COMPUTER SIMULATION IN NATURAL HAZARD ASSESSMENT

Don G. Friedman

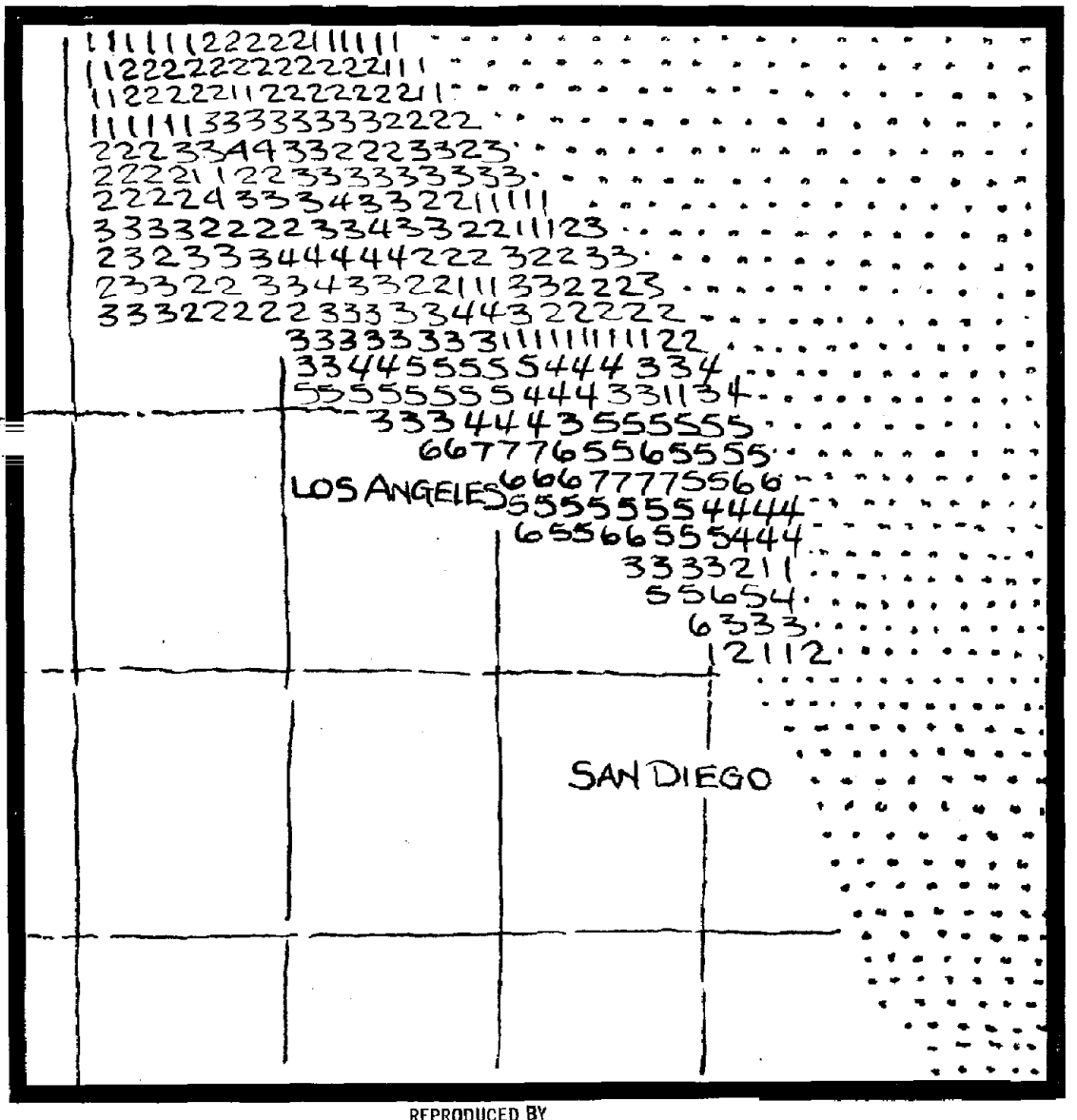

NSF-RA-E-75-002

COMPUTER SIMULATION IN NATURAL HAZARD ASSESSMENT

Don G. Friedman

The Travelers Insurance Company

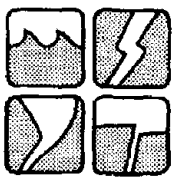

Program on Technology, Environment and Man

Monograph #NSF-RA-E-75-002

Institute of Behavioral Science

The University of Colorado

1975

ia

Prepared with the Support of the
National Science Foundation
Research Applied to National Needs
Washington, D.C. 20550

NSF Grant Number GI-32942

Library of Congress
Catalog Card No.
75-620036

Together, the entire staff of Assessment of Research on Natural Hazards (J. Eugene Haas and Gilbert F. White, Co-Principal Investigators) developed the objectives, approaches, methods and procedures, and gave assistance which contributed to the production of this volume.

Assessment of Research on Natural Hazards Staff

Robert S. Ayre	Neil J. Ericksen	Dennis S. Mileti
Earl J. Baker	J. Eugene Haas	Allan H. Murphy
Elwood M. Beck	Paul C. Huszar	Sarah K. Nathe
Mitchel J. Beville	Janice R. Hutton	Deanna J. Nervig
Karen K. Bird	Lee E. Kapaloski	Madalyn M. Parsons
Waltraud A. R. Brinkmann	Doris Knapp	John H. Sorensen
Anita Cochran	Brian A. Knowles	Patricia B. Trainer
Harold C. Cochrane	Sigmund Krane	Hazel Visvader
Frederick W. Dauer	Michael K. Lindell	Richard A. Warrick
Barbara S. Dunn	Gordon McPhee	Gilbert F. White

Ian Burton, Don G. Friedman, and Robert W. Kates served as regular consultants to the staff; Richard R. Nervig executed the original illustrations in this volume.

Advisory Committee

George W. Baker
National Science Foundation

Kenneth E. Boulding
Institute of Behavioral Science
University of Colorado

Earl Cook
College of Geosciences
Texas A & M University

Charles H. W. Foster
Secretary of Environmental Affairs
State of Massachusetts

George Housner
Earthquake Engineering
California Institute of Technology

Thad G. McLaughlin
U. S. Geological Survey

Daniel Price
Department of Sociology
University of Texas

E. L. Quarantelli
Disaster Research Center
Ohio State University

Will Reedy
Bureau of Reclamation

Robert Schnabel
Federal Disaster Assistance Administration

Herbert Temple, Jr.
Office of Emergency Services
State of California

Joseph Tofani
U. S. Army Corps of Engineers

John Townsend
National Oceanic and Atmospheric Administration

Neil P. Woodruff
U. S. Department of Agriculture

Cover sketch by Michael K. Alverson

Acknowledgment

The author wishes to thank Maryellen Bocaccino for her considerable contributions in the development of simulation procedures, mathematical analysis, and computer programming.

ASSESSMENT OF RESEARCH ON NATURAL HAZARDS
AIMS AND METHODS

The Assessment of Research on Natural Hazards is intended to serve two purposes: (1) it provides a more nearly balanced and comprehensive basis for judging the probable social utility of allocation of funds and personnel of various types of research on natural hazards; (2) it stimulates, in the process, a more systematic appraisal of research needs by scientific investigators in cooperation with the users of their findings.

The basic mode of analysis is to examine the complex set of interactions between social systems and natural systems which create hazards from the extreme geophysical events. The chief hazards investigated relate to: coastal erosion, drought, earthquake, flood, frost, hail, hurricane, landslide, lightning, snow avalanche, tornado, tsunami, urban snow, volcano, and windstorms. For each of those hazards the physical characteristics of the extreme events in the natural system are examined. The present use of hazardous areas and the variety of adjustments which people have made to extreme events are reviewed. The range of adjustments includes measures to modify the event, as by seeding a hurricane; modifying the hazard, as by adjusting building or land use to take account of the impact of the extreme event; and distributing the losses, as by insurance or relief. Taking all of the adjustments into account, the impact of the hazard upon society is estimated in terms of property losses, fatalities and injuries, and systemic disruption. An effort is made to identify the directions of change in the mix of adjustments and in their social impact. As a part of this review, those forces in the national society which shape the decisions about adjustments are appraised.

Authorities in the field are consulted through the medium of literature review, workshops on specific hazards, a national conference which was held in October, 1973, and individual reviews. Where appropriate and practicable, simulations of the extreme events and of their

social impacts are carried out. In selected areas scenarios of past and possible future events and their consequences are constructed.

In the light of this analysis the possible contributions of research to amelioration of the national condition with respect to each hazard are assessed. Each set of adjustments is reviewed in terms of its potential effects upon national economic efficiency, enhancement of human health, the avoidance of crisis surprise, the equitable distribution of costs, and the preservation of environmental options. Evaluation of particular research activities includes (1) the average sum of social costs and social benefits from application of a given adjustment in changing property use, and (2) reduction in average fatalities and casualties. In addition to the direct impacts of extreme events upon society, account is taken of the costs and benefits which society reaps in seeking to cope with the hazards, as in the case of costs of insurance or of control works.

In addition to calculating the average effects of hazard adjustments, an effort is made to estimate the degree to which the occurrence of a very rare event which has dramatic destructive potentialities, such as an 8.0 earthquake or a 200-year flood, would disrupt society.

Estimates also are made of the extent to which the adoption of an adjustment reduces the options of maintenance of environmental values, and the degree to which the pattern of distribution of income among various groups in society may be changed.

Research proposals are appraised in the light of the likelihood that the research undertaken could yield significant findings, and the likelihood that once the research is completed satisfactorily, the findings may be adopted and practiced by the individuals or public agencies in a position to benefit.

The United States as a whole is doing a competent job of dealing with some aspects of its natural hazards and a very ragged job of handling other aspects. The overall picture is one of rising annual property damage, decreasing loss of life and casualties, coupled with a marked growth in the potentiality for catastrophic events. On the whole, the public costs of adjustments are increasing.

The assessment reveals that very little is known about the dynamic relationships among many of the adjustments. It is difficult to predict with any confidence what the consequence of new Federal investments or initiatives will be in particular adjustments.

For each hazard a set of research opportunities deserving special consideration for early adoption is presented. In addition, three types of research which cut across the various hazards are assessed: warning systems, land management, and relief and rehabilitation.

Among the research basic to other aspects of natural hazards activity are: carefully planned post-audits of certain disasters and of adjustment measures by interdisciplinary teams; community observations over time of critical points (recovery policies and administration, health, mental health, and preventive measures) of change and of the effects of Federal-state-community interaction; and a clearinghouse service.

In most research fields it is noted that certain types of research which have claimed substantial amounts of public support offer little prospect of effecting a basic change in the character of the national hazard situation. In those instances there are new lines of emphasis which promise larger returns. Many of these involve more explicit collaboration of social scientists and natural scientists than has been customary in past. Wherever appropriate, the research recommendations include explicit provision for the translation of research findings into action by individuals or public groups.

To initiate effectively the desirable new lines of research will in some instances require a readjustment in legislative authority. In other cases it will require an increase in or reallocation of public funds for research. Much of it will involve changes in administrative procedures and policies of the responsible funding agencies. In many instances the effectiveness of the research will be linked strongly with the resolution of issues of public policy. These issues evolve around national land use management, financial assistance to sufferers from disasters, and the sharing of responsibility among local, state, and Federal agencies in designing and maintaining community preparedness.

TABLE OF CONTENTS

LIST OF TABLES

LIST OF FIGURES

SUMMARY

Every section of the United States is affected by one or more of such natural hazards as coastal and inland flooding, hurricanes, tornadoes, hailstorms and earthquakes. Each year hundreds of lives are lost and billions of dollars in damages occur. In recent years, the number and severity of natural disasters has increased sharply even though there is no conclusive evidence that storms and earthquakes are more severe than in past years. Growth in population size and susceptibility to natural hazard effects has increased the loss potential.

One approach to the reduction of this trend is the possible modification of adjustments to these hazards, or the addition of new adjustments. Major adjustments include warning systems, building codes and land use management. A number of these adjustments appear to be feasible for future loss mitigation, but the possible impact of these adjustments upon future natural hazard losses is difficult to assess. To make this assessment, there are two requirements. First, the assessment requires a means of estimating the present level and future trend of natural hazard losses in the United States using adjustments as they exist today. Second, it needs a vehicle by which the effect of modifying present or adding new adjustments can be evaluated. The use of past loss experience does not satisfy these requirements. An alternative approach is described, involving simulation techniques, which does provide a means of making the assessment.

A loss potential index is used to measure the present level and future trend of natural hazard losses in the United States. In the analysis, four factors interact to determine this index: natural hazard generator, local conditions, population-at-risk, and vulnerability. The natural hazard generator determines the frequency and severity of earthquakes and storms by section of the United States. It generates a geographical severity pattern (maximum wind speed for hurricanes, earthshock intensity for earthquakes) associated with each geophysical event. Local conditions express the modifying effect of local conditions on the severity pattern. Population-at-risk specifies the number and geographic

distribution of persons or buildings exposed to the natural hazards in various parts of the United States. An 85,000 point grid system is used. Vulnerability defines the susceptibility of population-at-risk to loss when an event of given severity occurs. The explicit relationship between the four factors and the loss potential index is used as a vehicle for measuring the effect of changing current adjustments or adding new ones.

The overlapping and resulting interaction of a geophysical event's severity pattern with the geographical array of population-at-risk determines the magnitude of the loss potential associated with the occurrence of an earthquake or storm. This index can vary from very low, when a weak earthquake or storm affects a sparsely populated area of the United States, to very high, when a severe geophysical event occurs over or near an urban area. A slight change in the positioning of the severity pattern relative to the population-at-risk array can drastically change the loss potential. When the index is large, it becomes a measure of catastrophe potential, indicating the likelihood of the production of a natural disaster. Loss potential cannot be determined solely from the use of any one of the four factors, for instance, the density of population-at-risk in a region or the seismicity and severe storm climatology of the area. The interaction of all four factors is needed.

To highlight problems and opportunities inherent in the use of this approach as a natural hazard assessment device, results of some applications to a number of natural hazards are given. Four populations-at-risk are defined: single unit residential buildings; other residential buildings; non-residential buildings; and population.

In the application to earthquakes, the development of the "earthquake generator" is described and the reasonableness of the computed severity patterns is discussed. Loss potential from the simulated recurrence of the moderate or severe earthquakes (Richter magnitude 5 or greater), that are reported to have affected Los Angeles since 1800, was calculated for the four populations-at-risk and tall buildings in that city. In addition, hypothetical earthquakes were simulated along the major fault zones in California. Three intensity levels were used--Richter magnitude 6, 7 and 8. Loss potential to the four populations-at-risk and tall buildings in California was estimated. Results of the application are used to point out the research and data requirements needed to improve the accuracy of the output.

For the hurricane hazard, the development and applications of the "wind speed generator" and the "storm surge generator" are discussed and computed patterns are compared with actual patterns. The simulated production of natural disasters is illustrated by the overlapping of the severity patterns of wind and storm surge with densely packed populations-at-risk along the Gulf and Atlantic coastlines. Severity patterns were calculated for hurricanes of five different intensity categories which were simulated to pass inland from 30 landfall locations set at intervals from southern Texas to Virginia.

The effect of modifying old adjustments and adding new adjustments on the level of loss potential is illustrated by the application to the inland flood hazard.

A major problem associated with the use of natural hazard simulation is the lack of information on the various populations-at-risk and their vulnerability to natural hazard effects. Another problem is the incomplete understanding of the physical relationships in the natural hazard loss-producing mechanism. Incorporation of the results of excellent work currently being conducted at a number of universities and government agencies could help to make the output of the natural hazard generators better approximations of the actual severity patterns. The question "how good is good enough?" must continually be asked; how close an approximation is needed for the purposes of the analysis?

One of the opportunities associated with the use of simulation techniques is that cross-hazard comparisons on a comparable basis can be made of the loss potential of various natural hazards, including the possible frequency and severity of future natural disasters. The impact of geophysical events can be simulated in any section of the United States and measures of the relative risk of various natural hazards can be estimated for any location.

CHAPTER I

COMPONENTS OF HAZARD

Assessment Needs

To some degree every section of the United States is affected by one or more of the natural hazards. These hazards include inland flooding, coastal storm surge, hurricanes, tornadoes, hail, windstorms and earthquakes. Damaging effects are measured each year in terms of hundreds of lives lost and billions of dollars in property damage. A substantial portion of these losses results from moderate or severe geophysical events (storms or earthquakes) occuring over or near populated areas of the United States.

In recent years the number and severity of natural disasters have increased sharply. One approach to reducing this trend is the possible modification of adjustments to these hazards, or the addition of new adjustments. Major adjustments include warning systems, land use management, insurance, and relief and rehabilitation. A number of time-sequenced combinations of these adjustments appear to be feasible possibilities for loss mitigation.

The possible impact of these adjustments upon future natural hazard losses is difficult to assess. To make this assessment, there are two requirements. First, the assessment requires a means of estimating the present level and future trend of natural hazard losses in the United States using adjustments as they exist today. Second, it needs a vehicle by which the effect of modifying present or adding new adjustments can be evaluated.

Some work has been done on developing techniques for estimating loss potential at an individual site in terms of a single maximum credible event. An example is an engineering study of natural hazard effects on a building at a given location. Information of this type is needed for the adjustment of building design and codes. However, for other types of adjustments it is desirable to have information on the loss-producing

characteristics of hurricanes or earthquakes that are less severe but more frequent than the maximum credible event. Planning must include the effect of storms and earthquakes with return periods of much less than once every 100 years or more, which is usually representative of the maximum credible event.

To approximate the natural hazard loss-producing mechanism, account must also be taken of the fact that a large percentage of the losses does not occur at random times and places in a region. Many losses from geophysical events can occur simultaneously to a population-at-risk spread over an area of hundreds of square miles. For natural hazard assessment, losses must be estimated over the entire area affected by the event rather than independently at individual sites. Work has recently been done on estimating the effects on the metropolitan areas of Los Angeles (NOAA, 1973) and San Francisco (NOAA, 1972) of a maximum credible earthquake occurring nearby. However, very little work has been done to estimate the regional effects of all potentially damaging geophysical events. Most of the work in this area has been done with evaluations at individual sites.

The purpose of this report is to describe a method of providing an order-of-magnitude measure of overall loss potential associated with natural hazards (Friedman, 1974). This loss potential index can be used to measure the present level and future trend of natural hazard losses in the United States. Four factors interact to determine this index: natural hazard generator, local conditions, population-at-risk, and vulnerability. Natural hazard generator determines the frequency and severity of earthquakes and storms by section of the United States. It generates a geographical severity pattern associated with each event. The maximum wind speed pattern associated with the passage of a hurricane and the earthshock pattern associated with an earthquake are examples of these severity patterns. Local conditions expresses the modifying effect of local conditions on the severity pattern of a geophysical event. Examples are the effect of urban-versus-rural exposures on wind speeds, and elevation and proximity to beach areas for storm surge. Population-at-risk specifies the number and geographic distribution of persons or buildings exposed to the natural hazards in various parts of the United States. Vulnerability defines the susceptibility of population-at-risk to loss when an event of given severity occurs. Vulnerability of buildings can vary from one section of the United States to another because of

differences in building codes, type, and quality of construction. The explicit relationship between the four factors and the loss potential index can be made a vehicle for measuring the effect of changing current adjustments or adding new adjustments.

Loss Potential

The interaction of a geophysical event's severity pattern with the geographical array of population-at-risk determines the magnitude of the loss potential associated with the occurrence of an earthquake or storm. This loss index can vary from very low, when a weak storm or earthquake affects a sparsely populated area of the United States, to very high, when a severe geophysical event occurs over or near an urban area (Table I-1a). A slight change in the positioning of the severity pattern relative to the population-at-risk array can change the loss potential drastically.

Table I-1 illustrates qualitative relationships that can be established between the four factors and the loss potential index. In this table, "natural hazard generator" represents the geographical pattern of severity associated with the occurrence of a geophysical event. These overall severity patterns are modified by the effect of "local conditions." The overlapping of these modified patterns with the geographic array of "population-at-risk" determines the number of persons or structures exposed to wind speeds or earthshocks of given severity. The number of these exposed persons or buildings that actually are affected and the degree of the effect are determined by the measure of "vulnerability." The index is also a measure of catastrophe potential, indicating the likelihood of the production of a natural disaster.

Loss potential cannot be determined solely from the use of any one of the factors such as the denseness of the population-at-risk in a region or the seismicity and severe storm climatology of an area; the interaction of all four factors is needed. When all four factors are considered, there are a number of combinations that can produce the same level of loss potential (Table I-1b).

Even simplified relationships implied in Table I-1 demonstrate the difficulties inherent in attempting to translate past loss experience into a measure of present loss potential. First, the natural hazard loss-producing process is not reversible. Past loss experience (realized loss potential) results from the particular overlapping of the event's

severity pattern with the then existent population-at-risk and its vulnerability. This particular combination of conditions will not occur again.

TABLE I-1

QUALITATIVE RELATIONSHIPS AMONG THE FOUR FACTORS WHICH COMBINE TO DETERMINE MAGNITUDE OF NATURAL HAZARD LOSS POTENTIAL

1a. Combination of Factors that Produce a Loss Potential Index Ranging from Very Low to Very High

Factor			
Natural hazard generator	weak	moderate	severe
Local conditions	good	medium	poor
Population-at-risk	sparse	moderately dense	dense
Vulnerability	low	moderate	high
Loss potential index	very low	moderate	very high

1b. Possible Combinations of the Four Factors that Yield the Same Loss Potential Index

Factor			
Natural hazard generator	severe	moderate	moderate
Local conditions	medium	poor	poor
Population-at-risk	moderately dense	dense	moderately dense
Vulnerability	high	moderate	high
Loss potential index	high	high	high

1c. Illustration of Changes Over Time in the Loss Potential Index Even Though the Natural Hazard Event Does Not Change in Severity

Factor	1945	1960	1975
Natural hazard generator	moderate	moderate	moderate
Local conditions	medium	medium	medium
Population-at-risk	sparse	moderately dense	dense
Vulnerability	moderate	moderate	moderate
Loss potential index	low	moderate	high

1d. Differences Between Condition of Factors When Past Loss Experience and Natural Hazard Simulation is Used for Estimating the Present Level of Natural Hazard Loss Potential

Factor	Past loss experience	Natural hazard simulation
Natural hazard generator	held constant	allowed to vary
Local conditions	held constant	held constant
Population-at-risk	allowed to vary	held constant
Vulnerability	allowed to vary	held constant

The second difficulty is illustrated in Table I-1c. An identical geophysical event occurring in, for example, 1945, 1960 and 1975 would produce different levels of loss potential due to the increased population-at-risk in hazard-prone areas such as on the coastal strip of the Eastern seaboard or in California. The direction of change in the vulnerability factor over time depends on a number of items. Improvements over time in materials and type of construction should reduce the loss susceptibility of buildings to natural hazard losses. However, these improvements may or may not counteract the effect of increased value-at-risk and the inflationary cost of repair when damage does occur.

When past experience is used as a proxy measure of present loss potential, the natural hazard events which happened to occur in the sampled period of years are held constant in the extrapolation. Population-at-risk and vulnerability, however, vary with time within the sampled period, as illustrated in Table I-1. To obtain a more realistic measure of present loss potential, these conditions should be reversed. Population-at-risk and vulnerability should be held constant at current levels, while the natural hazard generator is allowed to vary by producing geophysical events (Table I-1d). Generation of these events and their associated severity patterns, irregularly placed in time and space, should of course be consistent with the long-term seismicity or severe storm climatology of the particular geographical area being examined. We are interested in the effect of a recurrence of the 1906 San Francisco earthquake on the current population-at-risk and its current vulnerability, not on the 1906 population-at-risk and its vulnerability to loss at that time.

The relationships in Table I-1 are highly oversimplified. For example, the four factors are assumed to be constant throughout the geographical area that is affected, and a uniform overlapping of the patterns is supposed. In reality, the size, shape, orientation and intensity gradient in the event's severity pattern are not uniform over a geographical area. Local exposure conditions and population-at-risk can also vary greatly within a region. Even vulnerability is not constant throughout. In addition, the overlapping of the event's pattern with the geographical array of population-at-risk varies, depending upon the severity pattern's irregular shape, size and positioning relative to the usually non-uniform geographical array of population-at-risk. Consequently, the illustrative relationships in Table I-1 must be refined and quantified in order to be useful in producing estimates of present and future natural hazard loss

potential. Figure I-1 is a plot of the overlapping of the earthshock severity pattern of a California earthquake with the geographical array of population-at-risk. It is the interaction of patterns of this type that must be duplicated.

An approximation of the loss-producing mechanism shown in Table I-1 has been made through the use of a mathematical modeling of apparent relationships among the four factors and the loss potential index. Models have been constructed to produce a geographical pattern of severity associated with the occurrence of earthquakes or hurricane winds and storm surge (Friedman, 1972). Models for generating the geographical severity patterns of squall line storms (tornadoes, hailstorms, thunderstorm winds) and winter windstorms are under construction.

Population-at-Risk

One of the key elements required for the modeling is an approximation of the population-at-risk. The geographical distribution of properties is obtained by using a grid system.

An essential element involved in the application of a single computerized system for assessing loss potential of more than one natural hazard is definition of the grid network used for representing the geographical distribution of population-at-risk. Civil divisions (state, county, standard metropolitan areas, census track, city block, and ZIP code divisions) present varying amounts of difficulties because of their non-uniform sizes and shapes. Ideally, the area of the grid elements should be small compared to the size of the severity pattern associated with each hazard, and the grid elements should be uniform in shape to eliminate regional biases in loss estimation. The possible magnitude of these biases is not known. To reduce the effect of these size and shape irregularities upon the estimation of loss potential, a rectangular grid network was chosen for the test system described in this report. In actual practice, it would be much simpler to use a network based, for instance, upon census tracts so that population-at-risk information could be extracted directly from U. S. Bureau of the Census tapes. The use of a rectangular grid system which is ideal for the geographical evaluation of natural hazards requires the laborious task of gathering population-at-risk information by hand using an atlas and hard copy census tabulations for input into computer memory for each grid area.

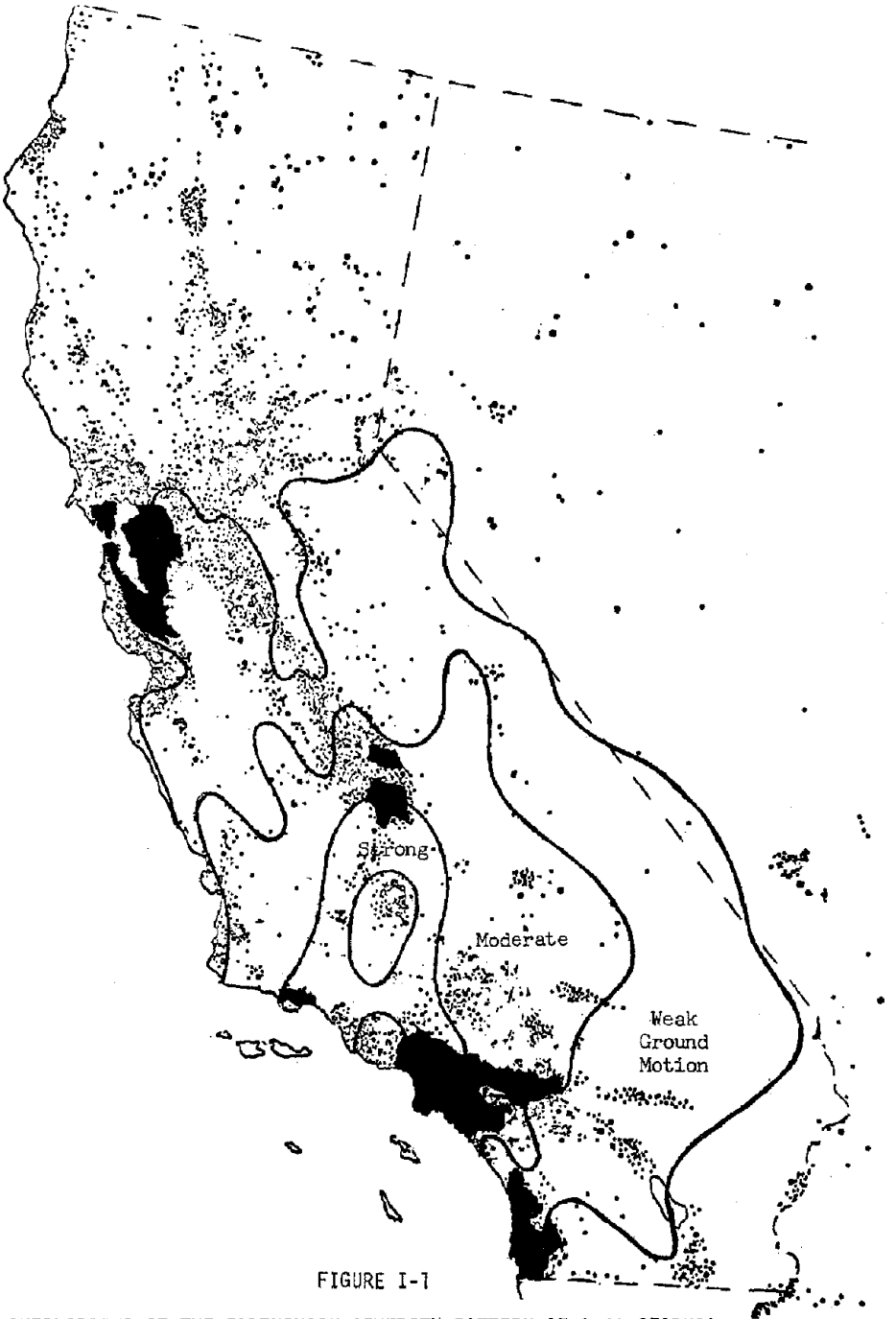

FIGURE I-1

OVERLAPPING OF THE EARTHSHOCK SEVERITY PATTERN OF A CALIFORNIA EARTHQUAKE WITH THE GEOGRAPHICAL ARRAY OF POPULATION

A rectangular grid system addressed in terms of uniform increments of latitude and longitude has been developed. Size of the individual grid areas depends upon the application. For a study of the earthquake hazard in the San Francisco Bay area, a system of grid areas of less than one-half of a square mile (.01° latitude by .01° longitude) was used. For general studies of the natural hazards in various parts of the United States, a system of grid areas of one-tenth of a degree longitude by one-tenth of a degree latitude is utilized.

Due to the convergence of the meridians, the grid areas vary in size from approximately 44 square miles in southern Florida to 32 square miles along the northern border of the United States. The magnitude of possible inaccuracies introduced by use of grid areas that are not uniform throughout the United States is reduced because natural hazards usually do not affect an area covering more than about ten degrees of latitude, and the effect of the convergence of the meridians has been built into the natural hazard generators which produce a computed geographical pattern of severity associated with a hurricane or earthquake. The size and shape of these patterns change from south to north to account for the meridian convergence.

Approximately 85,000 grid areas are needed to represent the land area of the contiguous forty-eight states. Population characteristics such as number, type, value, exposure, and vulnerability are stored in memory for each grid area. Two components of population-at-risk are used: number of persons, and number and value of one-family dwellings. Currently, information from the 1970 Census on a population-at-risk of 203,000,000 persons and property-at-risk of 47,000,000 one-family dwellings is being allocated to the grid areas in the computer system.

Vulnerability Relationships

The magnitude of the calculated loss potential is directly related to the vulnerability of the exposed population-at-risk. For example, the degree of vulnerability of dwellings measured relative to wind speed or earthshock severity is determined from claim records, engineering studies and other information that may be available. For other types of buildings, vulnerability relationships are different and may require an on-site engineering inspection. Casualty and social impact curves also are used as input.

A two-stage vulnerability relationship for dwellings has been found to be useful. First, the range and expected percentage of the exposed structures that would be damaged in a small geographical area by a given wind speed or earthshock is determined. Except for extremely severe geophysical conditions, only a percentage of dwellings in the area will be damaged because of differences in damage susceptibility due to age, type, quality of construction, and degree of exposure. In the second part of the relationship the range and expected amount of potential loss is calculated if the structure is one of those that is damaged. The range of possible damage amounts is related to the severity of the event. When winds are 150 miles per hour, the range and frequency distribution of possible damages are different from the damage possibilities when winds are only 50 miles per hour.

Natural Hazard Generator

Mathematical models have been constructed which produce a geographical pattern of severity with properly spaced contours that are consistent with the size, shape and configuration of observed patterns associated with hurricanes and earthquakes. Severe storm climatology and seismicity of various sections of the United States are used to provide tracks and intensity of past hurricanes, and epicenter locations and magnitude of past earthquakes.

Information from the physical sciences is used to relate the size and shape of the geographical pattern of maximum wind speed associated with the passage of a hurricane to input measures of storm intensity (central barometric pressure), storm size, storm speed, and direction and curvature of storm path relative to the coastline. Effect of friction and loss of energy source in causing hurricane winds to decrease as the storm moves inland is included in the model. Variations in the input parameters change the computed severity patterns. For earthquakes, isoseismal patterns of earthshock intensity are related to commonly available information on earthquake magnitude (Richter Scale), location, orientation of fault zone, and hypocenter depth.

Local Conditions

The geographical patterns obtained from natural hazard generators have smooth, regular-shaped contours. The superposition of local conditions causes these computed patterns to become irregular in shape, size, and contour spacing. For earthquakes, the effect of local ground

conditions on earthshock severity is approximated. For windstorms the measure of local conditions is the degree of exposure to high winds such as urban-versus-suburban or rural environments. Calculated and observed intensity patterns are compared whenever possible. Computer-derived patterns are good approximations of observed patterns when the effects of local conditions are included.

CHAPTER II

SIMULATION OF LOSS POTENTIAL

Approach

Given location, intensity and other pertinent characteristics of a simulated geophysical event, a geographical severity pattern is computed (Figure II-1). Due to the uniqueness of each event, it is almost impossible to duplicate exactly all observed severity patterns with a computer-derived version. The rationale for using computed patterns is that, although the patterns cannot exactly duplicate actual patterns, they can be made to represent the observed inherent physical constraints and limits on size, shape, and contour spacing as related to the intensity of a geophysical event. For example, past observations of earthshock patterns exhibit general consistencies in severity pattern properties which are common to all earthquakes. Computerized models are based upon these consistencies. There are variations from the most commonly observed dimensions but this variability can be statistically accounted for in the mathematical models.

Simulated interaction of the four factors yields a measure of the event's loss potential based upon its physical characteristics and positioning relative to the geographical array of population-at-risk. This evaluation of the loss potential of each individual natural hazard *event* is different from the frequently used approach of measuring natural hazard risk at a given geographic *location*. Thom (1968) has presented maps of the return period of high winds in the United States, including winds associated with Gulf and East Coast hurricanes. Algermissen (1969) developed a seismic risk map of the United States in terms of a measure of earthshock severity. To use either set of maps it must be assumed that the risk at one location is independent of the risk at surrounding locations. Because of this implicit lack of spatial correlation it is not possible to reconstruct the loss potential of each of the many individual geophysical events that, when accumulated over a long

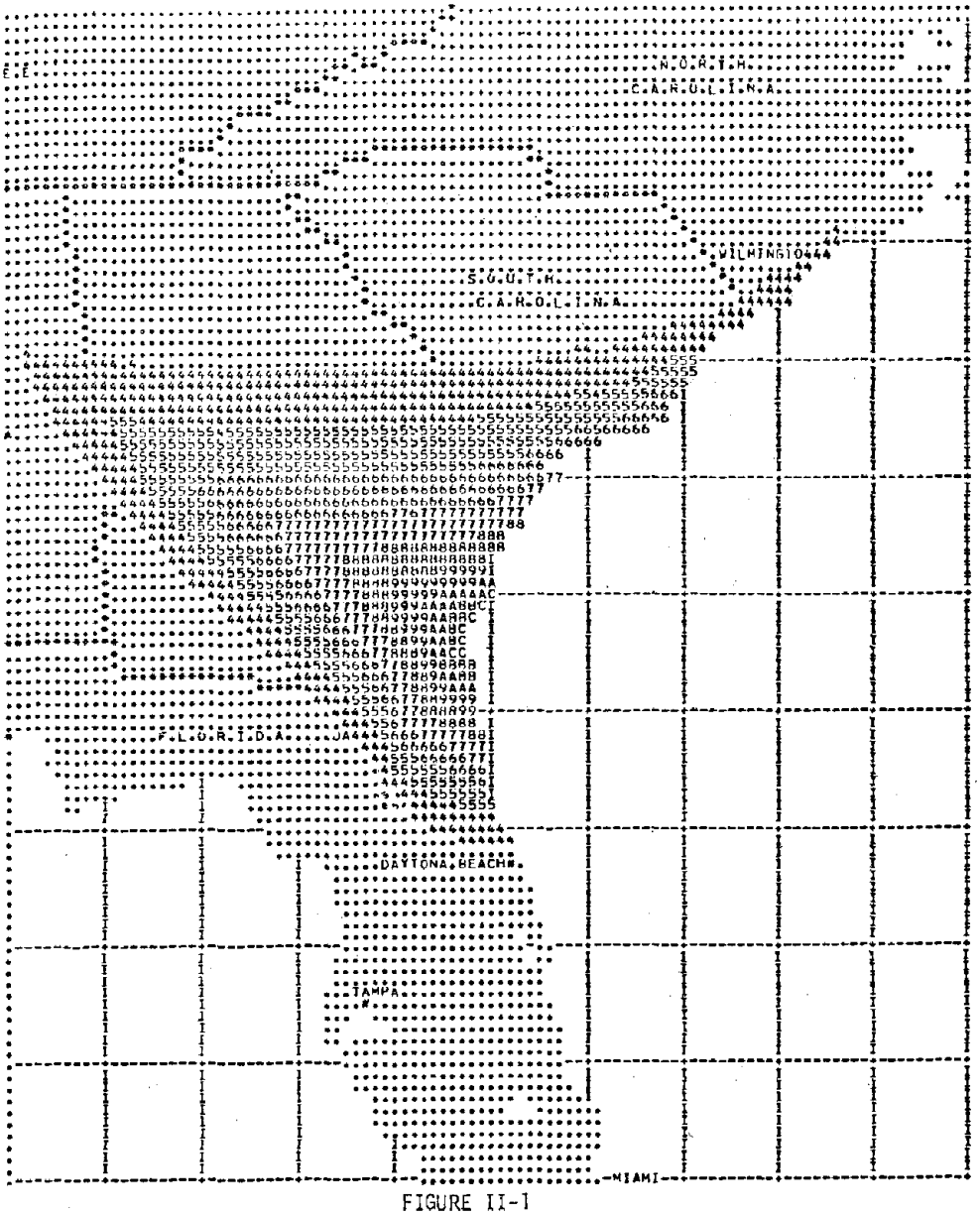

FIGURE II-1

EXAMPLE OF THE CALCULATED PATTERN OF MAXIMUM WIND SPEEDS ASSOCIATED WITH THE PASSAGE OF A HURRICANE ACROSS THE SOUTHEAST COASTLINE (Maximum wind speed is plotted as a single digit number on the chart. For example, a "7" denotes a computed windspeed which lies between 70 and 79 miles per hour. Effects of local exposure conditions are not incorporated in the wind speed pattern given in this exhibit.)

period of years, produce a measure of risk at each individual location. In addition, risk is measured in physical terms (windspeed or earthshock intensity) rather than as a loss potential.

Figure II-2 graphically illustrates the relationship between the event's severity pattern and the geographical distribution of population-at-risk in determining the loss potential of the event. In this figure the intensity of the event, including modification by local conditions, is plotted against the affected population-at-risk and its vulnerability. The diagonally trending curves represent idealized contours of loss potential. A weak storm or earthquake which affects a sparsely populated area produces a very low value of loss potential (lower left section of the graph). At the other extreme, a severe event over a densely populated area yields a very high loss potential which could lead to a natural disaster (upper right section of the graph).

The occurrence of a maximum credible event can be represented by a vertical line on the extreme right side of the chart. Loss potential of this most severe event clearly depends upon the size and vulnerability of the affected population-at-risk. Examples of possible levels of loss potential are given by points A, B and C, which lie on the vertical line. A simulation modeling approach to natural hazard assessment presents the opportunity to measure loss potential from the multitude of possible combinations of the overlapping a geophysical event's severity pattern with population-at-risk, represented by points anywhere on the Figure II-2 graph, for example, points D, E, F or G.

Frequency of Geophysical Events

A means for determining the loss potential when an event of given characteristics occurs has been outlined in the previous sections. To be useful in specifying the present and future trend in loss potential the frequency of events by intensity and geographic location must be included. Frequency has been incorporated into the analysis in two ways. First, a recurrence of past events is simulated. Secondly, events are generated by intensity, location and intervening time intervals consistent with available information on the seismicity or severe storm climatology of the region of the United States under study.

FIGURE II-2

GRAPHICAL REPRESENTATION OF THE RELATIONSHIP BETWEEN THE LOSS POTENTIAL INDEX AND THE FOUR FACTORS[1]

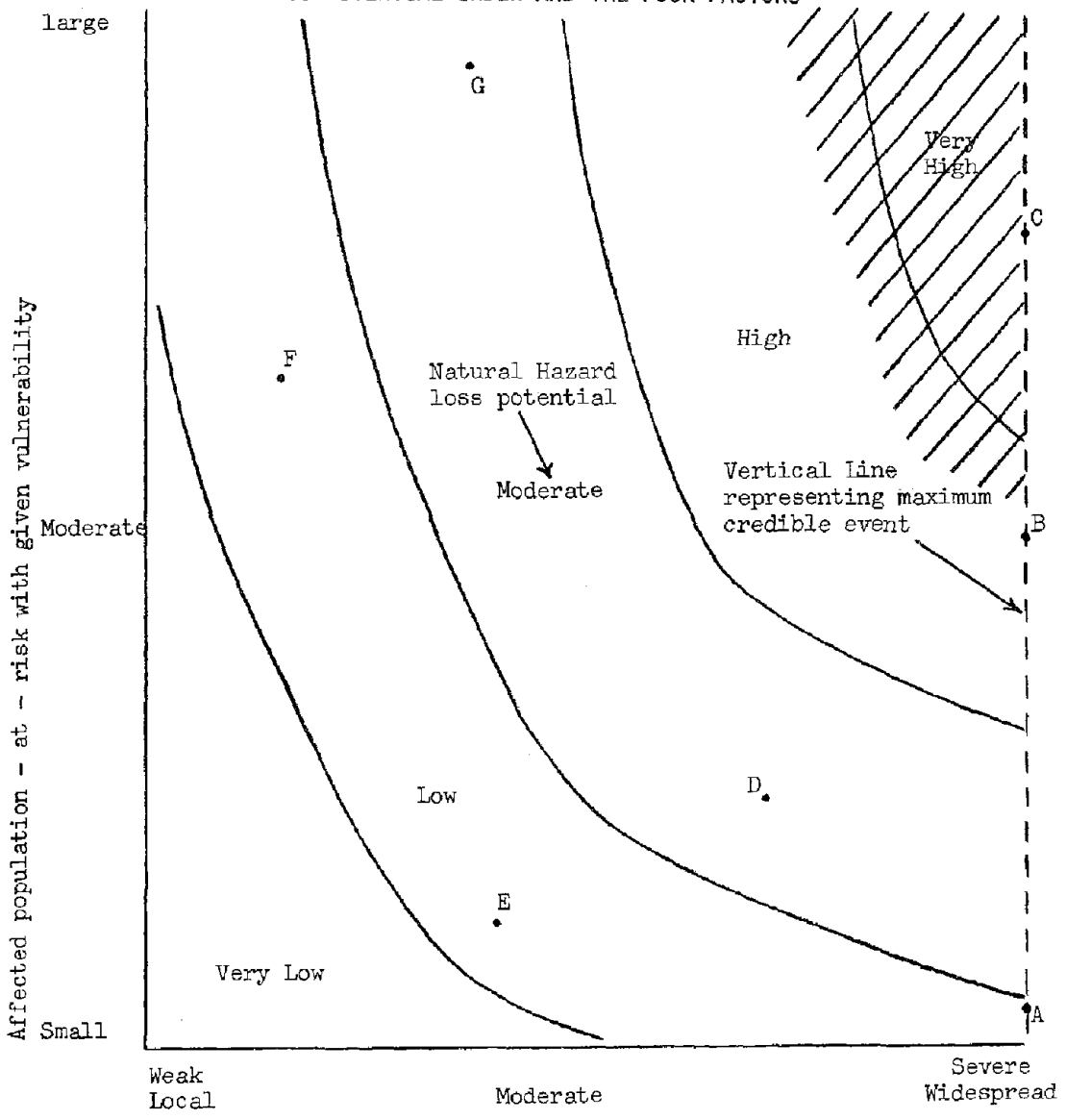

Generated severity pattern of geophysical event modified by local conditions

[1]Loss potential of a maximum credible event is given by a point somewhere on the vertical dashed line. The computer simulation approach produces a loss potential index in terms of a multitude of possible combinations of the four factors represented by any point on the chart. Examples are points A through G. Hatched lines represent the area in which there is a high likelihood of the production of a natural disaster.

Specification of Present Level and Future Trend

The present level in loss potential of the natural hazards in the United States, such as earthquakes and hurricanes, is determined by holding the population-at-risk and vulnerability at current levels and simulating the effect of an occurrence of natural hazard events on the exposed population.

Future trends in loss potential are obtained by applying differential growth factors to the geographical pattern of the population-at-risk, depending upon the assumptions regarding future growth in various parts of the region. Time changes in vulnerability are also specified. A year-by-year time simulation is then performed. Geophysical events are generated at irregularly spaced intervals within the sampled period of years, which may be of specified length, for instance, twenty years. A number of these twenty-year sequences are computed to provide a measure of the statistical variability inherent in the time-related sequencing of the simulated events.

Measuring Effects of Changing Adjustments

Relationships between loss potential and the four factors are changed to approximate the effect of adding new adjustments or modifying existing ones. The geographical distribution of population-at-risk is altered to reflect the effect of changing land use regulations; the hypothesized effect of weather modification is obtained by changing the character of the storm generator model; modification of vulnerability relationships is used to represent construction and building code changes. Insurance, which by itself does not alter loss potential, affects the distribution of the output of the system--the aggregated loss potential. This distribution flow is incorporated into the model. The relative influence of changes in the various adjustments on loss potentials is shown by the time-sequencing of them over the simulated periods of 20-year length.

Application

Of fifteen major natural hazards*, a number of them represent geophysical phenomena which can affect population-at-risk spread over a

---

*Snow avalanche, coastal erosion, drought, earthquake, flood, frost, hurricane, landslide, severe squall-line storms (tornadoes, wind, hail, lightning), urban snow, volcano, windstorms.

large geographical area in a short period of time. Currently, computer simulation techniques are being applied as an assessment tool to these hazards which include earthquakes, hurricanes (wind and storm surge), severe squall-line storms (tornadoes, wind, hail) and large-scale windstorms. A somewhat different approach has been taken on the simulation of the inland flood hazard. The 85,000 unit computerized grid system representing the land area of the United States was not used for evaluating the magnitude of the flood hazard. The approach that was taken is described in a later section.

In making these applications, the objective has been to keep the mathematical models as simple and flexible as possible and still be able to obtain useful information on the workings of the actual natural hazard mechanisms by the use of these rough mathematical approximations. No attempt has been made to further complicate the models in order to extract the usually small amount of useful additional information that a complicated model might yield over a simple one. The present state of knowledge does not warrant the construction of highly complicated models with a great amount of detail because there is a lack of pertinent input data and information on the intricate relationships among variables that combine to determine the magnitude of natural hazard losses.

CHAPTER III

EARTHQUAKES

Development of Original Model

During the development of the joint insurance industry/Federal government National Flood Insurance Program, simulation techniques were used in assessing the magnitude of the flood hazard to dwellings in the United States (Friedman and Roy, 1966; Kaplan, 1972). Upon completion of the flood work in 1967, the possibility of applying similar techniques to an evaluation of the earthquake hazard to United States dwellings was discussed.

Results of feasibility studies carried out over the next year and a half at The Travelers Insurance Company were reported by Friedman and Roy (1969). It was concluded that a simple mathematical generator could be constructed which, along with the use of an index of local ground conditions, could produce realistic geographical patterns of earthshock severity. Modified Mercalli intensity units were used to represent earthshock intensity in the 1969 earthquake model. Size, shape and contour gradient of the computed patterns were good approximations of observed Modified Mercalli isoseismal patterns for various combinations of earthquake magnitude (Richter Scale), epicenter location, hypocenter depth, and fault zone type and orientation. This possibility of producing realistic isoseismal patterns using a mathematical model was recently confirmed by Evernden, Hibbard and Schneider (1972).

Population-at-risk was defined as the total number of single family dwellings in the San Francisco metropolitan area. Vulnerability relationships used in the feasibility study were derived from damage experience of a number of past earthquakes. A brief description of the characteristics of the 1969 earthquake model is given in the following sections, along with some results of an application of the model to an evaluation of the catastrophe potential of earthquakes in the San Francisco metropolitan area (Friedman, 1969) and in the Los Angeles

metropolitan area (White and Haas, 1975).

For the first time, a large number of strong motion earthshock measurements were made at a dense network of nearby observation points during a moderately strong earthquake (1971 San Fernando earthquake). These newly published data, along with results of recent research studies, have provided the basis for modification of the 1969 earthquake model. The objective of the updating is to express the computed patterns of earthshock severity in more meaningful physical terms such as spectral acceleration, velocity, duration and wave length of the earthshocks.

When the original model was being developed, the Modified Mercalli intensity unit was the only earthshock index that was available in sufficient enough detail for a generator to be based upon it. The Modified Mercalli intensity unit taken by itself is a poor index of earthshock severity because it is based upon a qualitative and nonstationary mixture of earthquake effects on people (lower part of scale), buildings (middle of scale) and geology (upper part of scale). A description of it is given in Appendix A. In the 1969 earthquake model, the measure of earthshock severity is a continuous scale which runs parallel to the Mercalli Scale. It is assumed that fractions of the severity unit have a physical significance. An increasing degree of severity is represented, for instance, by readings of 6.5, 6.7 and 7.1 on this continuous scale.

The Modified Mercalli Scale is discrete. The use of a continuous unit that parallels the Mercalli Scale reduces somewhat the detrimental effects that would be inherent in a direct use of Mercalli intensity categories as measures of severity. In addition, the measure of earthshock severity, no matter how it is defined, is used in the simulation analysis as a connecting variable between the input (physical characteristics of the earthquake--magnitude, location, depth) and the output (number of buildings or persons exposed, number affected, and degree of the effect). It does not have to be explicitly used in the output. Inadequacies in the index as a measure of earthshock severity can be adjusted for in the vulnerability relationships which relate potential damage to degree of earthshock severity.

A discussion of the construction and use of the updated earthquake model is given at the end of this chapter.

1. Earthshock Severity at a Given Location

Construction of the original earthquake model was based upon the determination of relationships between the size, shape and gradient within the geographical pattern of earthshock severity, with the following factors:

(1) Magnitude of the earthquake (Richter Scale). This is a measure of the amount of energy released.

(2) Distance of the locality from the earthquake's epicenter. Earthshock intensity normally decreases with an increase in distance from the epicenter for low magnitude earthquakes.

(3) Orientation of the locality relative to the fault zone. For earthquakes of moderate or great magnitude, surface faulting stretches out along the fault zone in most of California. Earthquake magnitude is related to the length of faulting (NOAA, 1972):

Length faulting (miles)	Earthquake magnitude (Richter)	Total surface displacement (horizontal movement)
15 to 20	6.0	3 feet
40 to 50	7.0	5 feet
200 to 300	8.3	20 feet

(4) Depth of the hypocenter. Radiation of vibrational energy upward to the earth's surface is affected by the depth of the energy source. If the hypocenter is deep, energy reaching the earth's surface is spread over a large area and is not very intense at any given point on the surface. On the other hand, when the hypocenter is near the earth's surface, the radiated energy is distributed over a smaller surface area. Intense motion along the faulted area decreases rapidly with distance from the fault zone. Earthquakes in California are usually of shallow depth.

(5) Duration of the earthshock. Length of faulting determines the duration of the earthshocks. In this sense, duration is related to magnitude of the earthquake because both measures are dependent upon fault length. The damage producing potential of earthquakes is dependent upon both the earthshock severity and the duration of the intense shaking. The severity of the earthshock probably reaches a maximum when earthquake magnitude is about 6.5 (Richter). For earthquakes of larger magnitude, the earthshock intensity does not increase much above the severity level of a 6.5 earthquake. However, the duration of intense earthshaking is greater and the area affected by the intense ground motion is large because of the distribution of intense motion along the length of the faulted zone. The increased duration of intense

motion at a given locality is caused by the addition of time increments required for vibrational waves to reach the locality from various points along the faulted zone. Duration of a large earthquake may be as much as one minute because of the great length of the faulted zone.

(6) Geology of the intervening area between the locality and the earthquake's faulted zone. Geological formations through which the seismic waves must pass can amplify or dampen these waves.

(7) Local conditions. Certain types of local ground conditions can amplify or dampen the earthshock intensity. The influence of local ground conditions upon the severity of ground motion is still an open question. There is reported evidence that the effect of certain types of local ground conditions is deterministic, that is, the earthshock at a given site will be modified in the same way each time an earthquake of given physical characteristics--magnitude, depth, location--recurs (Richter, 1959; Medvedev, 1962). However, recent studies suggest that there may be a range of responses due to local ground conditions at each location. In this case, earthshocks associated with a recurrence of an earthquake of identical physical characteristics would not necessarily be affected in exactly the same way by the local ground conditions. An index of local ground conditions would be an indicator of a frequency distribution of possible responses rather than an indicator of a single deterministic response such as a fixed amount of amplification.

Available information on these factors and their interrelationships was used to construct the generator. An explicitly stated set of assumptions tying these factors together was assembled which appeared to be consistent with the currently accepted ideas among seismologists regarding the earthquake mechanism and resultant ground motions.

2. Construction of Earthquake Generator

Size, shape and spacing of isoseismic contours in the computed patterns on bedrock, as related to the magnitude and depth of an earthquake, were based upon information given in a number of sources (Slemmons, *et al.*, 1965; Isacks and Oliver, 1964; Gutenberg and Richter, 1942 and 1956; Medvedev, 1962; Furumoto, 1966; Richter, 1959; U. S. Department of Commerce, 1967). Figure III-1 illustrates some of the relationships graphically. On a bedrock surface, the size and shape of the computed pattern changes from small and circular for low magnitude earthquakes to large and elliptical for high magnitude ones. The degree of elliptical

distortion of the isopleths is greatest near the faulted area so that there is a differential change from the outer contour, which is the level of perceptibility (Modified Mercalli I), to inner contours near the faulted zone.

Depth of the hypocenter, the level at which the energy is released, is assumed to have an influence upon the overall size of the computed isoseismal patterns. An earthquake of shallow depth produces a surface pattern of small size with a tight gradient of earthshock severity. An earthquake of great depth results in a large-sized surface pattern with generally less intense earthshocks (see Figure III-1). The depth factor can be used as a scaling factor on the size of the earthshock pattern. Alternatively, the "felt area" which is reported for early earthquakes has been made a proxy measure of depth.

3. Effect of Local Conditions

The computed earthshock patterns on bedrock are represented by smooth contours with either circular or elliptically shaped isopleths, depending upon the assumed magnitude of the earthquake (see Figure III-2a). A comparison of these smooth synthetic patterns with observed irregular shaped isoseismal patterns indicated that the effect of other factors such as local conditions had to be introduced into the model in order to improve the reasonableness of the computed patterns. Based upon information that was available in 1968, the effect of local ground conditions was introduced as a simple, deterministic factor in the model. Material presented by Richter (1959) and Medvedev (1962) formed the basis for this "local ground condition" index.

It was assumed that local ground conditions could result in the addition of an increment of intensity to the intensity computed for bedrock. To quantify this factor, ground conditions were indexed for the entire state of California. As a first approximation, a geology map of California was used as a basis for the index determination (California Division of Mines and Geology, 1966; Jenkins, 1965). An index of five levels was constructed:

Index	Ground Condition
1	bedrock
2	moderately firm
3	sandy ground
4	alluvial
5	moist fill

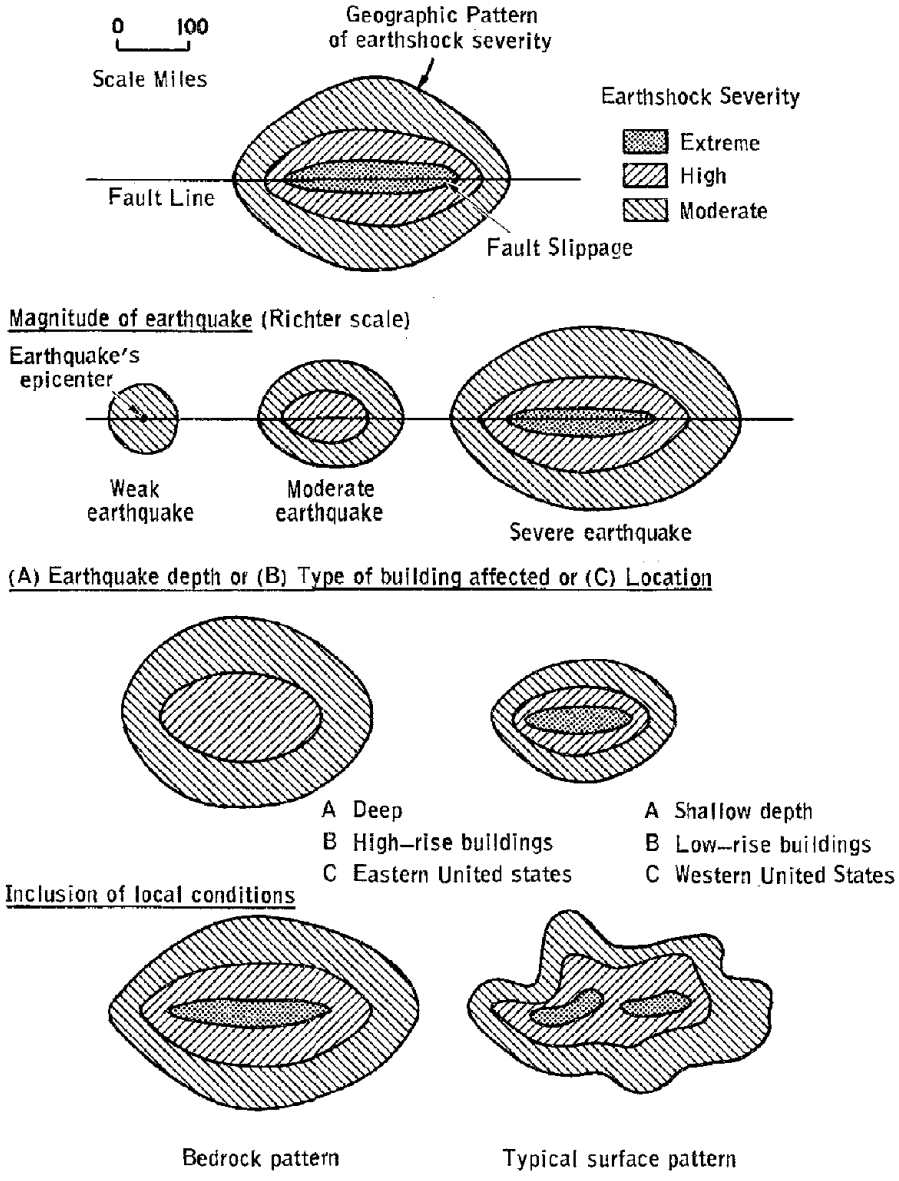

FIGURE III–I

SIZE AND SHAPE OF THE GEOGRAPHIC PATTERN OF EARTHSHOCK SEVERITY RELATED TO PHYSICAL PROPERTIES OF AN EARTHQUAKE FOR A COMMON TYPE OF FAULTING MECHANISM

FIGURE III-2

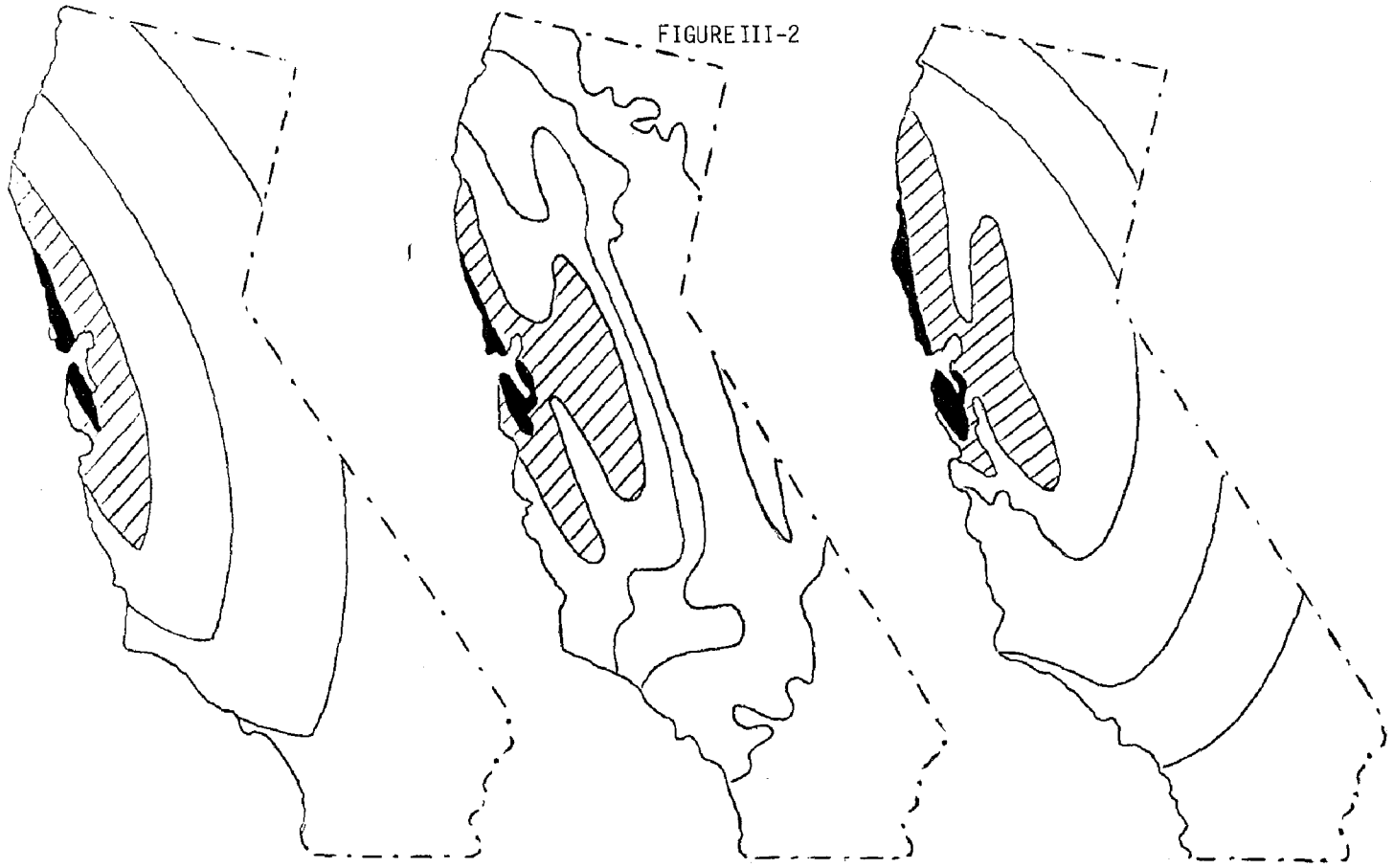

a. Computed pattern on bedrock

b. Computed pattern including effects of local ground conditions

c. Observed pattern based on Richter (1958)

COMPUTED EARTHSHOCK SEVERITY PATTERNS FOR THE 1906 SAN FRANCISCO EARTHQUAKE COMPARED WITH THE OBSERVED PATTERN

Each of the five index numbers represents a different equation in the computer program for calculating local ground condition increments to be added to the bedrock intensity. For bedrock conditions the index is equal to one (the local ground condition affect is negligible) and the increment to be added is zero. Magnitude of the increment to be added depends upon soil conditions and relative position of the locality within the isoseismal pattern. When the increment is added, the intensity patterns become irregular and begin to simulate the observed isoseismal patterns. Figure III-1 illustrates how the computed pattern becomes irregularly shaped when effects of local ground conditions are superimposed upon the bedrock pattern. The use of this simple index produces synthetic isoseismal patterns which are much closer in shape and size to observed patterns than the bedrock patterns.

4. Frequency and Magnitude of Future Earthquakes

To apply the earthquake hazard model, assumptions must be made about location and magnitude of future earthquakes. The state of knowledge regarding causes of earthquakes is such that a number of alternative sets of assumptions are needed. Possible alternative assumptions are:

(1) The location of future earthquakes of various magnitudes will follow the same pattern of earthquakes observed in the historical past, for example, in the past 168 years in San Francisco. The likelihood of an exact recurrence of past earthquakes is very small.

(2) Future earthquakes of various magnitudes are likely anywhere along the major fault zones, and future occurrences are independent of past occurrences. This alternative is not likely.

(3) The location of future earthquakes of higher magnitudes is dependent upon the location of high magnitude earthquakes in the recent past. Frequencies of larger earthquakes are probably not independent in either time or space. Occurrence of a large earthquake on a segment of fault line may decrease the likelihood of another large earthquake in the vicinity for a period of years, discounting occurrence of aftershocks. The greater the magnitude, the greater the time-space dependence. Earthquakes sufficiently intense to cause damage usually occur in fault zones. Moderate earthquakes (Richter 4 or 5) may be distributed at random along the fault zone. Earthquakes of lower magnitude (3 or less) may be associated with minor seismic features not connected with fault zones (Allen, *et al.*, 1965).

The third alternative, based upon a memory in both time and space, is the most likely (Friedman, 1973; Lomnitz, 1974).

Application of Earthquake Model to San Francisco

To test the models, isoseismal patterns of larger earthquakes that have affected the San Francisco Bay area in the past 168 years (since 1800) were calculated. This is equivalent to using frequency alternative number one mentioned in the previous section. Actual detailed isoseismal patterns for these early earthquakes are not available. The Earthquake History of the United States tabulated by the U. S. Coast and Geodetic Survey (1966) was used to estimate the magnitude (epicenter intensity), location, and depth (felt area) of the past earthquakes that affected San Francisco.

For those early earthquakes where no epicenter intensity was listed in the Earthquake History, an estimate was obtained from Descriptive Catalog of Earthquakes of the Pacific Coast of the United States (Townley and Allen, 1939). Rossi-Forel intensity units used prior to 1931 were converted to Modified Mercalli units for early earthquakes.

Earthshock intensity patterns were computed for earthquakes that occurred since 1800, had an epicenter intensity of VI or greater (Modified Mercalli), and were near enough to affect the San Francisco Bay area. Intensity patterns were computed for 100 earthquakes that occurred in central or northern California and Nevada in the historical past. Eighty earthquakes satisfied the above conditions. Computed isoseismal patterns of the remaining 20 earthquakes indicated that these earthquakes would not have been felt in the Bay area. This was substantiated by actual records of these earthquakes. Two grid systems were used to measure the effect of local ground conditions:

(1) Specification of the isoseismal pattern using indices of local ground conditions representative of tenth-of-a-degree latitude and longitude grid areas covering the state of California. There are 4300 of these grid areas each covering an area of about 36 square miles.

(2) Specification of detailed isoseismal patterns in the San Francisco Bay area. Somewhat less than half of the area is land. A total of 3500 grid points were used to cover this land area. One hundred and twenty-nine grid areas represented the 45.4 square mile area of the City of San Francisco. Each grid point represented a one-third of a square mile area. An index of local ground conditions was assigned to each area using a geologic map (Jenkins, 1965).

The purpose of the large grid application was to compare the overall size, shape and isopleth spacing of simulated isoseismal patterns with available information on actual patterns. The small grid application was to determine if the model could produce a realistic pattern over a system of small size grids.

Computed isoseismal patterns were compared with information on observed patterns, when available. Results of the comparisons were encouraging. The model worked equally well for earthquakes of low, moderate and high magnitude.

Figure III-2b is based on a computer printout of the isoseismal pattern associated with the 1906 earthquake. Cross hatching covers the area affected by severe earthshocks. This area stretches along the San Andreas fault zone from extreme Northern California to south of Monterey Bay. Effects of alluvial ground conditions extend the severity contours into the Central Valley of California. The observed isoseismal pattern for the 1906 earthquake based on a map by Richter (1958) is given in Figure III-2c. Although intensities were measured on a different scale (Rossi-Forel), shapes of the simulated and actual patterns are similar. In both patterns, an extension of severe earthshock intensities extends into the Central Valley. Simulated isoseismal contours for lower intensities are much more irregular in shape than the actual contours--it is not known if smoothness of contours in the "actual" pattern was caused by lack of data or if irregularities in the simulated patterns are physically meaningful.

Actual isoseismal patterns are not available for early earthquakes. However, these patterns can be simulated if one is willing to accept assumptions upon which the model is based. An example is the great earthquake that occurred at Fort Tejon in California on January 9, 1857. The simulated isoseismal pattern is given in Figure III-3. A large area representing extensive structural damage potential surrounds the epicenter. Areas of possible moderate damage extend in pockets from the Imperial Valley northward to near San Francisco. The light damage area extends north to Redding. A reported intensity of VI (Rossi-Forel) is close to a computed V (Modified Mercalli) intensity at Sacramento nearly 175 miles from the epicenter. At Visalia, 60 miles from the epicenter, a reported VIII (Rossi-Forel) is of the same order of magnitude as a simulated VIII (Modified Mercalli). Reported intensities were obtained from information compiled by Townley and Allen (1939).

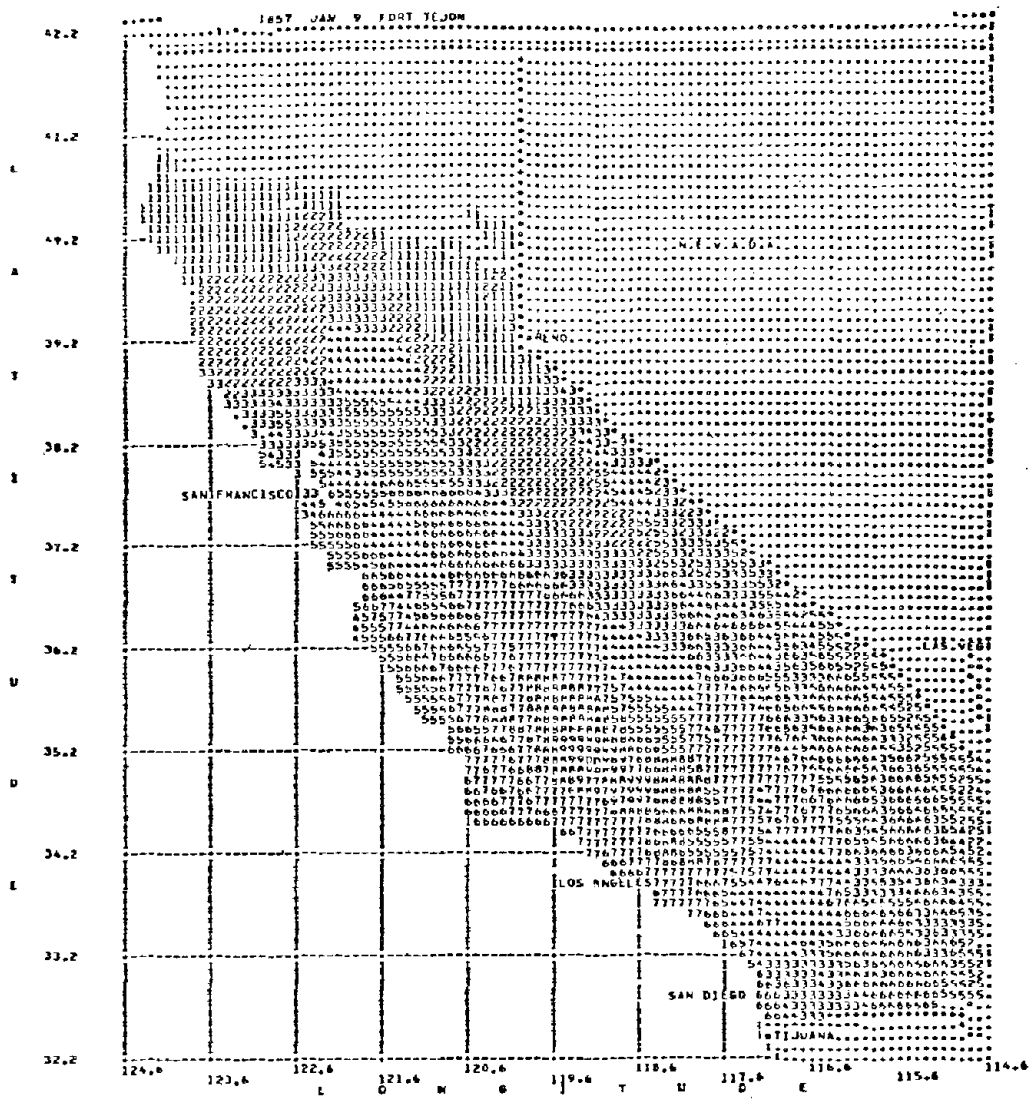

FIGURE III-3

COMPUTED EARTHSHOCK SEVERITY PATTERN OF 1857 FORT TEJON EARTHQUAKE IN SOUTHERN CALIFORNIA

1. Validity of Model

Usefulness of results derived from the earthquake model depends upon how accurately simulated earthshock severities approximate actual intensities for a large number of earthquake occurrences where intensity is measured on the Modified Mercalli scale. Designing a meaningful test of "goodness-of-fit" is a difficult task because actual intensities have generally been reported in the past as a single value for each city, while simulated severities suggest a range of values due to differences in local ground conditions within each city. To provide a rough measure of the degree of correspondence between simulated earthshock severity and actual intensities, a simple comparison has been used.

Of the 80 earthquakes that were simulated on the small grid, actual reported intensity for the City of San Francisco was available on 60 earthquakes. Reported intensities were obtained from Townley and Allen (1939), and U. S. Department of Commerce (1933-1970). A measure of goodness-of-fit was obtained by counting the number of times that reported intensity for the City of San Francisco was within the simulated range (Table III-1).

In 46 of the 60 earthquakes (77%), reported intensity was within the computed range. Note that the percentage of earthquakes in which the reported intensity was within the computed range is greatest when reported intensity is high, that is, when potential for structural damage is greatest. Deviations of reported intensity from the computed range are not as important when the level of intensity is below the threshold value of damage potential. The relationship between reported intensity and computed severity was checked in four other Bay area cities. The results were approximately the same as given in Table III-1 for the City of San Francisco.

On the basis of various comparisons between the computed and actual patterns, it was concluded that the earthquake model could produce realistic synthetic geographical patterns of earthshock severity. The next step was to apply these computed patterns to a population-at-risk. Potential loss resulting from a recurrence of these past earthquakes could then be estimated using vulnerability of the population-at-risk to loss.

TABLE III-1

COMPARISONS OF ACTUAL AND SIMULATED INTENSITIES

Reported intensity in San Francisco (Modified Mercalli)	Number of earthquakes	Number of times reported intensity was within range of simulated severities	Percentage
VII or greater	6	6	100%
VI	8	7	88
V	18	14	78
IV	18	14	78
III or less	10	5	50
	60	46	77%

2. *Population-at-Risk and Its Vulnerability*

The geographical distribution of single unit owner-occupied dwellings in California was defined as the population-at-risk. In the large grid system (individual grid area of about 36 square miles), there were about 625,000 dwellings in the San Francisco Metropolitan area, using 1960 U. S. Bureau of the Census data. The system of small grid areas (individual grid areas of about 1/3 square mile) covered the 45 square mile area of the City of San Francisco. In 1960 there were 110,000 single-unit dwellings within the city limits.

Vulnerability was based upon damage-versus-earthshock severity relationships derived from loss experience to dwellings in the 1957 San Francisco earthquake, the 1952 Kern County earthquake, and the 1933 Long Beach earthquake. No attempt was made, because of lack of data, to classify by type of dwelling construction, such as frame versus brick or the existence of a brick chimney. To give an example of the type of vulnerability relationship used, an earthshock severity of 6 would result in 15% of dwellings in a grid area damaged with a loss of 1% of value-at-risk per damaged dwelling. In addition to the most likely percentage, the ranges of percentage of dwellings damaged and percentage of value lost as related to the level of earthshock severity experience were also used.

The effect of a recurrence of each of the earthquakes that affected San Francisco since 1800 was simulated under these assumptions and the loss potential calculated. Of the 80 moderate or severe earthquakes that affected the San Francisco area in the past 168 years, 54 recurrences would have produced damages in the City of San Francisco and

65 would have caused damages somewhere within Metropolitan San Francisco. In the City of San Francisco, 30 of the 54 damaging earthquakes, when taken together, accounted for only 1% of the total damage. Most damages result from infrequent occurrences of severe earthquakes which are located near enough to densely populated areas to produce a natural disaster.

If losses resulting from the damaging earthquakes are summed and the percentage contribution of each earthquake to the total damage is calculated, a large percentage of the total losses would be attributed to four earthquakes as shown in Table III-2.

TABLE III-2

PERCENTAGE CONTRIBUTION OF THE FOUR MOST DAMAGING EARTHQUAKES TO TOTAL ACCUMULATED DAMAGES FROM THE RECURRENCE OF ALL EARTHQUAKES IN THE 168-YEAR PERIOD

Earthquake	City of San Francisco	Metropolitan San Francisco
1906 San Francisco	44%	33%
1838 San Francisco	24	21
1868 Hayward	12	17
1836 San Francisco Bay	6	13
Total	86%	84%

The four earthquakes account for about 85% of the total simulated damages. If these rare severe earthquakes were spread equally over the past 168 years, one would occur about every 40 years. However, the time interval between occurrences is highly variable. In fact, two of the four earthquakes occurred within two years of one another, and three of the four within a period of 32 years.

Major earthquakes are usually followed by a series of aftershocks with predictable frequency characteristics (Lomnitz, 1966). Locations of the epicenters of aftershocks do not necessarily follow the fault line, but are spread at random in a geographical pattern sometimes at a considerable distance from the original epicenter. Damage can occur from aftershocks because the epicenter of an aftershock may have a great proximity to exposed structures, and structures damaged by the initial shock, if not repaired, may fail during subsequent earthshocks. This happened during the 1952 Kern County earthquake. Aftershock patterns have been simulated in the computer analysis. Allen, *et al.* (1965) points

out the fallacy of attempting to specify the seismic hazard solely on the basis of the location of active faults or past epicenters.

3. Use of Loss Potential Information

Computer-derived loss potential data is applicable to insurance as one of the adjustments to the natural hazards (Friedman, 1969). Insurance is one means of protection against the earthquake hazard. To provide protection, actuaries must find answers to two basic questions:

(1) How much premium should be charged each year to cover long-term average annual earthquake caused losses?

(2) How much of a reserve should be established to cover losses in a year when a major earthquake occurs near a populated area.

To answer these questions, two kinds of information are needed. The first is a measure of extent of the geophysical hazard as given by frequency and magnitude of earthquakes. The second kind is the type, geographical distribution, and susceptibility to damage of structures to be covered by insurance. Information for a long series of years is needed to establish adequately the magnitude of the geophysical hazard. If a short period of years is used, chance occurrence (or non-occurrence) of a strong earthquake within the series of years could highly bias estimates of hazard severity. On the other hand, information on characteristics and vulnerability of structures to be insured must be current. The loss potential data provides some of the background information needed for answering the actuarial questions.

Regarding the first question, the effect of using damage experience derived from a short time interval to estimate the long-term earthquake hazard is shown in Table III-3, which lists the average annual damage-per-dwelling obtained by simulating the recurrence of earthquakes that originally occurred in each of the eight 20-year periods between 1808 and 1967.

TABLE III-3

AVERAGE ANNUAL DAMAGE-PER-DWELLING BASED UPON SIMULATED DAMAGES ASSOCIATED WITH RECURRENCE OF EARTHQUAKES THAT ORIGINALLY OCCURRED IN EACH 20-YEAR PERIOD

20-year period	Dwellings in the City of San Francisco	Dwellings in Metropolitan San Francisco
1948-1967	$ 4.20	$ 2.00
1928-1947	.30	.80
1908-1927	1.60	.70
1888-1907	79.90	38.70
1868-1887	19.00	16.30
1848-1867	10.20	6.30
1828-1847	48.70	32.70
1808-1827	.60	.40
168-year period	$19.70	$11.70

An average annual damage-per-dwelling of $4.20 is indicated if simulated damages associated with recurrence of earthquakes that were recorded between 1948 and 1967 are assumed to be a measure of the long-term earthquake hazard to dwelling properties. For dwellings spread throughout the San Francisco area, the average annual damage based upon the same 20-year period was $2.00. Possible reasons for the lower damage rate in Metropolitan San Francisco are:

(1) Geographical spread of exposed structures reduces the average annual damage.

(2) Difference between effects of using an index of local ground condition to represent a 36 square-mile grid and use of an index for each 1/3 square-mile grid area.

(3) The earthquake risk is greater in the City of San Francisco.

In the City of San Francisco, the average annual damage varies from 30¢ per dwelling on one 20-year period to $80 per dwelling in another 20-year period. The average annual damage in Metropolitan San Francisco based on 20-year averages, ranges from between 40¢ and nearly $40 per dwelling. As mentioned previously, chance occurrence (or non-occurrence) of a severe earthquake can highly bias estimates of the long-term earthquake hazard to dwelling properties, using small samples of years.

The long-term average annual damage-per-dwelling based upon the 168-year period (1800-1968) is $19.70 in the City of San Francisco and $11.70 in Metropolitan San Francisco. An estimate of the magnitude of the earthquake hazard using the period from 1928 to 1947 would have *underestimated* the long-term expected damage by a multiple of 60 in the City of San Francisco. If the period from 1888 to 1907 had been used, the long-term expected damage would have been *overestimated* by a multiple of four. This extreme variability emphasizes the need to use a long period of years for estimating magnitude of the earthquake hazard. The simulation approach provides a means of translating a long record of seismological data (earthquake location and intensity) into a measure of hazard in an insurance context.

Random rearrangements of year of occurrence of the 80 earthquakes during the 160-year period could produce 20-year averages which are much above, equal to, or much below the long-term average. Simulation techniques can assist in estimating the long-term annual damage by providing long series of damage "experience," based upon various possible sequenced combinations of earthquakes that occurred in the historical past (frequency alternative number one discussed in a previous section) or possible future sequences based on a time and space memory (frequency alternative number three).

Regarding question number two, if actual damages each year exactly equaled the average long-term expected damages, estimation of long-term average damage would be the only requirement. However, for geophysical hazards in general and the earthquake hazard in particular, annual damages vary widely from year to year. For an insurance operation, measures of both *average* and annual *variability* of loss are needed.

The concentration of damages to a few infrequently occurring events gives critical importance to the insurance reserve problem. When the rare but severe earthquake occurs near a populated area, actual damages can exceed the average annual damage by many times. Average damage-per-dwelling associated with the four most severe earthquakes in the historical past in the San Francisco area is expressed in Table III-4 as a multiple of average annual damage-per-dwelling. An amount 73 times larger than the average annual damage-per-dwelling would have been required to cover losses associated with a single event--the 1906 earthquake. In other words, it would have taken 73 years of annual average damage-per-dwelling to cover losses from a single occurrence if a proper

estimate of the long-term average annual loss were available. However, if the magnitude of the hazard had been estimated from damage experience of the most recent 20-year period, the 1906 earthquake would have caused losses 339 times the estimated annual damage-per-dwelling.

TABLE III-4

DAMAGE-PER-DWELLING IN NATURAL DISASTERS AS A MULTIPLE OF AVERAGE ANNUAL DAMAGE-PER-DWELLING BASED ON ALL EARTHQUAKES IN SAN FRANCISCO

Recurrence of earthquake of comparable intensity	City of San Francisco (110,000 dwellings in detailed grid)		Metropolitan San Francisco (625,000 dwellings in large grid)	
	168-year average	20-year average	168-year average	20-year average
1906	73 times	339 times	56 times	326 times
1838	40	184	35	202
1868	19	90	28	163
1836	10	45	21	126

Measures of both annual average damage and annual variability in damages are needed in risk evaluation involving rate and reserve calculations. Examples of other factors needed are (1) effect of taxation on the accumulation of a reserve over a number of years, and (2) effect of inflation on structure value and cost of repair in future earthquakes. These factors can be built into the computer program to study characteristics of an insurance operation needed to cover the earthquake hazard.

Catastrophe Potential of Los Angeles Earthquakes

Natural hazard simulation has been utilized as one means of determining the present level and future trend of natural hazard losses in the United States for various mixes of adjustments (White and Haas, 1975). Loss potential to a number of different populations-at-risk has been calculated for various hazards, including earthquakes. The purpose of the application to the earthquake hazard was to determine if there was sufficient information currently available which could be synthesized by simulation techniques to produce useful estimates of loss potential. If results indicated that currently available information was not sufficient, a secondary purpose was to outline research and data needed eventually to produce more realistic loss indicators.

For this application, the original earthquake model was used to estimate the loss potential to a number of different populations-at-risk from a recurrence of each of the moderate and severe earthquakes that were reported to have affected the greater Los Angeles area in the past 200 years. The impact of hypothetical earthquakes was also calculated. Methods of evaluating the effect of possible future sequences of earthquakes were then reviewed. Population-at-risk was defined in terms of:

(1) Single unit residential buildings
(2) Other residential buildings
(3) Non-residential buildings
(4) High-rise buildings
(5) Population

An estimate of the vulnerability of buildings to earthquake-induced damage was obtained from damage experience of the 1971 San Fernando earthquake. Casualty curves were based in part upon relationships presented in the San Francisco and Los Angeles studies by NOAA (1972, 1973). Results of the analysis were expressed in terms of loss potential given either as an absolute measure (number of buildings affected) or as a relative measure (ratio of losses for a particular earthquake to losses associated with the most severe earthquake). The following sections outline the assumptions underlying the applications, the results of the analysis, and informational needs to produce a more realistic estimate.

1. Generation of Severity Patterns

Appendix B contains a listing of moderate or severe earthquakes (estimated to have been of magnitude 5 or greater on the Richter Scale) that affected the Los Angeles area in the past 200 years. This tabulation is based upon data in Table I of the NOAA's Los Angeles report (1973). Forty-two earthquakes are listed. Two additional earthquakes of an estimated 4.8 Richter magnitude were included for comparative purposes.

Epicenter location, Richter magnitude, fault type and orientation, and hypocenter depth were used to denote the physical properties of each earthquake. A depth of 10 kilometers was used for those past earthquakes that do not have an estimated depth. The size of the "felt area" was taken as a proxy measure of depth for several of the earthquakes for which observed isoseismal patterns were available.

Comparisons were made between the computed and observed earthshock severity patterns whenever possible. An example of these patterns

is given in Figure III-4 for the most recent highly damaging California earthquake--the 1971 San Fernando earthquake. Note that in this case we have restricted the simulation to the California grid points.

Although relatively smooth contours were drawn in the earlier versions of the observed isoseismal patterns published in United States Earthquakes (U. S. Department of Commerce, 1933-1970), including the San Fernando earthquake, improved techniques for plotting observed isoseismal patterns of very recent earthquakes imply a much greater local variation in Modified Mercalli intensity than was suggested in the early smooth contoured versions of these patterns. An illustration of the new plotting routine is shown in Figure III-5a which represents the observed isoseismal pattern associated with the Point Mugu earthquake of February 21, 1973 (U. S. Department of Commerce, 1973). The computed pattern of the 5.7 magnitude earthquake is given in Figure III-5b. Large local variations in the earthshock severity pattern are also characteristic of the calculated pattern.

2. Reasonableness of Calculated Patterns

Modified Mercalli intensity observed in downtown Los Angeles is available for 24 of the 44 earthquakes in NOAA's Los Angeles report. Table III-5 provides a comparison between these observed and calculated values for downtown Los Angeles.

TABLE III-5

COMPUTED EARTHSHOCK SEVERITY VERSUS OBSERVED MODIFIED MERCALLI INTENSITY IN DOWNTOWN LOS ANGELES FOR 24 PAST EARTHQUAKES

		Computed Earthshock Severity							
		1	2	3	4	5	6	7	8
Observed Modified Mercalli Intensity	I	0	0	0	0	0	0	0	0
	II	0	0	0	0	0	0	0	0
	III	0	0	1	1	1	0	0	0
	IV	0	1	2	1	0	0	0	0
	V	0	0	1	0	3	1	0	0
	VI	0	0	0	0	1	7	0	0
	VII	0	0	0	0	0	1	3	0
	VIII	0	0	0	0	0	0	0	0

FIGURE III-4

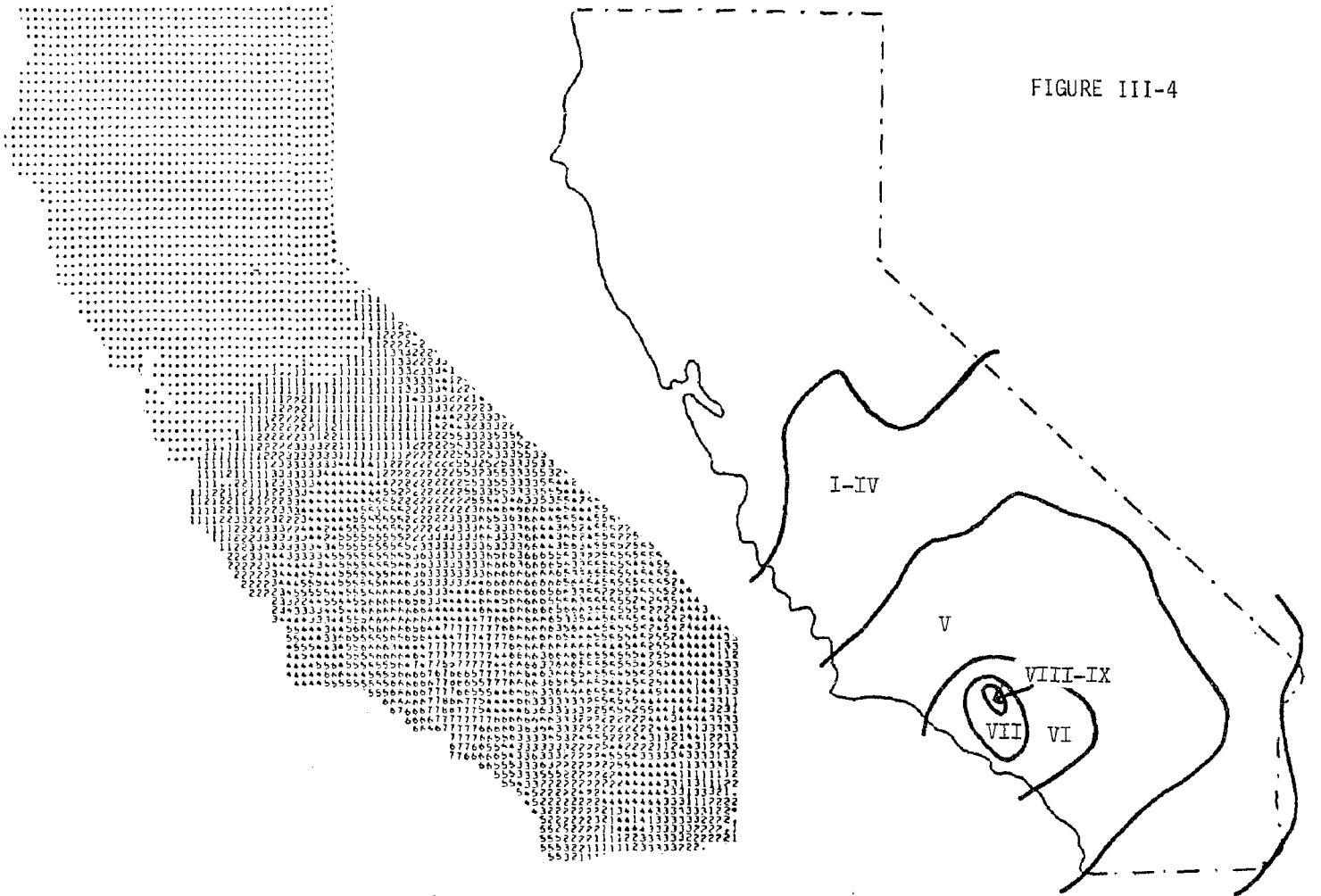

a. Computed earthshock pattern.

b. Observed modified Mercalli pattern.

COMPUTED EARTHSHOCK SEVERITY PATTERN OF THE 1971 SAN FERNANDO EARTHQUAKE COMPARED WITH THE OBSERVED PATTERN

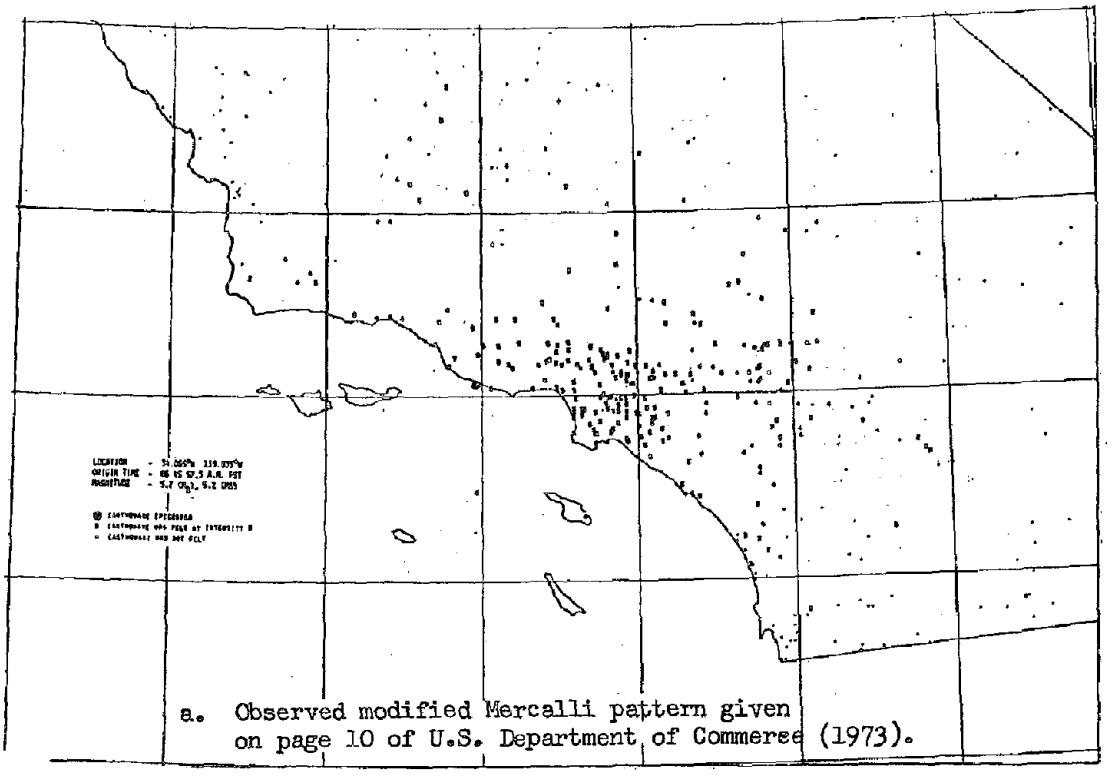

a. Observed modified Mercalli pattern given on page 10 of U.S. Department of Commerce (1973).

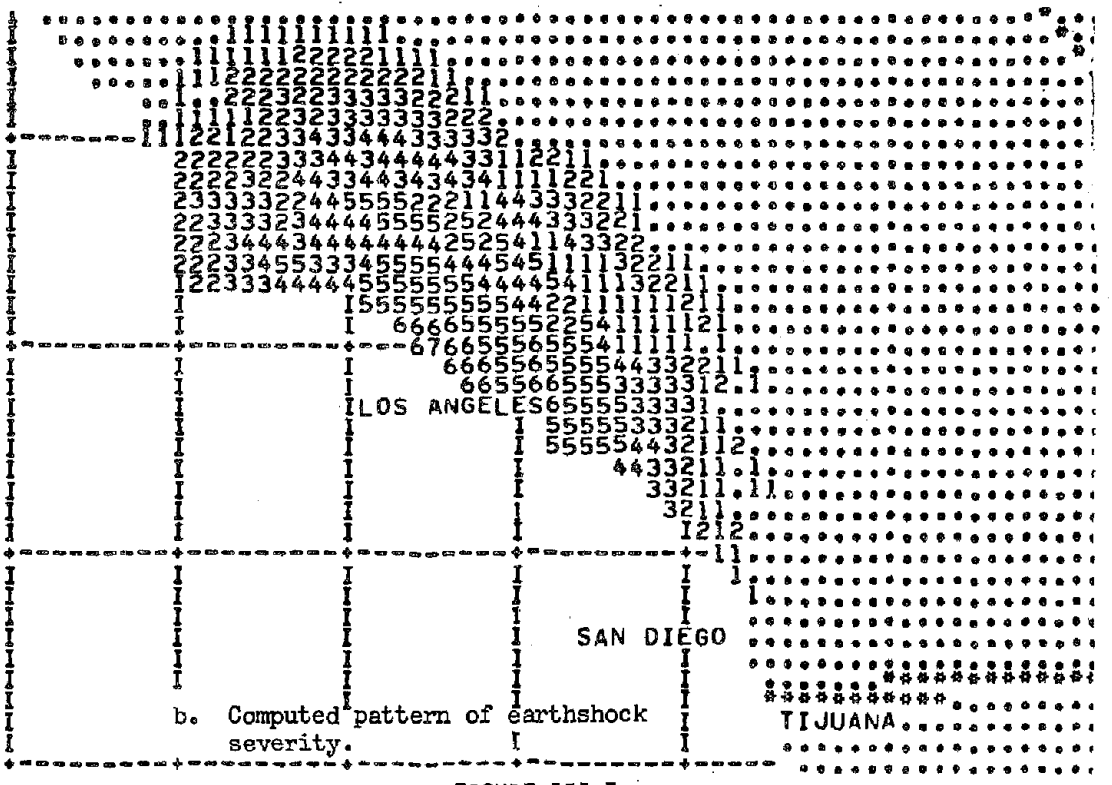

b. Computed pattern of earthshock severity.

FIGURE III-5

OBSERVED AND COMPUTED GEOGRAPHICAL PATTERNS OF EARTHSHOCK SEVERITY CAUSED BY THE POINT MUGU, CALIFORNIA, EARTHQUAKE OF FEBRUARY 21, 1973

In 64% of the cases, the computed severity equalled the observed Modified Mercalli intensity. In 88% of the cases, the computed severity was within plus or minus one unit of the observed intensity. The closeness-of-fit is roughly comparable to that given in Table III-1 for San Francisco earthquakes and indicates the level of inherent consistencies among earthquake severity patterns approximated by the generating model. These consistencies in size, shape, and gradient of the severity pattern for various combinations of earthquake location, magnitude, fault orientation and hypocenter depth do provide some information through the use of a simple model in specifying the character of the earthshock severity pattern as it is defined in this study. The question is whether the unique qualities of each earthquake, which prevent a completely deterministic specification of the severity pattern, are large enough to negate the usefulness of the model's output.

The closeness-of-fit illustrated in Tables III-1 and III-5 is not good enough to be used by an earthquake engineer in the analysis of a specific building at a given site. However, when loss potential is based upon the overlapping of the irregularly shaped geographical pattern of earthshock severity with the geographical array of population-at-risk spread haphazardly over an area of hundreds of square miles, the possibility of obtaining a deterministic solution is very small and the need to resort to a statistical approach is great. This is the reason why simulation techniques have been applied. There are too many unknowns and possible unanticipated interrelationships to use anything but statistical methods. Consequently, the estimation of loss potential must be based upon the integrated effect of a number of earthquakes, rather than on the loss-producing characteristics of any one earthquake in the sample. Deviations around the most likely value are measurable if a large group of earthquakes is considered. Not much significance should be assigned to the results from any one earthquake taken from the sampled sequence.

Even though local ground conditions measured from a geologic map have been shown recently to have very little explicit physical basis, the incorporation of the local condition index does contribute additional information to the earthshock severity pattern over that given by a bedrock pattern. The patterns based upon the inclusion of local ground conditions are much closer in shape, size and gradient to observed patterns than are those obtained using the bedrock patterns.

3. Population-at-Risk

A number of different populations-at-risk were considered in the analysis for Los Angeles earthquakes.

a. Single unit residential buildings:

The number and geographical distribution of single unit residential buildings are approximated by the allocation of 4,700,000 buildings in the 1970 U. S. Census to the 4300 grid areas in computer memory representing the land area of California. The median value of dwellings by county was also allocated to each area.

b. Other residential buildings:

All buildings used primarily for housing purposes and containing two or more housing units were classed as "other residential buildings." Special tapes of the U. S. Bureau of the Census contain information on these buildings, but these data were not available in a hard-copy format. For the purposes of this test application, an estimate of the number of such buildings was obtained using the estimated population and single-unit dwellings in each grid area. The population was converted into an index of the number of households. The difference between households and single-unit dwellings is a measure of the number of housing units needed in addition to the use of single-unit dwellings. Division by the average number of units in each building provides an index of the number of other residential structures in the grid area.

c. Non-residential Buildings:

An inventory of the number, type and geographical distribution of non-residential buildings is not available for California. To provide an index by grid area, several assumptions were made. The first assumption is that there is a rough relationship between the population of a town or city and the number of non-residential buildings in that town or city. Secondly, that the ratio of the number of these buildings to population varies with size of the city. A reference level was established by the use of the estimate of 2,000,000 structures in Los Angeles county made by the Office of the Assessor (1973). The 1970 U. S. Census listed 1,550,000 single family dwellings in the county. The difference (450,000) represents the non-residential buildings. The ratio of non-residential buildings with population (7,000,000) yields a ratio of 64 buildings per 1000 population.

To obtain an estimate of the change in this ratio with population size, the number of reporting units listed in the County Business Patterns (U. S. Department of Commerce, 1972) for each California county was plotted against county population. A close fitting non-linear trend was obtained. By assuming that a rough correspondence exists between number of reporting units and number of non-residential buildings in an area, an estimate of the change in ratio with population size was obtained. For example, for a population of 500, 31 buildings are assigned to the grid area (6.2%); for 1000 persons, 60 buildings (6.0%); and for 10,000 persons, 570 buildings (5.7%).

d. High-rise buildings:

An inventory of the number and geographical distribution of high-rise buildings in California was not available. However, a summary of the information gathered on high-rise buildings in the Los Angeles and San Francisco areas during the recent NOAA studies is given in Appendix C. The results of an independent inventory of high-rise buildings in Los Angeles county by Whitman, *et al.* (1973) is also given in Appendix C. By combining this information with estimates of building numbers, an approximate indication of the height distribution of California buildings is obtained.

Building Height	Number per 100,000 buildings
1-3 story	98,500
4-7 story	1,308
8-11 story	134
12-15 story	33
16-19 story	12
20 or more stories	13

The population-at-risk of high-rise buildings exposed to Los Angeles earthquakes was defined in terms of the Whitman survey data for Los Angeles county, and in terms of this height distribution for buildings in general throughout the state of California.

e. Population

The 20,000,000 persons in California allocated to the 4300 grid areas in computer memory defines the geographical distribution of this population-at-risk.

4. Vulnerability of Population-at-Risk

Vulnerability of buildings in the three broad categories was derived from damage experience resulting from the 1971 San Fernando earthquake (Steinbrugge, *et al.*, 1971). Table III-6 outlines these relationships.

TABLE III-6

VULNERABILITY OF BUILDINGS TO DAMAGE WHEN AN EARTHSHOCK OF SPECIFIED SEVERITY OCCURS

Earthshock Severity	Most Likely Percentage of Buildings Affected in a Grid Area: Single-Unit Residential	Other Residential	Non-Residential
5	3.3%	5.3%	3.9%
6	5.4	8.8	6.6
7	8.2	13.0	10.0
8	11.6	18.5	14.5
9	16.0	25.0	20.5
10	21.4	33.0	28.2

Earthshock Severity	Most Likely Amount of Damage (1971 Dollars) If Building is One of Those Affected in Grid Area: Single-Unit Residential	Other Residential	Non-Residential
5	$ 30	$ 100	$ 2
6	110	540	10
7	380	2,400	200
8	1,070	8,800	2,500
9	2,600	27,000	14,000
10	5,800	76,000	105,000

In this test application only the most likely values were used. The range of possible numbers of buildings affected and amounts of damage, which increases with the degree of earthshock severity, was not incorporated into the analysis.

Vulnerability of high-rise buildings in Los Angeles county to earthquake damage has been examined in detail by Whitman in terms of a number of different building characteristics. For this application, the buildings were grouped into two categories depending upon year of construction--pre-1933 and post-1933. Table III-7 gives an approximation of Whitman's mean damage ratio for these two categories.

TABLE III-7

APPROXIMATION OF THE MEAN DAMAGE RATIO FOR HIGH-RISE BUILDINGS FIVE STORIES OR ABOVE BASED ON YEAR OF CONSTRUCTION (Whitman, *et al.*, 1973)

Earthshock Severity	Pre-1933 Construction	Post-1933 Construction
6	.00045	.00032
7	.02000	.00700
8	.21000	.09100
9	.50000	.28000
10	1.00000	.64000

The number of casualties was related directly to size of population exposed. The casualty rate varied from 1 per 100,000 persons exposed to an earthshock severity of 5, to 1 per 1000 persons when the severity is at level 10. For this test application, no attempt was made to include the effect of other pertinent factors such as time of day of the earthquake occurrence.

5. Simulated Loss Potential

Earthshock severity patterns have been computed for each of the 44 earthquakes listed in Appendix B. The mathematical overlapping of these patterns with the geographical array of the populations-at-risk provides three measures of loss potential--number exposed, number affected and damage index. Appendix D is a tabulation of the loss potential indices for the various populations-at-risk resulting from a simulated recurrence of these earthquakes. Figure III-6 is a map of the numbered epicenter locations of these earthquakes.

a. Single Unit Residential Buildings

In Appendix D-1 the "number exposed" refers to the number of single-unit residential buildings in California that were exposed to an earthshock severity of at least 4.5 (moderate earthshocks) during the simulated earthquake. There are a total of about 4,700,000 of these buildings in California. Nearly 80% of these dwellings would be exposed to moderate earthshocks during a recurrence of the 1857 Fort Tejon earthquake. Of these exposed dwellings, 275,000 would have been affected (damaged) to some degree using the vulnerability relationship previously

FIGURE III-6

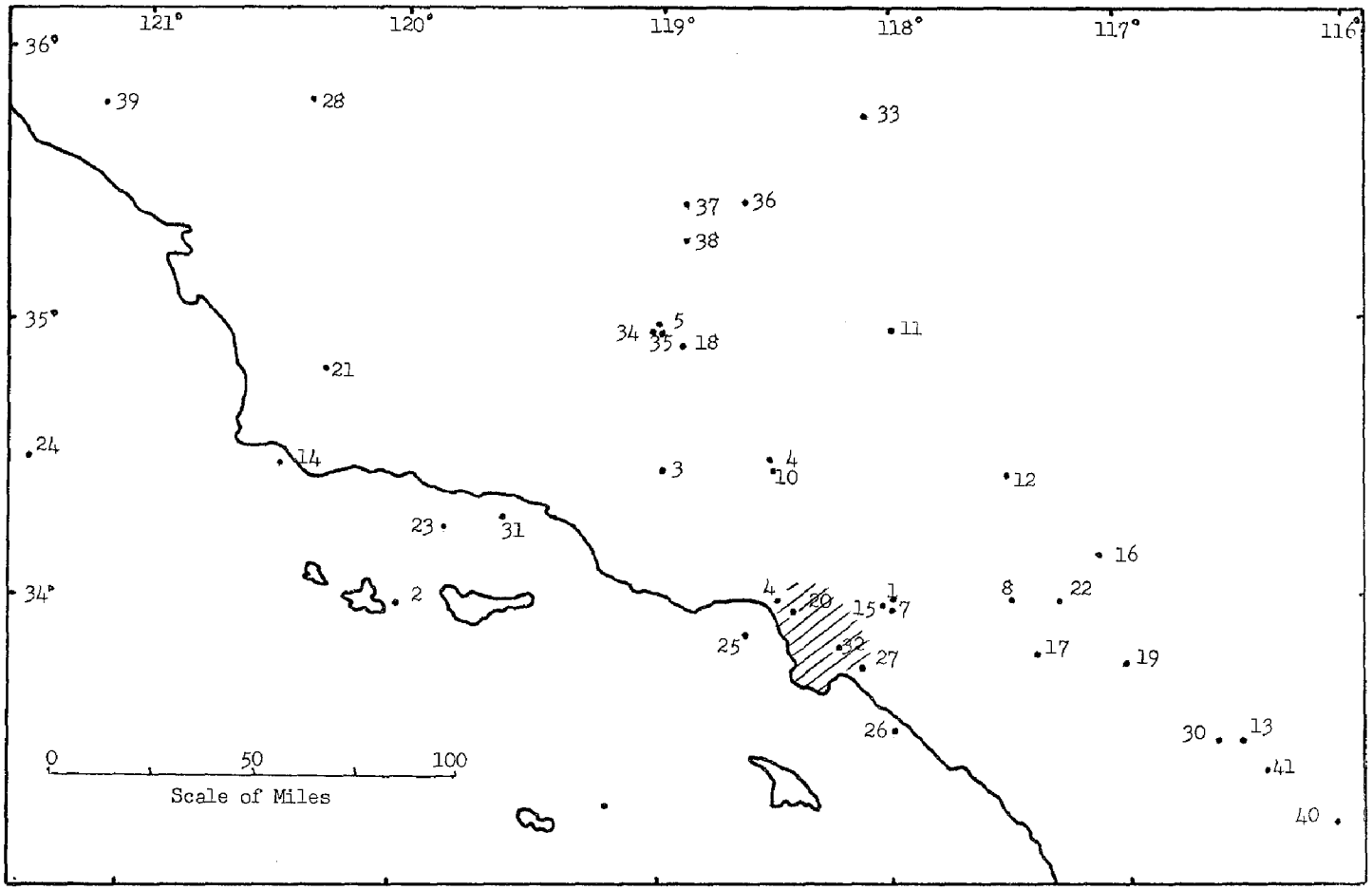

EPICENTER LOCATION OF EARTHQUAKES LISTED IN APPENDIX B. EPICENTER LOCATIONS OF EARTHQUAKES NUMBERED 6, 9 AND 29 ARE OFF THE MAP

discussed. The greatest damage from any of the 44 earthquakes would have resulted from the 1857 Fort Tejon earthquake. A damage index can be constructed by relating losses due to other earthquakes relative to those resulting from the 1857 earthquake. The earthquakes are listed by the size of this damage index.

None of the three measures of loss potential is directly related to the magnitude of the earthquake or the distance of its epicenter from the center of the densely populated Los Angeles area. In addition, a plot of each of the loss potential indices against a combination of earthquake magnitude and distance does not yield a clearly defined relationship. Direction and orientation of the earthquake relative to the irregularly shaped population density pattern in southern California must also be incorporated. Distance is measured in miles from the earthquake's epicenter to downtown Los Angeles.

Only three of the 44 earthquakes have an index of 500 or more (damages equal to 1/2 or more of damages resulting from the Fort Tejon earthquake). At the other extreme, 30 of the 44 earthquakes have a damage index of less than 100 (less than 10% of the damages induced by the Fort Tejon earthquake). In 32 of the earthquakes, more than 1,000,000 single-unit residential buildings would be exposed to moderate earthshocks. However, the number damaged and the amount of loss in most cases would be minimal.

The magnitude of the damage index decreases more rapidly than the number of exposed dwellings. The reason is that because the vulnerability relationships are non-linear, the number of dwellings exposed to moderately severe and severe earthquakes has a great effect upon the size of the damage index. Appendix D-2 provides a breakdown of number of dwellings exposed to various earthshock severity categories which shows the close relationship between exposure of dwellings to higher earthshock severities and the overall magnitude of the damage index.

b. Other Residential Buildings

Appendix D-3 represents synthetic damage experience to "other residential" buildings resulting from a recurrence of each of the 44 earthquakes. A damage index was constructed in the same manner as that for the single-unit residential buildings. The damage index drops off more rapidly than with single-unit dwellings. Thirty-four of the earthquakes had an index of less than 100 (less than 10% of the damage resulting from the

1857 Fort Tejon earthquake). The reason is that the vulnerability relationship is more sensitive to high values of earthshock severity and less sensitive to moderate severities.

c. Non-residential Buildings

Appendix D-4 contains simulated damage experience for non-residential buildings in California resulting from a recurrence of each of the 44 earthquakes. The damage potential for these structures is not the same as for residential buildings because of the geographical distribution of the buildings and because of differences in the vulnerability relationships. Non-residential buildings are assumed to be unaffected by moderate or moderately severe earthshocks. As earthshocks become severe, the amount of damage increases very rapidly.

In only six earthquakes are damages greater than 10% of the 1857 Fort Tejon losses. Twenty-six earthquakes have a potential loss less than 1% of the Fort Tejon earthquake damages. A large number of non-residential buildings would be exposed to earthshocks of at least moderate severity during a recurrence of the earthquakes. However, the earthshocks would be of sufficient severity to produce significant damage in only a few of these earthquakes.

d. High-rise Buildings

Aggregate replacement cost (millions of dollars) of high-rise buildings located in each grid area was used to represent the geographic distribution of this population-at-risk in Los Angeles county. The earthshock pattern of the simulated earthquake produced a level of severity in each affected grid area which was converted into a measure of Whitman's mean damage ratio. This damage ratio (as a percentage factor) was applied to the replacement cost to obtain the potential damage by grid area. Replacement costs and damage ratios were calculated separately for buildings with a pre-1933 and post-1933 construction date.

The accumulated potential damages over the affected grid areas in Los Angeles county for each earthquake are listed in Appendix D-5. As with the other populations-at-risk, a recurrence of the 1857 Fort Tejon earthquake would produce the greatest amount of loss. Thirty-eight of the earthquakes would have caused damages of less than 10% of the Fort Tejon losses, including 29 of these earthquakes with losses of less than 1% of the 1857 earthquake's potential damages.

The information in Appendix D-5 represents damage experience to high-rise buildings in Los Angeles County only. To obtain a very rough estimate of the number of high-rise buildings in California exposed to an earthshock severity of 4.5 or more during a recurrence of the 44 earthquakes, height distribution factors previously discussed were applied to the number of non-residential exposed buildings listed in Appendix D-4. In five earthquakes, at least 1000 high-rise buildings of eight stories or more would have been exposed:

Earthquake Number	Year	Number of High-Rise Buildings Exposed
5	1857	1590
1	1769	1480
2	1812	1130
44	1971	1080
34	1952	1050

At the other end of the scale, in 11 of the 44 earthquakes, less than 500 high-rise buildings would be exposed.

e. Population

The casualty experience associated with a recurrence of the 44 earthquakes is given in Appendix D-6. Casualty potential is expressed by an absolute index (number of persons exposed to an earthshock of 4.5 or more) and a relative index (casualty index is based on a simple non-linear relationship between number of persons exposed to various earthshock categories and the resulting number of casualties). Appendix D-7 illustrates how population exposure to higher earthshock severities greatly affects the size of the casualty index. Note that even though the number of persons exposed during a recurrence of the 1812 earthquake (11,500,000 people) is less than the number exposed during a recurrence of the 1872 earthquake (11,800,000 people), the casualty index of the 1812 earthquake (753) is nearly twice as large as the index for the 1872 earthquake (381). The reason is the relative numbers of persons exposed to very high earthshock severities.

Catastrophe Potential of Hypothetical California Earthquakes

Loss potential based upon some sets of assumptions regarding a recurrence of past earthquakes has been presented for illustrative purposes. The probability of a recurrence of the 44 earthquakes with exactly the same magnitude and location in the next 200 years is very small. A simple extrapolation of past events is a poor measure of future occurrences.

Methods of generating possible sequences of future earthquakes have been discussed by Lomnitz (1974) and Friedman (1973).

One method of examining the catastrophe potential of future earthquakes is to specify the physical characteristics of hypothetical earthquakes (magnitude, epicenter location); to calculate the economic and sociological effects as given by loss or catastrophe potential; and to assign a probability of occurrence to the results. Characteristics of the hypothetical earthquakes can be assigned even though a comparable event has not occurred in the recorded past.

An example of the use of natural hazard simulation in following this approach is obtained by referring to Figure III-7, which is a map giving the epicenter location of 11 simulated earthquakes. The epicenters of these earthquakes were placed at equidistant intervals along the major fault zones in California and Nevada. Nine of the locations are along the San Andreas fault zone. By holding the epicenter location and other physical characteristics of these earthquakes constant, the effect of earthquake magnitude upon loss potential can be shown. Earthquakes of three magnitudes (6, 7, 8 on the Richter Scale) were simulated at each of the 11 locations and the loss potential to four populations-at-risk in California was examined. Possible length of the fault break was considered in setting the location and magnitude of these earthquakes.

Results of the analysis are given in Appendix E. Appendix E-1 is a listing of the loss potential to single unit residential buildings measured by an absolute index (number of buildings exposed to an earthshock severity of at least 4.5) and a relative index (damage index of the amount of damage for a particular earthquake relative to losses of the most damaging earthquake). Of the 4,700,000 dwellings in California, over 4,100,000 would be exposed to moderate earthshocks by a Richter magnitude 8 earthquake located on the San Andreas fault near Salinas, California. However, the potentially most damaging magnitude 8 earthquake would occur somewhere along the San Andreas fault zone to the north, northeast or east of Los Angeles. A magnitude 8 earthquake at location 6 near Gorman, California, would produce the greatest amount of damage to dwellings in California under assumptions on which this study is based. The epicenter location of the 1857 Fort Tejon earthquake is near Gorman. The simulated earthquake of comparable magnitude at location 7 near San Bernardino produces a damage index nearly as large as the Gorman index. A location halfway between locations 6 and 7 was used. The damage index at this

FIGURE III-7

EPICENTER LOCATIONS OF HYPOTHETICAL EARTHQUAKES LISTED IN APPENDIX E

point was lower than at locations 6 or 7 because of the sparcity of population-at-risk in the immediate vicinity of the epicenter.

The catastrophe potential of Richter 8 earthquakes is much lower for other epicenter locations. An epicenter near San Francisco yields a damage index of about one-half as much as an epicenter near Los Angeles. It should be noted that one of the underlying assumptions is that the vulnerability of single-unit residential buildings is the same throughout California. No account has been taken of possible regional differences in age, type and quality of construction which could have an effect upon damage susceptibility of these buildings when an earthshock of a given severity occurs.

The great sensitivity of the loss potential indices to changes in the magnitude of the earthquake is illustrated by comparing the number of dwellings exposed and damage index of a Richter 6 and 7 earthquake with that of a Richter 8 earthquake. The damage index decreases by a factor of about 7 for a Richter 7 earthquake at Gorman, as compared with that of a Richter 8 earthquake. The damage index is reduced by a factor of over 50 when the damage potential of a Richter 6 earthquake is compared with that of a Richter 8 earthquake at Gorman, California.

The relative size of the damage index between locations also changes as the magnitude of the earthquake is decreased. For instance, a Richter 8 earthquake at San Bernardino produces an index of 97, compared to an index of 100 at Gorman. For a Richter 6 earthquake, the relative size reverses (2.7 at San Bernardino, compared to 1.8 at Gorman). The reversal occurs because of proximity of a large population-at-risk near San Bernardino which can be affected by the smaller localized severity pattern of a magnitude 6 earthquake. Gorman is in a mountainous area with a very small local population-at-risk.

The loss potential index based on the number of dwellings exposed to at least moderate earthshocks is less sensitive to changes in earthquake magnitude. With an epicenter at Gorman, the number of dwellings exposed decreases from about 4,000,000 for a Richter 8 earthquake, to 2,700,000 for a Richter 7 event. The number of dwellings exposed decreases by a factor of 2 when magnitude is changed from Richter 8 to Richter 6.

Appendix E-2 provides the same type of loss potential information for the other residential buildings. Results for this category of buildings track closely with those for single-unit residential buildings. However, the sensitivity of the damage index of these structures to

changes in earthquake magnitude is greater than for single-unit dwellings because of differences in the vulnerability assumptions.

Appendix E-3 lists the loss potential for non-residential buildings. The most damaging earthquake shifts from location 6 (Gorman) for residential buildings to location 7 (San Bernardino) for non-residential buildings. The damage index is two times as large for an earthquake located at San Bernardino, as compared with the index for Gorman, and five times as large for San Bernardino, than for an earthquake located near San Francisco. It is extremely sensitive to changes in earthquake magnitude. At San Bernardino the index decreases by a factor of over 30 when magnitude is changed from Richter 8 to Richter 7. The factor increases to over 100 when magnitude is decreased from Richter 8 to 6. As mentioned previously, buildings in this broad category are assumed to be relatively insensitive to moderate earthshocks, but are highly vulnerable to severe earthshocks. The loss index based upon "number of buildings exposed" for non-residential buildings follows the pattern for residential buildings.

Calculations of loss potential for high-rise buildings were not made for earthquakes depicted in Figure III-7. However, height distribution factors were applied to the number of non-residential buildings exposed which are given in Appendix E-3. The number of high-rise buildings (eight stories or more) exposed to an earthshock severity of 4.5 was estimated for each earthquake. In Table III-8 these numbers are expressed as percentage of the total number of high-rise buildings (eight stories or more) in California. It is assumed that there are slightly more than 1900 of these buildings.

It is not known if the percentages of high-rise exposed structures given in Table III-8 are realistic. The percentages are listed merely to illustrate the fact that high magnitude, distant earthquakes can affect a large percentage of the high-rise buildings in area the size of California. In establishing the height distribution factors used in constructing this table, recognition was given to the facts that the size and age of a city has an effect upon the height distribution of buildings in the city, and that the large number of high-rise buildings concentrated in large metropolitan areas such as Los Angeles and San Francisco service not only the City of Los Angeles and the City of San Francisco, but also populations in a wide surrounding territory (Appendix C).

TABLE III-8

PERCENTAGE OF THE TOTAL NUMBER OF HIGH-RISE BUILDINGS IN CALIFORNIA THAT ARE EXPOSED TO AN EARTHSHOCK SEVERITY OF 4.5 OR MORE DURING EACH OF A SERIES OF SIMULATED EARTHQUAKES; EPICENTER LOCATION SHOWN IN FIGURE III-7

	PERCENTAGE OF TOTAL CALIFORNIA HIGH-RISE BUILDINGS		
Epicenter Location	Richter 8 Earthquake	Richter 7 Earthquake	Richter 6 Earthquake
1	30%	9%	< 1%
2	37	27	5
3	71	32	21
4	91	32	15
5	90	64	5
6	89	61	44
7	81	59	43
8	61	46	1
9	52	8	< 1
10	64	44	< 1
11	49	< 1	0

Appendix E-4 illustrates the casualty potential of the simulated earthquakes. Nearly 17,600,000 of the 20,000,000 persons in California would be exposed to moderate earthshocks from a Richter 8 earthquake centered near Salinas, California. However, the highest casualty count would occur (of the earthquakes that are considered) when the epicenter is near Gorman. The casualty factor is reduced by a factor of 4 with a Gorman epicenter when magnitude is reduced from Richter 8 to 7. The reduction factor is about 20 when the magnitude is reduced from Richter 8 to 6. The "number of persons exposed" index follows the pattern for residential and non-residential buildings.

1. Production of a Natural Disaster

A natural disaster is produced when the severity pattern of a geophysical event overlaps and adversely affects a large segment of the exposed population-at-risk. The number of casualties and the total amount of damages required to create a natural disaster are not clearly defined. For property insurance, a "catastrophe code" is assigned to losses resulting from an event when aggregate insured losses from the event exceed $1 million. Because of the effect of the increased density of population-at-risk in hazardous areas and the inflationary trend in claim costs, the

annual number of events that qualify as catastrophes has increased rapidly from year to year even though there is no indication that the frequency and severity of geophysical events has changed. Figure III-8a shows this upward trend in number of catastrophes over the past 25 years.

An illustration of the probable changes over time in the percentage of the potentially damaging geophysical events that become natural disasters is shown in Figure III-8b. As density and geographical spread of the population-at-risk increases, the number of events that result in a natural disaster also increases. In the extreme case, where the maximum possible density of a vulnerable population-at-risk exists, the number of natural disasters (realized damages) equals the number of (potentially damaging) geophysical events.

To provide an order-of-magnitude estimate of the current percentage of potentially damaging earthquakes near Los Angeles which could become natural disasters, a count was made of the number of past Los Angeles area earthquakes that produced a sizable amount of damage to one of the populations-at-risk. In this case, if simulated damages to current single-unit residential buildings was $20 million or more, that event was called a natural disaster. In practice, the definition of a natural disaster appears to be a complicated combination of number of casualties and aggregate damage from an array of populations-at-risk. Eleven of the 44 past earthquakes exceeded the $20 million limit. If a natural disaster were defined in this manner the return period of earthquake-caused disasters near Los Angeles would be about once every 18 years (11 events in 200 years).

A supplement to this estimate of frequency is an indication of how the severity of a natural disaster is dependent upon earthquake magnitude, when the epicenter location is held constant relative to the geographical distribution of population-at-risk. The epicenter of the 1920 Englewood, California, earthquake was chosen because it is near the center of metropolitan Los Angeles. The original earthquake had a magnitude of 5.0 on the Richter Scale and caused a considerable amount of damage to the 1920 populations-at-risk. Five earthquakes were simulated at 0.5 increments on the Richter Scale between 5.5 and 7.5. Simulated damages to single-unit residential buildings were $10 million for a 5.5 Richter Scale earthquake. Damage multiples of the earthquakes for various populations-at-risk relative to the 5.5 Richter Scale earthquake were obtained. For instance, a 6.5 Richter Scale earthquake would cause damage

FIGURE III-8a

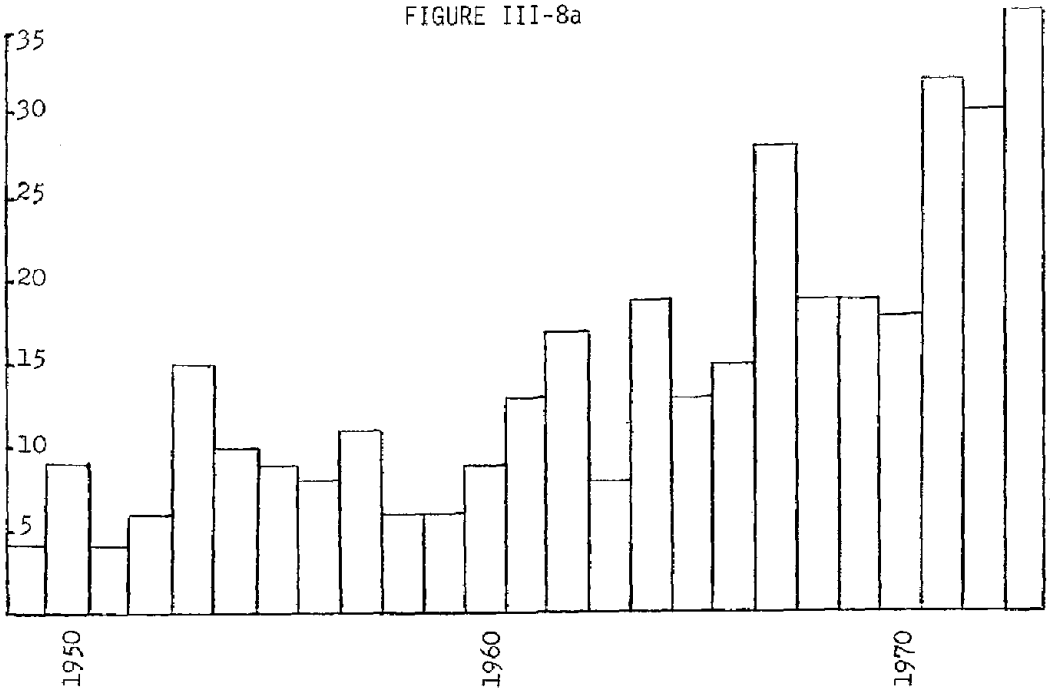

ANNUAL NUMBER OF CATASTROPHES (IN WHICH INSURED PROPERTY LOSSES EXCEEDED $1 MILLION) CAUSED BY NATURAL HAZARDS (Based on information prepared by Insurance Information Institute, 1949-1974)

FIGURE III-8b

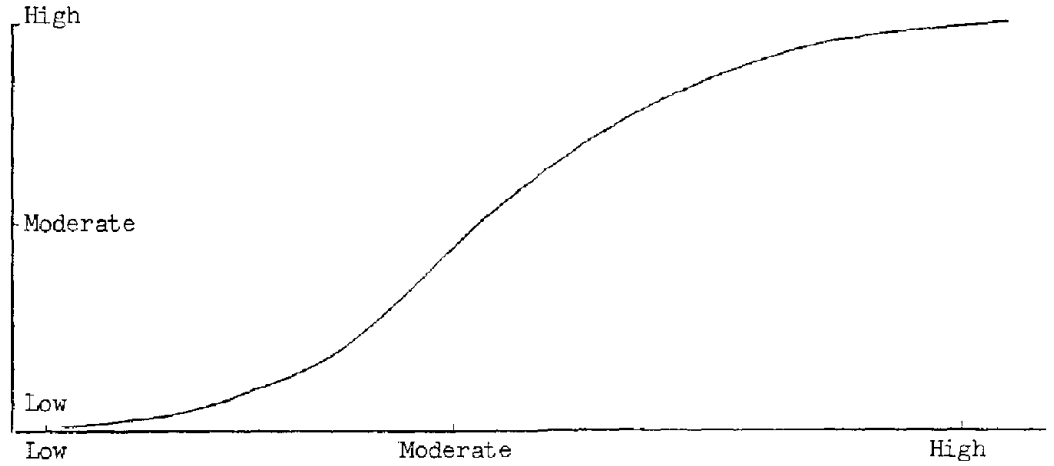

Density and Vulnerability of Population-at-Risk

PERCENTAGE OF THE NUMBER OF MODERATE OR SEVERE GEOPHYSICAL EVENTS THAT PRODUCE NATURAL DISASTERS (The loss producing potential of these events is more effectively realized when density and vulnerability of the population-at-risk is high.)

to non-residential buildings which were 45 times larger than losses caused by a 5.5 Richter Scale event. A 7.5 would cause 1200 times the loss to non-residential buildings than a 5.5.

A 7.5 Richter is considered to be the maximum credible earthquake that could occur on the Inglewood fault because of its relative length and other characteristics (NOAA, 1973). The probability of occurrence decreases rapidly with an increase in the magnitude of an earthquake. The probability of the maximum credible event is very small.

2. Validity of Loss Potential Estimates

Loss potential of the 1971 San Fernando earthquake to single-unit residential buildings was calculated to be $47 million, using the simulation model. Steinbrugge, *et al.* (1971) estimated losses to be $114 million. The computed damages are a conservative estimate of actual losses. Inasmuch as the same vulnerability relationships were used for each of the simulated recurrences of the 43 other earthquakes, the loss potentials calculated for the other earthquakes are probably also conservative. For example, calculated losses for the 1933 Long Beach earthquake are lower than what might be expected. However, the damage index used in Appendix E is probably representative as a relative measure among the earthquakes. One reason the calculated losses are low is that damage estimates are based upon value lost and not replacement costs, which can be as much as three times larger (U. S. Department of Commerce, 1967).

It should be noted in Appendix E that the estimated number of single-unit residential buildings affected during the 1971 San Fernando earthquake by moderate earthshocks (4.5 or above on the severity scale) is 162,000 buildings. This number is nearly an order of magnitude larger than the 20,500 dwellings reported to have been damaged. The vulnerability relationships in the simulation model are continuous curves that represent very minor non-structural damages (such as plaster cracks) for moderate earthshocks. The resulting amount of damage is negligible.

The original estimate of the magnitude of the 1971 San Fernando earthquake was 6.6 on the Richter Scale, with a hypocenter depth of 13 kilometers. An updated estimate lowers the magnitude to 6.4 and changes the depth to 8.4 kilometers (Whitcomb, *et al.*, 1973). Inasmuch as the simulation model was calibrated by using data for the San Fernando earthquake at Richter 6.6 and 13 kilometers depth, the effect on the simulated damages of a recalibration of the model using the 1971 San Fernando

earthquake at 6.4 and 8.4 kilometers is not known.

Simulation of Earthquakes in Central and Eastern United States

The model has been used for simulating earthquakes in the central and eastern United States. Figure III-9 is an example of the calculated earthshock severity pattern of a South Carolina earthquake. The effect of local ground conditions has not been included. Observed earthshock patterns occurring in the central and eastern sections of the United States are different in size, shape, and severity gradient from those observed in California. An "earthquake generator" is being constructed which reproduces these modified patterns. Loss potential of eastern earthquakes can be estimated based upon various sets of assumptions regarding populations-at-risk and their vulnerability to earthquakes.

Interpretation of Results in Terms of Research and Data Needs

The model has been applied to Los Angeles earthquakes to illustrate the type of output that can be obtained from a simulation approach and, secondly, to point out the research and data needs necessary to improve the usefulness of the output.

1. Data Needs

A number of restricting assumptions were required in these applications because of a lack of basic information on the character and geographic distribution of the populations-at-risk. The greatest informational deficiency exists for non-residential and high-rise buildings. An inventory of these buildings similar to that given in the U. S. Census for the 47 million single-unit dwellings and nearly 5 million other residential buildings is not available. A means of updating 1970 census information on population and residential buildings would also be desirable.

Much additional information needs to be gathered on various aspects of damage potential to various kinds of buildings. The accuracy of vulnerability estimates is closely related to the broadness of categories used to classify the exposed buildings or population. It is difficult to define vulnerability of buildings in the very broad categories used in this study because of the conglomeration of buildings that were mixed together in each of the four categories. As more information becomes available, the number of categories can be increased and the vulnerability definitions tightened to make them more realistic. In the extreme case, each building would be analyzed and its particular

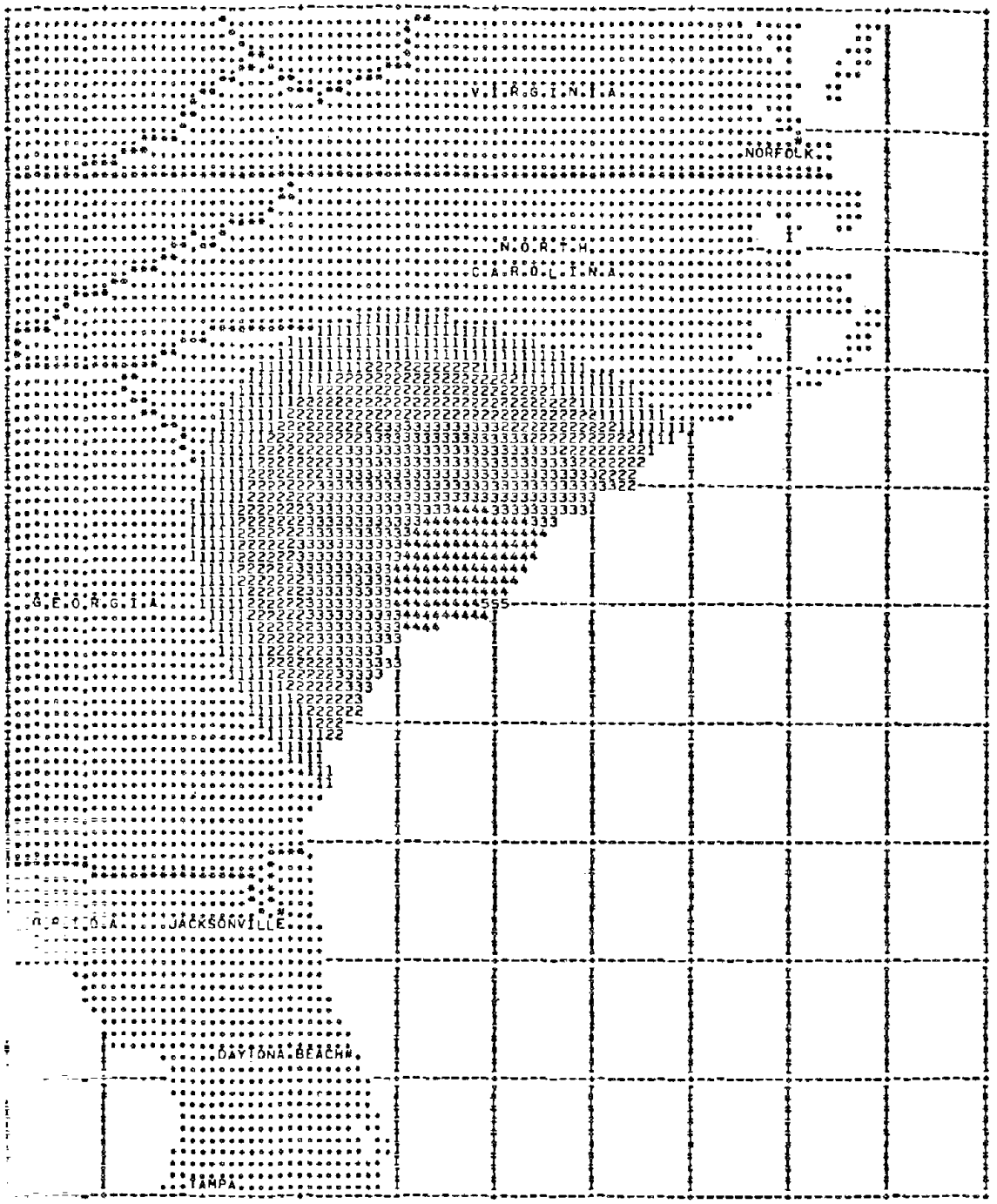

FIGURE III-9

SIMULATED EARTHSHOCK SEVERITY PATTERN OF AN EARTHQUAKE IN SOUTH CAROLINA

vulnerability to earthquake loss evaluated. However, the cost and time involved in this procedure eliminates it as a practical method. At the other extreme is the use of broad categories of buildings. In this case, "most likely" levels of vulnerability are used based upon the consistency of statistical properties inherent in the use of a large number of buildings in each category. The range of possible vulnerabilities due to differences in building type, value, age, height and quality of construction is probably very large in the broad groupings of non-uniform structures.

Work has been done on determining of vulnerability of single-unit residential buildings (U. S. Department of Commerce, 1969; Steinbrugge, 1973); other residential and non-residential buildings (Steinbrugge, *et al.*, 1971); and high-rise buildings (Whitman, *et al.*, 1973).

2. Research Needs

Results of these earthquake model applications suggest that useful information can be obtained on the loss potential of earthquakes to various populations-at-risk even when the output of the simple model is in Modified Mercalli-type severity units. It is likely that the usefulness of the output can be much improved by incorporating ideas and information that have been developed in seismology and earthquake engineering since the construction of the model in 1969. Some of the new ideas and information follow:

(1) The severity of earthshocks during a Richter magnitude 8 earthquake is not any greater than that associated with a Richter magnitude earthquake of about 6.5. However, the earthshocks of the magnitude 8 earthquake are of longer duration, cover a larger geographical area, and have a different mixture of long and short earthshock waves.

(2) The long waves attenuate slower with distance than the short waves. Consequently the mixture of long and short waves changes with distance from the area of faulting. Short waves predominate near the fault zone, while longer waves predominate at distances away from the faulted zone.

(3) The characteristics of the population-at-risk determine the wave lengths that produce the greatest damage potential to various types of buildings. High-rise buildings are most affected by long earthshock waves. Low-rise buildings are most affected by the high frequency, short waves.

(4) A measure of earthshock severity, as given by a Modified Mercalli-type unit, does not explicitly include the effect of changes in this mixture of wave lengths. For example, a Modified Mercalli intensity of VII observed 25 miles from the earthquake's epicenter has a much different mixture of wave length, and a different effect upon high and low-rise buildings than a Modified Mercalli VII observed 100 miles from the faulted area. A Modified Mercalli VII observed far from the faulted zone implies an occurrence of a high magnitude earthquake. The predominant wave length at these distances would be long and high-rise buildings would be affected. This is one of the drawbacks in the use of vulnerability based solely on a Modified Mercalli-type unit. Note in Appendix D that the 1952 Kern County earthquake, a large but distant earthquake (distant relative to the Los Angeles Metropolitan area), has a large damage index for single-unit dwellings because the calculated earthshock severities in the densely populated Los Angeles area were as high as 7 (equivalent to a Modified Mercalli VII). This is probably an overestimate of damage potential to these low-rise buildings from this relatively distant earthquake. On the other hand, a severity level of 7 at this distance from the epicenter probably produces an underestimate of damage potential to the high-rise buildings listed in Appendix D. The size of the effect of changes in wave length mixture with distance on damage potential is not known.

(5) The production of long wave lengths of sufficient severity to cause damage to high-rise buildings is related to earthquake magnitude. The greater the magnitude, the larger the production of long waves at distances from the faulted area. Consequently, the change in wave mixture with distance is also related to earthquake magnitude. It is not known if the earthshock severity patterns of moderate earthquakes can be extrapolated into a measure of the earthshock pattern of a great earthquake (Richter 8.3) using a simple model.

(6) The effects of local ground conditions are not completely deterministic and should be considered from a statistical viewpoint. The recurrence of an identical earthquake at the same epicenter and hypocenter depth may produce a significantly different earthshock pattern at a given site.

An earthquake model which incorporates these ideas has been developed and is being tested. The output of the model is response spectra acceleration for various wave lengths. This physical unit is used as a measure of earthshock severity rather than a Modified Mercalli-type unit. Geographical patterns of earthshock severity are calculated for a

number of wave length categories. Each category corresponds to a type of building. Geographical patterns calculated for short wave lengths are small in area. The area and shape changes with earthquake magnitude to moderately large, elongated patterns for the high magnitude earthquake. The patterns closely follow and encompass the length of the faulted area. For long waves, the patterns are larger in size. The size and shape changes with magnitude of the earthquake but the changes are not as drastic as with the short-wave patterns. High-rise buildings many miles away from an earthquake's faulted zone may be damaged significantly while adjacent low-rise structures are not affected.

Vulnerability relationships between building damage, spectral acceleration and earthshock duration have been hypothesized using recent loss experience. Scholl (1974) has studied the relationship between damage to low-rise buildings and spectral acceleration for the 1971 San Fernando earthquake. The explicit effect of earthshock duration on damage potential has not been measured. It is possible that earthquake magnitude can be used as a proxy measure of duration. The magnitude of a California earthquake can usually be related to the length of faulting. The greater the earthquake magnitude, the longer the length of the faulted zone, and hence, the larger the area affected by maximum ground accelerations and the longer the duration of maximum ground motion at any one location. Possible secondary effects associated with an earthquake occurrence such as tsunami, fire, landslide, dam breakage, and soil failure are not presently included in the model. Only the vibration of the ground is considered.

Information for developing the updated earthquake model has been gathered from a number of sources, including the following:

(1) Physical Characteristics of Earthquakes:

Nuttli, 1973; Thatcher and Hanks, 1973; Trifunac and Brune, 1970; Douglas, *et al.*, 1970; Blume, 1970; Brune, 1970; Shteinburg, 1969; Wesson and Ellsworth, 1973; Ergin, 1969; Nuttli, 1973a.

(2) Effect of Local Conditions:

Davis and West, 1973; Duke, *et al.*, 1972; Hudson and Udwadia, 1973; Schnabel and Seed, 1973; Udwadia and Trifunac, 1973; Seed and Idriss, 1969; Lysmer, *et al.*, 1970; Hays, *et al.*, 1972; Perez, 1973; Seed and Idriss, 1969; Schnabel, Seed and Lysmer, 1972; Lastrico, Duke and Ohta, 1972.

(3) Physical Measures of Earthshock Severity:

Housner and Jennings, 1973; Trifunac, 1973; Trifunac, 1971; Hudson, 1972; Hudson, *et al.*, 1971-1973; Seed and Idriss, 1970; Trifunac, Udwadia, Brady, 1973; Murphy, *et al.*, 1972; Lynch, 1969; Murphy and Lahoud, 1969; Udwadia and Trifunac, 1973a; Algermissen, 1973; Johnson, 1973.

(4) Measures of Vulnerability:

Blume and Monroe, 1971; Housner, 1973; Scholl and Farhoomand, 1973; Steinbrugge, *et al.*, 1971; Whitman, *et al.*, 1973; Donovan, 1973; Jennings, 1971; Munich Reinsurance, 1973; Blume, 1972; Duke and Jacobsen, 1973; Nadolski, 1969; Blume, 1969; Newmark and Hall, 1973.

Natural hazard simulation, when applied to earthquakes, can yield realistic information about the orders-of-magnitude of loss potential to the geographical array of a given population-at-risk. Recently available information from seismology and earthquake engineering, when incorporated into the model, should improve the usefulness of its output. In addition, the output can be improved by use of better information about the various populations-at-risk and their vulnerability to earthquake-induced loss. One objective is to keep the model as simple as possible and yet maintain the required accuracy of the output for the problem at hand.

Cross-hazard comparisons of loss potential for combinations of adjustments can be made, and incorporated into relative measures of riskiness for various sections of the United States.

CHAPTER IV

HURRICANES

Importance of Wind and Storm Surge Hazards

In the past decade, hurricane-induced damages have exceeded $3 billion. Two components are the hurricane wind and storm surge hazards. Appendix F is a tabulation of pertinent data on a group of hurricanes that have affected the Gulf and south Atlantic States in the past 100 years. Data on 90 hurricanes are listed based on a tabulation of "memorable hurricanes" prepared by Sugg, *et al.* (1971). The authors selected these memorable storms from the over 300 tropical storms and hurricanes that have affected the United States since 1873. Criteria for inclusion were landfall on the United States coastline or a near hit; severe intensity as measured by sea-level pressure within the hurricane's eye; or unusually large property damage or loss of life even though the hurricane's strength was not great.

One method of estimating future hurricane risk is to use past experience as a guide. However, an inspection of Appendix F illustrates the difficulties inherent in using past experience to predict the future level of risk. If a long period of years is used, the effect of changes in property density and characteristics is a dominant factor in determining the level of loss. A high loss figure for a recent storm does not necessarily mean that the storm was more severe than past storms. Density and geographical distribution of population and structures at risk have increased markedly along the Gulf and south Atlantic seaboard over the years. A large portion of this increase is in the most hazardous seacoast areas. In the past 50 years the population of Florida has increased at a rate 3.5 times greater than that of the United States as a whole.

Structure value and cost of repair has also increased many times over the past years. For example, construction costs have changed by a multiple of five in the past 30 years. Improved building codes, construction methods and quality of materials over time may have decreased

vulnerability of these structures to wind damage. Although the amount of decrease is not known, apparently it does not compensate for increases in the cost of repair and number of exposed structures. Consequently, the effect of time changes in geographical distribution, property characteristics, and vulnerability have a considerable influence upon the measure of loss potential. These time changes seriously hamper efforts to convert this information directly into a measure of future risk. On the other hand, there is no indication that the frequency of memorable hurricanes has trended upward in the past 100 years even though the number of natural disasters resulting from these storms has exhibited a large increase.

Hurricane intensity is important because of a relationship between intensity (central atmospheric pressure), the speed of winds and the height of the storm tides that are produced. The lower the central pressure, the greater the tendency for extreme wind speeds and high tides to occur. Dunn and Miller (1964) devised the following intensity classification:

Hurricane Intensity	Minimum Pressure (Inches of Mercury)	Maximum Winds
Minor	above 29.40 in.	less than 74 mph
Minimal	29.01-29.40	74 to 100
Major	28.01-29.00	101 to 135
Extreme	28.00 in. or less	136 or greater

The intensity of each of the 90 storms in Appendix F is designated according to this classification system. An inspection of the number of different designations indicates that the frequency of extreme storms has not increased during the past 100 years.

If the length of years used for specifying past experience is decreased to reduce the effect of time changes in number of properties and the property characteristics, a distorted estimate is obtained of the frequency and magnitude of hurricanes that affect various sections of the Gulf and south Atlantic coastlines. For instance, if experience of the past ten years is converted into a future risk, the lack of severe hurricanes along the coasts of Georgia, South Carolina and North Carolina might imply a very low storm frequency in these areas. Although no intense hurricane has affected this stretch of coastline in the past decade, the long-term probabilities of severe storm occurrence are relatively large, especially along the North Carolina coast. The same type of bias could be

obtained with regard to the southern tip of Florida, using experience in the past 10-20 years. The metropolitan area of Miami has been relatively free of severe hurricanes during this time period. Conversion of this experience into a measure of future risk could be misleading because long-term probabilities of hurricane occurrence, based upon the past 100 years, indicate that the Miami area has the highest potential for severe hurricane occurrences in the United States.

An alternative method of measuring present and future risk can be obtained by (1) utilizing the long record of hurricane occurrences by location and intensity along the Gulf and south Atlantic coastlines (severe storm climatology), and (2) eliminating the effect of changes over time in property characteristics, number and vulnerability, which minimizes the usefulness of past experience as a basis for measuring risk.

The disproportionate increase in damage vulnerability with an increase in wind speed makes it necessary to distinguish between hurricanes of different intensities. All hurricanes do not have the same damage-producing potential (Frank, 1974). An extreme hurricane with winds exceeding 135 mph is a much more dangerous storm than a minimal hurricane with winds of 100 mph or less. In addition, the land area covered by high winds increases with intensity of the storm. The area swept out by winds of 100 mph by an extreme intensity hurricane as it moves inland may be ten times larger than the area covered by 100 mph winds associated with a major intensity storm. By definition, winds are less than 100 mph in a minimal hurricane. The area covered by strong winds is important because it is the overlapping of these high wind patterns with the geographical array of exposed properties that can result in the production of a natural disaster.

Development of Wind Model

A computed severity pattern which represents the geographical pattern of maximum wind speeds experienced during the passage of a hurricane across the Southeast coastal area is shown in Figure II-1. The mathematical model that produced this pattern incorporates the combined effects of a number of physical characteristics of the tropical cyclone (Friedman, 1961, 1964, 1966, 1972). Figure IV-1 illustrates some of the relationships that are built into the model.

The calculated patterns of maximum wind speed associated with a hurricane that moves inland at right-angles to the coastline are typically bell-shaped. The base of the bell lies along the shoreline. Winds are

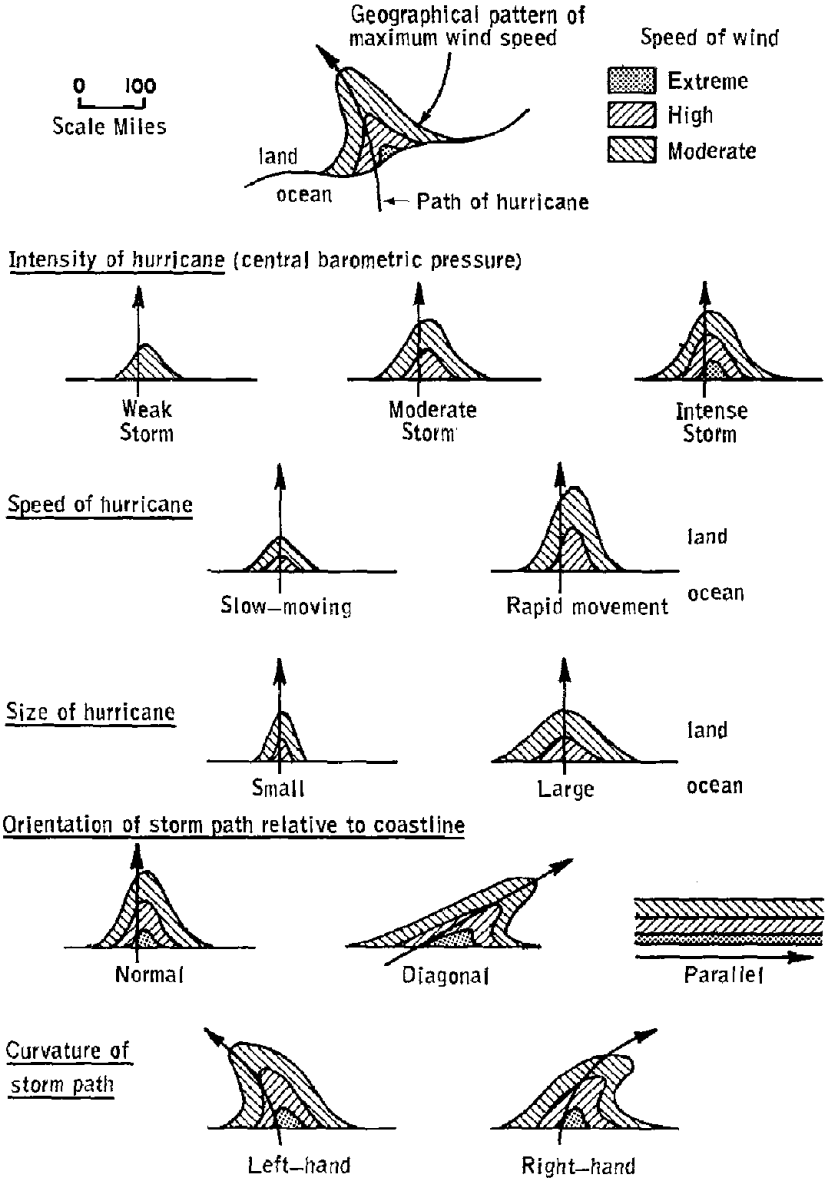

FIGURE IV–1

SIZE AND SHAPE OF THE GEOGRAPHIC PATTERN OF MAXIMUM WIND SPEED RELATED TO PHYSICAL PROPERTIES OF A HURRICANE

highest along the immediate coastline and decrease with distance inland. Winds decrease in magnitude as the hurricane moves inland because its major source of energy (warm ocean waters) is no longer available and also because the frictional effect of land-based obstructions (topography, forests, urbanized areas) tends to reduce the wind speed. Inasmuch as highest winds on the coastline are near or slightly to the right of the storm center, the dissipation of these winds takes longer as the storm moves inland than the dissipation of less intense winds near the storm's fringes. Hence, the development of the bell-shaped patterns centered on or near the storm path. Distortions of this basic wind speed pattern result from the effects of storm speed, size and path relative to the coastline, taken individually or in combination.

Specification of the geographical pattern of wind speed severity in terms of these physical measures was obtained through the construction of a mathematical generator. Incorporation of the affect of the various measures into the model was as follows:

(1) Storm intensity ideally is measured by the minimum sea level pressure at the storm's center as it nears or crosses the coastline. The effect of increasing the intensity of a hurricane is assumed to be an increase in the geographical area affected by high winds, and an increase in the overall magnitude of the wind speed. These changes tend to enlarge the number of wind speed contours within the pattern. The new contours are also bell-shaped. Relationships between storm intensity and characteristics of the wind severity pattern that were used in the model are based, among other things, on empirical information on past storms, which include 44 hurricanes (winds greater than 75 miles per hour) and 24 tropical storms (winds less than 75 miles per hour) that affected the Gulf and East coasts since 1950. Patterns of maximum wind speed (peak gusts) for each of these storms were plotted using data given in annual issues of Climatological Data-National Summary (U. S. Department of Commerce, 1950-1973).

Figure IV-2 is a graphical illustration of relationships that were derived from this information. The graph shows the length of coastline, to the right and left of the storm's center (vertical axis), that is affected by winds of various magnitudes for different storm intensities (horizontal axis) as the hurricane moves onshore. For illustration, two wind speed categories are shown--winds in excess of 50 miles per hour and winds in excess of 100 miles per hour. The plotted points represent

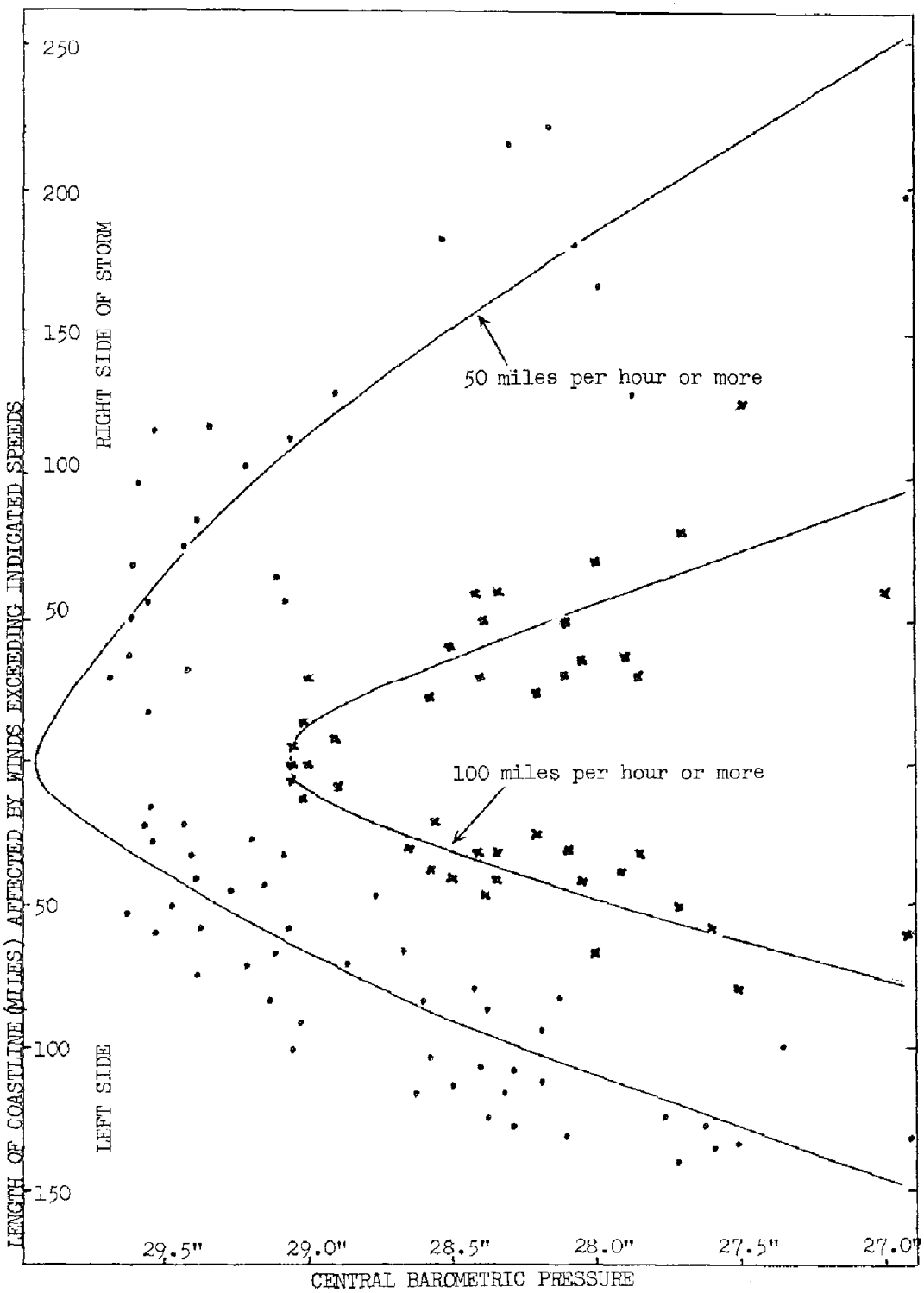

FIGURE IV-2

RELATIONSHIP BETWEEN HURRICANE INTENSITY AND LENGTH OF COASTLINE AFFECTED BY HIGH WIND SPEEDS (Path of storm nearly perpendicular to shoreline.)

the length of coastline encompassed by these wind speeds during the inland passage of past hurricanes on paths which were nearly perpendicular to the shoreline. The gradual increase in the length of coastline affected with an increase in intensity was incorporated in the model through the construction of a "most likely" curve drawn through these data points on the right and left sides of the storm center. An envelope of maximum winds on the coastline was obtained by constructing similar curves for a number of wind speed categories. The inland bell-shaped pattern was defined by applying dissipation rates to the coastal envelope of wind speeds. The size of the dissipation factor was related to inland distance along the storm path. These factors were consistent with rates observed during the past storms.

(2) Speed of the storm is measured by the rapidity of movement of the storm's center. An increase in storm speed distorts the shape of the wind pattern by increasing wind speeds to the right of the storm path (looking in the direction toward which the storm is moving) and reducing wind speeds by an amount equal to the speed of the storm on the left-hand side. The location of maximum wind speed lies to the right of the hurricane path for a moving storm. Highest winds are usually in the right quadrant of the hurricane's eye wall. The effect of this wind field distortion as the speed of the storm increases is to stretch out the right-hand side of the bell and squeeze it together on the left-hand side. A slow moving storm produces a nearly symmetrical bell-shaped pattern as it moves inland.

Note that the coastline distances are not symmetrical around the storm path for hurricanes represented in Figure IV-2 because of storm movement. The "most likely" curves relating coastline distance affected by various wind speeds to storm intensity were based upon storms with an average rate of movement. The "speed-of-storm" factor that was incorporated into the model adjusted the wind patterns for deviations from this average speed. With other conditions held constant, a fast-moving storm carries high winds further inland than a slow-moving storm. The effect is to stretch the pattern further inland for storms with an above-average rate of movement. The inland extent of the wind pattern is depressed for storms with a slower-than-average rate of movement. The duration of the period of high winds at any one location is shorter for a fast-moving storm. Duration of severe conditions can affect the degree of vulnerability of exposed populations-at-risk in much the same way that the duration of severe earthshocks affects damage potential during an earthquake.

In the hurricane model, the effect of deviations from the average storm speed was approximated by

changing the inland dissipation rates using relationships between wind patterns and speed of past hurricanes.

(3) Storm size refers to the areal extent of the storm. The scatter of the data points in Figure IV-2 indicates that an additional size adjustment would be needed in the model over and above that given by the "most likely" size-versus-intensity relationship described in item 1 of this section. It was evident that the size of a hurricane and its intensity were not always completely consistent. For the same intensity, there is a range of possible storm sizes, as indicated by the scatter of the data points in Figure IV-2. Consequently, a storm size factor was introduced into the model which modifies the wind pattern to account for the variability in storm size not accounted for by the hurricane intensity adjustment. By its use, the size of the wind pattern can be changed independent of the size effect of storm intensity. The size of the entire pattern or the patterns only on the left or right-hand side of the storm path (including appropriate modification of wind gradients with the pattern) can be made using the size adjustor.

(4) Orientation of storm path relative to the coastline distorts the shape of the bell-shaped pattern which is characteristic of a right-angle path with the shoreline. As the angle of the storm path with the coastline changes from perpendicular to parallel, the bell-shaped pattern becomes elongated and increasingly distorted. In the extreme case, if the storm path is parallel to the coastline and the storm center remains a short distance offshore, a continuing supply of energy is available to the storm resulting in wind speed contours that run parallel to the coastline. The change in shape and size of the wind pattern produced by the model is consistent with observed patterns in past hurricanes.

(5) Curvature of the hurricane path distorts the wind pattern as the storm makes a right-hand or left-hand turn of a specified radius. A factor which modifies the wind pattern based upon a measure of the storm track's curvature is also an input variable for the hurricane generator. Refer to Figure IV-1 which graphically illustrates modifications in the shape and size of the wind pattern to account for the effect of some of these physical characteristics of a hurricane.

(6) Inherent gustiness of hurricane winds is simulated by the use of a random number generator which modifies the calculated wind speed for each 35 square mile grid area. The effect of this factor is to reduce the smoothness of the wind speed contours.

1. Effect of Local Conditions

Local differences in exposure to high wind speeds are incorporated into the model by designating an exposure factor to each grid point in computer memory. Topography, tree-covered land and urban areas can have a marked effect upon local wind speeds. The exposure factor is based upon information provided by Thom (1968). Inclusion of the effect of this adjustment factor acts to further change the smooth contoured wind patterns over a frictionless surface, obtained by using the first five input variables described in the previous section, into an irregularly shaped pattern which more closely approximates observed wind patterns.

2. Reasonableness of Computer Wind Speed Patterns

To verify the reasonableness of computed patterns, input conditions representing a number of past hurricanes were used to compute wind patterns which were then compared with observed patterns. The degree of correspondence between the calculated and observed patterns varied from storm to storm, as it did when the earthquake model was used to approximate the observed earthshock severity patterns. The overall degree of correspondence is surprisingly good when it is remembered that the calculated patterns are based upon a simple set of assumptions which attempt to tie together and utilize the observed consistencies in the size and shape in the wind speed patterns that can be related to the physical properties of hurricanes.

Figure IV-3 is an example of a comparison between the calculated and observed wind speed patterns. Hurricane Carla, which affected the Texas coastline in 1961, is shown because it was an especially large and violent storm. Winds were estimated to have gusted to 175 miles per hour near its landfall location, and gusts of nearly 75 miles per hour or more affected the entire Texas coastline. The size of the computed wind pattern for this hurricane had to be increased using the size adjustment factor because the actual pattern was much larger than the intensity-versus-size relationship in the model would have indicated. In this case the use of the hurricane model is reversed. For a given wind pattern, the combination of physical measures that would have produced a prototype pattern is specified.

Estimation of loss potential to various populations-at-risk can be made for a variety of assumptions regarding the physical properties of the hurricane. The effect of a recurrence of past hurricanes can be

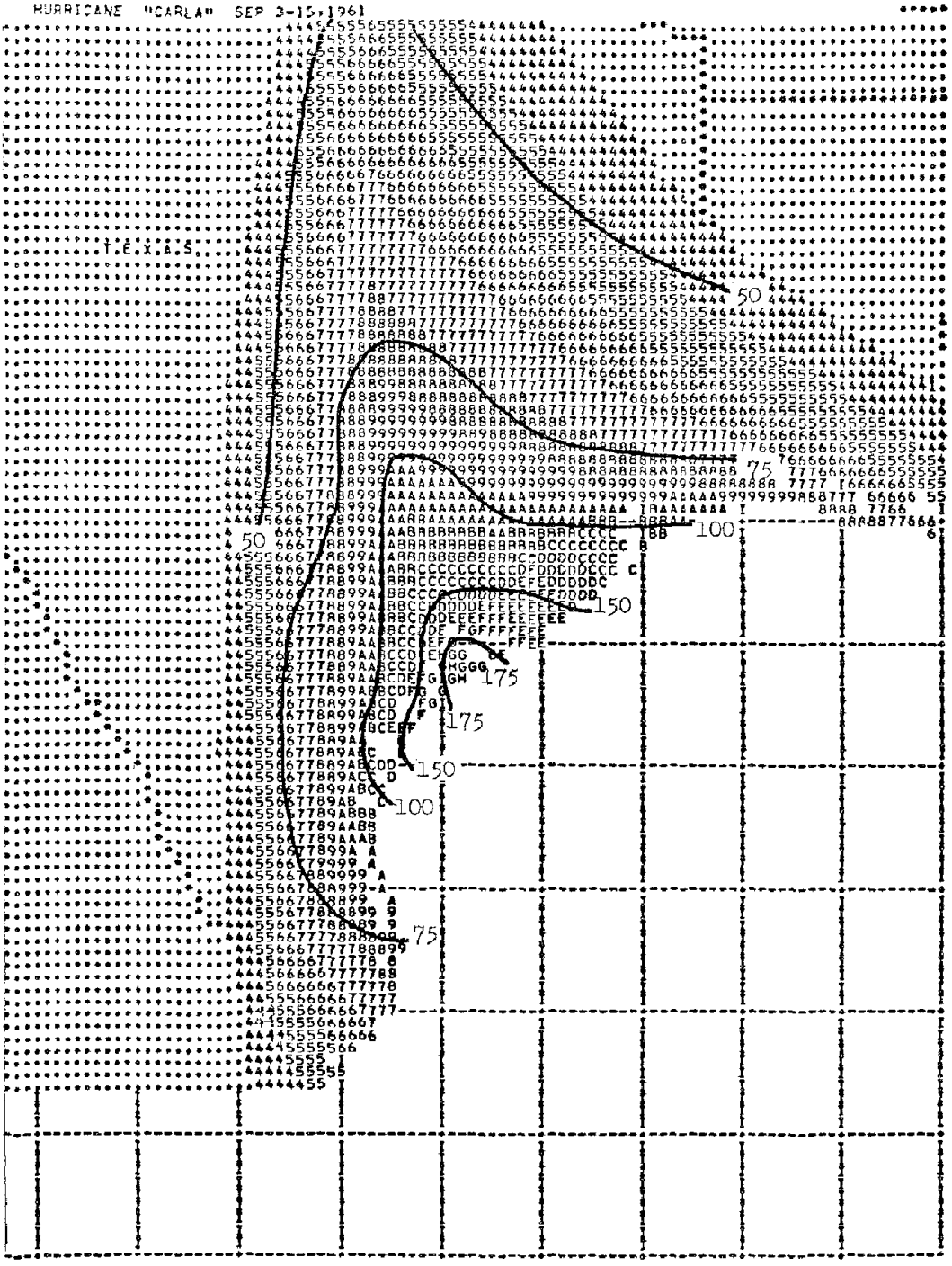

FIGURE IV-3

COMPUTED PATTERN OF MAXIMUM WIND SPEED (PEAK GUSTS) OF HURRICANE CARLA COMPARED WITH OBSERVED PATTERN BASED ON FIGURE 2, PAGE 67, OF U. S. DEPARTMENT OF COMMERCE (1961) (Wind speed intervals above 100 miles per hour represented by alphabetic code: A denotes 100 to 109 mph, B represents 110-119 mph and so forth.)

estimated using whatever information on the storm's characteristics available. An alternative approach is to determine the loss potential of the most likely hurricane; the largest; or the most rapidly moving storm. As with the use of the earthquake model, the question that must be answered is how good an approximation of actual patterns is needed in order to produce useful estimates of loss potential to a particular population-at-risk.

3. Population-at-Risk and its Vulnerability

Four populations-at-risk are exposed to the hurricane hazard in the application: single-unit residential, other residential, non-residential buildings, and population. A description of the sources and assumptions required to obtain this information was given in Chapter III. Measures of these populations-at-risk have been placed in computer memory for the 22 states that are adjacent to the Gulf and Atlantic coastlines. Land area of these states is represented by 26,500 grid points and contains 50% of the population and 50% of the single-unit residential buildings in the United States.

Vulnerability of these populations-at-risk to the hurricane wind hazard is expressed in terms of two measures, the percentage of the buildings or people in a grid area which would be affected if a wind speed of a specified magnitude were to occur in the area, and the degree of the effect.

Value of single-unit residential buildings is in computer memory for each grid area, based upon median value given by county in U. S. Bureau of the Census tabulations. For this application, the value of each building in the "other residential" and "non-residential" categories was arbitrarily set at $50,000 and $100,000 respectively. Estimates of aggregate losses to these two populations-at-risk can be adjusted by the application of a multiplicative factor to these incremental estimates of value. The casualty factor was assumed to be a ratio of casualties to number of persons affected by various wind speeds.

TABLE IV-1

VULNERABILITY OF BUILDINGS IN THE THREE CATEGORIES TO HURRICANE WINDS

1a. Percentage of Buildings Affected in Grid Area

Maximum Wind Speed in Grid Area (peak gust)	Single-Unit Residential	Other Residential	Non-Residential
40 mph	0.1%	0.08%	0.07%
60	1.8	1.5	1.2
80	8.4	7.0	5.6
100	25.0	20.9	16.7
120	51.0	42.5	34.0
140	72.0	60.0	48.0
160	100.0	83.4	66.7

1b. Most Likely Percentage of Value Lost to Affected Buildings

Maximum Wind Speed in Grid Area (peak gust)	Single-Unit Residential	Other Residential	Non-Residential
40 mph	1.0%	0.5%	0.4%
60	1.7	0.9	0.8
80	2.9	1.8	1.7
100	3.9	2.4	2.3
120	5.5	3.5	3.4
140	9.3	6.0	5.9
160	16.0	11.0	10.9

TABLE IV-2

CASUALTY FACTOR FOR POPULATION RELATED TO MAGNITUDE OF HURRICANE WIND SPEEDS

Maximum Wind Speed (peak gust)	Number of Casualties per Number of Persons
40 mph	1 per 5,000,000
60	1 per 300,000
80	1 per 50,000
100	1 per 11,000
120	1 per 3,000
140	1 per 1,000
160	1 per 400

4. Frequency and Magnitude of Future Hurricanes

If the past 100 years is indicative of general conditions in the future, extreme hurricanes are more likely along some sections of the Gulf and East coast than at others. Figure IV-4 is a count of the number of

times in the past 100 years that segments of the coastline were affected by minimal, major and extreme hurricanes. It is possible that some of these storms were beyond the stage in their life cycle at landfall when maximum wind speeds are generated.

An examination of Figure IV-4 suggests that there are differences in the frequency patterns along the Gulf and South Atlantic coastlines between the minimal, major and extreme hurricanes; however, reasons for the differences (if they are statistically significant) are not clear. In an attempt to determine if these apparent differences in hurricane frequency by intensity grouping do have a physical basis, the offshore tracks of all recorded tropical storms and hurricanes during the past 100 years were studied (Friedman, 1971). The Gulf of Mexico, Caribbean and adjacent Atlantic Ocean areas were divided into an array of 1° latitude by 1° longitude grid areas. A count was made of the number of times that the track of extreme hurricanes, for instance, passed through each grid area.

a. Extreme Hurricanes

The number of times tracks of extreme hurricanes passed through each grid area in the past 100 years was counted regardless of the particular stage of development of the storm as it moved across any given grid area. The only criterion for an extreme hurricane was that sometime during the storm's life cycle its central pressure dropped below 28.00 inches of mercury or its maximum winds exceeded 135 mph in peak gusts. Figure IV-5 represents the resulting frequency pattern for extreme hurricanes using this definition. Sixteen times during the past 100 years, the path of extreme hurricanes passed through 1° latitude by 1° longitude grid areas to the southwest of Cuba and also to the northeast of Cuba. One track which runs south of the Cuba--Puerto Rico island chain extends into the Gulf of Mexico through the gap between the Yucatan Peninsula and Cuba. Another track runs north of the island chain across or near tne southern tip of Florida and then westward into the Gulf of Mexico. A third major track curves northward off the East coast of the United States. In the past 100 years, extreme storms that entered the Gulf of Mexico have tended to continue on a west or northwesterly track across the Gulf of Mexico eventually striking Mexico, Texas or the exposed Mississippi delta region of Louisiana. Very few of these storms curved northward sufficiently to affect western Florida or the Florida panhandle. This overall frequency pattern appears to confirm the physical reasonableness of coastline counts

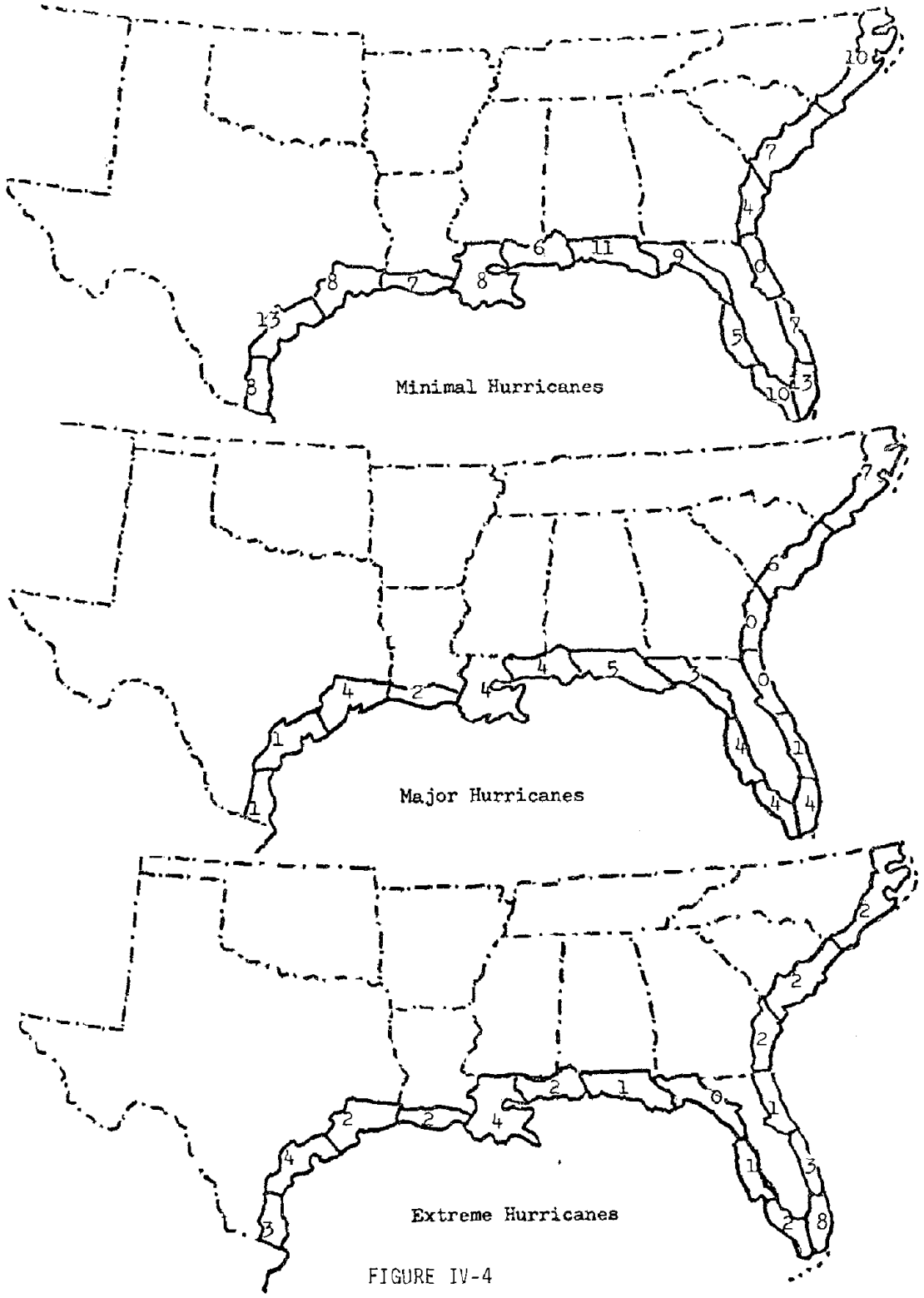

FIGURE IV-4

NUMBER OF TIMES IN THE PAST 100 YEARS THAT SEGMENTS OF THE COASTLINE WERE AFFECTED BY MINIMAL, MAJOR AND EXTREME HURRICANES

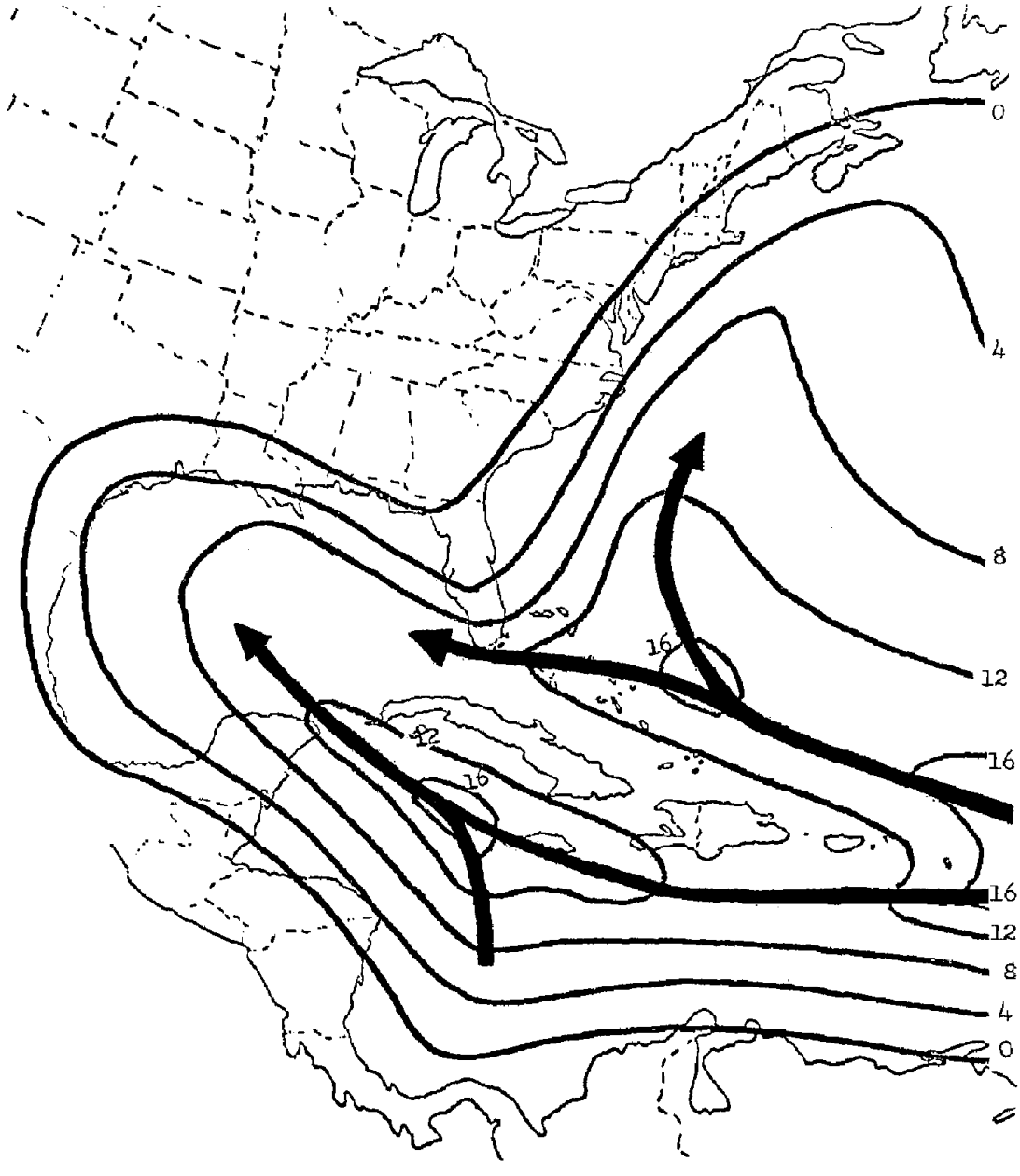

FIGURE IV-5

NUMBER OF TIMES IN THE PAST 100 YEARS THAT THE PATH OF AN EXTREME HURRICANE (WINDS REACHING MORE THAN 135 MILES PER HOUR SOMETIME DURING THE STORM'S LIFE CYCLE) PASSED THROUGH 1 DEGREE LATITUDE BY 1 DEGREE LONGITUDE SQUARES (Implied storm tracks are superimposed.)

of extreme hurricane occurrences.

b. Major Hurricanes

For major hurricanes, with winds reaching 100 to 135 mph sometime during the lifetime of storm, two major tracks are apparent: one to the south, and the other to the north of the Cuba-Puerto Rico island chain. The major difference between the frequency pattern of extreme and major hurricanes is the greater tendency for major hurricanes to curve northward or northeastward as they move through the Yucatan-Cuban gap; lines of equal frequency bend northward into the eastern Gulf of Mexico exposing coastal areas in the eastern Gulf to major hurricanes. All of the coastal sections of the Gulf states had a frequency of about four major storms in the past 100 years (return period of about once every 25 years). This contrasts with the apparent greater frequency of extreme hurricanes affecting western Gulf coastal areas as compared with areas in the eastern Gulf.

c. Minimal Hurricanes

In the frequency pattern of minimal hurricanes (maximum winds between 75 and 100 mph sometime during the storm's life cycle), the center of maximum frequency shifts from south of Cuba northward into the eastern Gulf of Mexico. The center of maximum frequency in the Atlantic has become more intense and lies just to the east of the southern tip of Florida at the intersection of two storm tracks. One track follows the warm water of the Gulf stream as it moves around the western tip of Cuba, eastward between Cuba and Florida, and then northward parallel to the south Atlantic coastline. The second track moves in a west-northwest direction along a line parallel to, and north of, the Cuba-Puerto Rico island chain. The track south of this island chain, was pronounced with the extreme and major hurricanes, is indistinct with the minimal hurricanes. In the Gulf of Mexico, the lines of equal frequency converge along the coastal areas of western Florida, Alabama and Mississippi. The frequency of minimal hurricanes is higher along the eastern coast of the Gulf of Mexico than along the western Gulf coast. A storm track is directed northeastward toward the Florida panhandle. Along the south Atlantic coastline extreme, major and minimal hurricanes are most frequent near the tip of Florida. Frequencies decrease as one moves northward to the Georgia coastline. Frequencies increase again further northward to a secondary

maximum along the coast of North Carolina. One reason for the lower number of hurricanes along the Georgia coastline, as compared with areas further north or south, is the pronounced inward bending of the coastline from Florida northward to Georgia.

d. Tropical Storms

Frequencies of tropical storms (winds reaching a maximum of between 50 and 75 mph sometime during the storm's life cycle) were tabulated only along the coastlines. The area of maximum frequency apparently lies just off the Florida panhandle with a storm track directed northeastward toward the Florida mainland. Along the Atlantic coastline, the frequency of tropical storms is highest at the southern tip of Florida and also along the eastern tip of North Carolina.

Overwater frequency patterns of extreme, major and minimal hurricanes in the past 100 years suggest that there are frequency differences along the coastlines affecting catastrophe potential and production of future natural disasters.

5. Variation in Loss Potential Caused by Changes in Path of Hurricane

To illustrate how path affects natural disaster production, a series of computer runs was made, assuming that a sequence of simulated storms would follow one of the most frequently traveled routes of extreme hurricanes. This route lies just to the north of the Cuba-Puerto Rico island chain. Hurricanes of five intensities were approximated (Friedman, 1973a):

Central Barometric Pressure	Level of Hurricane Intensity
27.00 in.	Extreme (upper limit)
27.50 in.	Extreme (midpoint)
28.00 in.	Extreme (lower limit), Major (upper limit)
28.50 in.	Major (midpoint)
29.00 in.	Major (lower limit), Minimal (upper limit)

Thirty-two locations were assumed as possible landfall positions. Landfall is the point where the hurricane crosses the coastline. These locations were equally spaced at intervals of about 50 miles from south Texas to North Carolina, as depicted in Figure IV-6. Direction and curvature of the path followed by these storms is also shown.

FIGURE IV-6

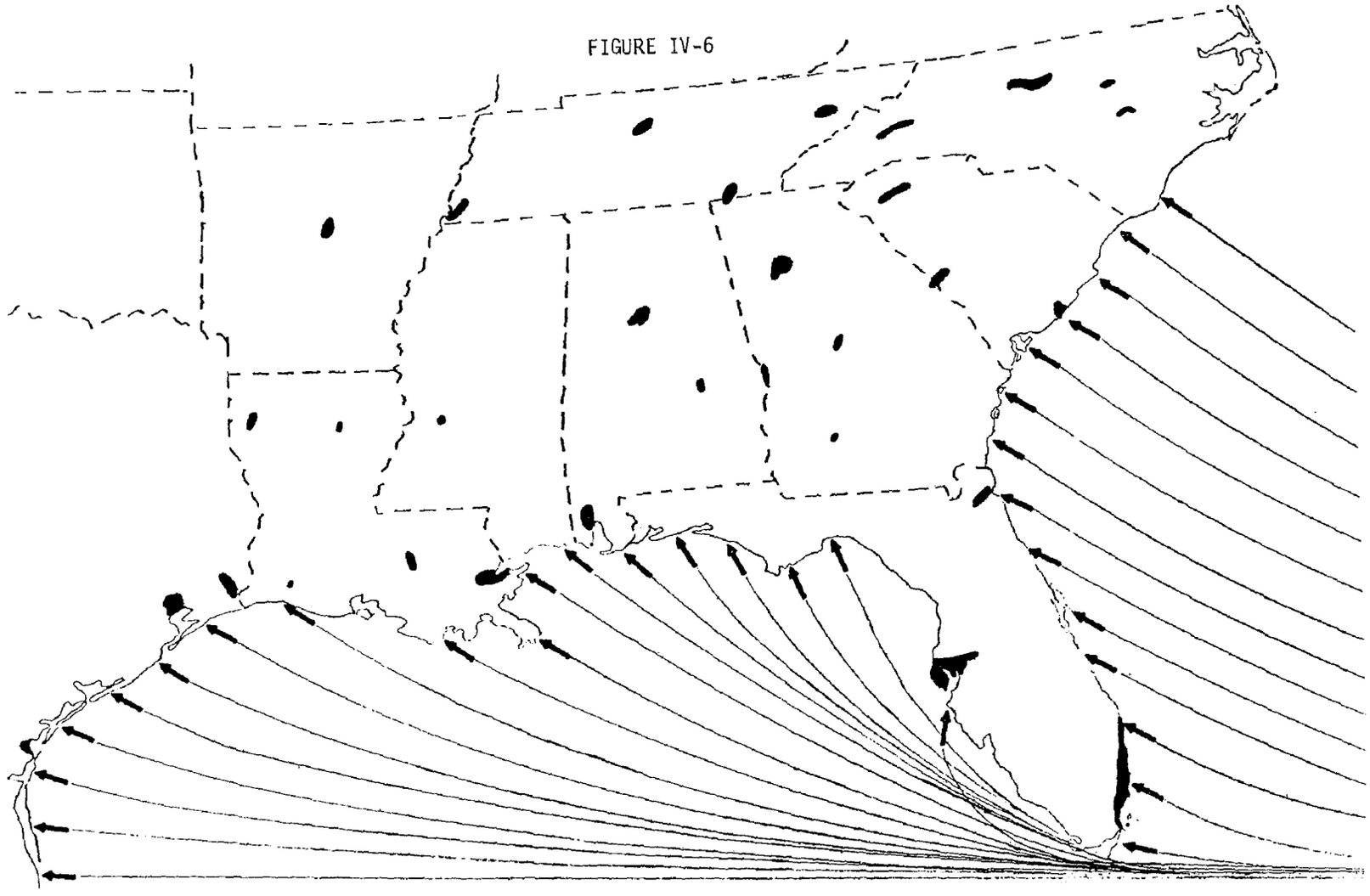

DIRECTION AND CURVATURE OF STORM PATH WITH LANDFALL LOCATION USED IN SIMULATED ANALYSIS

For each of the 160 simulated hurricane occurrences (32 landfall locations times 5 hurricane intensity groups) the number of dwellings exposed to peak gusts in wind speed categories (80-89 mph, 90-99 mph, and so forth) was obtained by summing over the affected grid areas. The expected number of dwellings damaged and the accumulated amount of damage for each wind speed category was also tabulated based on the vulnerability relationships, which were assumed to be representative of all dwellings in the coastal regions.

Figure IV-7 illustrates the loss potential measured in terms of number of single-unit residential buildings exposed. The number of dwellings exposed to wind speeds of 60 mph-or-more and 120 mph-or-more from the passage of an extreme hurricane (27.00 in.) is plotted versus landfall location from Texas to North Carolina. The effect of the overlapping of the wind speed patterns with the geographical array of properties yields two coastal areas in which more than 1 million dwellings would be exposed to winds of 60 mph-or-more if an extreme hurricane were to move onshore following the indicated paths. One area is on the northern Texas coast. The other is on the panhandle of Florida. The densely populated coastal areas of western Florida contribute to the number of dwellings in Alabama and Georgia which would be exposed if an extreme storm were to move northward just skirting the western Florida coastline. The number of dwellings exposed to winds of 60 mph-or-more would be at a minimum if landfall were in southern Florida. The reason for the low exposure in southern Florida is that the wind speed pattern would overlap only the array of dwellings located on the Florida peninsula.

However, when the dwellings exposed to winds of 120 mph-or-more are considered, the landfall locations in southern Florida produce the greatest number of exposed structures. A landfall near New Orleans yields the second greatest amount, and a Houston area landfall is the third greatest number. The reason for the shift in patterns is that, even though the total number of dwellings exposed to moderately strong winds (60 mph) is low in southern Florida, a large percentage of these structures is located close to the coastline, making them susceptible to very high winds as the storm moves onshore. On the other hand, in the Houston metropolitan area, the smaller number of dwellings exposed to extreme high winds results from the fact that even though there are more dwellings in the general area, a large percentage of these structures is located some distance inland and takes advantage of the decrease in maximum wind speed

FIGURE IV-7

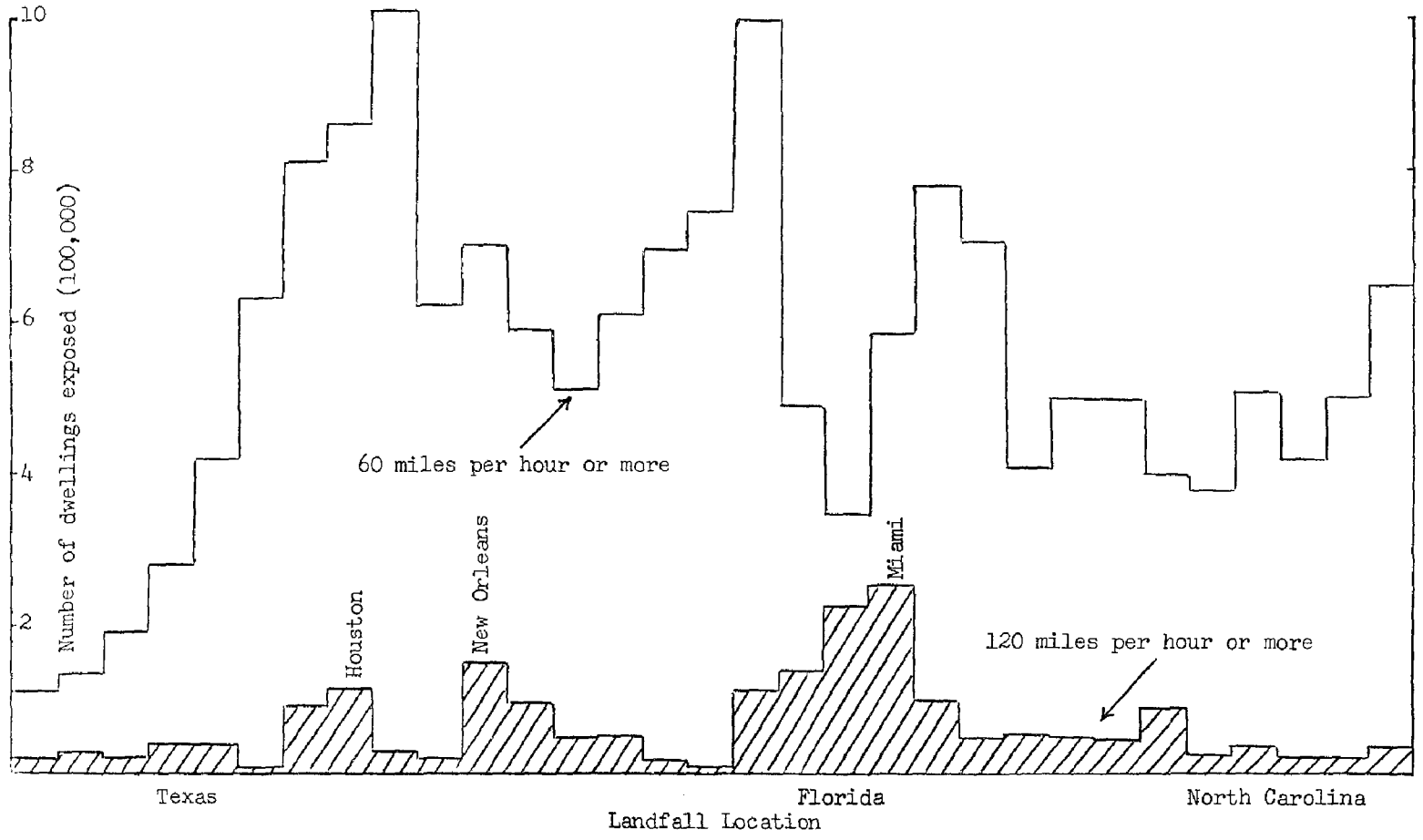

NUMBER OF SINGLE-UNIT RESIDENTIAL BUILDINGS EXPOSED TO HIGH WIND SPEEDS DURING PASSAGE OF AN EXTREME INTENSITY HURRICANE WITH SIMULATED LANDFALL AT EQUALLY SPACED INTERVALS FROM SOUTHERN TEXAS TO NORTH CAROLINA

as the hurricane moves inland.

Application of the vulnerability factors to the number of dwellings represented by the 60 mph and 120 mph categories yields a much different result. The percentage of the 1 million dwellings that would sustain damage in the Houston metropolitan area (at 60 mph-or-more) is much smaller than the percentage of the 250,000 structures in the Miami area that would be damaged (at 120 mph-or-more), assuming that building codes in Houston are comparable to those in Miami. The relative amount of loss per damaged structure is much greater for winds of 120 mph than for 60 mph, based upon the vulnerability factors. Consequently, the potential for producing a natural disaster from an extreme hurricane with the various landfalls is greatest in southern Florida. A landfall near New Orleans yields the second highest natural disaster potential, and a landfall near Houston would produce the third largest potential. This conclusion applies only to the hurricane wind hazard. When the storm surge hazard is concurrently evaluated for these landfall locations, the coastal area with the greatest catastrophe potential will likely change. In addition, the natural disaster potential of an extreme hurricane at each of the 32 landfall locations must be weighted by the probability of occurrence implied from long-term frequencies. The probability of an extreme storm with landfall in (1) south Florida, (2) the delta area of Louisiana, and (3) the central coastal section of Texas is relatively high compared with other coastal areas based on occurrences in the past 100 years.

Some of the most damaging extreme hurricanes have been those with two landfall locations; namely, that pass over southern Florida, move across the Gulf, and then go inland near the New Orleans or Houston metropolitan areas. These storms can produce extensive damage in both Florida and Texas or Louisiana. Examples of extreme hurricanes that were of this type are as follows:

Hurricane	Lives Lost	Economic Loss
Sept. 2-15, 1919	900	22,000,000 (1919 dollars)
Sept. 11-22, 1926	243	112,000,000 (1926 dollars)
Sept. 4-21, 1947	51	110,000,000 (1947 dollars)
Aug. 27-Sept. 12, 1965 (Betsy)	75	1,420,500,000 (1965 dollars)

6. Variation in Loss Potential Caused by Level of Hurricane Intensity

In the previous section, the effect of the overlapping and interaction of an extreme hurricane's wind speed pattern with the coastal array of the populations-at-risk was considered. Landfall of the extreme hurricane at several locations along the coast created a high catastrophe potential. In this section, the effect of hurricane intensity upon catastrophe potential is discussed.

Five hurricanes with identical path, speed and relative size were simulated at each of the 32 landfall locations. Storm intensity ranged from 27.00 inches (upper limit of extreme hurricane category) to 29.00 inches (upper limit of minimal hurricane category). When the number of dwellings affected was plotted against landfall locations for the four other intensity levels, the resulting relationships were different from those of the extreme hurricane. The reason is that changes in size, shape and gradient of the wind speed patterns due to the change in storm intensity result in a different set of interactions with the geographical array of population-at-risk spread over the coastal states from Texas to North Carolina.

In Table IV-3 an indication of the effect of changing hurricane intensity upon loss potential is expressed in terms of number of buildings exposed to a given wind speed and relative amounts of damage, as compared with that caused by an extreme hurricane.

TABLE IV-3

LEVEL OF LOSS POTENTIAL AS A PERCENTAGE INDEX OF DAMAGES CAUSED BY AN EXTREME HURRICANE WITH LANDFALL NEAR HOUSTON, NEW ORLEANS AND MIAMI

3a. Comparison of the number of single-unit residential buildings exposed to winds of 100 miles per hour or more during passage of an extreme hurricane with the number exposed during the passage of hurricanes of lesser intensity.

	HURRICANE INTENSITY				
	EXTREME			MAJOR	MINIMAL
Landfall location	27.00 in.	27.50 in.	28.00 in.	28.50 in.	29.00 in.
near Houston	100 %	59 %	19 %	5 %	< 1 %
near New Orleans	100	79	38	19	< 1
near Miami	100	92	66	12	< 1

3b. Comparison of the amount of wind-caused damages incurred during the passage of an extreme hurricane with damages caused by the passage of hurricanes of lesser intensity.

HURRICANE INTENSITY

Landfall location	27.00 in.	27.50 in.	28.00 in.	28.50 in.	29.00 in.
near Houston	100 %	54 %	23 %	7 %	2 %
near New Orleans	100	60	26	9	2
near Miami	100	56	24	8	2

The number of dwellings exposed to winds in excess of 100 miles per hour for a 28.00 in. intensity hurricane would be about 66% of the number exposed during an extreme hurricane when landfall is near Miami. The percentage is only 19% when the landfall is near Houston. The difference between Houston and Miami is due to the distribution of dwellings relative to the coastline. However, the amount of damage for a major hurricane (28.00 in.) is about the same (25%) at both cities when compared to losses incurred during the passage of an extreme hurricane. At Miami, the absolute amount of damage is greater than at Houston for an extreme hurricane.

7. Combined Effect of Storm Path and Intensity on Loss Potential

One way to look into the future is to examine the past. Estimation of the current catastrophe potential associated with a recurrence of past hurricanes would be dependent upon the known physical characteristics of the hurricane (storm intensity, speed, size and age) and its path relative to the spatial array of the current populations-at-risk and their vulnerabilities. It is difficult to integrate the multitude of interactions necessary to make this estimate, especially when the only information that is commonly available are maps of the storm's track (Cry, 1965). There is much additional information available on characteristics from a number of different sources which is pertinent to this estimation problem and which should form the basis of a severe storm climatology. Natural hazard simulation is one means of synthesizing this information with population-at-risk data and translating it into a measure of catastrophe potential.

A recurrence of a number of past hurricanes was simulated in order to examine how the level of catastrophe potential is related to

storm intensity (central barometric pressure in inches of mercury) and storm path. In the past 100 years, 66 hurricanes affected those coastal areas that adjoin the western Gulf of Mexico. The effect of a recurrence of each of these hurricanes upon populations-at-risk in Texas and Louisiana was calculated. Damages resulting from each hurricane were indexed relative to losses caused by the most damaging storm. Frequency by index size is as follows:

DAMAGES AS A PERCENTAGE OF LOSSES CAUSED BY THE MOST DAMAGING HURRICANE	NUMBER OF HURRICANES
1 - 19 %	49
20 - 39	7
40 - 59	5
60 - 79	2
80 - 100	3
TOTAL	66

In nearly 75% of the simulated recurrences, the calculated losses were less than 20% of damages associated with the most damaging hurricane. This result reinforces the idea that all hurricanes do not have the same catastrophe potential. The path of the storm relative to populated areas must also be considered. No matter how intense a storm might be, it is not a damaging storm unless it affects a population-at-risk which is vulnerable to damage. Climatological information taken by itself cannot be used to determine loss potential.

Seventeen of the past hurricanes would have been classed as extreme hurricanes using Dunn and Miller's (1964) criteria. Twelve would be major events and the remaining 37 would be of minimal intensity. Calculated damages resulting from the 17 extreme storms exhibited a wide range in amounts in spite of the fact that all of the storms were of severe intensity.

The level of loss potential is dependent upon a combination of storm intensity and path. To define the form of this dependence, calculated damages from each of the simulated hurricanes with landfall locations given in Figure IV-6 were indexed relative to losses from the most damaging hurricane of extreme (27.00 in.) intensity.

If the production of a natural disaster can be defined in terms of relative amounts of damage, then data in Table IV-4 suggest that hurricane intensity is a necessary condition, but not a sufficient condition for the creation of a natural disaster. There are a number of occurrences

listed in the table exceeding, say, a 20% index for high intensity (extreme) storms and none for low intensity (minimal) storms. However, it should be noted that calculated damages are indexed relative to the most damaging 27.00 in. intensity hurricane. A 27.00 in. hurricane is a relatively rare event. Consequently, a similar indexing was made using the most damaging storm with a central pressure of, in succession, 27.50 in., 28.00 in., or 28.50 in. as the intensity level for the most damaging storm. In these cases the lower intensity (minimal) hurricanes have a greater number of higher index numbers, but the importance of storm intensity as a necessary condition in producing a high level of loss potential still holds.

TABLE IV-4

SIZE OF DAMAGE INDEX FOR EACH OF FIVE HURRICANE INTENSITIES AT 32 LANDFALL LOCATIONS[1]

Calculated Damages as a Percentage of Losses Caused by Most Damaging Hurricane	HURRICANE INTENSITY				
	EXTREME			MAJOR	MINIMAL
	27.00 in.	27.50 in.	28.00 in.	28.50 in.	29.00 in.
0 - 9%	1	11	24	32	32
10 - 19	11	10	5	0	0
20 - 29	7	5	3	0	0
30 - 39	3	1	0	0	0
40 - 49	4	2	0	0	0
50 - 59	2	1	0	0	0
60 - 69	0	1	0	0	0
70 - 79	1	1	0	0	0
80 - 89	1	0	0	0	0
90 -100	2	0	0	0	0
TOTAL	32	32	32	32	32
Maximum wind speed (peak gust)	165	145	130	115	100

[1]The index for the most damaging hurricane is 100%.

The fact that high intensity is not a sufficient condition for producing a high loss potential can also be shown in Table IV-4. Even though the simulated hurricanes were of extreme intensity, a number of them did not produce large amounts of damage. There are still stretches along the Gulf and South Atlantic coastlines across which an extreme

hurricane can move and yet produce only a small aggregate damage. However, because of the rapid growth in density and spread of population-at-risk in hazardous coastal areas, this situation will not continue very far into the future. This possibility can be tested by increasing the density and spread of population-at-risk in hazardous coastal areas on the computerized grid system using various sets of assumptions about future growth.

8. *Other Factors Affecting Estimation of Loss Potential*

Additional factors must be considered when possible reasons for various levels of loss potential are being sought. The effects of the speed and size of a hurricane in setting the level of loss potential are fairly obvious with other factors held constant. A fast-moving storm will expand the size of the overland wind speed pattern but reduce the duration of the period of high winds. Increasing the size of the storm increases the size of the inland wind pattern and its resultant loss potential. Both of these factors were held constant in the simulation of hurricanes at the 32 landfall locations.

A less obvious, but important, consideration is the degree of effectiveness of the interaction of the wind speed severity patterns with the geographical arrays of populations-at-risk in influencing loss potential. The level of effectiveness is dependent upon the existence and horizontal extent of areas containing very high wind speeds which cause a disproportionate amount of damage. Vulnerability relationships are highly non-linear. Given that a hurricane has sufficient strength (as determined by its intensity) to produce very high wind speeds, the realization of its inherent loss potential depends upon the overlapping of these areas of very high winds with the population-at-risk.

In general, the size of areas affected by wind speeds of various severities depends upon storm intensity. In the computer model, when a hurricane moves onshore on a path perpendicular to a straight coastline, the land area affected by winds of, for instance, 90 miles per hour is 80 square miles for a minimal intensity (29.00 in.) hurricane; 2000 square miles for a major (28.00 in.) hurricane; and 4800 square miles for an extreme (27.00 in.) hurricane. However, when the angle of the storm path is different from a right angle course to the coastline, the size and shape of the high wind areas become distorted. This is also true when the path has a curvature. In addition, irregularity in coastline configurations,

including the existence of offshore islands close to the mainland, makes it difficult to define the location of the "effective coastline" for placing the hurricane's landfall position. In the hurricane model, the factor for decreasing the wind speed with distance inland begins at the landfall location.

To illustrate the effect of these two factors upon the determination of simulated loss potential, the hurricanes were rerun for five intensity categories at each of the 32 landfall locations, assuming a uniform (saturated) density of the populations-at-risk throughout the coastal states. In effect, this assumption eliminates the influence of the geographical variability of populations-at-risk in determining whether a particular hurricane will attain its inherent loss potential. As a result, the variability in calculated damages among the 32 landfalls is dependent solely upon the relative sizes of the areas affected by very high wind speeds. All of the physical characteristics of the storms were held constant except the angle and curvature of the path relative to the coastline. The degree of coastline irregularity varies widely among the 32 landfall locations. Damage amounts were indexed against losses in the most damaging storm. The following is a frequency count by size of the damage index for the 32 extreme intensity (27.00 in.) hurricanes. For comparative purposes the frequency count is also given using the current population-at-risk, as listed in Table IV-4.

Calculated Damages as a Percentage of Losses Caused by the Most Damaging Extreme (27.00 in.) Hurricanes	Current Population-at-Risk	Uniform (Saturated) Population-at-Risk
0 - 9 %	1	0
10 - 19	11	0
20 - 29	7	1
30 - 39	3	3
40 - 49	4	6
50 - 59	2	5
60 - 69	0	5
70 - 79	1	6
80 - 89	1	3
90 - 100	2	3
TOTAL	32	32

The wide variation in the frequency counts for a saturated population-at-risk indicates that the effectiveness of the pattern interactions can be significantly influenced by a storm's path and curvature

relative to the coastline and by the irregularity of the coastline at landfall.

Interpretation of Wind Results in Terms of Research and Data Needs

Several examples have been given of some applications of the wind model to estimate loss potential of hurricane winds to populations-at-risk along coastal sections of the southern and eastern United States. The purpose has been to use results of these applications as a vehicle for enumerating the type of research and data needed to improve the usefulness of output from this type of analysis.

1. Data Needs

The same definitions are used to represent the four populations-at-risk in the eastern United States as were used in California so the informational requirements are comparable. Refer to the section on data needs in Chapter III for a discussion of the current deficiencies in population-at-risk and vulnerability specifications.

2. Research Needs

As with the earthquake model, useful estimates of the loss potential evidently can be obtained with the use of a simple mathematical model. The output of the hurricane wind model can be improved by use of the local exposure factor which is currently being put into computer memory for each grid point. Additional work must be done to test the physical validity of various assumed combinations of hurricane characteristics (intensity, storm speed, storm size, path, landfall on an "effective coastline") in altering the size and shape of geographical areas affected by very high winds during the passage of a hurricane.

The Storm Surge Hazard

The worst storm surge catastrophe, in terms of lives lost, occurred in 1900 at Galveston when 6000 persons were killed. Early warning procedures of the United States government have drastically reduced loss of life in the United States from storm surge occurrences in recent years. Unfortunately, an early warning of an impending surge was not made several years ago in East Pakistan, and resulted in the death of 500,000 people. Property damage in the United States resulting from storm surges has increased very rapidly over the years because of such things as

increased numbers of structures built in exposed areas, value of these structures, and cost of repair or replacement. In the 14-year period (1957-1970), property damage amounting to nearly $2 billion can be attributed to coastal flooding resulting from four hurricanes that affected coastal areas of the Gulf: Hurricane Audrey, Louisiana, 1957; Hurricane Carla, Texas, 1961; Hurricane Betsy, Louisiana, 1965; Hurricane Camille, Louisiana and Mississippi, 1969. A recurrence of other hurricanes that occurred in the years prior to 1957 would probably also cause comparable storm surge losses to the geographical distribution and value of current structures located in coastal areas of the Gulf. Computer simulation is being used to make damage estimates based upon a recurrence of these earlier hurricanes.

A storm surge is defined as an increase in water level above normal tidal action, caused by storm conditions. Along the Gulf and lower eastern coastline of the United States, a storm surge usually accompanies the passage of a hurricane. It may be as small as one to two feet above normal tide levels or it may exceed 20 feet, as happened when Hurricane Camille moved across the Mississippi coastline in 1969. Storm surge-caused damages exceed wind-caused losses in many hurricanes. The depth of the hurricane surge, as it is sometimes called, is dependent upon a complicated set of interactions between the path, intensity, speed, and size of the hurricane with sea bottom and coastline configurations. Local conditions can cause a variability in surge depth of a number of feet within a distance of only a few miles. However, some general relationships can be constructed about the magnitude of the surge as influenced by the major causative factors. These relationships are the basis for the development of the storm surge model. The storm surge pattern associated with each hurricane has its unique qualities, but there are also consistencies among hurricane surges which can form the basis for the development of a simple mathematical model to approximate the process.

1. Factors that Influence Depth of the Hurricane Surge

A number of factors can affect the depth of the storm surge along coastal areas (Friedman, 1971).

a. Effect of Reduced Barometric Pressure

Over the open ocean, the only factor that contributes to the still water depth of the ocean surface is reduced atmospheric pressure. The level of the ocean surface increases in areas of low atmospheric pressure. Beneath the center of a severe hurricane, the ocean surface may be drawn upward by as much as two or three feet. The level of the sea surface is increased by about one foot for each inch of mercury reduction in atmospheric pressure. Severe hurricanes can have central atmospheric pressures of only 27 to 28 inches of mercury, or two to three inches below a normal atmospheric pressure of 30 inches. However, waves of 50 feet or more in height may be superimposed upon this deep ocean "surge" of two or three feet. The effect of reduced atmospheric pressure on the depth of the surge probably also holds near coastlines but the wind effect overshadows its influence.

b. The Wind Effect

The wind effect does not increase the still water depth of deep ocean waters. However, as the hurricane crosses the Continental shelf and moves toward a coastline, its influence on surge depth increases rapidly as the ocean depth decreases. The still water level may be increased by 15 feet or more as onshore winds of hurricane-force drive the water shoreward where it "piles up" along the coastline. This wind-caused portion of the storm surge, along with the portion caused by reduced atmospheric pressure, is added to the level of the normal lunar tide which happens to be occurring as the hurricane moves onshore. Finally, superimposed upon the confined still water level of the storm surge and lunar tide are the wind-induced waves. The still water level is defined as that level which is approximately midway between the aggregate of the troughs and peaks of these storm waves.

Onshore winds of a hurricane approaching the Gulf or East coast occur to the right of the storm track (as one looks in the direction toward which the hurricane is moving). The peak level of the surge is usually 10 to 20 miles to the right of the storm track. In some cases it may be as much as 35 miles to the right of the track. Occasionally, because of sea bottom and coastline conditions, the peak surge may even occur to the left of the track of the hurricane's center.

The configuration of the sea bottom near the shoreline and the coastline itself can greatly influence the resulting storm surge level and

produce large unpredictable local variations in depth. In general, a gently upward-sloping sea floor producing shallow ocean depths near the shoreline contributes to a maximum buildup of wind-driven water along an open coastline. Bays, estuaries or irregular shaped coastlines that cause a convergence of the wind-driven waters can produce storm surge levels that are twice as great as the depth of the surge on an open coastline. When the surge is forced up a narrow channel, such as a river bed, it may appear as a wall of water.

If the ocean remains relatively deep near the coastline, there is much less tendency for the water to pile up on the seacoast as a hurricane approaches and the resulting storm surge will not be as deep as it would be along a coastline where offshore waters are shallow. To offset this affect, wind-driven waves will be much higher on the coastline where the ocean is deep near the shoreline than waves along coastline areas where offshore water is shallow. Portions of the Texas and Louisiana coastlines represent areas where offshore water is shallow, and there are deep storm surges and less intense wave action when a hurricane occurs. On the other hand, oceanside sections of Miami represent a coastline where offshore water is relatively deep, leading to a relative shallow storm surge, but intense wind-driven wave action when a hurricane strikes that area. The bay effect increases the storm surge depth potential on the west side of Biscayne Bay as compared with that on the oceanside.

c. The Effect of Waves

A brief description of the damage potential of wave action is given by the Environmental Science Services Administration (1967):

> Wave and current action associated with the surge also causes extensive damage. Water weighs some 1700 pounds per cubic yard; extended pounding by giant waves can demolish any structures not specifically designed to withstand such forces. Currents set up along the coast by the gradient in storm-surge heights and wind combine with the waves to weaken coastal structures. Many buildings withstand hurricane winds until, their foundations undermined by erosion, they are weakened and fail.

Some account must be taken of the damaging effect of the superposition of wind-driven waves upon the (still water) depth of the tidal surge. Runup from breaking waves on a sloping surface can add a number of feet to the effective depth of coastal flooding. In addition, the

battering effect of the rapidly moving water can add appreciably to the damage potential of the surge.

Wind-driven waves transport very little water in the open sea, but near shore these waves may produce a significant transport of water shoreward. Waves parallel to a beach carry considerable water onshore. Water moving shoreward from a wave breaking on a beach has a large amount of momentum and it may run up a sloping surface to an elevation above the still water line which is twice the height of the wave before breaking. As a result, run-up water can spill over into areas which are a number of feet higher than the still water level on the seaward side of the beach. This overtopping process is dependent upon such things as wave height, wave frequency, wave steepness, slope of the beach, wind conditions, and the depth of water near the beach which determines how close to shore these waves can get before breaking. The U. S. Army Corps of Engineers estimates run-up to be five to seven feet along beach areas on southern Florida beaches near Miami and also along eastern North Carolina beaches. In other coastal areas where offshore waters are shallower and large waves are less likely to occur, the run-up is less. Two to three feet appears to be a representative increment. In bays and estuaries, the run-up is even less because only short period waves of low height can form in the shallow waters.

Shallow-water waves, when the fetch is short, are not high and will produce a run-up of only one or two feet. Under these conditions the greatest wave wash damage potential will occur near the natural shoreline. Consequently, when offshore waters are relatively deep close to the shoreline, depth of the surge (still water depth) will not be large, but superimposed wave action will be great with considerable run-up potential. On the other hand, when offshore waters are relatively shallow (still water), depth of the storm surge may be large, but the superimposed wave action will be less with lower run-up distances.

If waves break offshore before reaching the coastline, very little run-up occurs; however, the water carried shoreward by the breaking waves cannot move back to sea as rapidly as new water is sent shoreward by subsequent wind-driven waves. This effect is called "wave set-up", which is the piling up of water near the shore caused directly by wave action. The maximum amount of wave set-up occurs at the beach line. The set-up of breaking waves may amount to three feet of the total storm surge on a beach. It is estimated that under certain conditions wave set-up may even

amount to as much as six feet of the surge. Wave set-up would be important on an open coast, such as those near Miami, where ocean depth increases rapidly with distance from the shoreline and enables large waves to approach to very near the coast before breaking. Peak water elevation measured on a beach will be higher than recorded at tide gages which are located some distance seaward in order to also give information on low tide. Therefore, the effect of wave set-up is less pronounced on the gage recording than actually occurs on the beach.

If the land is low-lying and level, the surge depth will be greatest a short distance inland. Depth of the surge decreases both seaward and landward of this point. The amount of decrease landward will be about one foot for each 2.75 miles inland on low-lying land similar to that found in the Mississippi River delta of Louisiana (Corps of Engineers, 1965). For instance, if the maximum surge were 12 feet near the coast, the surge would be ten feet deep approximately six miles inland. Wave heights at this distance inland could add another two to three feet to the surge depth if winds were blowing onshore at nearly 100 mph. However, in the Mississippi delta area, swamp grasses help to dampen the height of waves developed on storm surge waters forced inland by the wind.

d. The Effect of Rainfall

A foot or more of rainfall in a 24-hour period over a large area can easily be produced by an approaching hurricane (Goodyear, 1968). Resulting flood waters can be trapped in rivers, bays and estuaries along the coastline by the tidal surge which reverses direction of the normal drainage flow patterns. These trapped flood waters then add to the depth of the storm surge.

e. Effect of Lunar Tides

Lunar tides, as defined in this report, refer to the predictable astronomical tides which normally affect coastal areas. Lunar tides in coastal sections of the Gulf could add (or subtract) a foot or more to the depth of the storm surge, depending upon the timing of storm occurrences with times of high or low tide. As one moves northward from Florida along the Atlantic coastline, the maximum lunar tide increment that could be added (or subtracted) increases in size.

f. Effect of the Earth's Rotation

The rotation of the earth produces an acceleration to the right in any current in the Northern Hemisphere. If motion in this direction is impeded by a coastline, the acceleration is balanced by an increase in water level to the right. Consequently, the effect of the earth's rotation can increase or decrease the depth of the surge, depending upon the shape of the coastline where the hurricane crosses.

g. Effect of Land Elevation

Various factors have been discussed which have an influence upon the frequency and severity of the storm surge. Elevation of the land along the coastline is a major factor in determining the magnitude of the storm surge hazard.

Elevation conditions can vary from where the land rises abruptly near the beachline, to levels above the maximum expected storm surge, to the case where the land is level and near sea level for many miles inland. Along the Gulf and Atlantic coastlines both extremes and many middle variations exist. Barriers and other protective structures have been built to offset the lack of land elevation.

An index of the degree of exposure to the storm surge due to land elevation and distance to open water is given in Appendix G, which contains maps of the approximate location of the 10, 20 and 30 foot contours along the coastline from Texas to Maine. Along the Texas coast, the 10-foot contour is generally more than five miles from the coastline. Without some sort of protection, the population-at-risk along this seacoast strip of Texas is highly exposed to the relatively frequent occurrence of deep surges. An example of the possible geographical extent of coastal flooding is shown in Figure IV-8, which represents nigh water marks resulting from Hurricane Carla in 1961. Portions of the entire Texas coastline were inundated up to five to ten miles inland; coastal flooding depths were four to five feet near Brownsville; 150 miles up the coastline, near Corpus Christi, water depths increased to nine feet; another 75 miles northward along the coast, near where Hurricane Carla moved onshore, water depths varied from about 12 feet on open beach areas to 22 feet in an adjacent bay (high water mark). One hundred and twenty-five miles further north in the vicinity of Galveston, water depths on the beaches were about nine feet; along shores of Galveston Bay, water ranged up to 16 feet deep; at the Texas-Louisiana border, another 75 miles

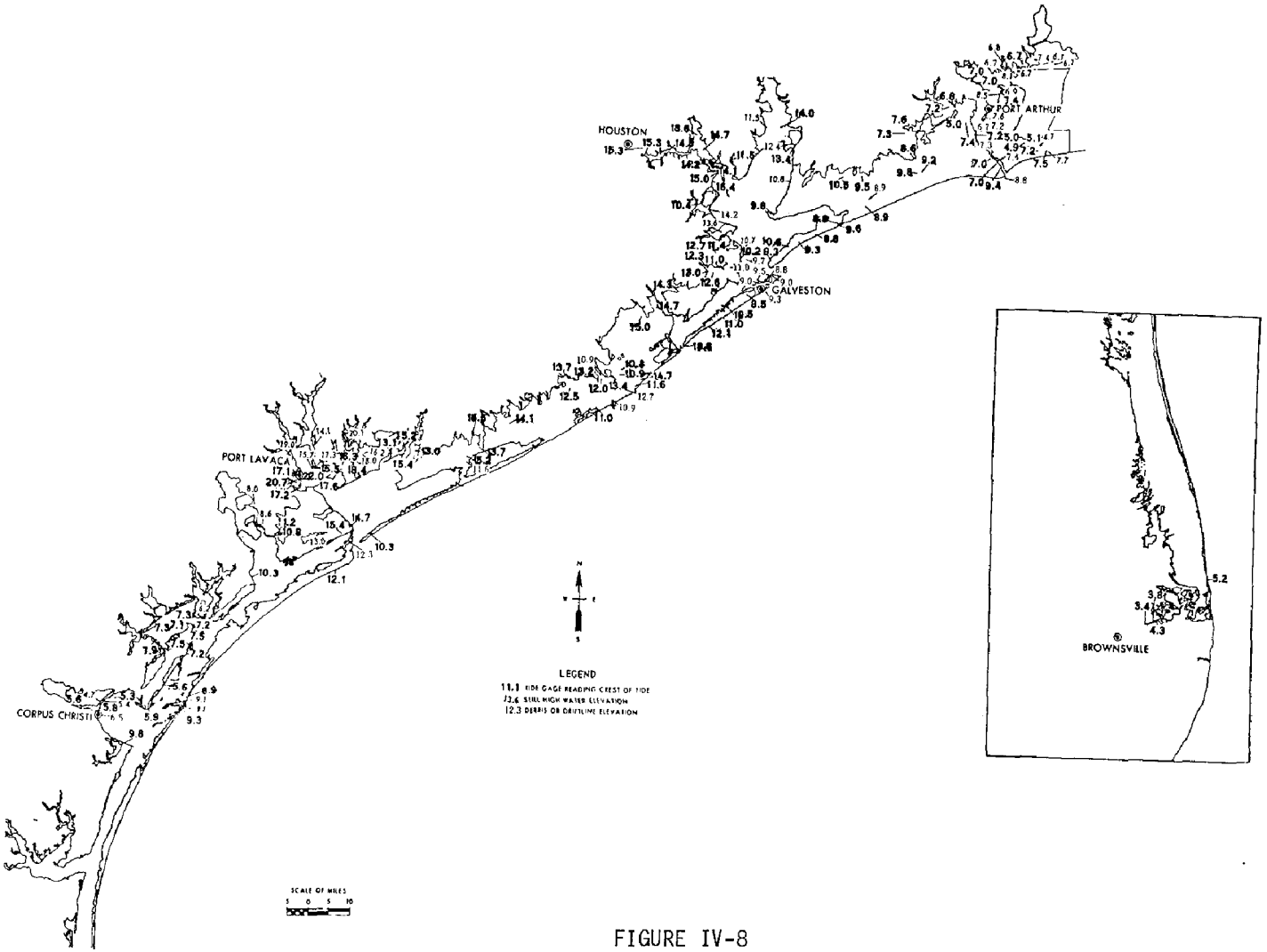

FIGURE IV-8

HIGH WATER MARKS FOR HURRICANE CARLA, SEPTEMBER 10-12, 1961. SHADED AREA INDICATES EXTENT OF FLOODING (This exhibit was prepared by the Galveston District Office of the Corps of Engineers, U. S. Army and was presented as Figure 1 on page 62 of U. S. Department of Commerce, 1961.)

up the coast, water depths were seven feet on the beaches; coastal areas of western Louisiana were also inundated. It should be noted that Hurricane Carla was an unusually large and slow-moving storm.

The ten-foot contour lies about 30 miles inland in southwestern Louisiana and more than 50 miles inland in the Mississippi delta area of southeastern Louisiana. The storm surge hazard is especially great in coastal Louisiana because of the combination of the vast extent of low-lying ground with the relatively high frequency of extreme hurricanes. In 1957, Hurricane Audrey caused an inundation of many square miles of land in southwestern Louisiana. Maximum water depth was 14 feet. Three hundred and eighty persons were drowned. Eight years later, Hurricane Betsy pushed Gulf waters across most of the Mississippi delta area of southeastern Louisiana to depths of ten to 12 feet. In some places the water was 15 feet above mean sea level. Fifty-eight persons were killed and property damage was above $1 billion. The greatest loss of life as a result of a storm surge in Louisiana occurred in 1893 when 1800 people perished in the vicinity of New Orleans.

Four years after Hurricane Betsy, one of the most powerful storms ever to strike the United States, Hurricane Camille crossed the Mississippi coastline with a storm surge depth of up to 24 feet on beach areas a few miles to the right of the storm's center. Storm surge depths reached 15 feet on Louisiana's Mississippi River delta. Total property damage was estimated to exceed $1.4 billion. A large portion of the total damage can be attributed to the storm surge. Two hundred and fifty-six persons died; most were drowned. Nearly $1 billion in damages occurred in Mississippi in spite of the fact that the 10, 20 and 30-foot elevation contours are close to the shoreline.

In coastal Alabama the contours are close to the shoreline in most areas. However, the shallow upper sections of Mobile Bay appear to present a target for deep surge waters from a hurricane with an optimally oriented track. Many areas of the Gulf and south Atlantic coastlines are protected by hurricane flood protection systems. If an exceptionally severe storm surge breached one of these protective facilities, severe damage could result because the building of dikes and other barriers greatly encourages construction of homes and industrial buildings close to highly hazardous coastal areas, as in the case of the City of New Orleans. Further east, the elevation contours along the Florida panhandle to Panama City are close to tne shoreline, minimizing the geographical

extent of the storm surge hazard area.

East of Panama City to about 50 miles north of Tampa Bay the ten-foot contour moves inland and exposes a five to ten-mile strip of low-lying land. The contours are close to the shoreline further south, including most of Tampa Bay. However, the concentration of population-at-risk and the possibility of deep surges at the head of Tampa Bay increase the catastrophe potential for the area. Water depths up to 14 feet above sea level have been observed in Tampa Bay during a hurricane passage. From Tampa to Fort Myers, the ten-foot contour lies generally five miles or less from the beachline. South of Fort Myers, the ten-foot contour moves inland. The southern tip of Florida, including the Florida Keys, is generally less than ten feet above mean sea level.

The most intense storm to strike the United States (central pressure 26.35 inches of mercury) occurred in 1935. A storm surge depth of 18 feet was reached on Long and Matacumbe Keys. Nearly 400 persons were drowned. In 1926, an extreme hurricane moved directly over Miami (barometer reading 27.61 inches at Miami). Surge depths in excess of 12 feet were reached in at least one water front location of Biscayne Bay. Damages from this hurricane (wind and storm surge combined) were estimated at $100 million (1926 dollars). More than 100 persons were killed in Miami. A recurrence of the 1926 storm would produce damages to current properties many times in excess of the original losses.

It should be noted that wind setup on a large inland lake near the coastline, such as Lake Okeechobee in south Florida, can pile large amounts of water onto leeward shores. A hurricane in 1928 caused the death of 2000 persons by drowning along the shoreline of the lake. A hurricane in September, 1947, caused water pile-up to 21.6 feet msl at Clawiston, and 20.9 feet msl at Moore Haven on the southwestern shore of Lake Okeechobee. Two years later a hurricane in August, 1949, piled water to 24.0 feet msl at Belle Glade, and 23.1 feet msl at Okeechobee on the shores of the lake. The elevation of Lake Okeechobee is about ten feet msl.

North of Miami, the ten-foot contour is close to the shoreline from Boca Raton upshore to Melbourne Beach. South of Boca Raton the land is generally less than ten feet above mean sea level. This includes Ft. Lauderdale, Hollywood, Miami and Miami Beach. The storm surge hazard in the southern tip of Florida is increased because of the low-lying land and the high frequency of extreme hurricanes. Fortunately, offshore

waters near Miami are deep. This reduces the probability of large storm surges. However, wave action can be significant on beach properties.

North of Melbourne, a large section of coastal land is less than ten feet above mean sea level. From Cape Canaveral to St. Augustine, the ten-foot contour is within a few miles of the shoreline. The general ten-foot contour is five miles or more inland from St. Augustine to Jacksonville. However, dune elevations may exceed ten feet along the beach line.

The ten-foot contour along the coast of Georgia averages ten miles or more inland, so the geographical area with a potential storm surge hazard is large. Fortunately, extreme hurricanes have not been frequent along the Georgia coast in the past 100 years. When an extreme storm does occur, and other factors are favorable, the resulting storm surge can cause considerable destruction. A hurricane in 1898 caused a 16-foot surge on the Georgia coastline and inundated portions of Brunswick, Georgia to a depth of eight feet.

The general ten-foot contour along most of the South Carolina coastline is ten or more miles inland, establishing a wide area of high storm surge hazard. A tidal surge in 1893 killed about 1500 persons near Charleston, South Carolina. In the northern part of the South Carolina coastline and the first half of the North Carolina coastline, the three contours (10, 20 and 30 feet) are located close to the shoreline. The eastern half of the North Carolina shore has a large amount of land that is less than ten feet above sea level. At one point this low-lying area measures nearly 40 miles across. From Virginia northward to New England, the open coast areas below ten feet are relatively narrow. However, because of the high density of population-at-risk, the catastrophe potential is high in a number of coastal locations.

2. Development of Storm Surge Model

For a given stretch of coastline, the depth of the storm surge will be maximized if, among other things, the track of the hurricane is perpendicular to the coastline; the atmospheric pressure at the storm's center is extremely low; the hurricane is slow moving; and it is large in size. Inasmuch as most of the important meteorological factors that contribute to the severity of the storm surge are related to the intensity of the hurricane, and intensity is directly related to the minimum atmospheric pressure at the storm's center, there is a relationship between maximum storm surge depth and central pressure. The lower the central

pressure, the greater the storm surge, with other factors held constant.

Surge depths in bays and estuaries must also be considered separately. If a bay or estuary widens inland from its mouth, the surge will dampen. On the other hand, if it narrows from its mouth to its head, the piled-up water will converge and amplify the magnitude of the surge as observed on the coastline. The effect of the offshore bottom conditions is to make the expected maximum surge dependent upon the location at which the hurricane crosses the coastline. The expected depth would be greater along the coast of Texas than in the Miami area of Florida, if hurricanes of comparable intensity were to strike each area.

The storm surge generator incorporates the various factors in the following manners.

(1) The maximum surge depth along an open coastline usually occurs near, and to the right of the storm center. In the model, an estimate of maximum depth is obtained by using procedures suggested by Jelesnianski (1967, 1972). First, an approximation of the maximum surge was obtained using a relationship between surge depth and hurricane intensity. This depth is modified by a "shoaling factor" which accounts for offshore bottom conditions. Data from a nomogram of shoaling factors for the Gulf and Atlantic coastline given in Jelesnianski was put into computer memory for each grid area along these coastlines. The maximum surge depth is also modified by a multiplicative factor which represents the effect of storm speed and the orientation of its path to the coastline. A mathematical surface was fit to Jeslesnianski's graphical representation of this adjustment factor and equations defining this surface were built into the model.

(2) Jelesnianski also presented a method for defining the location of the maximum surge depth and the shape and size of the surge depth pattern to the left and right of the location of maximum depth. However, after reviewing the literature (Nickerson, 1971; Bodine, 1969 and 1971; Harris, 1963; Jelesnianski, *et al.*, 1973) and inspecting available data on storm surge patterns associated with past hurricanes (including the 44 hurricanes and 24 tropical storms that were discussed earlier), it was decided that an approximation of the envelope of maximum surge depths could be obtained by the use of the envelope of maximum wind speeds for coastal locations that is computed in the hurricane wind model. The combined effects of storm intensity, storm speed, storm size and storm path on the shape and size of this envelope of maximum wind have already been included in the wind model. The possible distortion in this

pattern caused by combinations of the physical properties of the hurricane has been outlined. Consequently, it was assumed that the envelope of maximum surge depth on an open coastline could be derived from the computed winds. Maximum storm surge depth that occurs during the passage of a hurricane is used as a measure of severity rather than the storm depth observed at any given time during the hurricane passage, for instance, at the time of occurrence of the maximum surge. Maximum storm surge depth is a better indicator of damage producing potential for the same reason that maximum wind speeds are used as a measure of the damage potential of high winds.

A plot of observed (maximum) wind speeds versus observed (maximum) storm surge depths to the right and left of the storm center for past hurricanes suggested the use of non-linear relationship involving storm intensity as a means of converting calculated wind speeds on the coastline into a measure of surge depth. As with the earthquake and hurricane wind generators, the objective is to attempt to devise a mathematical model which is based upon consistencies among occurrences of past events. It is not expected that the simple model would be capable of exactly reproducing the storm surge pattern of each individual hurricane. However, it is hoped that when the calculated surge patterns of a number of hurricanes are obtained, the overall results will yield useful indications of loss potential.

The surge depth obtained from the calculated wind speed is also modified by the shoaling factor that is assigned to the grid point.

(3) The effect of lunar tide is approximated by the addition or subtraction of a depth increment at each grid point, depending upon the assumption regarding the timing of the maximum surge depth relative to the timing of lunar tides. The size of increment can be varied. It is larger along the middle Atlantic and New England coastlines than along the Gulf or Southeast coasts.

The basic model produces an approximation of the distribution of maximum storm surge depths along an open coastline.

a. Effect of Local Conditions

For the storm surge hazard, the effect of local conditions is of utmost importance in estimating its loss potential. The assumed influences of the following local factors were built into the generator.

(1) Offshore conditions adjacent to each grid area, as measured by Jelesnianski's "shoaling factor", are stored in computer memory as described above.

(2) Elevation of the land in each grid area was roughly estimated by superimposing a grid overlay upon elevation maps given in Appendix G. An "average" elevation of each 35-square-mile area was approximated for about 3000 grid points that represent coastal sections of Gulf and Atlantic states susceptible to the surge hazard. These elevation estimates are stored in the computer.

(3) Land character of each of these exposed grid areas was designated as "level" or "sloping." An estimate of the character of the topography was necessary for determining the percentage of the various populations-at-risk in a grid area which is exposed to a surge of a given depth. A representative variability in elevation across the grid area is assigned. The amount of variability depends upon whether the area was given a "level" or "sloping" land character code.

(4) Coastline configuration is a major influence upon the determination of a realistic estimate of surge depths. Jelesnianski and other researchers have not described, at least in published papers and reports, a method of estimating surge depth along an irregularly shaped shoreline that may include bays and estuaries. The work that has been reported relates to open, straight coastlines. In the surge generator, an attempt has been made to produce depths along an irregular shoreline that are closer to what is actually observed than the calculated depths obtained using the open coastline assumption.

A very simple set of assumptions was constructed. Each grid area from Texas to Maine, that is exposed to open water, is assigned a coastline configuration designation:

(a) Open coastline;
(b) Coastline indentation with a restricted opening to the sea--the width of the indentation becomes larger with distance inland;
(c) Coastline indentation with an opening to the sea--the width of the indentation does not change with inland distance;
(d) Coastline indentation with a wide opening to the sea--the width of the indentation narrows with inland distance.

The calculated storm surge at each of these grid areas is modified by a factor that represents the effect of the coastline configuration. The size of this multiplicative factor depends upon the type of coastline and the location of the grid area to the left or right of the storm's path:

Coastline Factor	Grid Area Lies to Left of Storm Path	Grid Area Lies to Right of Storm Path
1) Open Coastline	1.0	1.0
2) Restricted Bay	0.8	1.2
3) Bay	0.7	1.3
4) Open Bay	0.6	1.4

The assumption is that surge depths in coastline indentations on the right-hand side of the hurricane path will be greater than on an open beach. Onshore winds drive the ocean water against the coastline on the right-hand side as the hurricane makes landfall. To the left of the path, it is assumed that offshore winds reduce the surge depth within coastline indentations more than along an open coastline.

(5) Distance from water is a factor that must be included for those grid areas that have a low elevation but do not adjoin an open water area. It is assumed that surge depth decreases at a rate of two feet per six miles (the distance across a grid area) if land elevation is held constant. The duration of the period of high winds is important in determining how far inland a surge will flow. In a fast-moving storm, the surge waters have little time to be driven a great distance inland before the winds change direction and decrease in magnitude. In a slow-moving storm, the storm tide has sufficient time to move far inland if the elevation of the land is near sea level. Storm surge water moved many miles inland along the Texas coast during the slow approach of Hurricane Carla in 1961. An average storm speed is assumed for the two feet per six mile rate mentioned above.

All of the 3000 grid points that are not adjacent to open water are coded as second, third, or fourth tier grid areas away from an open beach, a restricted bay, or an open bay. The depth of the maximum surge in these areas is based upon four factors: the surge depth in the closest open water area; the distance from open water; the average elevation of the grid area; and the character of the intervening land.

(6) "High water level" is defined as the minimum level below which buildings would not ordinarily be placed. The high water level is related to the maximum height of the highest annual lunar tide. For illustrative purposes, mean high water level is assumed to vary from about three feet above mean sea level along the Gulf coast to nearly seven feet along New England coastlines.

b. Reasonableness of Computed Storm Surge Depths

The surge generator requires the same input information as is needed for the hurricane wind generator. These parameters are location of landfall, direction and curvature of path, storm intensity, storm speed, and storm size. Data on Hurricane Carla were used to obtain the computed storm surge pattern shown in Figure IV-9. Depth is expressed in feet. For depths greater than or equal to ten feet, an alphabetic designation is used: the letter A stands for ten feet, B denotes 11 feet, and so forth. The indicated depth in Figure IV-9 represents the maximum surge expected within the grid area. The depth used in the vulnerability relationships is much more shallow than the maximum depth because it is based upon a combination of the effects of elevation, land character, mean high water, distance from open water, and an averaged surge depth for that portion of the grid area covered by water.

A comparison between the calculated and observed patterns is given in Figure IV-10 for open coast and bay areas. Observed still water depths are plotted. The superimposed effect of wave action increases the effective depth of the surge as signified by gage depths in Figure IV-8. Calculated depths do not include the effect of wave action. Correspondence between calculated and observed depths is good when it is considered that very simple assumptions were used in order to obtain the open coast and bay area estimates.

An example of the use of the storm surge generator to calculate surge depths when a hypothetical storm affects the Florida peninsula is shown in Figure IV-11. The simulated hurricane moves northward, closely paralleling the Florida west coast, making landfall on the Florida panhandle. The storm then weakens as it moves northeastward across Georgia and South Carolina. Note the increased depth of water in Tampa Bay as compared with adjacent beach areas. Minor surge depths of one to three feet are calculated for the Georgia and South Carolina coastlines as the storm moves past these areas. The surge depth drops off rapidly to the left (west) of the storm path.

Major improvement in the accuracy of the estimates can be obtained by further refinement of the storm surge generator. However, results of the preliminary runs using the present model suggest that it can produce an adequate approximation of the actual storm surge mechanism for the illustrative purposes of this report.

FIGURE IV-9

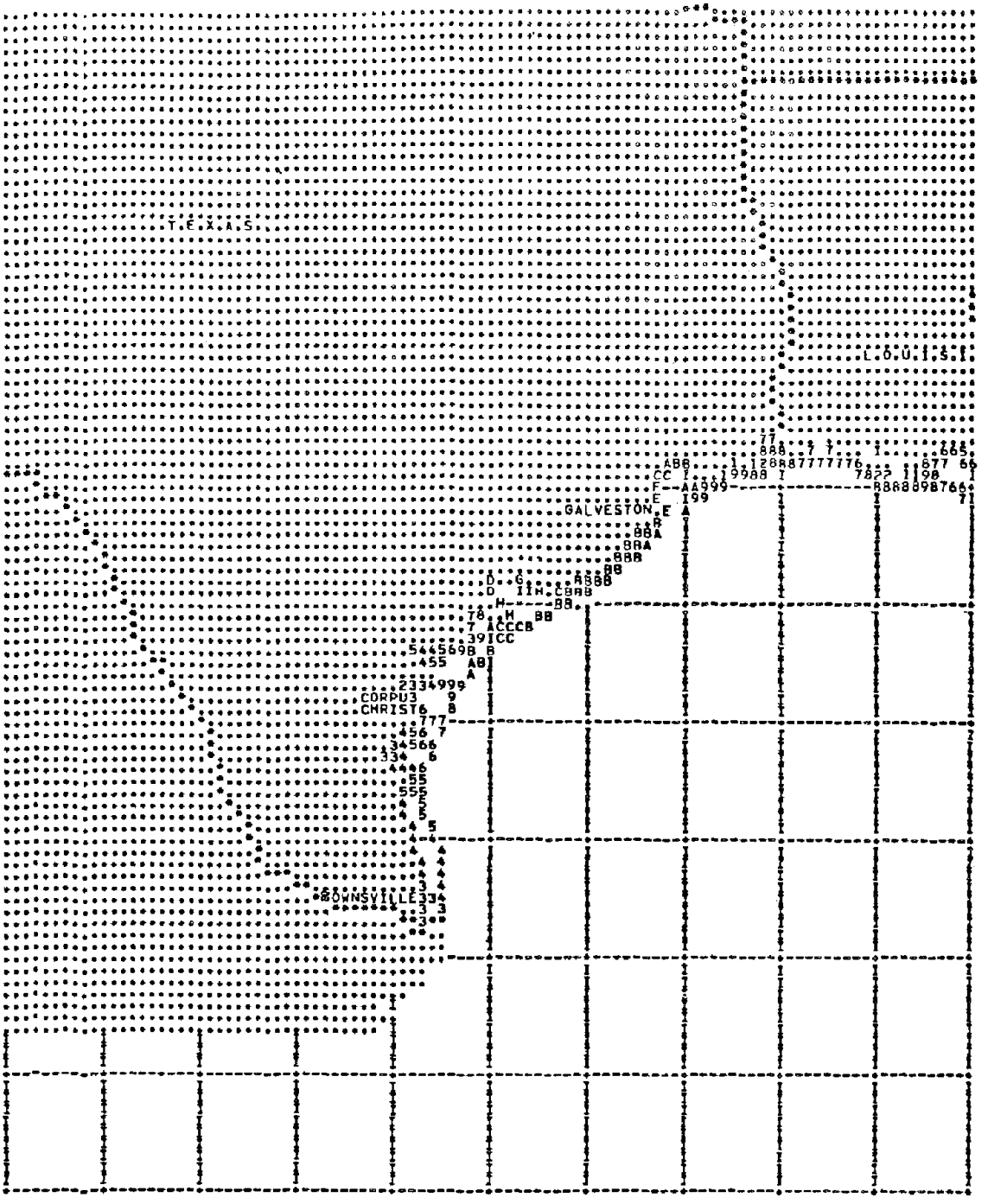

COMPUTED PATTERN OF MAXIMUM STORM SURGE DEPTH ASSOCIATED WITH THE PASSAGE OF HURRICANE CARLA IN SEPTEMBER 1961 (Depths greater than 10 feet designated by alphabetic code: A represents a depth between 10 and 11 feet, B denotes 11 to 12 feet and so forth. Superimposed wind-driven waves not included.)

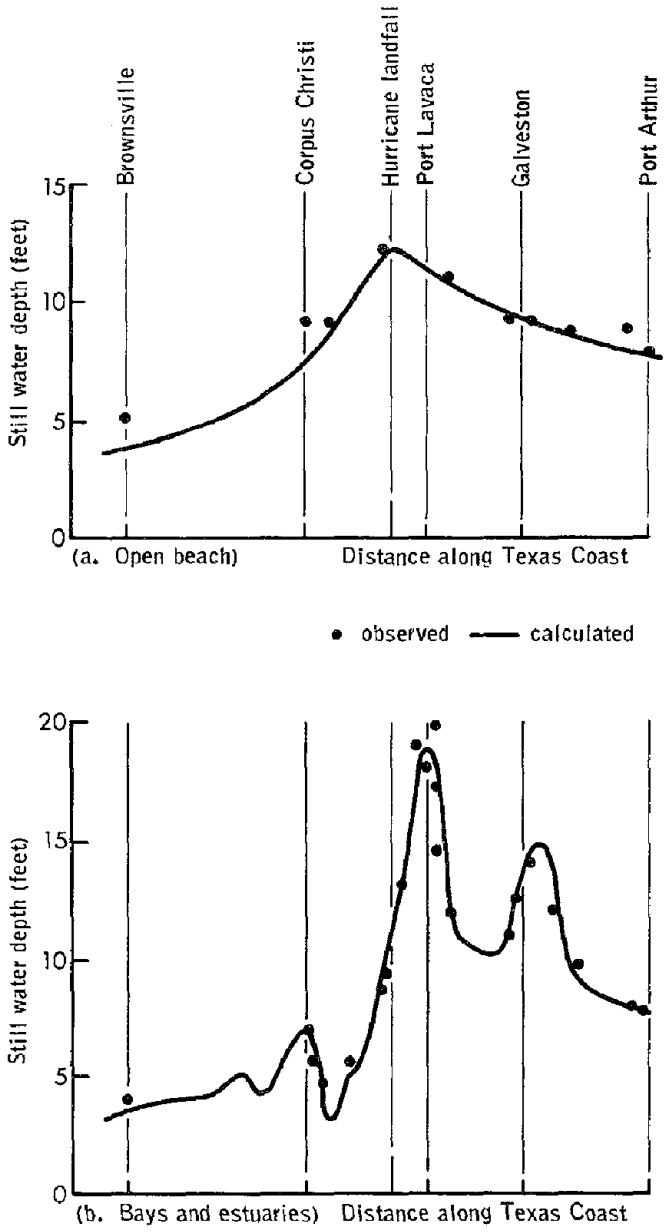

FIGURE IV–10

COMPARISON OF CALCULATED STORM SURGE DEPTH ALONG THE TEXAS COAST ASSOCIATED WITH PASSAGE OF HURRICANE CARLA (FIGURE IV–9) WITH OBSERVED STILL WATER DEPTHS (FIGURE IV–8) (effect of wind–driven waves not included)

FIGURE IV-11

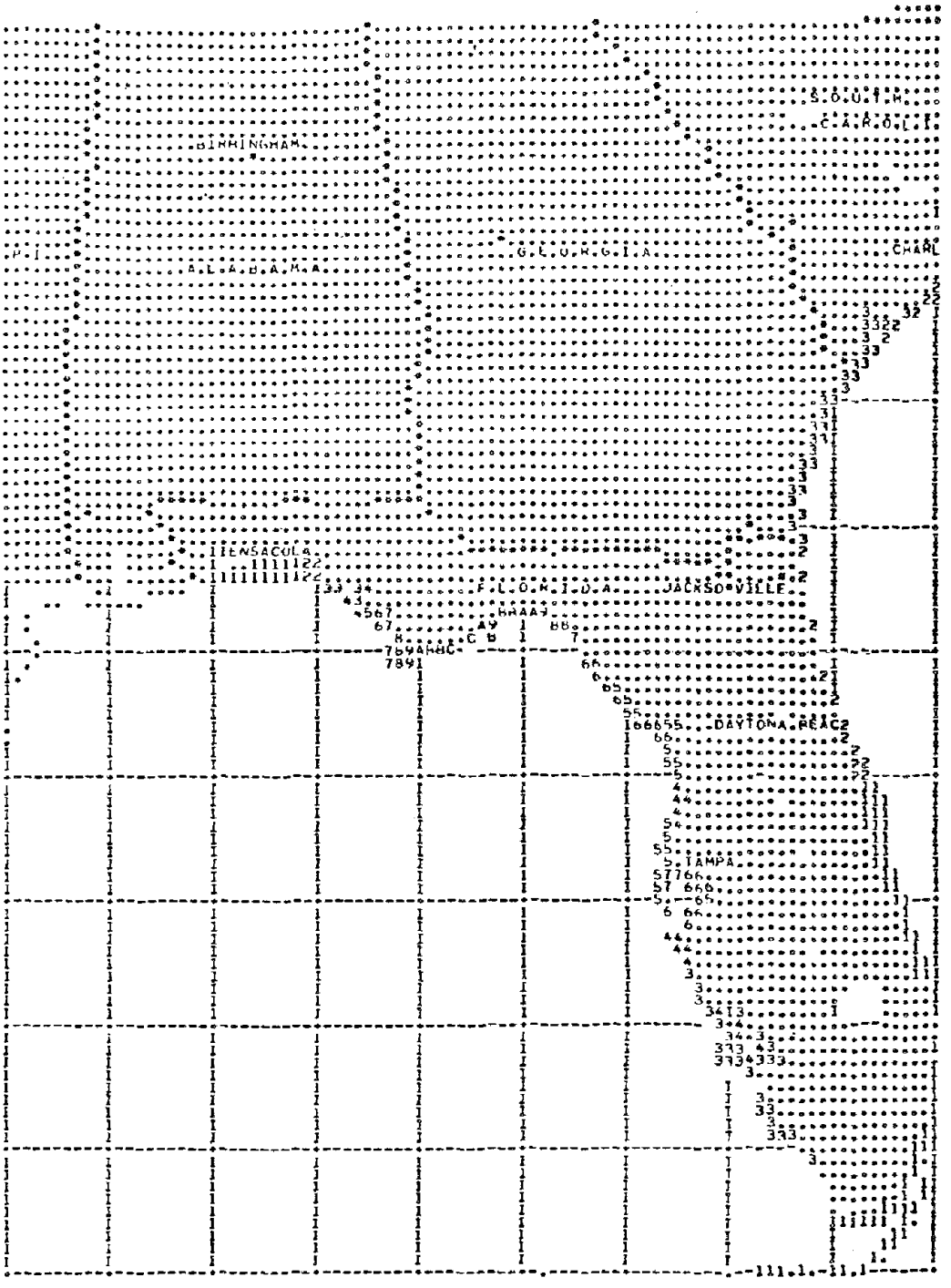

COMPUTED PATTERN OF STORM SURGE DEPTHS ASSOCIATED WITH A SIMULATED NORTHWARD-MOVING HURRICANE WHICH SKIRTS THE WESTERN COAST OF FLORIDA AND MAKES LANDFALL ON THE FLORIDA PANHANDLE

c. Population-at-Risk and its Vulnerability to Storm Surge

The four populations-at-risk described in Chapter III are represented in the 3000 grid areas that have an average elevation of less than 30 feet along the Gulf and Atlantic coastlines. Vulnerability relationships are composed of two segments for buildings. First, the percentage of the total number of buildings in a grid area that are affected by the storm surge is based upon a relationship between computed maximum surge depth, mean high water, distance to open water, land character, coastline configuration and elevation of that grid area. Secondly, the "most likely" amount of value lost when a building is affected is given in Table IV-5. The value of single unit residential buildings is based on U. S. Bureau of the Census information. As with the hurricane wind hazard, the value of other residential and non-residential buildings is expressed in a basic increment of $50,000 and $100,000, respectively.

TABLE IV-5

ASSUMED PERCENTAGE OF VALUE LOST TO AFFECTED BUILDINGS WHEN A STORM SURGE COVERS ALL OR A PORTION OF A GRID AREA

Storm Surge Depth (Feet)	Single-Unit Residential Buildings	Other Residential Buildings	Non-residential Buildings
1	18.0	9.0	4.5
2	30.0	15.0	5.9
3	40.0	20.0	7.3
4	48.0	24.0	8.4
5	56.0	28.0	9.3
6	66.0	33.0	10.2
7	72.0	36.0	11.0
8	80.0	40.0	11.7
9	86.0	43.0	12.3
10	94.0	47.0	13.0
11	100.0	50.0	13.6
12	100.0	53.0	14.2

For population, the percentage of the number of people affected in a grid area was calculated in the same manner as buildings-at-risk. Time did not permit the inclusion of social disruption relationships developed on the "Assessment of Research on Natural Hazards" project. However, to provide at least an order-of-magnitude estimate, an over-simplified casualty curve was used. Some ratios read from the curve are:

Storm Surge Depth (Feet)	Ratio of Casualties to Number of Persons Affected
1	1 per 100,000
7	1 per 10,000
14	1 per 1,000
20	1 per 100
25	1 per 10

Assumed vulnerabilities for storm surge, hurricane winds and earthquakes are based upon the very meagre amount of information that is presently available. Much additional research is needed to establish more realistic relationships.

Application of Storm Surge Model

Local conditions (land elevation, offshore configuration, coastline shape) have an important effect upon the severity of the surge hazard at any given coastal location. The character of coastal lands also controls the possible number and density of population-at-risk exposed to the hazard, as shown in the topographic maps in Appendix G. As a result of these influences, there is a greater variability in catastrophe potential of the storm surge hazard than in the hurricane wind hazard for hurricane landfalls spaced along the coast from Texas to Maine.

Loss potential of the storm surge associated with these landfalls exhibits a large variation in terms of the size of populations-at-risk exposed, the number affected, and the relative degree of the effect as measured by a damage index. The simulated influences of current protection devices, such as seawalls and sand dunes along the coast, tend to reduce the magnitude and variability of loss potential along the coastline.

The physical characteristics of the hurricane also exert a major influence upon the loss-producing capabilities of the storm surge. It was indicated during the discussion of the wind hazard that all hurricanes do not have the same damage potential for winds; the same holds for surge. Intensity of the storm, as given by the minimum barometric pressure, is a good measure of inherent damage-producing capabilities. Table IV-6 illustrates the calculated variation in loss potential of a hurricane's storm surge with change in storm intensity when other physical variables are held constant (location of landfall, storm speed, storm size and path).

Landfall of the hypothetical hurricane is on the central Texas coast about 25 miles northeast of Corpus Christi.

TABLE IV-6

VARIATION IN LOSS POTENTIAL OF THE STORM SURGE ASSOCIATED WITH AN OCCURRENCE OF A HURRICANE WITH LANDFALL ON THE TEXAS COAST NORTHEAST OF CORPUS CHRISTI

a. SINGLE-UNIT RESIDENTIAL BUILDINGS

Hurricane Intensity Description	Intensity (Minimum Barometric Pressure)	Index of Number Affected	Index of Damage
Minimal	29.5 in.	0	0
	29.0	2	2
Major	28.5	76	24
	28.0	300	158
Extreme	27.5	610	469
	27.0	1000	1000

b. POPULATION

		Casualty Index
Minimal	29.5 in.	0
	29.0	1
Major	28.5	43
	28.0	174
Extreme	27.5	478
	27.0	1000

In the past 100 years, there were 13 minimal intensity hurricanes that affected the stretch of Texas coastline, which includes the simulated landfall (refer to Figure IV-4). Calculated loss potential of these storms as given in Table IV-6 is very small (damage index 2 or less). On the other hand, there were four extreme hurricanes during the same period. The relative loss-producing capabilities of the surge associated with an extreme intensity storm are large if the other physical factors are comparable (damage index between 400 and 1000).

The variability of loss potential due to landfall location can be shown by shifting landfall of a 28.00 in. intensity hurricane from the point northeast of Corpus Christi to a location near, say, the Texas-Louisiana border (see Figure IV-6). The damage index associated with the new landfall increases to 5750 for single-unit residential buildings, as compared with an index of 158 for a 28.00 in. intensity storm and 1000 for

a 27.00 in. intensity storm near Corpus Christi. The casualty index increases to 7740, as compared with index of 174 for an identical hurricane with a landfall near Corpus Christi.

The effect of hurricane intensity upon the level of loss potential to a vulnerable urbanized area can be shown by simulating the occurrence of two extreme intensity hurricanes with landfall at Miami, Florida. The first hurricane has an intensity of 28.00 in. (the least intense storm within the range defined for the extreme category). The second storm, with other physical characteristics identical to the first storm, has an intensity of 27.00 in. (near the most intense storm in the extreme category). The path of the simulated storms is across the tip of southern Florida into the Gulf of Mexico on a path slightly north of west, after making landfall at Miami Beach. Figures IV-12 and 13 denote the simulated maximum wind speed patterns associated with the 28.00 in. and 27.00 in. intensity storms. Figures IV-14 and 15 represent the storm surge patterns of these hurricanes.

The ratio of the number of people exposed to the storm surge as compared with the number exposed to high winds during passage of a 28.00 in. intensity hurricane over Miami is about 1 in 4. This compares with a ratio of 1 in 300 for a comparable storm with landfall near Corpus Christi.

Table IV-7 gives the percentage increase in two measures of loss potential--number exposed and damage index--when the effects of a 28.00 in. intensity storm are compared with those of 27.00 in. storm which both pass over Miami.

A relatively small change in hurricane intensity can change its loss potential by a considerable amount.

Interpretation of Storm Surge Results in Terms of Research and Data Needs

Informational deficiencies on population-at-risk and vulnerability mentioned in connection with the earthquake and hurricane wind hazards also exist for the storm surge hazard. As far as could be ascertained, an inventory of buildings along the coastal sections of the Gulf and Atlantic coasts of the United States does not exist. Information on vulnerability to damage of exposed buildings is also needed.

Results of preliminary computer runs using the storm surge generator suggest that a realistic approximation of the actual storm surge mechanism can be obtained by the use of a simple model. The question of

FIGURE IV-12

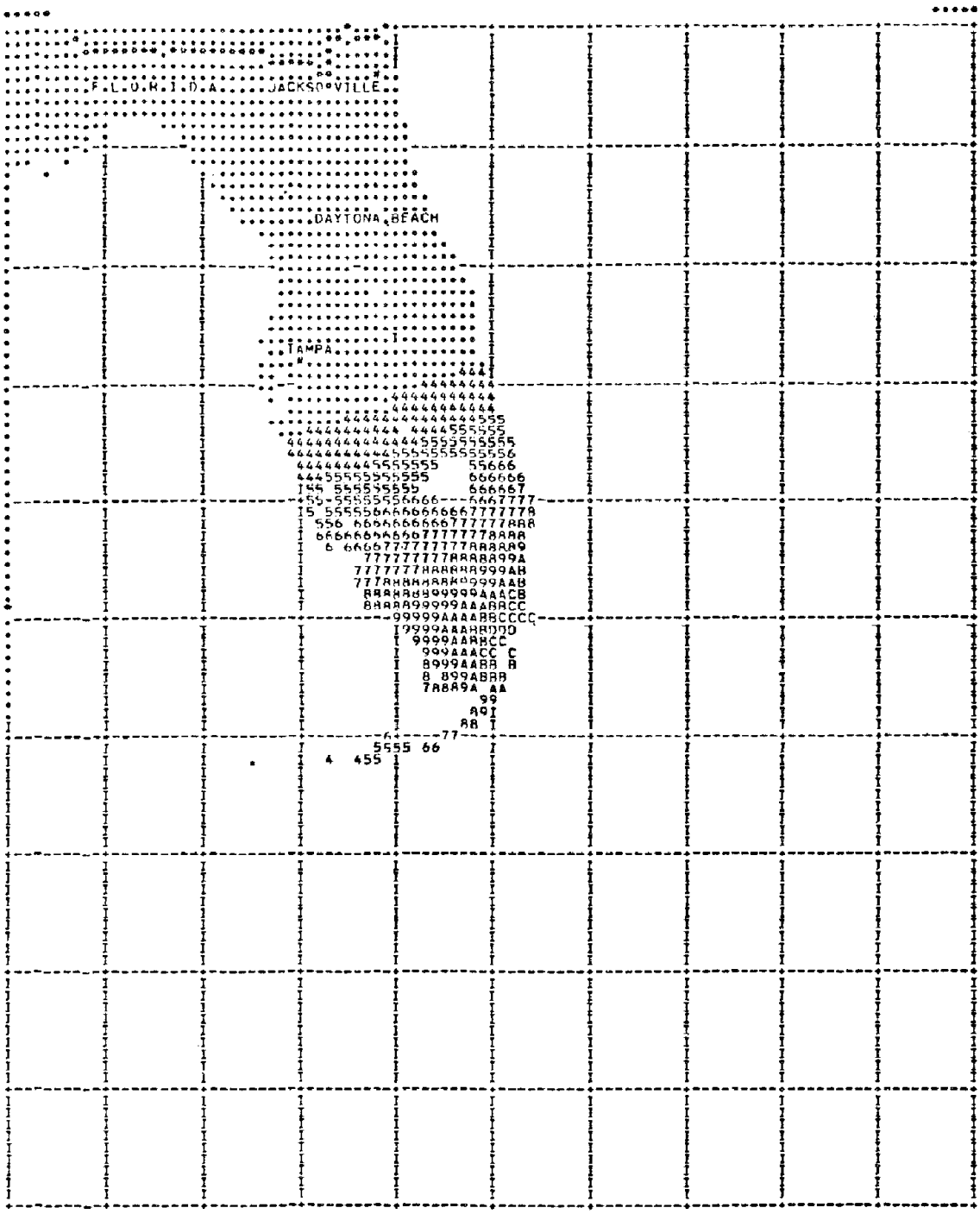

COMPUTED PATTERN OF MAXIMUM WIND SPEED ASSOCIATED WITH PASSAGE OF AN EXTREME INTENSITY HURRICANE (28.00 INCH CENTRAL PRESSURE) (Landfall of the westward-moving simulated storm is Miami, Florida.)

FIGURE IV-13

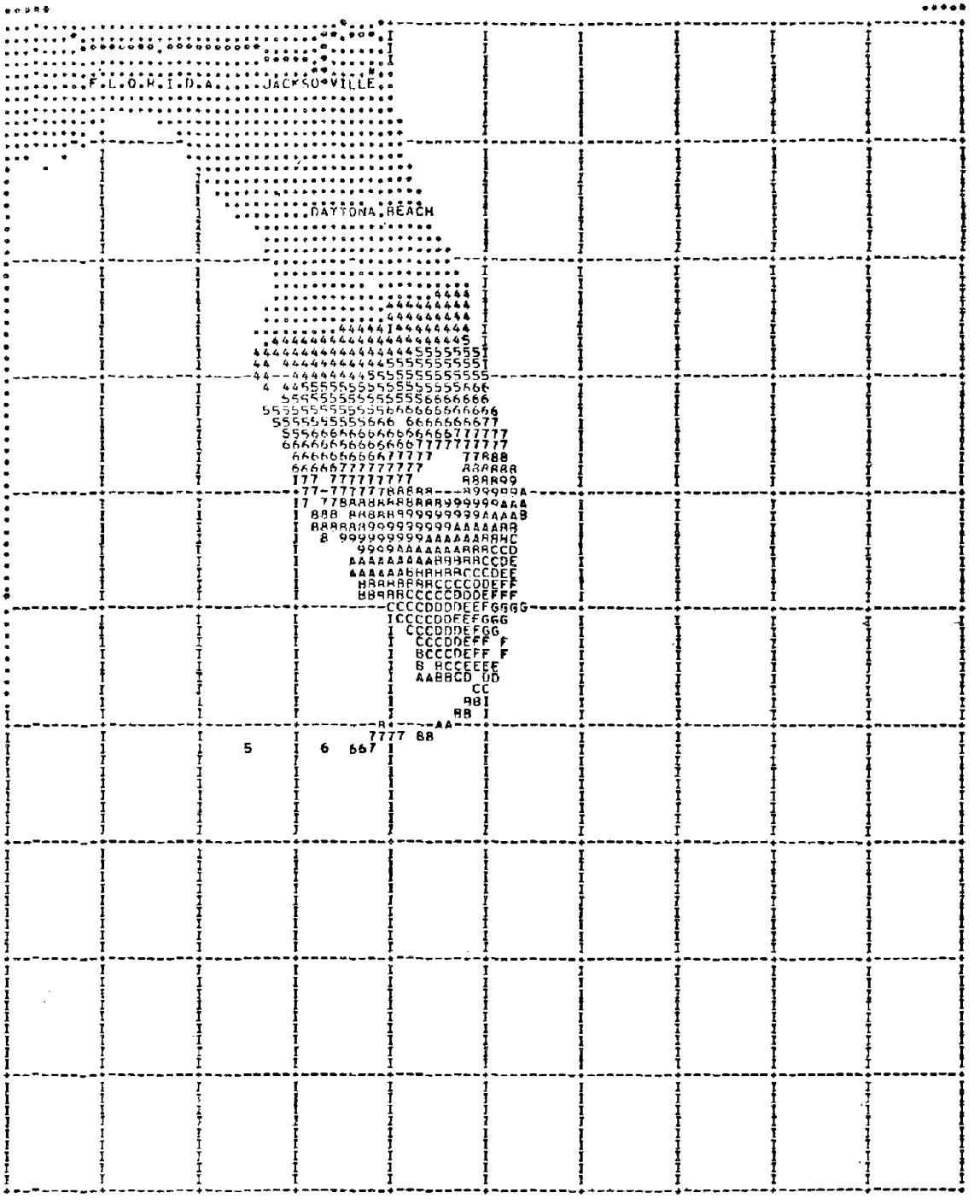

COMPUTED PATTERN OF MAXIMUM WIND SPEED ASSOCIATED WITH THE PASSAGE OF AN EXTREME INTENSITY HURRICANE (27.00 INCH CENTRAL PRESSURE) (Landfall of the westward-moving simulated storm is Miami, Florida.)

FIGURE IV-14

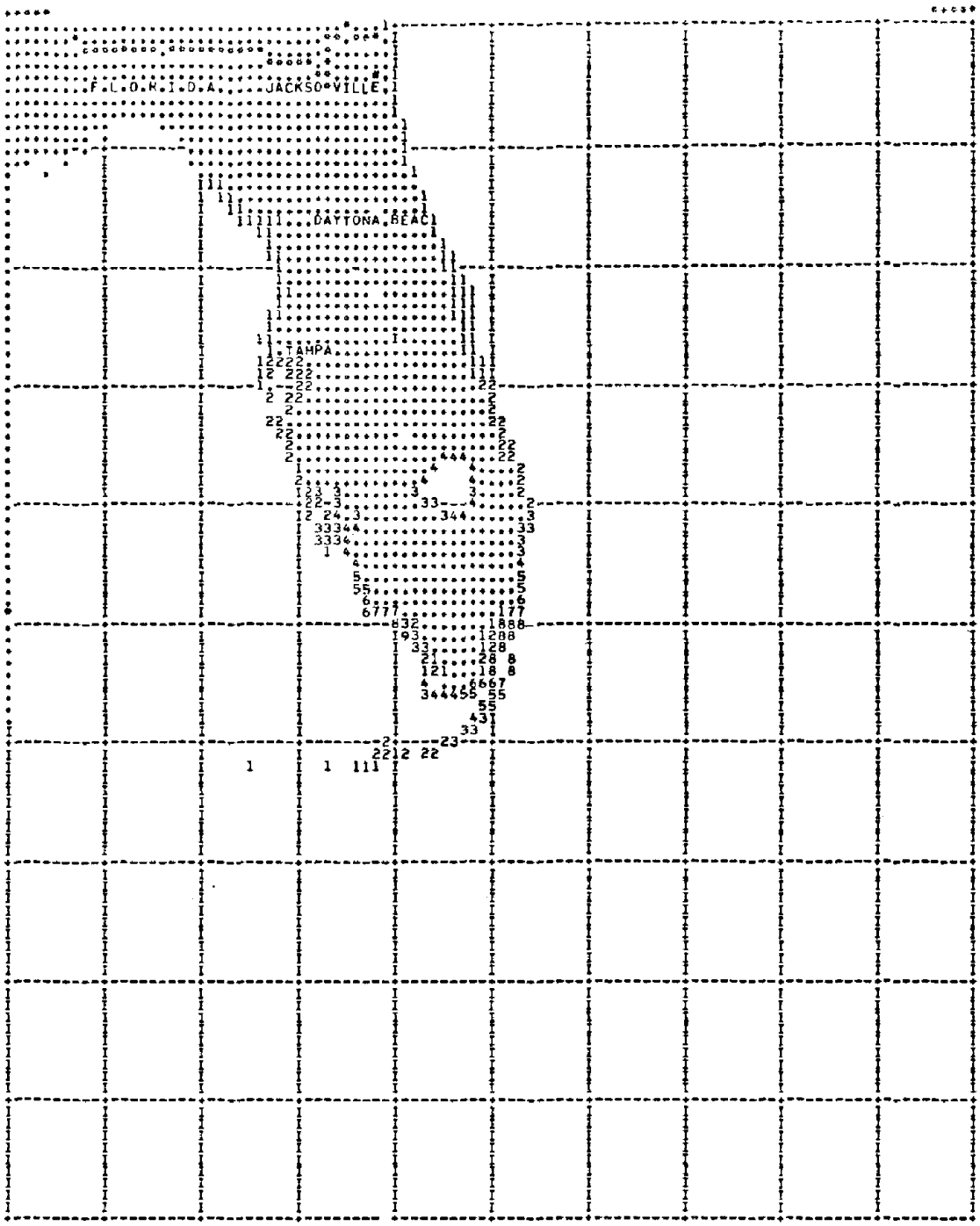

COMPUTED PATTERN OF MAXIMUM STORM SURGE DEPTH (FEET) ASSOCIATED WITH THE PASSAGE OF AN EXTREME INTENSITY HURRICANE (28.00 INCH CENTRAL PRESSURE)
(Landfall of the westward-moving simulated storm is Miami, Florida.)

FIGURE IV-15

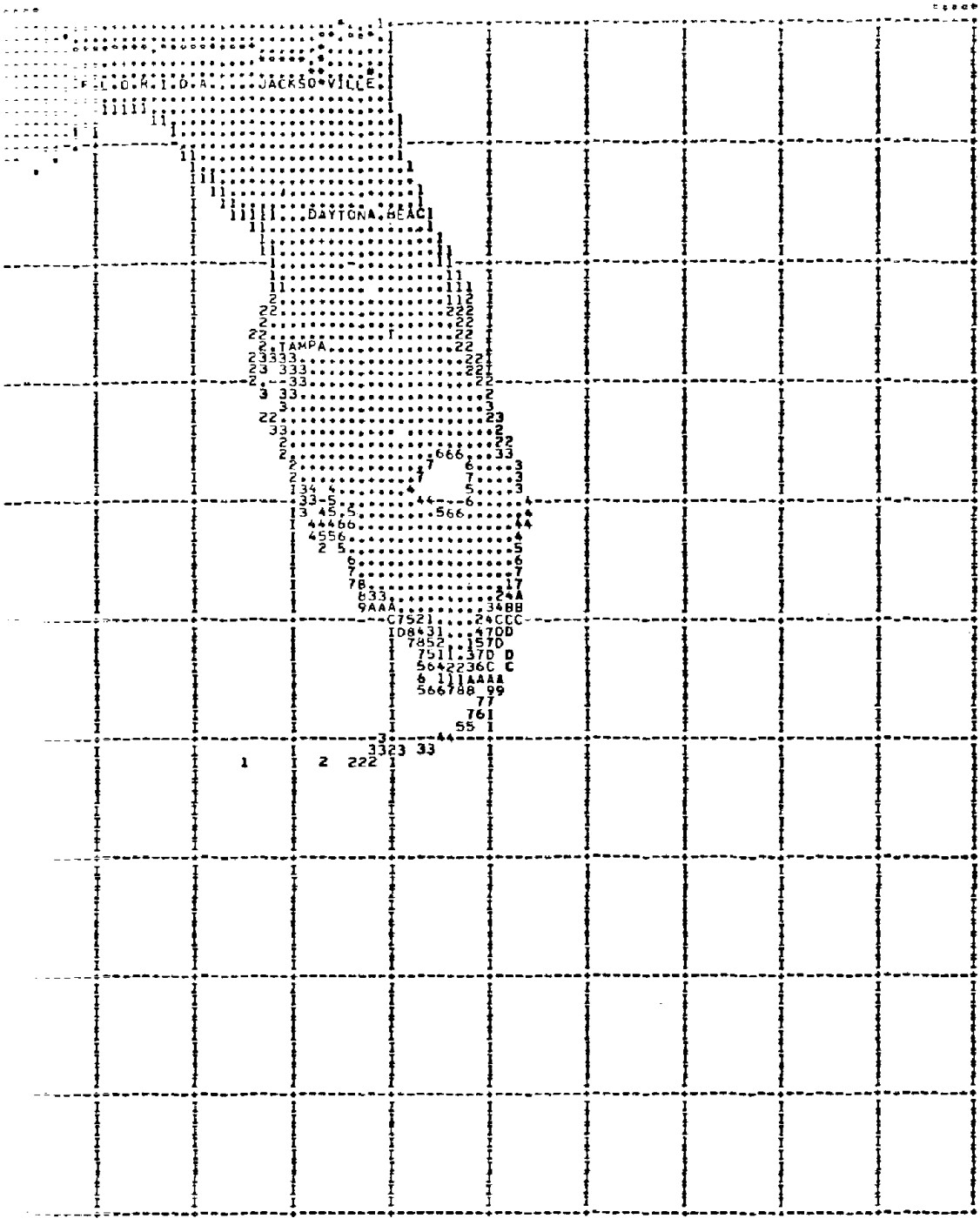

COMPUTED PATTERN OF MAXIMUM STORM SURGE DEPTH (FEET) ASSOCIATED WITH THE PASSAGE OF AN EXTREME INTENSITY HURRICANE (27.00 INCH CENTRAL PRESSURE)
(Landfall of the westward-moving simulated storm is Miami, Florida.)

how close the approximation must be in order to provide usable estimates of loss potential is yet to be answered. A series of additional runs must be made to test the sensitivity of the output to changes in the input information and to compare calculated patterns with actual storm surge patterns.

TABLE IV-7

PERCENTAGE CHANGE IN THE LEVEL OF LOSS POTENTIAL WHEN THE EFFECTS OF A HURRICANE WITH A MINIMUM PRESSURE OF 28.00 INCHES (Lower end of extreme hurricane category) ARE COMPARED WITH EFFECTS OF A 27.00 INCH HURRICANE (Near upper end of extreme category)

7a. Wind Hazard

	Populations-at-Risk			
	Single-Unit Residential Buildings	Other Residential Buildings	Non-residential Buildings	Population
Number Exposed	67%	33%	67%	57%
Damage Index	530%	380%	379%	540%

7b. Storm Surge Hazard

	Populations-at-Risk			
	Single-Unit Residential Buildings	Other Residential Buildings	Non-residential Buildings	Population
Number Exposed	100%	82%	92%	90%
Damage Index	340%	280%	210%	590%

When testing and model adjustment is completed, a recurrence of Gulf and Atlantic hurricanes from the past 100 years will be simulated and the effect upon the current populations-at-risk ascertained, using hurricane wind and storm surge generators as a unit. In addition a number of 25-year periods will be simulated with various sequences of hurricane occurrences along the Gulf and Atlantic coasts within the simulated time periods. An estimate will be obtained of the magnitude and frequency of future natural disasters caused by the storm surge hazard by changing the density, geographical spread, and vulnerability of populations-at-risk in accordance with assumptions about future growth in the exposed coastal plains.

The effect of adjustments to the hurricane hazard are incorporated by modifying the various input factors:

(1) Weather modification which could affect the output of the *natural hazard generator;*

(2) Land use changes which might affect the geographical distribution of *population-at-risk;*

(3) Building code changes which affect *vulnerability;* and

(4) Insurance which could affect the distribution of the output of the system--the *aggregated loss potential.*

CHAPTER V

INLAND FLOODING

A computer simulation model was prepared for the U. S. Department of Housing and Urban Development (HUD) to provide a means for estimating the overall magnitude of the inland flooding hazard to dwellings in the United States. This information was used during the development of the joint insurance industry/Federal government National Flood Insurance Program (Friedman and Roy, 1966). This model has been modified to provide a basis for estimating the effects of various adjustments to the inland flood hazard (Friedman and Bocaccino, 1972). Although the inland flood simulation model does not utilize the grid system, it can be used as an example of the computer simulation approach for estimating the effects of the natural hazards.

The purpose of the study was to determine the present level and future trend in inland flood-loss potential to populations-at-risk located in the 5539 towns and cities in the United States that are reported by the U. S. Army Corps of Engineers to have a flood problem. The present level and trend of loss potential was determined on the basis of the present mix of adjustments to the flood hazard and the probable change in mix of these adjustments if there is no deliberate effort to alter it. In the second stage of the analysis, the effect of changing old or adding new adjustments on the magnitude and trend of the loss potential index was examined.

Population-at-Risk and its Vulnerability

The 5539 cities in the United States determined to have flood problems were broken down by city size category shown in Table V-1. The total number of dwelling structures in each city was taken from the 1970 Census. A percentage of these structures was determined to be on the flood plain. These percentages were based upon studies of certain flood-prone cities requested in 1966 by the U. S. Department of Housing and Urban Development from the U. S. Army Corps of Engineers, the Tennessee Valley Authority, and the U. S. Geological Survey.

TABLE V-1

NUMBER OF PLACES WITH FLOOD PROBLEMS

City Size (Population)	Number of Places	Size Distribution Used in Simulations of 1000 Cities
1,000 to 2,499	1812	328
2,500 to 4,499	1098	198
4,500 to 9,499	992	179
9,500 to 24,499	903	163
24,500 to 49,499	390	70
49,500 to 99,499	204	37
99,500 to 249,499	88	16
249,500 to 499,499	30	5
499,500 to 999,499	16	3
greater than 999,500	6	1
	5539	1000

The flood plain was divided into six hazard zones, defined in terms of return period of floods of various depths. The most hazardous zone had a flood return period of less than five years, the least hazardous more than one hundred years. Residential properties on the flood plain were distributed on the basis of results of the empirical studies of selected flood-prone areas. City size appeared to have no effect on the distribution of dwelling properties by hazard zone.

As with other hazards, it was difficult to obtain an estimate of the commercial structures in the cities, since a total count was not available. As a first approximation, it was assumed that the ratio of total commercial to residential properties was the same in each of the cities. A plot of the rates of commercial to residential properties on the flood plain indicated that commercial properties may follow the same relationship to city size as residential properties, the only difference being a reduction in the overall number of commercial structures as compared with the number of residential properties. The distribution of commercial properties by hazard zone was estimated, using the 1966 study, and found to be slightly different from the residential distribution. As with residential structures, city size had no effect on distribution by hazard zone.

The distributions of value for residential properties used in the 1966 simulation studies (Friedman and Roy, 1966) were updated to 1972 prices. City size again had no effect. Very little information was available on value of commercial structures. However, it was assumed that

if commercial structures included "manufacturing" structures, a value of $100,000 would be representative for all zones and city sizes. An annual growth rate, identical for both residential and commercial structures, was included in the simulation. A growth rate of 3.5% per year was assumed to be "normal" growth.

In these simulations no attempt was made to use census data to determine population in the flood-prone areas. An estimate of the number of people exposed to floods was obtained by multiplying the number of dwellings exposed in each hazard zone by a conversion factor. In the preliminary simulation runs, it was assumed that 3.0 (persons per dwelling) was an appropriate factor for converting a measure of the number of dwellings to the number of people. This factor was derived from summary tabulations of the 1970 Census.

Vulnerability relationships utilized in the 1966 studies for HUD (Friedman and Roy, 1966) were used in the current simulations. The general shape and level of this loss function compares closely with functions derived from information in other studies (Jones, 1971). Table V-2 shows these relationships.

TABLE V-2

VULNERABILITY OF RESIDENTIAL STRUCTURES TO DAMAGE FROM FLOODING

Depth Above First Floor (feet)	Percentage of Value Lost	Depth Above First Floor (feet)	Percentage of Value Lost
1	6.5%	11	29.0%
2	10.5	12	30.5
3	13.5	13	32.0
4	16.5	14	34.5
5	19.0	15	36.5
6	21.3	16	40.0
7	23.0	17	46.5
8	24.5	18	53.0
9	26.0	19	60.0
10	27.5	20	60.0

The vulnerability relationships for commercial structures was obtained by weighting the residential structure relationship by a constant factor of 0.3. The rationale for using this particular weight was to insure that the total structural commercial damages would be, on the average, approximately 40% of the total residential plus commercial structure flood damages. The 40% figure was obtained from the U. S. Department of Commerce, National Weather Service annual estimates of flood damages in the United States by type of structure (U. S. Department of Commerce, 1950-71).

Vulnerability relationships were also developed for damage to residential and commercial contents. The loss to residential contents was determined using an estimated weighted composite of depth damage relationships given in the Federal Insurance Administration's report, Flood Hazard Factors (1970), for various types of residential structures. Losses for commercial contents were obtained by weighting the residential depth-damage curve by a factor 0.3, as was done for commercial structures.

Number of casualties was determined by the number of damaged residential structures. An estimate of the expected number of casualties was obtained by multiplying the number of dwellings damaged by a simulated flood by a factor of one casualty per 170 damaged dwellings. For flash floods, the casualty rate became one per 85 dwellings damaged. The casualty rates were derived from the annual flood tabulations of the American Red Cross.

In the simulations, the number of persons who became unemployed as a result of floods was considered. An estimate of this was given by the number of commercial structures affected times a factor denoting the average number of employees per commercial establishment. This factor varied by city size: for example, a city of 1000 to 2499 persons had an estimated five employees per commercial establishment; a city of 49,500 to 99,499 had an estimated ten.

Construction of a Flood Generator

The flood generator was designed to develop synthetic loss experience over a period of years. Memory from year to year was not included in this model. During each year of the simulation, each city is individually checked by the program for occurrence or non-occurrence of a flood, through the use of a random number generator.

TABLE V-3

FLOOD ZONE PROBABILITIES

Flood Hazard Type	Return Period of Floods	Probability of Occurrence
No flood	--	.600
A	Less than 5 years	.267
B	5 - 10 years	.076
C	10 - 25 years	.030
D	25 - 50 years	.014
E	50 - 100 years	.006
F	Over 100 years	.007

When a flood occurs in a given location, the type of flood is also given. A flood of type A in a city will affect zone A on the flood plain, but not zone B. A type C flood will affect zones A, B, and C, but not zone D (refer to Figure V-1). Flood zone probabilities, which were used in the basic simulations, are given in Table V-3. Alternative sets of assumptions concerning the level were used in later simulations.

Within the various flood types, a range of possible depths was assumed. Table V-4a shows the minimum depth by hazard zone for each flood type. Table V-4b gives the range of flood depth by zone and flood type.

TABLE V-4

FLOOD DEPTHS

4a LOWER LIMIT OF FLOOD DEPTHS WITHIN ZONE (FEET)

Hazard Zone	Flood Type A	B	C	D	E	F
A	0	3.6'	6.6'	9.6'	12.8'	16.0'
B	0	0	3.6'	6.6'	9.6'	12.8'
C	0	0	0	3.6'	6.6'	9.6'
D	0	0	0	0	3.6'	6.6'
E	0	0	0	0	0	3.6'
F	0	0	0	0	0	0

4b RANGE FOR FLOOD DEPTHS WITHIN ZONE (FEET)

Hazard Zone	Flood Type A	B	C	D	E	F
A	3.5'	2.9'	3.0'	3.2'	3.2'	3.0'
B	0	3.5'	2.9'	3.0'	3.2'	3.2'
C	0	0	3.5'	2.9'	3.0'	3.2'
D	0	0	0	3.5'	2.9'	3.0'
E	0	0	0	0	3.5'	2.9'
F	0	0	0	0	0	3.5'

When a flood of a certain type is simulated to occur in a city, deptn of the flood water in each hazard zone is specified by use of these tables. A random number generator is used to determine the depth of water in the highest zone affected. This is accomplished by specifying a portion of the range of depth for that particular zone using a random number draw.

Having determined the magnitude of the flood, the model then calculates damages to populations-at-risk using the vulnerability functions outlined previously.

FIGURE V–1

GRAPHICAL REPRESENTATION OF FLOOD DEPTHS ASSOCIATED WITH VARIOUS FLOOD TYPES IN HAZARD ZONES

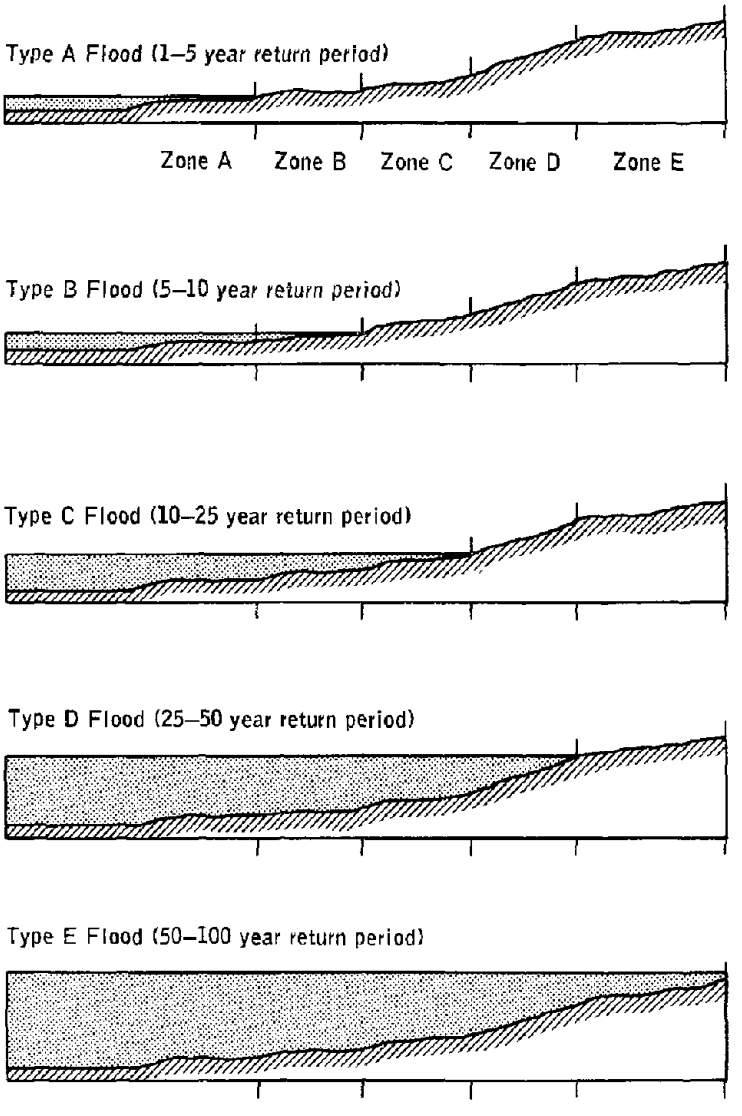

* A Type F Flood has a return period of over 100 years.

Adjustments to the Flood Hazard

In order to determine the present level of loss potential of the flood hazard, it was necessary to determine the current level of adjustments in effect at each of the locations. These adjustments include dams, levees and land use regulations. To obtain a quick estimate of the type and combination of present adjustments to the inland flood hazard, a hand count was made of the number of cities with works constructed by various agencies. The percentage of places with different types of adjustments was as follows: no flood protection (61.7%), dam only (5.4%), land use only (1.5%), levee only (21.8%), dam and land use (0.4%), land use and levee (3.1%), dam and levee (4.6%), and dam, land use and levee (1.5%).

Modifications in the flood generator, the distribution of population-at-risk in the hazard zones, and the vulnerability relationships were made as a means of representing the effect of these adjustments on the flood-loss potential at each city. Type of adjustment was assumed to be independent of city size. The present level of loss potential, including the frequency of occurrence of events producing very high loss potential (natural disasters), was estimated from a series of 20-year simulations holding population-at-risk, vulnerability, and combination of adjustments constant at current levels.

Time-Phased Changes in Adjustments

To determine the future trend of aggregate loss potential at the 5539 places, probable growth rates by hazard zone were applied to the population-at-risk, and hypothesized time-related changes in the future were incorporated into the vulnerability relationships. In addition, it was necessary to develop a means of estimating the "normal" year-to-year change in adjustment combinations at various places when there was no explicit effort to alter the time-phased pattern of adjustments. Table V-5 shows a change of state probability matrix derived from currently available information (Friedman and Bocaccino, 1972).

This change of state matrix incorporates an average annual rate of introduction of a levee adjustment to about 24 out of 1000 cities per year. The annual rate for dams is set at about 13 cities per year. The land use rate was established at 25 cities per 1000 per year. Probabilities in the change-of-state matrix operate in such a way that the rate at the beginning of a simulated period of years is greater than the rate near the end of the period. The introduction of the levee, land use, and

dam adjustments can occur singly or in combination with other adjustments that already are in operation.

TABLE V-5

CHANGES OF STATE PROBABILITIES BY TYPE OF ADJUSTMENT (STATE 2)

...of Adjustment (State 1)	No Protection	Dam	Land Use	Levee	Dam & Land Use	Levee & Land Use	Dam & Levee	Dam Levee & Land Use	Total
protection	.9027	.0125	.0225	.0300	.0020	.0100	.0200	.0003	1.0000
	0	.9590	.0000	.0000	.0300	.0000	.0100	.0010	1.0000
...Use	0	0	.9795	.0000	.0085	.0100	.0000	.0020	1.0000
	0	0	0	.9360	.0000	.0500	.0100	.0040	1.0000
... & land use	0	0	0	0	.9995	.0000	.0000	.0005	1.0000
... & land use	0	0	0	0	0	.9850	.0000	.0150	1.0000
... & levee	0	0	0	0	0	0	.9995	.0005	1.0000
... levee & land	0	0	0	0	0	0	0	1.0000	1.0000

Use of the matrix is illustrated by assuming that a city has no flood protection in a given year. From the matrix, the probability that it will still not be protected is about 90 out of 100. The probability that the place will be protected by a levee in the next year is 3 out of 100. Determination of the future trend in loss potential, when the "normal" time sequencing of flood adjustments is in effect, was obtained by simulating aggregate loss experience during each year of a series of 20-year periods. The trend in the production of natural disasters was also tabulated.

The final stage of the analysis was to use the model as a vehicle for measuring the effect on aggregate loss potential of modifying old adjustments, introducing new adjustments and altering the time sequencing of adjustments implied in Table V-5. A number of 20-year periods were computed using various combinations of adjustments, including improved warning systems and flood proofing. Comparisons were made between the present level and future trend of loss experience based on current adjustment patterns, and loss experience resulting from the use of the modified or new adjustment combinations.

CHAPTER VI

OTHER HAZARDS

Tornadoes, Wind and Hail

Large-scale winter windstorms and severe local storms (tornadoes, hailstorms, local windstorms) are other natural hazards that produce natural disasters in the United States. An idea of the annual production of natural disasters is given in Table VI-1, which lists the number of times in each of the past 25 years that tornadoes, wind or hail (singly or in combination) have caused $1 million or more in insured property losses.

TABLE VI-1

NUMBER OF TIMES THAT TORNADOES, WIND OR HAIL CAUSED INSURED PROPERTY LOSSES EXCEEDING $1 MILLION

Year	Number of Coded Catastrophes	Year	Number of Coded Catastrophes
1949	3	1962	17
1950	8	1963	8
1951	4	1964	14
1952	5	1965	12
1953	15	1966	14
1954	7	1967	26
1955	6	1968	18
1956	7	1969	18
1957	10	1970	17
1958	5	1971	27
1959	4	1972	26
1960	8	1973	24
1961	11		

(Insurance Information Institute, 1949-1974)

The annual number of occurrences of losses exceeding $1 million is dependent upon the percentages of the populations-at-risk that are insured, the amount of coverages, and the effects of inflation upon the cost of repair. However, the numbers given in Table VI-1 provide at least a rough measure of the annual frequency of catastrophes caused by these hazards. In the recent past, there have been about 25 occurrences per year.

The amount of loss when a catastrophe of this type occurs can be roughly estimated by adjusting damage amounts for each of the 348 coded events that occurred between 1949 and 1973 to current dollars. When this adjustment is made, losses exceed $5 million in 50% of the occurrences. In 10% of the cases, losses are in excess of $25 million. Extreme damage amounts include losses of nearly $175 million (1950 dollars) from a winter windstorm in the northeastern United States in November of 1950. A recurrence of this storm would probably result in losses between $500 million and $1 billion to present day populations-at-risk. The April, 1974, tornado catastrophe caused insured losses of about $400 million.

1. Squall Line Hazards

Tornadoes, hailstorms and thunderstorm winds are occasional byproducts of severe thunderstorm activity that frequently occurs in various sections of the United States. Many times this thunderstorm activity occurs along a squall line. Realized (actual) damages caused by these severe local storms are highly variable because of the small geographical area affected by the event's severity pattern; there is a low probability that the storm will overlap a densely packed population-at-risk array (Friedman and Shortell, 1967). In contrast, the severity pattern of high winds associated with a hurricane and the earthshock pattern resulting from an earthquake may be several orders of magnitude larger than the severity patterns associated with tornadoes, hailstorms, or thunderstorm winds.

A measure of severity of a hailstorm is the size of the hailstones, the duration of hailfall, and whether the stones are wind-driven. The severity of thunderstorm winds is determined by the maximum wind gusts. For a tornado, the measure is the distance of its path from the exposed population-at-risk and the severity level of the particular tornado (Fujita, 1970).

The damage potential of a tornado is very large because of its extreme severity. Fortunately its full potential is very seldom realized because of the small area affected. The width of a tornado is usually measured in fractions of a mile; the length of the affected area averages less than ten miles. The overlapping of this small area with the geographical array of populations-at-risk is needed to convert potential damage production into actual damages. Over the Great Plains, where the density of populations-at-risk is very low, a large percentage of the tornadoes

cause only minor and scattered damages. However, when a squall line with accompanying tornadoes of great severity occurs over more densely populated areas of the Middle West, the Great Lakes area, or the eastern United States, a much larger portion of the potential damage production is realized. In April of 1974, a squall line produced a number of tornadoes that caused hundreds of millions of dollars in damages from Ohio southward.

The area affected by hail of damaging size may be an order of magnitude larger than the area affected by a tornado. Strong thunderstorm wind areas may be several orders of magnitude larger than the geographical area affected by tornadoes as a squall line sweeps across an area.

Figure VI-1 illustrates the importance of the overlapping of the severity patterns of the severe local storms with population-at-risk in the creation of a natural disaster. Isolines on VI-1a represent a measure of the frequency and severity of severe local storms in the Middle West. If the population-at-risk were spread uniformly across the area, western Oklahoma and Kansas would probably have the highest frequency of natural disasters caused by these storms. However, the density and geographic spread of the population-at-risk is not uniform across the eastern and middle sections of the United States. Density drops off rapidly west of the Mississippi River. Consequently, the overlapping of the local storm severity patterns with a closely packed population-at-risk array is more likely over eastern sections of the Middle West. The location of Insurance Service Office coded catastrophes is plotted on Figure VI-1b. As expected, the dots are not concentrated in the area of highest frequency of severe local storms (Oklahoma and Kansas), but are displaced eastward where there is a greater probability that the severity pattern will affect a dense population-at-risk. Even though these storms occur less frequently east of the Mississippi, when they do occur, there is a better chance that the pattern overlap will result in the creation of a natural disaster.

Natural hazard simulation is being used to examine the future natural disaster potentials of severe local storms in various sections of the United States. A mathematical generator for producing severity patterns of tornadoes, hailstorms and thunderstorm winds is currently being tested. The generated severity patterns can be applied to the population-at-risk defined by the currently used system of rectangular grid points, each of which represent 35 square miles of land area.

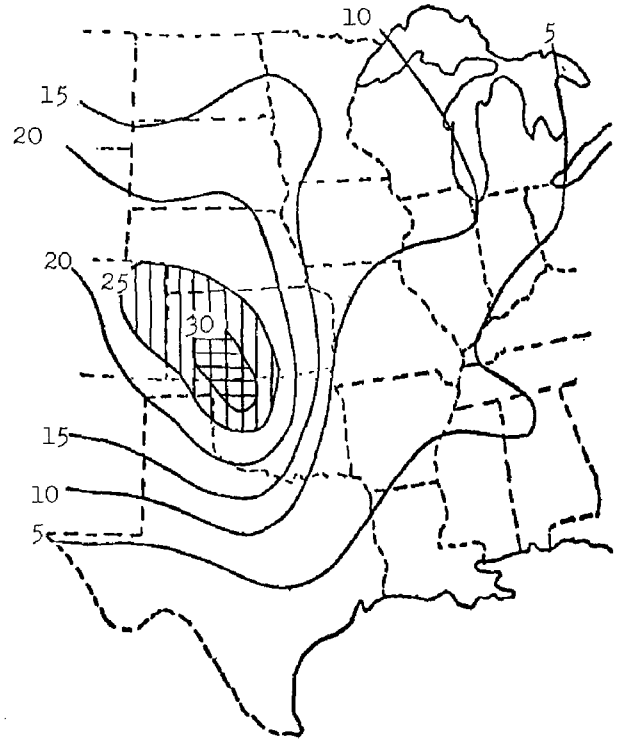

a. Geographical measure of the frequency and severity of tornadoes, hailstorms and thunderstorm winds.

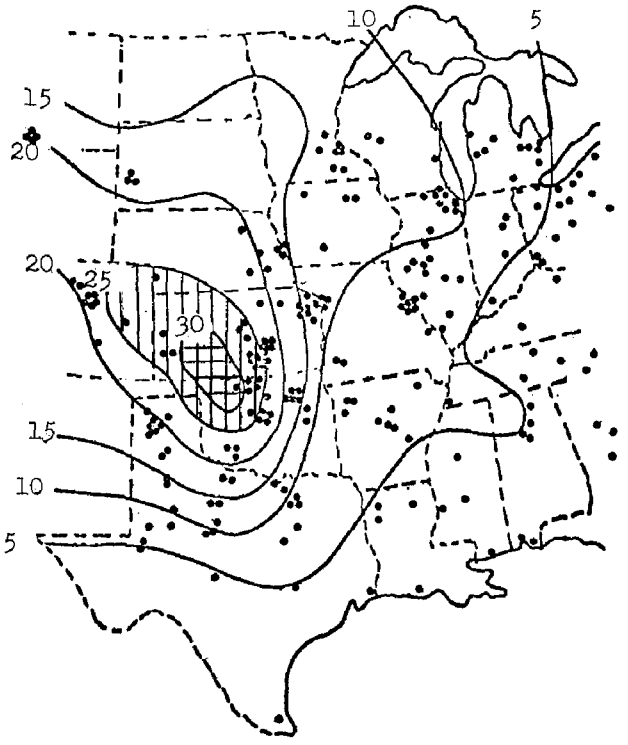

b. Location of catastrophes caused by severe local storms in past twenty years.

FIGURE VI-1

LOCATION OF CATASTROPHES CAUSED BY SEVERE LOCAL STORMS (TORNADOES, HAIL AND WIND), RELATIVE TO THE GEOGRAPHICAL PATTERN OF THE FREQUENCY AND SEVERITY OF THE GEOPHYSICAL EVENTS (Severe local storms occur most frequently in Kansas and Oklahoma.)

However, probability techniques are needed to estimate the percentage of the population-at-risk in a grid area that will be affected and the degree of the effect when a simulated tornado path or hailstreak crosses the grid area. A tornado would normally affect less than 1/10 of the 35-square-mile grid area. Hailstreaks could cover a larger percentage of the area, and strong winds could affect the entire grid area as the thunderstorm moved by.

As mentioned previously, the size of the grid point areas representing the population-at-risk should be determined by the expected size and shape of the severity pattern of the geophysical event. Tornadoes which usually affect a geographical area of a few square miles spread along the narrow path of the storm ideally should interact with a population-at-risk array represented by a grid system in which the individual grid areas are, for example, 1/10 of the size of the present grid areas. Other local windstorms requiring a finer grid include the Boulder, Colorado storms.

The natural hazard generators can be applied to any size grid. A graphical illustration of the generation of very simple severity patterns is given in Figure VI-2. Vulnerability relationships have been developed for several populations-at-risk for tornadoes, hailstorms, and local windstorms using information derived from insurance claim records (Friedman, 1966). The effect of possible changes in the density, geographic spread and vulnerability of populations-at-risk on the production of future natural disasters caused by severe local storms will be ascertained by using various sets of assumptions in the computer analysis.

2. Other Windstorms

Windstorms not associated with tropical cyclone (hurricane) or thunderstorm activity are considered separately because of differences in the size, shape and gradient in the severity patterns. There are two types of windstorms in this category: those caused by and tied to local topographic features of a region--the "Santa Ana" winds in Southern California and the "Boulder" winds in Colorado; and those not related to topography, but the result of a tight gradient in atmospheric pressure usually associated with an intense extratropical cyclone.

Characteristics of the wind speed severity patterns are related to local topography for the first type of storm and to the size and shape of the atmospheric pressure pattern for the second type. Winter windstorms

FIGURE VI-2

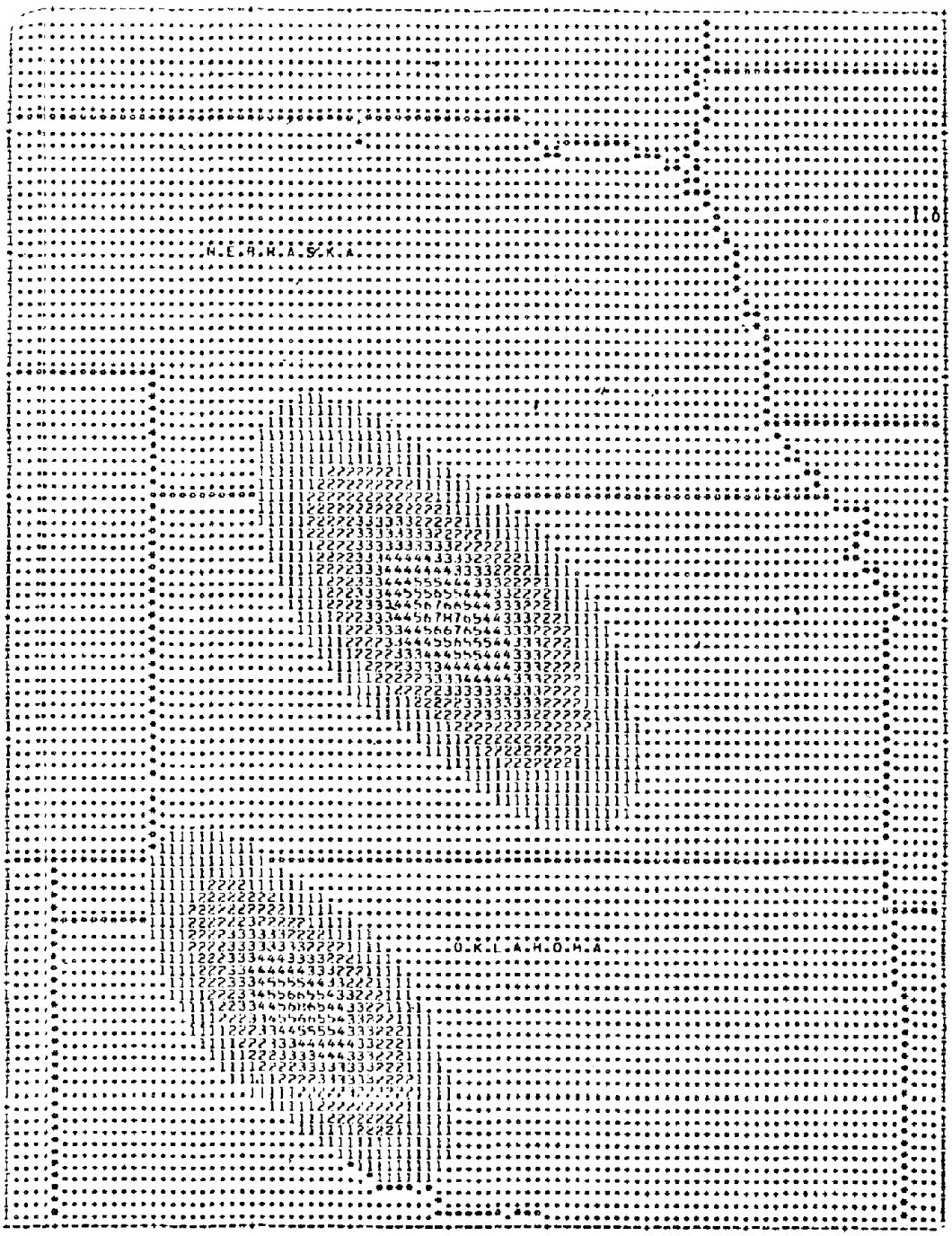

EXAMPLE OF POSSIBLE SEVERITY PATTERNS ASSOCIATED WITH SEVERE LOCAL STORM HAZARD (The patterns are oversimplified and are for illustrative purposes only.)

are of the latter type and can cover many thousands of square miles. However, the maximum wind speeds (peak gusts) usually do not exceed 100 miles per hour, as compared with winds in excess of 200 miles per hour which are possible over a small area during the passage of an extremely intense hurricane. These widespread windstorms can occur in the fall, winter and spring seasons, usually in northern or western sections of the United States. Examples of the level of catastrophe potential of these storms in the past 25 years are given in Table VI-2.

TABLE VI-2

EXAMPLES OF INSURED LOSS AMOUNTS CAUSED BY WIDESPREAD WINDSTORMS IN THE PAST 25 YEARS[1]

Date	Location	Estimated Insured Loss
Nov. 24-27, 1950	Northeastern United States	$174,000,000
Oct. 11-13, 1962	Calif., Oregon, Washington	81,000,000
Nov. 11-13, 1968	Eastern United States	17,000,000
Nov. 6 - 7, 1953	Northeastern United States	12,000,000
Dec. 18-23, 1955	California	12,000,000
Feb. 19-20, 1972	Northeastern United States	11,000,000
Mar. 25-26, 1954	Midwestern United States	7,000,000
Nov. 25-27, 1952	Great Lakes Area	7,000,000

[1]Loss amount not adjusted to current levels.

(Based upon information in the Insurance Information Institute, 1949-1974)

Vulnerability relationships for widespread winter windstorms have been developed from insurance claim records. The general shape of the non-linear curves relating wind speed to damage is similar to the vulnerability curves for the hurricane wind hazard. However, there are sufficient differences that the relationships are not interchangeable. Reasons for these differences are probably duration of the high winds, degree of gustiness, steadiness in wind direction, type of building construction, winterizing of the property, and type and condition of trees.

A mathematical model is currently being constructed which will generate the synthetic severity patterns of the widespread windstorm. These patterns can be applied to populations-at-risk in various sections of the United States.

Drought

It is possible that simulation techniques can also be applied to creeping natural hazards such as drought as one means of estimating loss potential. In this case, the mathematical model would have to generate a time-dependent series of severity patterns that are autocorrelated, rather than a single pattern needed to represent the instantaneous hazards such as earthquakes and hurricanes. The populations-at-risk would be types of crops, and the vulnerability to loss would have to be time-dependent as related to the period of the growing season.

CHAPTER VII

PROBLEMS AND OPPORTUNITIES

Major Problems

Simulation techniques provide one approach to natural hazard loss assessment. Results of the analysis can provide unique insights into catastrophe potential, including conditions leading to the production of future natural disasters. Information in this form is not readily obtainable by other means. The natural hazard loss-producing mechanism is approximated by simulating the effects of the overlapping of the geographical severity pattern associated with a geophysical event (earthquake, hurricane, hailstorm) with the spatial array of a population-at-risk (buildings or population). Major components of the system are a natural hazard generator which produces the geographical pattern of severity (wind speed, earthshock intensity), based upon the physical characteristics of the geophysical event and modified by the effect of local conditions. The spatial distribution of the exposed population-at-risk is designated by use of a computerized grid system representing the land area of the United States. The vulnerability of population-at-risk to loss at given levels of intensity (wind speeds, earthshocks) is also included.

Examples of applications of the simulation approach to various natural hazards have been presented to emphasize some of the problems inherent in this type of analysis:

(1) The number and constraining effects of underlying assumptions that must be made;

(2) Lack of pertinent input data and information on relationships among physical variables;

(3) The difficulty of obtaining an adequate representation of the natural hazard loss-producing system without making the mathematical model unduly complicated and unyielding--how good is good enough; and

(4) Uniqueness in some of the characteristics of each geophysical event which cannot be reproduced by a simple model.

Opportunities

The simulation approach provides some unique analysis opportunities.

(1) It provides a method for tying together information from a number of sources, including the physical sciences, which are not ordinarily used for natural hazard assessment. Implications of the synthesis of this information are expressed in the context of the problem-at-hand.

(2) Long-term climatology of severe storms can be translated into a measure of loss potential to a given population-at-risk. For example, information implicitly contained in charts of the paths of past hurricanes along the Gulf and East Coasts can be expressed in terms of loss potential to a specified population-at-risk array. This is done by utilizing consistencies inherent in relationships between such things as storm path and intensity which imply resultant size, shape and gradient of the high-wind pattern produced as the hurricane moves through an area. The same translation can be made for the earthquake hazard by converting information contained in long-term maps of epicenter location and intensity of past earthquakes into measures of loss potential to a specified geographical array of exposed population-at-risk.

(3) Natural hazard simulation can create a natural disaster from the occurrence of a moderate or severe geophysical event near a populated area in a fashion similar to that produced in nature. Natural hazard loss potential is expressed on a continuous scale ranging from zero to very high (implying a natural disaster), depending upon the interaction of the severity pattern of the geophysical event with the population-at-risk and its vulnerability to loss.

If this approach were to be extended and refined for use as a natural hazard assessment tool, productive areas for further research and development would include the following:

(1) Refinement of the natural hazard generators could be achieved by incorporation of the results of current research being conducted in universities and government agencies on the physical characteristics of the natural hazards (earthquakes, hurricanes, tornadoes), including the effect of local conditions.

(2) More accurate specification of vulnerability of various populations-at-risk to the effects of the natural hazards, and improved definition of the

measure of severity for each hazard and its effect upon loss production are needed.

(3) Development of a meaningful population-at-risk inventory for all sections of the United States, including mobile homes, is desirable.

(4) Better definitions of current adjustments to the natural hazards, the relationships among them, and the time sequencing of possible new adjustment combinations in the future are necessary. For example, development of a method of projecting building code and land use changes is vital.

(5) More accurate specification of the geographical distribution of populations-at-risk can be accomplished by the development of a better inventory of the populations-at-risk, and by the use of a computer system with smaller-sized grid areas in which the population information is mapped. The current system, which is based upon 0.1° latitude by 0.1° longitude increments, utilizes grid areas of about 35 square miles (large-scale grid). Approximately 85,000 of these grid areas are needed to represent the land area of the 48 contiguous states. For a number of the natural hazards, including tornadoes, hailstorms, some windstorms and many riverine floods, it would be desirable to use a system based upon smaller-sized grid areas, since the size of the individual grid areas representing population-at-risk should be small relative to the size of the hazard's severity pattern. The number of grid areas needed to represent a geographical area increases nonlinearly as the size of the latitude and longitude increments used in defining the size of the grid areas is shortened. When the increment is changed from 0.1° to 0.01°, the number of grid areas required to represent a region increases by a factor of 100. The average size of the new grid area is about 1/3 of a square mile (small-scale grid). Eight and one-half million of these smaller grid areas would be needed to approximate the land area of the United States excluding Alaska and Hawaii. The lack of appropriate population-at-risk information for the entire land area of the United States, which is needed as input into this small-scale system, as well as the large number of grid areas, makes the construction of the entire system impractical. However, detailed mappings of selected urban areas using the small-scale grid system could be made by utilizing U. S. Bureau of the Census tabulations of city block and of smaller-sized census track information. Data preparation for these small-scale system segments would probably be comparable to the rates for the large-scale grid system which are about 2000 grid areas per man-month for preparation of 1970 Census information on population and single-unit residential structures. The rate for updating between censuses is approximately 3000 grid areas per man-month. Concurrent

simulation of the same geophysical event on the large- and small-scale grid systems would provide a means of estimating the overall catastrophe potential of the event (large-scale grid), and a detailed estimate of the effect of the event upon urban areas (small-scale grid) that happened to be affected by the event.

National Facility for Simulating Natural Hazard Effects

In mitigation efforts, there is recurrent need for an objective means to approximate the effects of natural hazards upon populations-at-risk in various sections of the United States under different combinations. Natural hazard effects, including the creation of natural disasters, result from the interaction of a number of factors--some known and some unknown. The interaction of all these factors provides a degree of uniqueness to the effects produced by each individual geophysical event. Some of the more important factors, including the physical properties of the geophysical event and the characteristics of exposed populations-at-risk, can be defined and quantified.

Computer simulation of natural hazard effects is based upon a representation of the interactions among the identifiable and measurable factors. The Assessment studies show that natural hazard simulation can provide realistic approximations of actual natural hazard effects. Results of the simulation analysis can be used to produce order-of-magnitude estimates. The influence of those other factors that cannot be included in the simulation model can then be superimposed subjectively. Usefulness of the results obtained with simulation can be increased by refining the simple mathematical models presented for illustrative purposes in this report. Improvements also can be made in the quality and quantity of computerized information on populations-at-risk and their vulnerability to the various natural hazards.

Output from the model could be expanded to express ranges of possible economic and social impacts that might reasonably be expected from a recently reported occurrence of a geophysical event somewhere in the United States. It could also be used to outline the range of catastrophe potential implied in the prediction of geophysical events. For example, if earthquake prediction is to include epicenter location and Richter Magnitude, it is likely that initially those forecasts will be couched in terms of a geographical area in which the epicenter is most likely to occur, and a range in which the actual magnitude will probably

fall. Estimates of catastrophe potential could be calculated for various combinations of epicenter location and magnitude which lie within the forecast geographical area and magnitude range. Likewise, the effect of possible error in predicting the intensity and landfall location of an on-rushing hurricane could be expressed in terms of a series of catastrophe potential estimates based upon selected landfalls located to the left and right of the predicted location, and a series of possible storm intensities. With a properly sized grid system and local conditions defined by information from flood hazard maps, effects of predicted floods could also be approximated.

Cross-hazard capability of the natural hazard simulation system includes comparison of the effects of a hurricane with those of an earthquake. It might be expanded to some of the man-made hazards. This extension would be consistent with the overall objective of providing estimates of hazard effects that can be used in work on disaster causation and impact, disaster operations, emergency systems evaluations, and on the use of various adjustments such as warning systems, land use restrictions, and building codes as a means of reducing the detrimental effect of future natural disasters. One of the more important applications could be in promoting the development of community hazard awareness and preparedness.

APPENDIXES

APPENDIX A

MODIFIED MERCALLI INTENSITY SCALE OF 1931

I. Not felt except by a very few under specially favorable circumstances (I Rossi-Forel Scale).

II. Felt only by a few persons at rest, especially on upper floors of buildings. Delicately suspended objects may swing (I to II Rossi-Forel Scale).

III. Felt quite noticeably indoors, especially on upper floors of buildings, but many people do not recognize it as an earthquake. Standing motorcars may rock slightly; vibration like passing of truck. Duration estimated (III Rossi-Forel Scale).

IV. During the day felt indoors by many, outdoors by few. At night some awakened. Dishes, windows, doors disturbed; walls make creaking sound. Sensation like heavy truck striking building; standing motorcars rocked noticeably (IV to V Rossi-Forel Scale).

V. Felt by nearly everyone, many awakened. Some dishes, windows broken; a few instances of cracked plaster; unstable objects overturned. Disturbances of trees, poles, and other tall objects sometimes noticed. Pendulum clocks may stop (V to VI Rossi-Forel Scale).

VI. Felt by all, many frightened and run outdoors. Some heavy furniture moved; a few instances of fallen plaster or damaged chimneys. Damage slight (VI to VII Rossi-Forel Scale).

VII. Everybody runs outdoors. Damage negligible in buildings of good design and construction; slight to moderate in well-built ordinary structures; considerable in poorly built or badly designed structures; some chimneys broken. Noticed by persons driving motorcars (VIII Rossi-Forel Scale).

VIII. Damage slight in specially designed structures; considerable in ordinary substantial buildings with partial collapse; great in poorly built structures. Panel walls thrown out of frame structures. Fall of chimneys, factory stacks, columns, monuments, walls. Heavy furniture overturned. Sand and mud ejected in small amounts. Changes in well water. Persons driving motorcars disturbed (VIII+ to IX Rossi-Forel Scale).

IX. Damage considerable in specially designed structures; well-designed frame structures thrown out of plumb; great in substantial buildings, with partial collapse. Buildings shifted off foundations. Ground cracked conspicuously. Underground pipes broken (IX+ Rossi-Forel Scale).

X. Some well-built wooden structures destroyed; most masonry and frame structures destroyed with foundations; ground badly cracked. Rails bent. Landslides considerable from riverbanks and steep slopes. Shifted sand and mud. Water splashed (slopped) over banks (X Rossi-Forel Scale).

XI. Few, if any, masonry structures remain standing. Bridges destroyed. Broad fissures in ground. Underground pipelines completely out of service. Earth slumps and land slips in soft ground. Rails bent greatly.

XII. Damage total. Waves seen on ground surfaces. Lines of sight and level distorted. Objects thrown upward into air.

APPENDIX B

EARTHQUAKES OF RICHTER MAGNITUDE 5 OR GREATER WHICH AFFECTED LOS ANGELES AND ORANGE COUNTIES FROM 1769 TO 1972

No.	Year	Date	(Lat(°N)	(Long(°W)	Mag	Location and Damage
1	1769	Jul 28	34.0	118.0	7.5*	Los Angeles Area. Four violent shocks. Many more during the following week. Alarmed the native Indians.
2	1812	Dec 21	34.0	120.0	7.7*	Santa Barbara Channel. Damaging in Santa Barbara, Ventura, and northern Los Angeles counties. Many mission buildings destroyed or damaged.
3	1852	Nov 27	34.5	119.0	6.3*	Lockwood Valley. Fissures 30 miles long in Lockwood Valley.
4	1855	Jul 10	34.0	118.5	6.1*	Los Angeles County. Almost every building in Los Angeles damaged.
5	1857	Jan 9	35.0	119.0	7.8*	Fort Tejon. Buildings and trees thrown down at the Fort. In Los Angeles motion slow and caused hanging grapes to swing up to the rafters.
6	1872	Mar 26	36.5	118.0	7.8*	Owens Valley. At Lone Pine 27 were killed and most houses destroyed.
7**	1889	Aug 28	34.0	118.0	4.8*	Near Pomona. At Los Angeles clocks stopped, ceilings cracked and people ran into the streets.
8	1890	Feb 9	34.0	117.5	6.0*	Los Angeles area. At Los Angeles most people were awakened and windows rattled.
9	1892	Feb 24	31.5	116.5	7.4*	Baja, California. Intensity probably X near epicenter in Mexico. Felt at Los Angeles.

APPENDIX B (continued)

No.	Year	Date	(Lat(°N)	(Long(°W)	Mag	Location and Damage
10	1893	Apr 4	34.5	118.5	6.4*	Newhall-Pico Canyon. Earth fissured and chimneys wrecked in Newhall and Pico Canyon, but not strong at Los Angeles.
11	1894	Jul 30	35.0	118.0	7.0	Los Angeles area. Broke some panes of glass in Los Angeles.
12	1899	Jul 22	34.5	117.5	6.1*	Cajon Pass. Slides in mountains 20 miles from Pass.
13	1899	Dec 25	33.5	116.5	6.7*	San Jacinto and Hemet. Nearly all brick buildings severely damaged at Hemet. Six killed near San Jacinto. People badly frightened in Los Angeles.
14	1902	Jul 28	34.5	120.5	6.1*	Near Santa Barbara. Some buildings damaged, pipeline twisted and broken, two oil tanks destroyed, ground fissured.
15**	1903	Dec 25	34.0	118.0	4.8	Los Angeles area. In Los Angeles, some plaster and bricks thrown down.
16	1907	Sep 20	34.2	117.1	6.0	Near San Bernardino. Damage to buildings in San Bernardino and San Jacinto. Large buildings swayed in Los Angeles.
17	1910	May 15	33.77	117.4	6.0	Lake Elsinore District.
18	1916	Oct 22	34.9	118.9	6.0	Tejon Pass.
19	1918	Apr 21	33.8	117.0	6.8	San Jacinto and Hemet. $200,000 property damage in two places.

(continued)

APPENDIX B (continued)

No.	Year	Date	(Lat(°N)	(Long(°W)	Mag	Location and Damage
20	1920	Jun 21	34.0	118.5	5.0*	Inglewood. Wrecked some buildings. Upset cemetary monuments.
21	1922	Mar 10	34.8	120.3	6.5	Cholame Valley. Felt feebly in Los Angeles.
22	1923	Jul 23	34.0	117.25	6.3	San Bernardino Valley. Damage to masonry buildings and many chimneys in San Bernardino.
23	1925	Jun 29	34.3	119.8	6.3	Santa Barbara. $8 million in Santa Barbara.
24	1927	Nov 4	34.5	121.5	7.5	West of Point Arguello. Chimneys wrecked at Lompoc.
25	1930	Aug 30	33.9	118.6	5.2	Santa Monica Bay. At Los Angeles minor cracks in buildings, fallen plaster, broken dishes.
26	1933	Mar 10	33.6	118.0	6.3	Long Beach. $41,000,000 damage. 120 killed. Buildings collapsed in Long Beach and Compton.
27	1933	Oct 2	33.8	118.1	5.4	Signal Hill. Cracked plaster, some damaged street lamps and broken dishes and windows in Los Angeles.
28	1934	Jun 7	35.8	120.4	6.0	Parkfield.
29	1934	Dec 30	32.0	114.8	7.1	Lower California. Crevices opened. Telephone poles shaken down.
30	1937	Mar 25	33.5	116.5	6.0	Terwilliger Valley.
31	1941	Jun 30	34.3	119.6	5.9	Santa Barbara Channel. $100,000 total damage, 25% of it to drug and liquor stocks and 10% to plate glass.

(continued)

APPENDIX B (continued)

No.	Year	Date	(Lat(°N)	(Long(°W)	Mag	Location and Damage
32	1941	Nov 14	33.8	118.2	5.4	Torrance-Gardena. Damage approximately $1,000,000.
33	1946	Mar 15	35.7	118.1	6.3	Walker Pass. Felt by many in Pasadena and Los Angeles. Near Walker Pass, damage to adobe structures, cracks in brick chimneys, fall of plaster.
34	1952	Jul 21	35.0	119.0	7.7	Kern County. Damage estimates upward of $50 million. Twelve persons killed, nine of them from the fall of a brick wall in Tehachapi.
35	1952	Jul 21	35.0	119.0	6.4	Major aftershock of Kern County earthquake.
36	1952	Jul 23	35.4	118.6	6.1	Major aftershock of Kern County earthquake.
37	1952	Jul 28	35.4	118.9	6.1	Major aftershock of Kern County earthquake.
38	1952	Aug 22	35.3	118.9	5.8	Heavy damage at Bakersfield. Aftershock of 7.7 mag. July 21 shock.
39	1952	Nov 21	35.8	121.2	6.0	
40	1968	Apr 8	33.2	116.1	6.5	Borrego Mountain. In two downtown Los Angeles buildings the only damage was reopened or slightly enlarged plaster cracks from the 1933 and 1952 shocks.
41	1969	Apr 28	33.35	118.35	5.9	Borrego Springs. In Los Angeles, tall buildings swayed. Brick walls cracked at Borrego Springs.
42	1969	Oct 24	33.3	119.2	5.1	Los Angeles, Orange and Ventura counties. Very slight plaster cracking at Downey.

(continued)

APPENDIX B (continued)

No.	Year	Date	(Lat("N)	(Long(°W)	Mag	Location and Damage
43	1970	Sep 12	34.3	117.5	5.4	Lytle Creek. At Lytle Creek, ground cracks, landslide, disturbed water. Chimneys, tombstones, elevated water tanks, etc., cracked, twisted and overturned.
44	1971	Feb 9	34.4	118.4	6.6*	San Fernando. Collapse and severe damage at Veterans Hospital and Olive View Hospital. In downtown Los Angeles, moderate damage, especially to older type buildings with brick and masonry facings; portions of one old building collapsed, killing one person.

* Richter magnitude estimated.

** Estimated earthquake magnitude less than 5 (Richter Scale); event included for comparative purposes.

(Based on Table 1 of Report by NOAA, 1973)

APPENDIX C

MULTISTORY BUILDING INVENTORIES

a. Multistory building inventory based on information given in NOAA Reports (1972, 1973)

Number of Buildings

City	4-8 Story	9-13 Story	14 or more Stories	Total
San Francisco	1287	165	102	1554
Los Angeles	1066	255	51	1372
Oakland	167	27	11	205
Long Beach	63	20	6	89
Berkeley	68	15	2	85
Santa Monica	35	14	9	58
Pasadena	42	11	2	55
San Jose	41	12	0	53
Palo Alto	18	4	1	23
Santa Ana	10	11	0	21

B. Multistory building inventory based on information given in Whitman (1973)

Number of Buildings

City	5-7 Story	8-13 Story	14-18 Story	19 or more Stories	Total
Los Angeles Area	916	588	85	57	1646

APPENDIX D-1

DAMAGE EXPERIENCE TO SINGLE-UNIT RESIDENCES CAUSED BY A RECURRENCE OF EARTHQUAKES LISTED IN APPENDIX B

Earthquake Number	Year	Magnitude	Distance[1]	Number Exposed	Number Affected	Damage Index
5	1857	7.8	80	3,707,000	275,000	1000
2	1812	7.7	105	2,631,000	203,000	650
1	1769	7.5	80	3,437,000	224,000	548
44	1971	6.6	30	2,503,000	162,000	355
34	1952	7.7	80	2,435,000	157,000	346
6	1872	7.8	170	2,734,000	167,000	291
4	1855	6.1	15	2,062,000	135,000	289
26	1933	6.3	35	2,239,000	135,000	244
10	1893	6.4	35	2,244,000	132,000	182
19	1918	6.8	65	2,411,000	130,000	165
22	1923	6.3	55	2,263,000	113,000	133
8	1890	6.0	45	2,151,000	106,000	103
32	1941	5.4	15	1,775,000	89,000	101
9	1892	7.4	205	2,231,000	107,000	101
11	1894	7.0	70	2,058,000	100,000	99
3	1852	6.3	55	2,145,000	107,000	91
27	1933	5.4	20	1,753,000	89,000	86
17	1910	6.0	55	2,179,000	104,000	73
13	1899	6.7	105	2,229,000	104,000	68
12	1899	6.1	45	2,210,000	97,000	59
40	1968	6.5	130	2,181,000	92,000	45
16	1907	6.0	65	1,774,000	67,000	35
18	1916	6.0	70	1,901,000	72,000	27
20	1920	5.0	15	1,419,000	57,000	26
37	1952	6.1	105	258,000	12,000	26
21	1922	6.5	130	1,372,000	45,000	25
25	1930	5.2	25	1,559,000	62,000	24
35	1952	6.4	80	1,566,000	56,000	24
7	1889	4.8	15	1,687,000	65,000	23
15	1903	4.8	15	1,665,000	63,000	22
24	1927	7.5	190	694,000	29,000	22
31	1941	5.9	80	1,602,000	57,000	17
43	1970	5.4	50	1,275,000	44,000	14
30	1937	6.0	100	1,330,000	45,000	12
38	1952	5.8	95	168,000	7,000	8
36	1952	6.1	95	396,000	15,000	8
33	1946	6.3	120	936,000	30,000	7
23	1925	6.3	90	637,000	22,000	7
29	1934	7.1	240	379,000	13,000	6
41	1969	5.9	110	587,000	19,000	5
28	1934	6.0	170	301,000	11,000	4
39	1952	6.0	205	124,000	5,000	2
14	1902	6.1	135	30,000	1,000	1
42	1969	5.1	75	0	0	0

[1]Distance is measured in miles from epicenter to center of Los Angeles

APPENDIX D-2

NUMBER OF SINGLE-UNIT RESIDENCES IN CALIFORNIA EXPOSED TO EARTHSHOCK SEVERITY EQUAL TO, OR GREATER THAN INDICATED VALUE FOR A RECURRENCE OF EARTHQUAKES LISTED IN APPENDIX B[1]

Earthquake Number	Year	Magnitude	Distance[2]	Casualty Potential[3]	Earthshock Severity 5	6	7	8	9	10
5	1857	7.8	80	1000	3,465,400	2,567,200	1,811,000	78,800	5,600	100
2	1812	7.7	105	650	2,526,400	2,138,000	1,416,500	19,300		
1	1769	7.5	80	548	3,138,900	2,180,700	828,700	23,700	400	100
44	1971	6.6	30	355	2,215,000	1,866,400	347,000	1,200		
34	1952	7.7	80	346	2,332,300	1,844,000	197,600	42,400	2,500	100
6	1872	7.8	170	261	2,634,500	1,929,200	50,800	1,900	200	100
4	1855	6.1	15	289	2,003,500	1,478,900	246,100	16,100		
26	1933	6.3	35	244	1,963,600	1,489,800	189,700			
10	1893	6.4	35	182	2,158,500	1,486,500	41,800	1,200		
19	1918	6.8	65	165	2,212,000	1,023,200	125,600	1,600	1,400	
22	1923	6.3	55	133	2,034,000	447,000	110,000			
8	1890	6.0	45	103	1,881,700	436,600	72,600			
32	1941	5.4	15	101	1,517,700	598,000	82,800			
9	1892	7.4	205	101	1,966,800	292,000	110,000			
11	1894	7.0	70	99	1,838,000	515,000	46,000	4,600		
3	1852	6.3	55	91	1,917,400	720,400	400	100		
27	1933	5.4	20	86	1,628,500	591,500	25,500			
17	1910	6.0	55	73	2,051,400	350,800	1,700	100		
13	1899	6.7	105	68	2,076,600	233,200	3,400			
12	1899	6.1	45	59	1,773,600	286,100	9,200	100		
40	1968	6.5	130	45	1,927,400	96,900	1,000	100		
16	1907	6.0	65	35	990,100	164,600	10,400			
18	1916	6.0	70	27	1,314,000	35,200	600	300		

(continued)

APPENDIX D-2 (continued)

Earthquake Number	Year	Magnitude	Distance[2]	Casualty Potential[3]	Earthshock Severity 5	6	7	8	9	10
20	1920	5.0	15	26	1,126,700	87,100				
37	1952	6.1	105	26	164,500	61,100	30,500	7,400		
21	1922	6.5	130	25	284,200	47,000	22,000	300		
25	1930	5.2	25	24	1,368,900					
35	1952	6.4	80	24	722,800	110,300	6,200	100		
7	1889	4.8	15	23	1,411,500					
15	1903	4.8	15	22	1,242,400	22,400				
24	1927	7.5	190	22	432,200	97,300	11,600			
31	1941	5.9	80	17	977,500	38,900				
43	1970	5.4	50	14	535,800	10,500	300			
30	1937	6.0	100	12	525,800	9,400				
38	1952	5.8	95	8	105,500	42,700	2,400			
36	1952	6.1	95	8	191,800	43,000	100	100		
33	1946	6.3	120	7	266,200	14,000	300			
23	1925	6.3	90	7	235,100	44,200				
29	1934	7.1	240	6	130,400	19,800	200			
41	1969	5.9	110	5	216,000	8,700	100			
28	1934	6.0	170	4	125,600	12,100	200			
39	1952	6.0	205	2	83,900	8,200	200	200		
14	1902	6.1	135	1	28,400	8,700	200			
42	1969	5.1	75	0	0					

[1]There are about 4,700,000 single-unit residences in California (1970 Census).

[2]Distance measured in miles from epicenter to the center of Los Angeles.

[3]The earthquakes have been sequenced according to the magnitude of a calculated measure of damage potential.

APPENDIX D-3

DAMAGE EXPERIENCE TO OTHER RESIDENTIAL BUILDINGS CAUSED BY A RECURRENCE OF EARTHQUAKES LISTED IN APPENDIX B

Earthquake Number	Year	Magnitude	Distance[1]	Number Exposed	Number Affected	Damage Index
5	1857	7.8	80	167,120	20,300	1000
2	1812	7.7	105	122,510	15,860	703
1	1769	7.5	80	158,570	16,750	499
44	1971	6.6	30	117,690	12,750	351
4	1855	6.1	15	102,940	11,350	339
34	1952	7.7	80	111,960	11,780	282
26	1933	6.3	35	110,810	10,940	247
6	1872	7.8	170	123,260	12,300	206
10	1893	6.4	35	108,310	10,480	157
19	1918	6.8	65	115,210	9,900	110
32	1941	5.4	15	91,361	7,600	91
22	1923	6.3	55	110,600	8,690	88
11	1894	7.0	70	100,700	7,950	87
9	1892	7.4	205	110,470	8,450	77
3	1852	6.3	55	104,990	8,640	69
8	1890	6.0	45	105,490	8,270	69
27	1933	5.4	20	90,150	7,500	68
17	1910	6.0	55	107,460	8,150	47
13	1899	6.7	105	108,450	8,000	42
12	1899	6.1	45	107,080	7,530	36
40	1968	6.5	130	107,420	7,220	30
20	1920	5.0	15	77,000	5,150	22
25	1930	5.2	25	83,600	5,510	17
16	1907	6.0	65	89,580	5,210	16
21	1922	6.5	130	71,630	3,710	16
18	1916	6.0	70	94,450	5,760	16
37	1952	6.1	105	8,580	590	15
7	1889	4.8	15	87,450	5,390	13
35	1952	6.4	80	77,820	4,410	13
15	1903	4.8	15	86,730	5,230	12
31	1941	5.9	80	84,690	4,930	11
24	1927	7.5	190	26,210	1,650	9
43	1970	5.4	50	62,600	3,330	6
30	1937	6.0	100	57,030	3,050	5
23	1925	6.3	90	36,450	1,880	4
33	1946	6.3	120	49,240	2,450	3
29	1934	7.1	240	14,190	810	3
38	1952	5.8	95	5,860	380	3
36	1952	6.1	95	15,650	890	3
41	1969	5.9	110	22,850	1,210	3
28	1934	6.0	170	7,630	450	2
39	1952	6.0	205	4,170	270	1
14	1902	6.1	135	1,140	80	1
42	1969	5.1	75	0	0	0

[1]Distance is measured in miles from epicenter to center of Los Angeles.

APPENDIX D-4

DAMAGE EXPERIENCE TO NON-RESIDENTIAL BUILDINGS CAUSED BY A RECURRENCE OF EARTHQUAKES LISTED IN APPENDIX B

Earthquake Number	Year	Magnitude	Distance[1]	Number Exposed	Number Affected	Damage Index
5	1857	7.8	80	826,210	74,250	10000
34	1952	7.7	80	544,970	42,320	3343
2	1812	7.7	105	589,960	55,620	3293
1	1769	7.5	80	771,058	60,290	3143
4	1855	6.1	15	470,294	37,470	1559
44	1971	6.6	30	562,330	44,150	1502
26	1933	6.3	35	509,006	36,706	923
6	1872	7.8	170	608,140	44,380	760
19	1918	6.8	65	542,950	34,580	718
11	1894	7.0	70	468,164	26,890	572
22	1923	6.3	55	512,730	29,970	433
10	1893	6.4	35	508,078	35,780	329
32	1941	5.4	15	407,820	24,470	250
37	1952	6.1	105	54,950	2,950	231
9	1892	7.4	205	507,490	28,490	177
8	1890	6.0	45	487,870	28,240	172
21	1922	6.5	130	318,840	11,980	164
27	1933	5.4	20	402,590	24,270	114
3	1852	6.3	55	487,100	29,000	68
40	1968	6.5	130	494,940	24,290	46
17	1910	6.0	55	494,350	27,550	43
13	1899	6.7	105	504,260	27,410	42
7	1889	4.8	15	388,200	17,370	38
35	1952	6.4	80	358,550	14,780	36
12	1899	6.1	45	499,680	25,670	35
16	1907	6.0	65	406,080	17,600	28
24	1927	7.5	190	150,280	7,350	26
38	1952	5.8	95	36,310	1,840	22
20	1920	5.0	15	332,100	15,730	17
18	1916	6.0	70	434,230	19,050	14
36	1952	6.1	95	86,420	3,680	8
29	1934	7.1	240	79,290	3,200	7
31	1941	5.9	80	373,090	15,467	5
25	1930	5.2	25	363,810	17,100	5
39	1952	6.0	205	26,510	1,200	4
15	1903	4.8	15	383,645	16,800	4
14	1902	6.1	135	6,700	350	3
23	1925	6.3	90	154,160	5,960	3
28	1934	6.0	170	60,500	2,500	3
41	1969	5.9	110	124,510	4,750	3
43	1970	5.4	50	289,090	11,390	3
30	1937	6.0	100	289,600	11,220	2
33	1946	6.3	120	218,740	7,940	2
42	1969	5.1	75	0	0	0

[1]Distance is measured in miles from epicenter to center of Los Angeles.

APPENDIX D-5

DAMAGE EXPERIENCE TO HIGH-RISE BUILDINGS IN LOS ANGELES COUNTY CAUSED BY A RECURRENCE OF EARTHQUAKES LISTED IN APPENDIX B

Earthquake Number	Year	Magnitude	Distance[1]	Pre 1933 Structures	Post 1933 Structures	Damage Index
5	1857	7.8	80	$81,075,000	$127,862,000	10000
2	1812	7.7	105	58,726,000	112,810,000	8210
4	1855	6.1	15	26,111,000	103,382,000	6198
1	1769	7.5	80	25,798,000	46,299,000	3451
44	1971	6.6	30	15,649,000	40,337,000	2680
34	1952	7.7	80	6,317,000	16,214,000	1078
6	1872	7.8	170	6,155,000	11,933,000	866
10	1893	6.4	35	4,932,000	10,327,000	730
32	1941	5.4	15	5,809,000	7,635,000	643
26	1933	6.3	35	3,904,000	7,264,000	534
27	1933	5.4	20	1,044,000	3,889,000	236
3	1852	6.3	55	1,152,000	3,348,000	215
11	1894	7.0	70	751,000	2,323,000	147
20	1920	5.0	15	302,000	2,588,000	138
19	1918	6.8	65	934,000	1,907,000	136
22	1923	6.3	55	462,000	1,008,000	70
8	1890	6.0	45	446,000	966,000	68
17	1910	6.0	55	337,000	754,000	52
12	1899	6.1	45	243,000	606,000	41
25	1930	5.2	25	136,000	657,000	38
9	1892	7.4	205	176,000	471,000	31
13	1899	6.7	105	175,000	425,000	29
18	1916	6.0	70	84,000	286,000	17
7	1889	4.8	15	91,000	219,000	15
40	1968	6.5	130	71,000	199,000	13
15	1903	4.8	15	80,000	187,000	13
35	1952	6.4	80	22,000	121,000	7
16	1907	6.0	65	26,000	71,000	5
21	1922	6.5	130	7,000	48,000	3
43	1970	5.4	50	9,000	23,000	1
33	1946	6.3	120	3,000	12,000	1
23	1925	6.3	90	1,000	17,000	1
30	1937	6.0	100	2,000	5,000	1
14	1902	6.1	135	0	0	0
24	1927	7.5	190	0	0	0
28	1934	6.0	170	0	0	0
29	1934	7.1	240	0	0	0
31	1941	5.9	80	0	0	0
36	1952	6.1	95	0	0	0
37	1952	6.1	105	0	0	0
38	1952	5.8	95	0	0	0
39	1952	6.0	205	0	0	0
41	1969	5.9	110	0	0	0
42	1969	5.1	75	0	0	0

[1]Distance is measured in miles from the epicenter to center of Los Angeles.

APPENDIX D-6

CASUALTY EXPERIENCE OF POPULATION CAUSED BY A RECURRENCE OF EARTHQUAKES LISTED IN APPENDIX B

Earthquake Number	Year	Magnitude	Distance[1]	Number Exposed	Casualty Index
5	1857	7.8	80	16,033,700	1000
2	1812	7.7	105	11,493,900	753
1	1769	7.5	80	14,983,400	647
44	1971	6.6	30	10,974,800	465
34	1952	7.7	80	10,599,900	409
4	1855	6.1	15	9,222,600	405
6	1872	7.8	170	11,831,700	381
26	1933	6.3	35	9,995,900	351
10	1893	6.4	35	9,926,000	294
19	1918	6.8	65	10,624,800	249
22	1923	6.3	55	10,050,900	200
3	1852	6.3	55	9,532,500	180
8	1890	6.0	45	9,569,800	178
9	1892	7.4	205	9,957,600	177
32	1941	5.4	15	8,042,000	177
11	1894	7.0	70	9,158,500	165
27	1933	5.4	20	7,936,700	163
17	1910	6.0	55	9,706,600	152
13	1899	6.7	105	9,882,400	147
12	1899	6.1	45	9,786,800	125
40	1968	6.5	130	9,712,100	108
25	1930	5.2	25	7,183,300	72
18	1916	6.0	70	8,510,000	71
20	1920	5.0	15	6,567,100	71
16	1907	6.0	65	7,979,400	71
7	1889	4.8	15	7,660,400	67
15	1903	4.8	15	7,574,200	63
31	1941	5.9	80	7,337,100	53
35	1952	6.4	80	7,020,300	52
21	1922	6.5	130	6,252,900	41
43	1970	5.4	50	5,684,200	37
30	1937	6.0	100	5,678,500	34
24	1927	7.5	190	2,853,000	31
37	1952	6.1	105	1,026,600	21
33	1946	6.3	120	4,279,400	21
23	1925	6.3	90	2,995,500	18
41	1969	5.9	110	2,422,600	13
36	1952	6.1	95	1,648,600	13
29	1934	7.1	240	1,536,000	10
38	1952	5.8	95	677,900	9
28	1934	6.0	170	1,126,800	7
39	1952	6.0	205	490,700	4
14	1902	6.1	135	124,900	2
42	1969	5.1	75	0	0

[1]Distance is measured in miles from epicenter to center of Los Angeles.

APPENDIX D-7

NUMBER OF PERSONS IN CALIFORNIA EXPOSED TO EARTHSHOCK SEVERITY EQUAL TO, OR GREATER THAN INDICATED VALUE FOR A SIMULATED RECURRENCE OF EARTHQUAKES LISTED IN APPENDIX B

Earthquake Number	Year	Magnitude	Distance[1]	Casualty Potential[2]	Earthshock Severity 5	6	7	8	9	10
5	1857	7.8	80	1000	15,072,700	11,205,700	8,128,600	316,700	24,000	500
2	1812	7.7	105	753	11,100,800	9,506,900	6,571,000	96,000		
1	1769	7.5	80	647	13,706,800	9,601,300	3,682,300	97,400	1,400	500
44	1971	6.6	30	465	9,804,800	8,443,500	1,695,300	6,100		
34	1952	7.7	80	409	10,195,147	8,264,100	793,100	152,700	8,700	500
4	1855	6.1	15	405	9,005,500	6,841,900	1,251,100	83,800		
6	1872	7.8	170	381	11,457,800	8,551,100	217,600	6,800	600	100
26	1933	6.3	35	351	8,787,000	6,852,300	894,300			
10	1893	6.4	35	294	9,595,700	6,814,000	183,000	6,100		
19	1918	6.8	65	249	9,820,300	4,341,400	459,200	5,300	4,700	
22	1923	6.3	55	200	9,083,800	1,800,500	427,300			
3	1852	6.3	55	180	8,605,200	3,424,600	900	300		
8	1890	6.0	45	178	8,463,400	1,760,900	293,400			
9	1892	7.4	205	177	8,850,900	1,256,300	484,400			
32	1941	5.4	15	177	7,037,800	2,772,800	378,600			
11	1894	7.0	70	165	8,169,500	2,410,800	210,300	20,000		
27	1933	5.4	20	163	7,438,900	2,697,000	96,400			
17	1910	6.0	55	152	9,167,300	1,470,600	4,300	400		
13	1899	6.7	105	147	9,289,600	905,700	14,200			
12	1899	6.1	45	125	7,971,100	1,152,900	35,100	300		
40	1968	6.5	130	108	8,665,130	422,500	8,500	1,800		
25	1930	5.2	25	72	6,403,600					
18	1916	6.0	70	71	5,961,500	150,300	1,900	1,100		

(continued)

APPENDIX D-7 (continued)

Earth-quake Number	Year	Magni-tude	Dis-tance[1]	Casualty Potential[2]	Earthshock Severity 5	6	7	8	9	10
20	1920	5.0	15	71	5,240,600	454,600				
16	1907	6.0	65	71	4,309,900	621,000	15,600			
7	1889	4.8	15	67	6,507,600					
15	1903	4.8	15	63	5,746,300	82,300				
31	1941	5.9	80	53	4,676,800	178,100				
35	1952	6.4	80	52	3,324,500	448,500	21,700	500		
21	1922	6.5	130	41	1,185,300	185,500	82,900	1,000		
43	1970	5.4	50	37	2,167,300	38,500	800			
30	1937	6.0	100	34	2,174,500	45,800				
24	1927	7.5	190	31	1,654,700	380,900	42,600			
37	1952	6.1	105	21	656,300	218,400	115,000	29,500		
33	1946	6.3	120	21	1,124,700	48,000	1,000			
23	1925	6.3	90	18	959,400	197,100				
41	1969	5.9	110	13	861,700	45,400	1,200			
36	1952	6.1	95	13	781,000	156,600	500	500		
29	1934	7.1	240	10	554,400	82,300	900			
38	1952	5.8	95	9	405,100	155,700	9,000			
28	1934	6.0	170	7	487,100	48,000	800			
39	1952	6.0	205	4	347,600	33,300	800	800		
14	1902	6.1	135	2	117,900	35,600	900			
44	1969	5.1	75	0	0					

[1]Distance is measured in miles from Epicenter to center of Los Angeles.

[2]Earthquakes have been sequenced according to magnitude of calculated measure of casualty potential.

LOSS POTENTIAL TO SINGLE-UNIT RESIDENCES IN CALIFORNIA ASSOCIATED WITH THE SIMULATED OCCURRENCE OF EARTHQUAKES OF SPECIFIED MAGNITUDES ALONG MAJOR FAULT ZONES

	Epicenter Location			Richter 8		Richter 7		Richter 6	
Loc. No.	Nearest Landmark	Lat.	Long.	Number Dwellings Exposed[2]	Damage Index[2]	Number Dwellings Exposed[1]	Damage Index[2]	Number Dwellings Exposed[2]	Damage Index[2]
1	Cape Mendocino, CA	40.4N	124.3W	1,428,000	4.77	401,000	.37	22,000	.05
2	Point Arena, CA	38.9N	123.4W	1,769,000	19.41	1,276,000	1.88	221,000	.09
3	San Francisco, CA	37.6N	122.6W	3,229,000	50.40	1,499,000	8.52	951,000	1.25
4	Salinas, CA	36.5N	121.1W	4,119,000	35.38	1,484,000	3.72	690,000	.35
5	Paso Robles, CA	35.5N	120.0W	4,083,000	35.42	2,827,000	3.05	222,000	.14
6	Gorman (Ft. Tejon), CA	34.8N	118.7W	3,994,000	100.00	2,718,000	14.15	1,965,000	1.83
7	San Bernardino, CA	34.2N	117.4W	3,600,000	96.71	2,649,000	17.72	1,895,000	2.68
8	Niland, CA	33.2N	115.6W	2,723,000	15.17	2,031,000	1.48	47,000	.10
9	Gulf of Calif., Mex.	31.9N	114.9W	2,324,000	4.58	372,000	.20	16,000	.01
10	Lone Pine, CA	36.5N	118.0W	2,871,000	16.93	1,963,000	1.03	33,000	.02
11	Hawthorne, NV	38.7N	117.8W	2,195,000	1.14	10,000	.01	200	.00

[1]The loss index is expressed in terms of number of dwellings exposed to an earthshock severity of 4.5 or more on a continuous scale paralleling the Modified Mercalli Intensity Scale.

[2]The damage index is measured relative to the most damaging earthquake.

APPENDIX E-2

LOSS POTENTIAL TO OTHER RESIDENTIAL BUILDINGS IN CALIFORNIA ASSOCIATED WITH THE SIMULATED OCCURRENCES OF EARTHQUAKES OF SPECIFIED MAGNITUDE ALONG MAJOR FAULT ZONES

	Epicenter Location			Richter 8		Richter 7		Richter 6	
Loc. No.	Nearest Landmark	Lat.	Long.	Number Apartments Exposed[1]	Damage Index[2]	Number Apartments Exposed[1]	Damage Index[2]	Number Apartments Exposed[1]	Damage Index[2]
1	Cape Mendocino, CA	40.4N	124.3W	53,000	2.23	16,000	.11	400	.01
2	Point Arena, CA	38.9N	123.4W	63,000	14.38	50,000	.95	10,000	.03
3	San Francisco, CA	37.6N	122.6W	140,000	48.18	57,000	6.39	42,000	.74
4	Salinas, CA	36.5N	121.1W	178,000	29.48	57,000	2.24	30,000	.16
5	Paso Robles, CA	35.5N	120.0W	179,000	26.34	134,000	1.42	7,000	.03
6	Gorman (Ft. Tejon), CA	34.8N	118.7W	177,000	100.00	126,000	10.86	97,000	1.08
7	San Bernardino, CA	34.2N	117.4W	164,000	82.43	123,000	11.37	95,000	1.25
8	Niland, CA	33.2N	115.6W	123,000	10.09	100,000	.71	1,000	.04
9	Gulf of Calif., Mex.	31.9N	114.9W	112,000	2.68	14,000	.10	700	.01
10	Lone Pine, CA	36.5N	118.0W	127,000	11.77	94,000	.42	600	.01
11	Hawthorne, NV	38.7N	117.8W	101,000	.42	200	.01	10	.00

[1]The loss index is expressed in terms of number of other residential buildings exposed to an earthshock severity of 4.5 or more on a continuous scale paralleling the Modified Mercalli Intensity Scale.

[2]The damage index is measured relative to the most damaging earthquake.

APPENDIX E-3

LOSS POTENTIAL TO NON-RESIDENTIAL BUILDINGS IN CALIFORNIA ASSOCIATED WITH THE SIMULATED OCCURRENCE OF EARTHQUAKES OF SPECIFIED MAGNITUDE ALONG MAJOR FAULT ZONES

	Epicenter Location			Richter 8		Richter 7		Richter 6	
Loc. No.	Nearest Landmark	Lat.	Long.	Number Buildings Exposed[1]	Damage Index[2]	Number Buildings Exposed[1]	Damage Index[2]	Number Buildings Exposed[1]	Damage Index[2]
1	Cape Mendocino, CA	40.4N	124.3W	304,000	.86	87,000	.04	4,000	.00
2	Point Arena, CA	38.9N	123.4W	372,000	2.80	275,000	.04	50,000	.00
3	San Francisco, CA	37.6N	122.6W	712,000	20.46	321,000	.57	210,000	.01
4	Salinas, CA	36.5N	121.1W	906,000	7.94	320,000	.13	153,000	.00
5	Paso Robles, CA	35.5N	120.0W	902,000	3.57	639,000	.06	47,000	.00
6	Gorman (Ft. Tejon), CA	34.8N	118.7W	886,000	49.17	609,000	1.84	448,000	.06
7	San Bernardino, CA	43.2N	117.4W	805,000	100.00	592,000	2.90	432,000	.06
8	Niland, CA	33.2N	115.6W	605,000	4.49	462,000	.12	10,000	.00
9	Gulf of Calif., Mex.	31.9N	114.9W	524,000	.28	78,000	.01	4,000	.00
10	Lone Pine, CA	36.5N	118.0W	637,000	1.14	444,000	.02	6,000	.00
11	Hawthorne, NV	38.7N	117.8W	491,000	.01	2,000	.00	100	.00

[1]The loss index is expressed in terms of number of buildings exposed to an earthshock severity of 4.5 or more on a continuous scale paralleling the Modified Mercalli Scale.

[2]The damage index is measured relative to the most damaging earthquake.

APPENDIX E-4

CASUALTY POTENTIAL TO THE POPULATION OF CALIFORNIA ASSOCIATED WITH THE OCCURRENCE OF EARTHQUAKES OF SPECIFIED MAGNITUDES ALONG MAJOR FAULT ZONES

	Epicenter Location			Richter 8		Richter 7		Richter 6	
Loc. No.	Nearest Landmark	Lat.	Long.	Number Persons Exposed[1]	Casualty Index[2]	Number Persons Exposed[1]	Casualty Index[2]	Number Persons Exposed[1]	Casualty Index[2]
1	Cape Mendocino, CA	40.4N	124.3W	5,817,000	7.35	1,667,000	.56	78,000	.06
2	Point Arena, CA	38.9N	123.4W	7,119,000	23.74	5,280,000	4.32	961,000	.29
3	San Francisco, CA	37.6N	122.6W	13,820,000	47.88	6,177,000	13.27	4,091 000	3.32
4	Salinas, CA	36.5N	121.1W	17,589,000	43.77	6,137,000	6.97	2,963,000	1.12
5	Paso Robles, CA	35.5N	120.0W	17,507,000	50.65	12,455,000	7.94	874,000	.32
6	Gorman (Ft. Tejon),CA	34.8N	118.7W	17,167,000	100.00	11,867,000	24.21	8,783,000	5.44
7	San Bernardino, CA	34.2N	117.4W	15,606,000	83.79	11,539,000	25.00	8,493,000	6.27
8	Niland, CA	33.2N	115.6W	11,762,000	22.97	9,057,000	3.65	178,000	.15
9	Gulf of Calif., Mex.	31.9N	114.9W	10,262,000	9.74	1,519,000	.56	70,000	.03
10	Lone Pine, CA	36.5N	118.0W	12,373,000	28.03	8,681,000	3.50	116,000	.03
11	Hawthorne, NV	38.7N	117.8W	9,577,000	3.79	36,000	.03	500	.00

[1]The exposure index is expressed in terms of number of persons exposed to an earthshock severity of 4.5 or more on a continuous scale paralleling the Modified Mercalli Intensity Scale.

[2]The casualty index is measured relative to the most dangerous earthquake.

APPENDIX F

NATURAL DISASTER SITUATIONS CAUSED BY THE HURRICANE WIND AND STORM SURGE HAZARDS ALONG THE GULF AND SOUTH ATLANTIC COASTLINES IN PAST 100 YEARS

No.	Intensity	Date	Lives Lost	Economic Loss	Areas Affected
1	Major	Sep 26-Oct 9, 1873	-	-	Tide 14.0 ft. Ponta Rosa, Fla., destroyed.
2	Extreme	Sep 8-18, 1875	176	$1,000,000	Tides destroyed most of Indianola, Texas.
3	Minimal	Sep 14-21, 1877	-	-	Tide 10.5 ft. at Indianola, Texas.
4	Minimal	Sep 21-Oct 5, 1877	-	-	Tide 12.0 ft. at St. Marks, Fla.
5	Major	Oct 18-25, 1878	-	-	Florida - North Carolina.
6	Extreme	Aug 13-19, 1879	-	-	Wind estimated at 165 mph in N.C.
7	Major	Aug 4-14, 1880	-	1,000,000	Brownsville, Texas nearly destroyed.
8	Major	Aug 24-Sep 2, 1880	-	-	Palm Beach and Okeechobee, Fla.
9	Major	Aug 21-29, 1881	700	-	Georgia - South Carolina.
10	Major	Sep 2-12, 1882	-	-	Damage was severe in Ala.
11	Minimal	Oct 5-15, 1882	-	-	Cedar Key, Fla., submerged by tides.
12	Major	Sep 4-13, 1883	53	-	North Carolina.
13	Extreme	Aug 21-26, 1885	21	-	South Carolina
14	Major	Jun 18-23, 1886	-	-	Tides high at Apalachicola, Fla.
15	Extreme	Aug 12-21, 1886	-	-	Indianola, Texas destroyed by tides.
16	Minimal	Oct 8-13, 1886	50	-	Tides 10 ft. Johnsons Bayou, La., destroyed.
17	Extreme	Aug 15-Sep 2, 1893	2000	10,000,000	South Carolina.
18	Major	Sep 25-Oct 15, 1893	22	-	North Carolina.
19	Extreme	Sep 27-Oct 5, 1893	2000	-	Tides 12.0 ft. at Pass Christian, Miss.
20	Major	Sep 18-30, 1894	-	-	Winds were 104 mph at Key West, Fla.
21	Major	Jul 4-12, 1896	-	-	Winds were 100 mph at Pensacola, Fla.
22	Major	Sep 22-29, 1896	116	7,000,000	Tide 10.0 ft. at Cedar Key, Fla.
23	Extreme	Sep 25-Oct 6, 1898	179	-	Georgia
24	Major	Oct 23-Nov 4, 1899	-	-	High tides in North Carolina.
25	Extreme	Aug 27-Sep 15, 1900	6000	30,000,000	Galveston, Texas.

(continued)

APPENDIX F (continued)

No.	Intensity	Date	Lives Lost	Economic Loss	Areas Affected
26	Major	Sep 3-18, 1906	-	-	North Carolina.
27	Major	Sep 19-29, 1906	34	$2,000,000	15.0 ft. tides at Coden, Ala.
28	Major	Oct 11-22, 1906	164	-	Miami, Fla.
29	Major	Jul 13-22, 1909	41	2,000,000	Tide 10.0 ft. at Galveston, Texas.
30	Extreme	Sep 10-21, 1909	350	5,000,000	Tides 15.0 ft. at Timbalier Bay, La.
31	Major	Oct 6-13, 1909	15	1,000,000	Southern Florida.
32	Major	Oct 9-23, 1910	30	365,000	Wind 125 mph, Sand Key, tide 15.0 ft. Key West, Fla.
33	Major	Aug 23-30, 1911	17	-	Charleston, S.C.
34	Extreme	Aug 5-23, 1915	275	50,000,000	Wind 120 mph, tide 16.1 ft., Galveston, Texas.
35	Extreme	Sep 22-Oct 1, 1915	275	13,000,000	Tide 11.8 ft. at Bay St. Louis, Miss.
36	Major	Jun 29-Jul 10, 1916	4	3,000,000	Wind 107 mph, tide 11.9 ft., Mobile, Ala.
37	Extreme	Aug 12-19, 1916	20	1,800,000	Wind 90 mph, tide 5.9, Corpus Christi, Texas.
38	Minimal	Oct 12-19, 1916	-	-	Wind 128 mph at Mobile, Ala.
39	Major	Sep 21-29, 1917	-	170,000	Wind 125 mph at Pensacola, tide 7.8 ft. at Ft. Barancas, Fla.
40	Extreme	Aug 1-6, 1918	34	5,000,000	Wind 125 mph at Sulphur, La.
41	Extreme	Sep 2-15, 1919	900	22,000,000	Wind 110 mph at Key West, Fla., tides 16.0 ft. at Corpus Christi.
42	Major	Oct 20-29, 1921	6	3,000,000	Tide 11.0 ft. at Ponta Rassa, Fla.
43	Major	Aug 22-27, 1926	25	4,000,000	Tide 15.0 ft. at Terre Bonne Parish, La.
44	Extreme	Sep 11-22, 1926	243	112,000,000	Wind 138 mph, tide 13.2 ft. Miami, Fla.
45	Extreme	Sep 6-20, 1928	2136	76,000,000	Tide 9.8 ft. at Ft. Pierce, Fla.
46	Extreme	Sep 22-Oct 4, 1929	3	800,000	Wind 150 mph Key Largo, Fla., tide 10.2 ft., Perrine, Fla.
47	Major	Aug 11-14, 1932	40	7,500,000	Wind 100 mph, Columbia, Texas.
48	Major	Aug 17-20, 1933	-	21,000,000	North Carolina and areas north.
49	Major	Aug 28-Sep 5, 1933	40	12,000,000	Wind 80 mph, tide 15.0 ft. Brownsville, Texas.
50	Major	Aug 31-Sep 7, 1933	2	4,100,000	Wind 125 mph, Jupiter, Fla.

(continued)

APPENDIX F (continued)

No.	Intensity	Date	Lives Lost	Economic Loss	Areas Affected
51	Major	Sep 8-21, 1933	21	$1,000,000	Wind 76 mph at Cape Hatteras, N.C.
52	Extreme	Aug 29-Sep 10, 1935	408	6,000,000	Wind 200 mph, Fla. Keys, tide 20 ft.-Long Key.
53	Minimal	Oct 30-Nov 8, 1935	19	5,500,000	Wind 75 mph at Miami, Fla.
54	Major	Sep 8-25, 1936	2	1,600,000	Wind 80 mph at Cape Hatteras, N.C.
55	Minimal	Aug 2-10, 1940	-	1,800,000	Wind 82 mph, tide 14.5 ft., Jennings, La.
56	Major	Aug 5-15, 1940	34	7,000,000	Tide 10.7 ft. at Charleston, S.C.
57	Minimal	Sep 16-25, 1941	4	6,000,000	Wind 83 mph, tide 11.0 ft.-Matagorda, Texas.
58	Major	Oct 3-14, 1941	5	700,000	Wind 123 mph, tide 8.0 ft., Miami, Fla.
59	Major	Aug 21-31, 1942	8	26,500,000	Wind 120 mph, Port Lavaca, tide 14.7 ft., Matagorda.
60	Major	Sep 9-16, 1944	390	100,000,000	North Carolina to New England.
61	Major	Oct 12-23, 1944	18	60,000,000	Wind 120 mph-Dry Tortugas, Fla., tides 11.0 ft., Naples.
62	Extreme	Aug 24-29, 1945	3	20,100,000	Wind 135 mph-Port Lavaca, Fla., tide 14.5 ft.
63	Extreme	Sep 11-20, 1945	26	54,100,000	Wind 196 mph-Homestead, Fla., tides 13.7 ft.
64	Minimal	Oct 4-14, 1946	-	7,200,000	Wind 80 mph-Ft. Myers, tides 5.1 Punta Gorda
65	Extreme	Sep 4-21, 1947	51	110,000,000	Wind 155 mph-Hillsboro, tide 21.6 ft. Clewiston, Fla.
66	Minimal	Oct 9-16, 1947	1	23,000,000	Wind 95 mph, Savannah, Ga.
67	Major	Sep 18-25, 1948	3	17,500,000	Wind 122 mph-Key West, tide 19.0 ft., Canal Pt.,Fla.
68	Minimal	Oct 3-15, 1948	11	5,000,000	Wind 100 mph-Fla. Keys, tide 6.2 ft. Homestead,Fla.
69	Extreme	Aug 23-31, 1949	2	52,000,000	Wind 153 mph-Jupiter, Fla., tide 24.0 ft. Belle Glade.
70	Major	Sep 27-Oct 6, 1949	2	7,000,000	Wind 135 mph-Freeport, Tex., tides 11.4 ft. Harrisburg.
71	Major	Sep 1-9, 1950	2	3,300,000	Wind 125 mph-tide wrecked Cedar Key, Fla.
72	Major	Oct 13-19, 1950	4	28,000,000	Wind 150 mph-Miami; tide 19.3 ft. Clewison, Fla.
73	Extreme	Oct 5-18, 1954	98	251,600,000	Wind 150 mph-Cape Fear, tide 17.0 ft. Wilmington,N.C.
74	Minimal	Aug 3-14, 1955	-	40,000,000	Wind 100 mph-Ft. Macon, N.C.tide 8.0 ft. Nags Head
75	Minimal	Aug 7-21, 1955	-	65,000,000	Wind 74 mph, tide 8.0 ft. Wilmington, N.C.

(continued)

APPENDIX F (continued)

No.	Intensity	Date	Lives Lost	Economic Loss	Areas Affected
76	Minimal	Sep 10-23, 1955	7	88,000,000	North Carolina.
77	Minimal	Sep 21-30, 1956	15	24,900,000	Wind 100 mph, tide 10.0 ft. Grand Isle, La.
78	Extreme	Jun 25-28, 1957	390	150,000,000	Wind 180 mph-Oil rig; tide 13.9 ft. Oak Grove Ridge, La.
79	Extreme	Sep 21-Oct 3, 1958	-	$11,200,000	Wind 160 mph, tide 7.5 ft., Cape Fear, N.C.
80	Extreme	Sep 20-Oct 2, 1959	22	14,000,000	Wind 175 mph, tide 12.0 ft., Beaufort, N.C.
81	Extreme	Aug 29-Sep 13, 1960	50	426,000,000	Wind 200 mph-Fla. Keys, tide 13.0 ft., Florida to New England.
82	Extreme	Sep 3-15, 1961	46	408,200,000	Wind 175 mph, tide 16.6 ft. Port Lavaca, Tex.
83	Major	Aug 20-Sep 5, 1964	3	128,500,000	Wind 135 mph, tide 5.5 ft., Miami, Fla.
84	Major	Aug 28-Sep 16, 1964	5	250,000,000	Wind 125 mph-St. Augustine, Fla., tide 14.0 ft. Brunswick, Ga.
85	Major	Sep 28-Oct 5, 1964	38	125,000,000	Wind 135 mph Franklin, tide 10.0 ft. Point-au-Fer, La.
86	Extreme	Aug 27-Sep 12, 1965	75	1,420,500,000	Wind 165 mph-Fla. and La., tide 15.2 ft. Pointe-a-la-Hache, La.
87	Extreme	Sep 21-Oct, 1966	48	5,000,000	Wind 165 mph-tide 5.0 ft. Big Pine Key, Fla.
88	Major	Sep 5-22, 1967	15	200,000,000	Wind 120 mph-Raymondville, Texas, tide 18.0 ft. Padre Island.
89	Extreme	Aug 5-22, 1969	256	1,420,700,000	Wind 135 mph-Columbia, Miss., tide 24.6 ft., Pass Christian
90	Extreme	Jul 31-Aug 5, 1970	11	453,000,000	Wind 161 mph, tide 9.2 ft. Corpus Christi, Tex.

(Sugg, *et al.*, 1971; Dunn and Miller, 1964)

APPENDIX G

GULF AND ATLANTIC COASTAL FLOOD PLAINS: 10', 20', AND 30' CONTOURS

The 10', 20', and 30' contours as shown on these maps represent an average contour line; irregularities were ignored and an estimated average line drawn where there was no continous contour.

The information for these maps came from the Topographic Maps prepared by the U. S. Geological Survey and made available through the Yale University Map Department. Approximately 1,000 maps were used to cover the coastal area from Brownsville, Texas, to Eastport, Maine. Maps with a scale of 1: 62,500, or approximately 1 mile to the inch, were used whenever possible; maps with a 1: 24,000 scale, or 2,000 feet to the inch, were used when the 1: 62,500 were not suitable or available.

Where no maps were available or the available maps did not show contours at 10 foot intervals, estimates were made on the basis of the contours of adjoining areas. Where large areas were not available, the best estimate was shown as a dotted line.

Some of the maps were quite old, though none dated prior to 1901 were used. These maps presented plotting problems since many towns and roads on recent maps were not shown on these older maps. It is possible that in some areas the contours may have changed.

The last two pages of this section show some of the larger cities in this area at a larger scale. These cities were chosen for their size, exposure to coastal flooding, and the completeness of contour information on them.

(Presented as Appendix in Friedman and Roy, 1966)

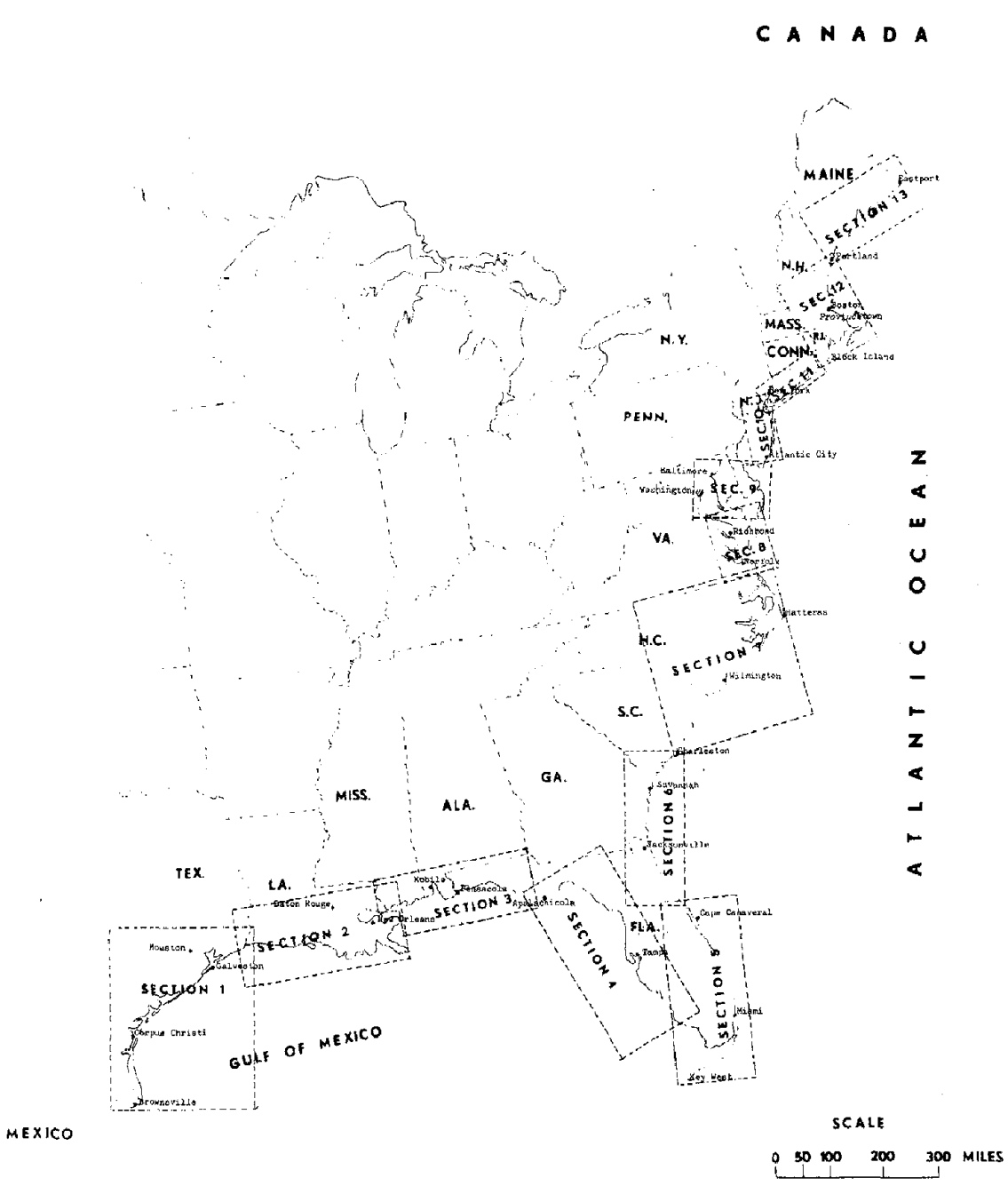
CANADA
MAINE
Eastport
SECTION 13
Portland
N.H.
SEC. 12
MASS.
Boston
Providence
R.I.
CONN.
Block Island
N.Y.
New York
PENN.
SECTION 10
Atlantic City
Baltimore
Washington
SEC. 9
VA.
Richmond
SEC. 8
Norfolk
Hatteras
N.C.
SECTION 7
Wilmington
S.C.
Charleston
GA.
Savannah
SECTION 6
Jacksonville
MISS.
ALA.
TEX.
LA.
Baton Rouge
Mobile
Pensacola
New Orleans
SECTION 3
Apalachicola
SECTION 2
SECTION 4
FLA.
Cape Canaveral
Houston
Galveston
SECTION 1
Tampa
SECTION 5
Miami
Corpus Christi
Key West
GULF OF MEXICO
Brownsville
MEXICO
ATLANTIC OCEAN
SCALE
0 50 100 200 300 MILES

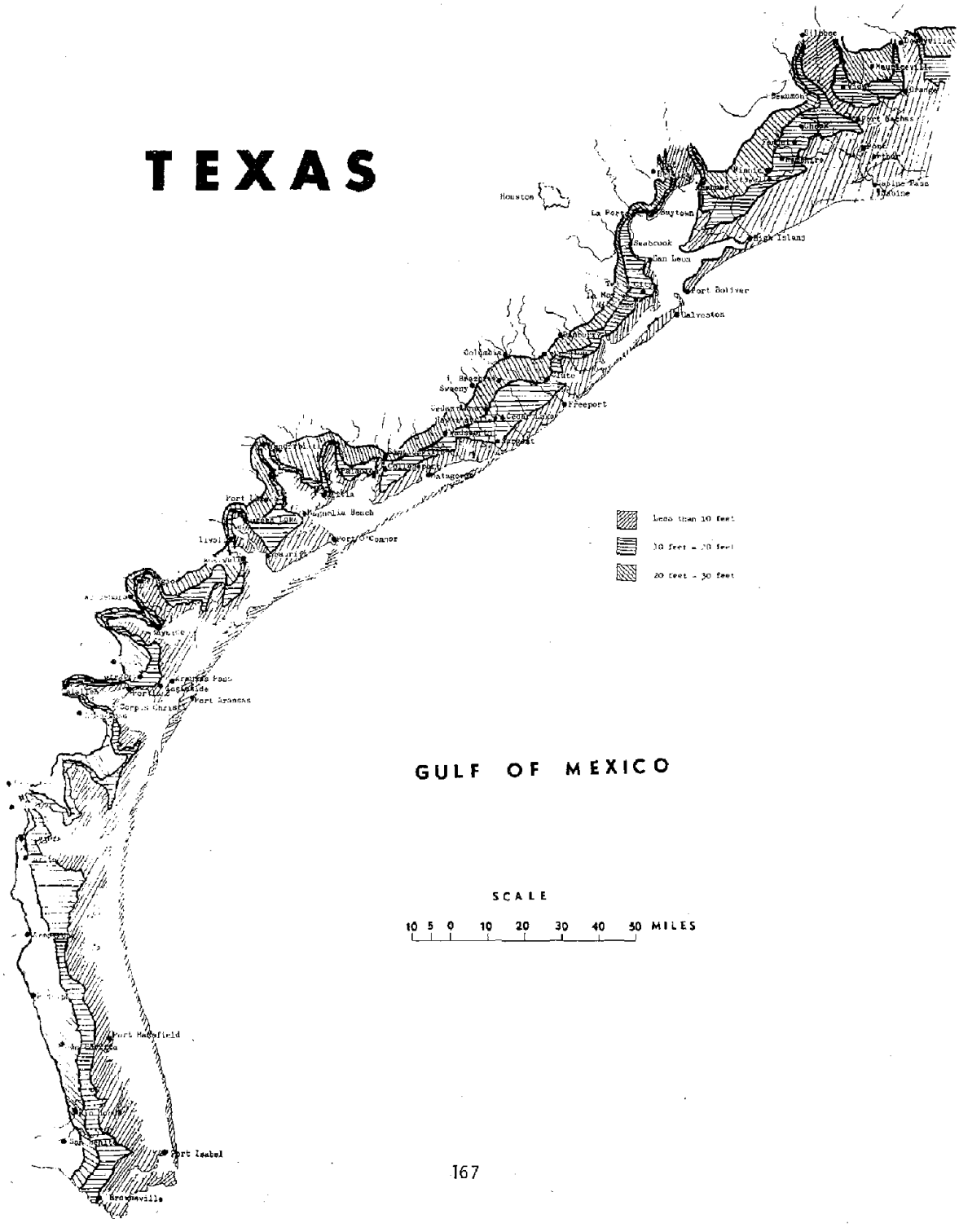
TEXAS
Houston
La Porte
Seabrook
Galveston
Freeport
Port Aransas
Port Isabel
Brownsville
Less than 10 feet
10 feet - 20 feet
20 feet - 30 feet
GULF OF MEXICO
SCALE
10 5 0 10 20 30 40 50 MILES

LOUISIANA

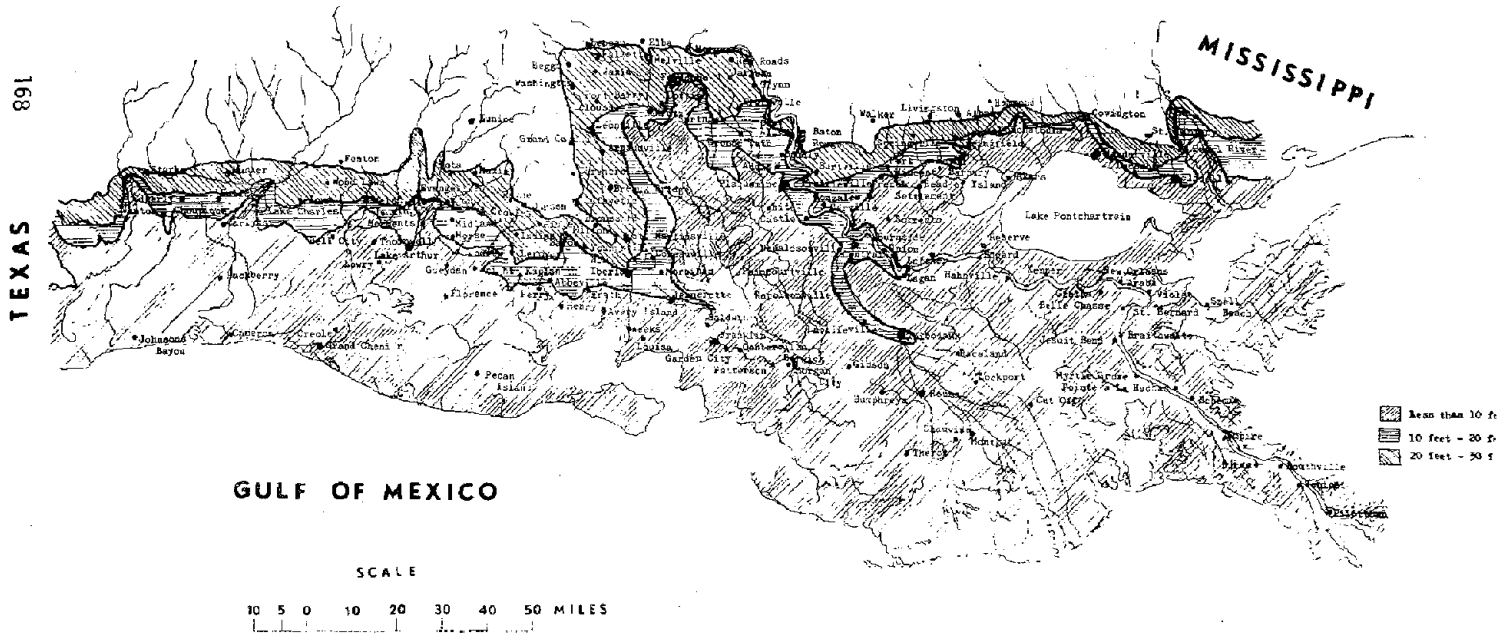
168
TEXAS
MISSISSIPPI
GULF OF MEXICO
Lake Pontchartrain
SCALE
10 5 0 10 20 30 40 50 MILES
Less than 10 ft
10 feet - 20 ft
20 feet - 30 f

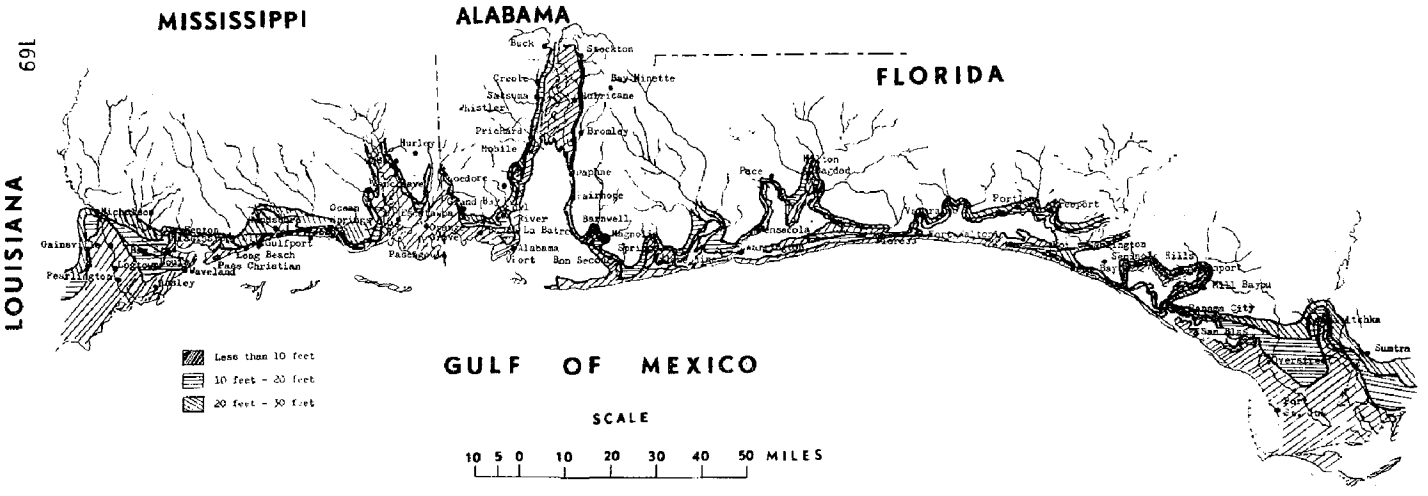
MISSISSIPPI
ALABAMA
FLORIDA
LOUISIANA
GULF OF MEXICO
Less than 10 feet
10 feet - 20 feet
20 feet - 30 feet
SCALE
10 5 0 10 20 30 40 50 MILES
Buck
Stockton
Creole
Bay Minette
Saksuma
Hurricane
Chistiler
Prichard
Bromley
Mobile
Hurley
Escatawpa
Theodore
Dauphine
Island
Fairhope
River
La Batre
Barnwell
Alabama
Port
Bon Secour
Pace
Milton
Crestview
Gainesville
Pascagoula
Gulfport
Long Beach
Pass Christian
Pearlington
Waveland
Ashley
Sumtra

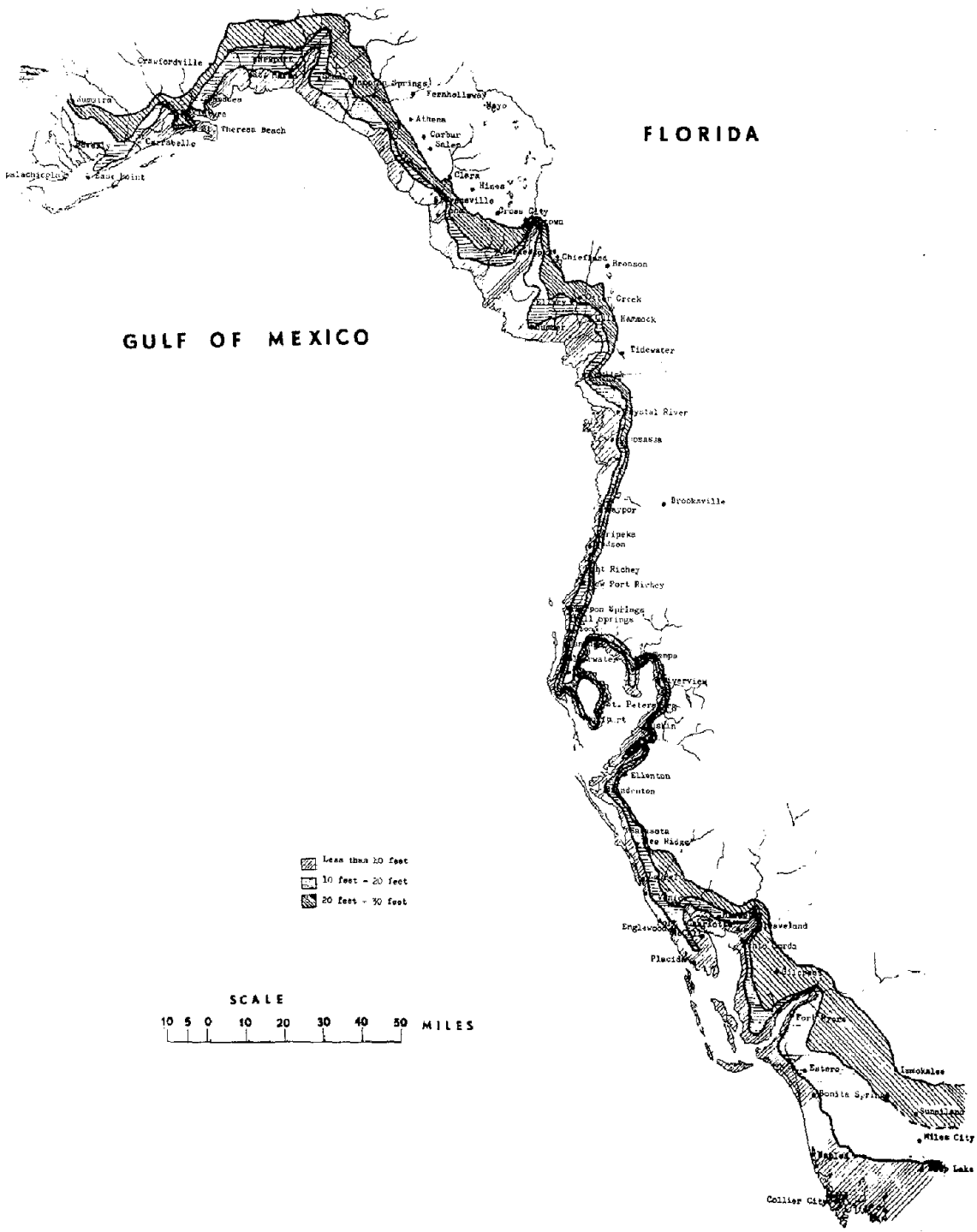
FLORIDA
GULF OF MEXICO
Crawfordville
Fernhollaway
Athena
Carbur
Salem
Clara
Hines
Chiefland
Bronson
Hammock
Tidewater
Brooksville
Ellenton
Englewood
Placida
Fort Myers
Estero
Immokalee
Miles City
Collier City
Less than 10 feet
10 feet - 20 feet
20 feet - 30 feet
SCALE
10 5 0 10 20 30 40 50 MILES

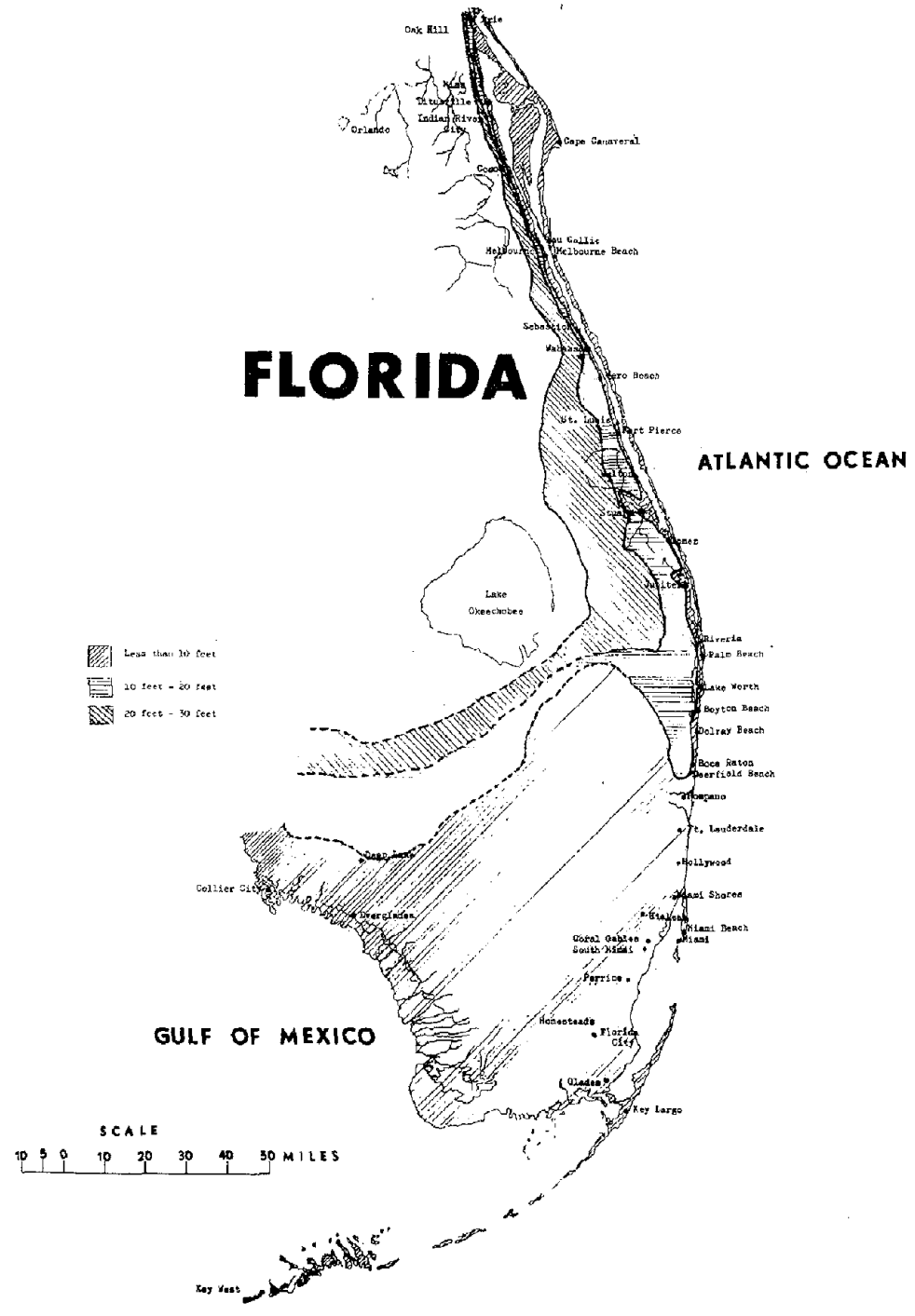
FLORIDA
ATLANTIC OCEAN
GULF OF MEXICO
Oak Hill
Orlando
Cape Canaveral
Melbourne Beach
Vero Beach
Fort Pierce
Lake
Okeechobee
Riviera
Palm Beach
Lake Worth
Boyton Beach
Delray Beach
Boca Raton
Deerfield Beach
Ft. Lauderdale
Hollywood
Miami Shores
Miami Beach
Miami
Coral Gables
South Miami
Perrine
Homestead
Florida City
Key Largo
Collier City
Everglades
Key West
Less than 10 feet
10 feet - 20 feet
20 feet - 30 feet
SCALE
10 5 0 10 20 30 40 50 MILES

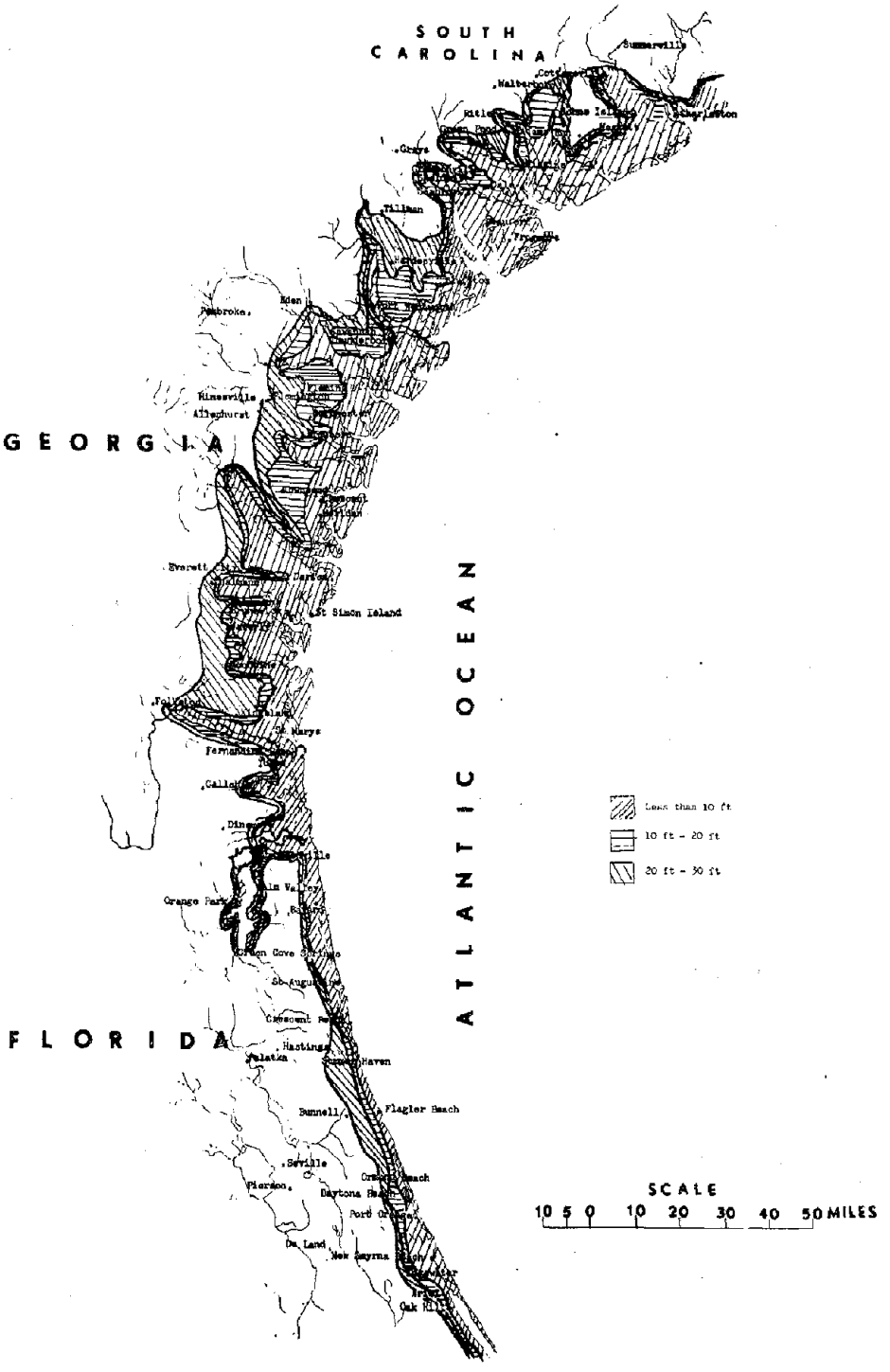
SOUTH CAROLINA
GEORGIA
FLORIDA
ATLANTIC OCEAN
Less than 10 ft
10 ft - 20 ft
20 ft - 30 ft
SCALE
10 5 0 10 20 30 40 50 MILES

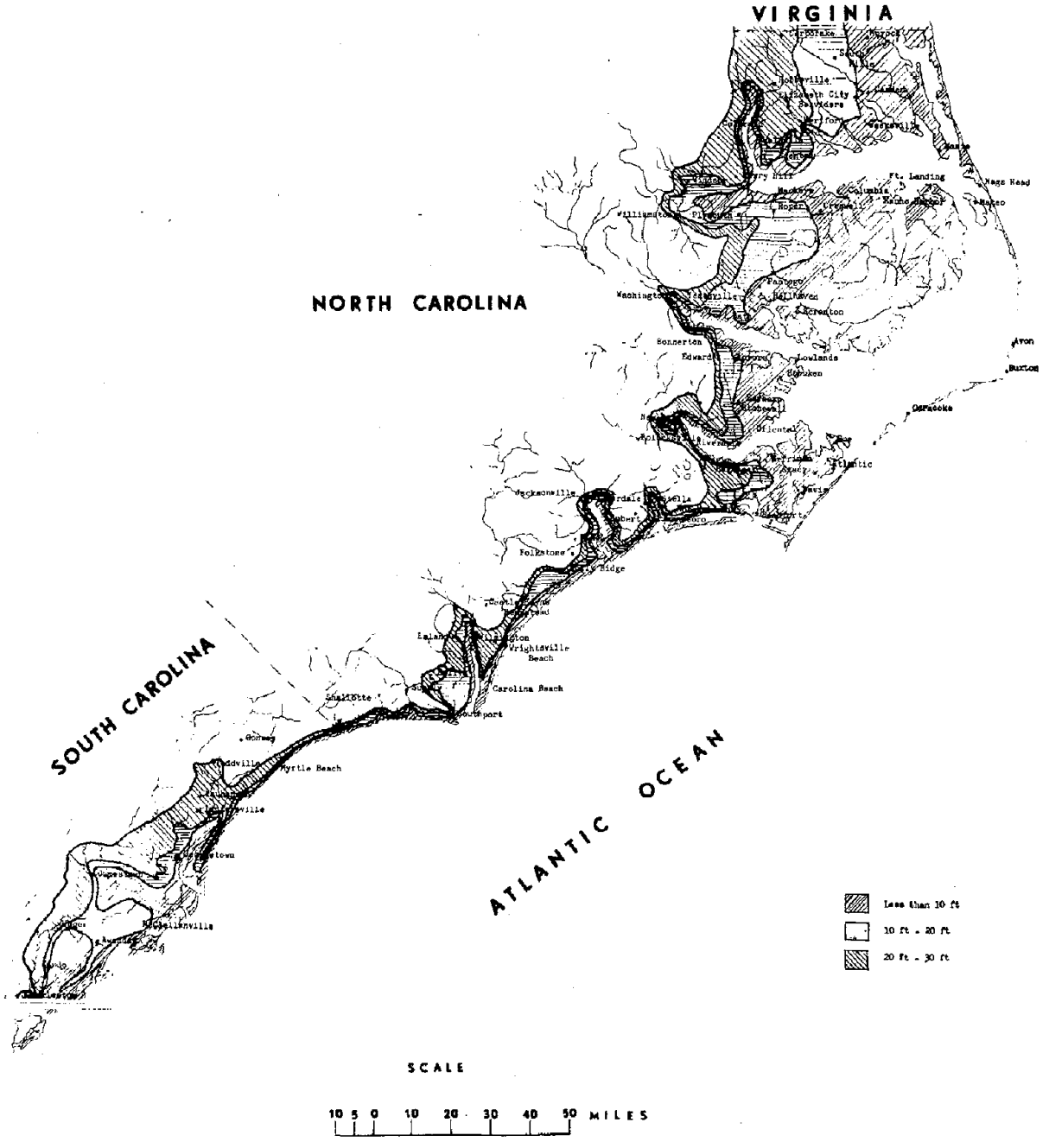
VIRGINIA
NORTH CAROLINA
SOUTH CAROLINA
ATLANTIC OCEAN
Kitty Hawk
Nags Head
Manteo
Ft. Landing
Columbia
Manns Harbor
Roper
Creston
Bonnerton
Edenton
Lowlands
Avon
Buxton
Ocracoke
Atlantic
Folkstone
Ridge
Wrightsville Beach
Carolina Beach
Southport
Myrtle Beach
Less than 10 ft
10 ft - 20 ft
20 ft - 30 ft
SCALE
10 5 0 10 20 30 40 50 MILES

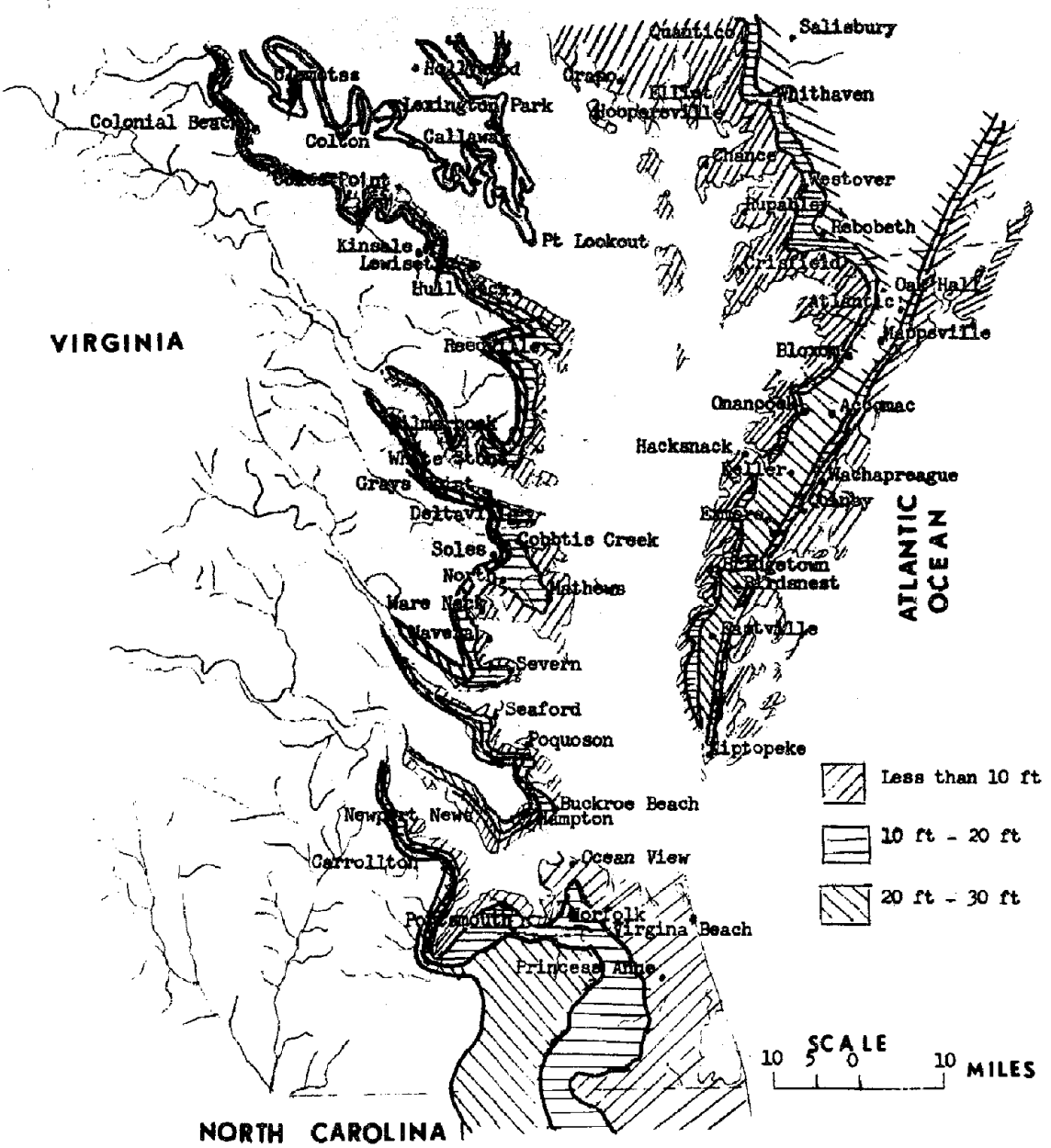
Quantico
Salisbury
Whithaven
Hooperesville
Chance
Westover
Rehobeth
Crisfield
Oak Hall
Atlantic
Pocomoke
Onancock
Accomac
Hacksnack
Wachapreague
Cobbtis Creek
Bridgetown
Birdsnest
Eastville
ATLANTIC OCEAN
Colonial Beach
Colton
Callaway
Pt Lookout
Kinsale
Lewisetta
Hull
Reedville
VIRGINIA
Grays
Deltaville
Soles
Mathews
Mare Neck
Severn
Seaford
Poquoson
Tiptopeke
Buckroe Beach
Hampton
Newport News
Carrollton
Ocean View
Norfolk
Virgina Beach
Princess Anne
NORTH CAROLINA
Less than 10 ft
10 ft - 20 ft
20 ft - 30 ft
SCALE
10 5 0 10 MILES

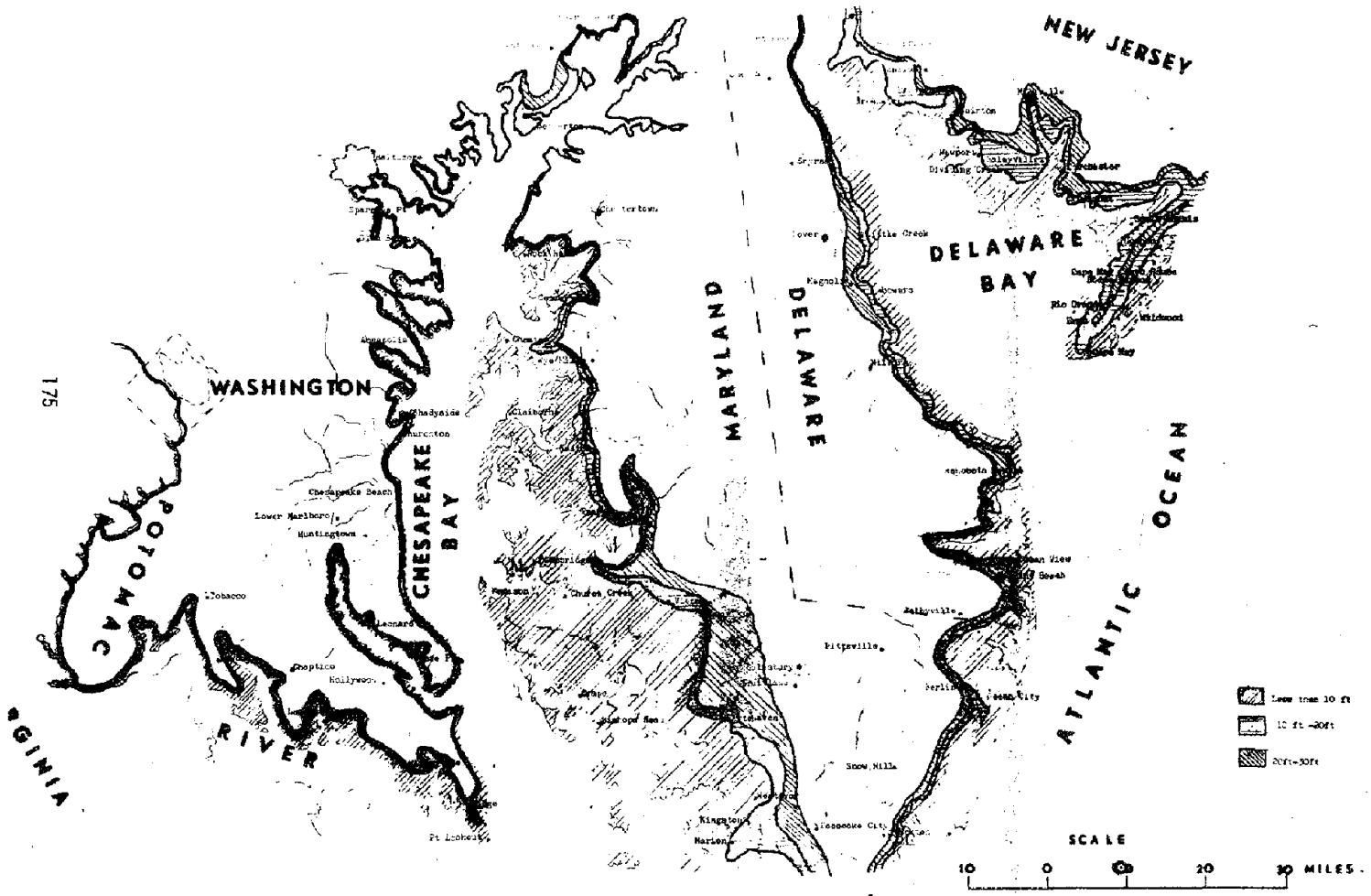
NEW JERSEY
DELAWARE BAY
MARYLAND
DELAWARE
WASHINGTON
CHESAPEAKE BAY
POTOMAC
RIVER
VIRGINIA
ATLANTIC OCEAN
Less than 10 ft
10 ft -20ft
20ft-30ft
SCALE
10 0 10 20 30 MILES

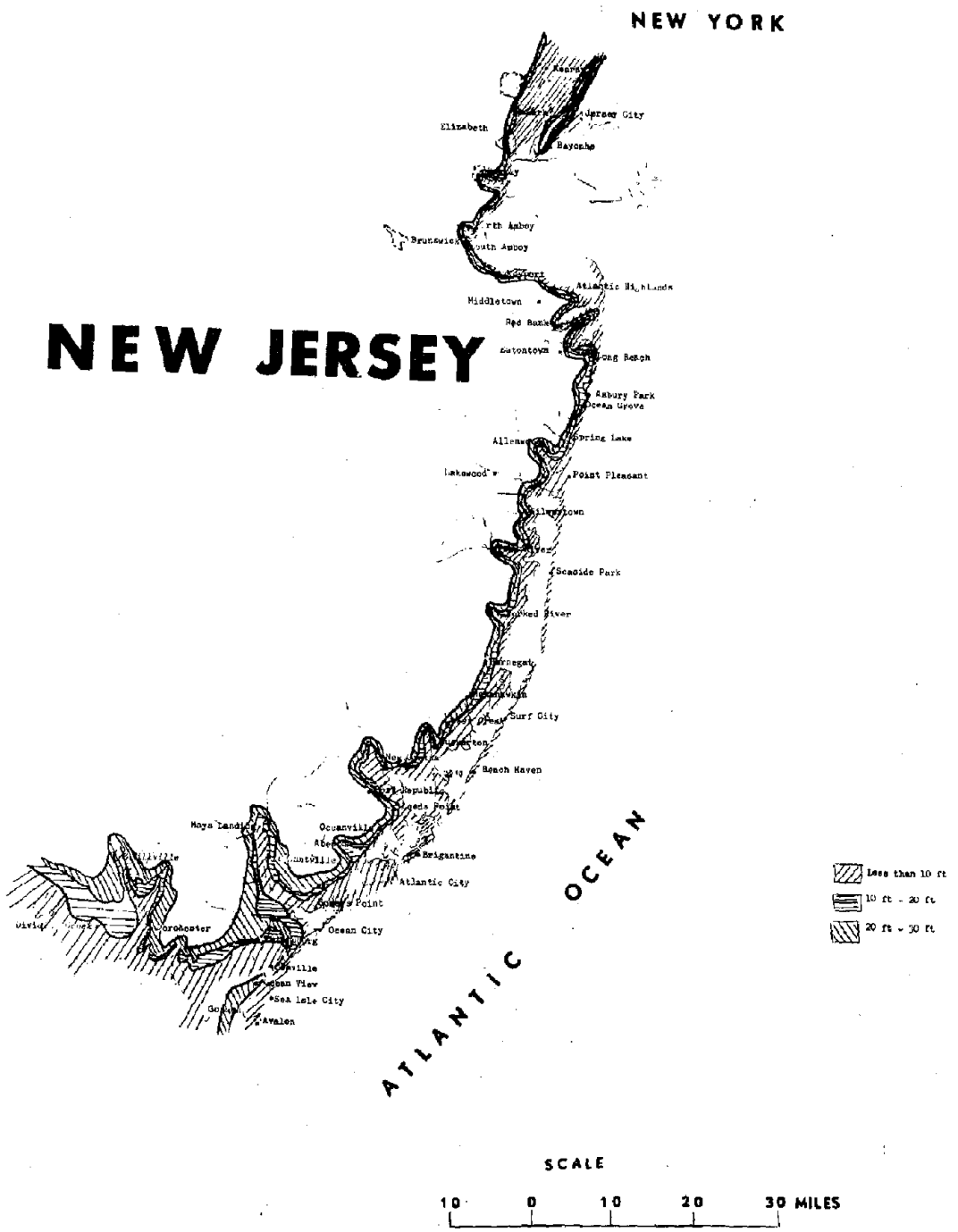
NEW YORK
NEW JERSEY
Elizabeth
Bayonne
Middletown
Asbury Park
Ocean Grove
Point Pleasant
Seaside Park
Surf City
Beach Haven
Brigantine
Atlantic City
Ocean City
Sea Isle City
Avalen
ATLANTIC OCEAN
Less than 10 ft
10 ft - 20 ft
20 ft - 30 ft
SCALE
10 0 10 20 30 MILES

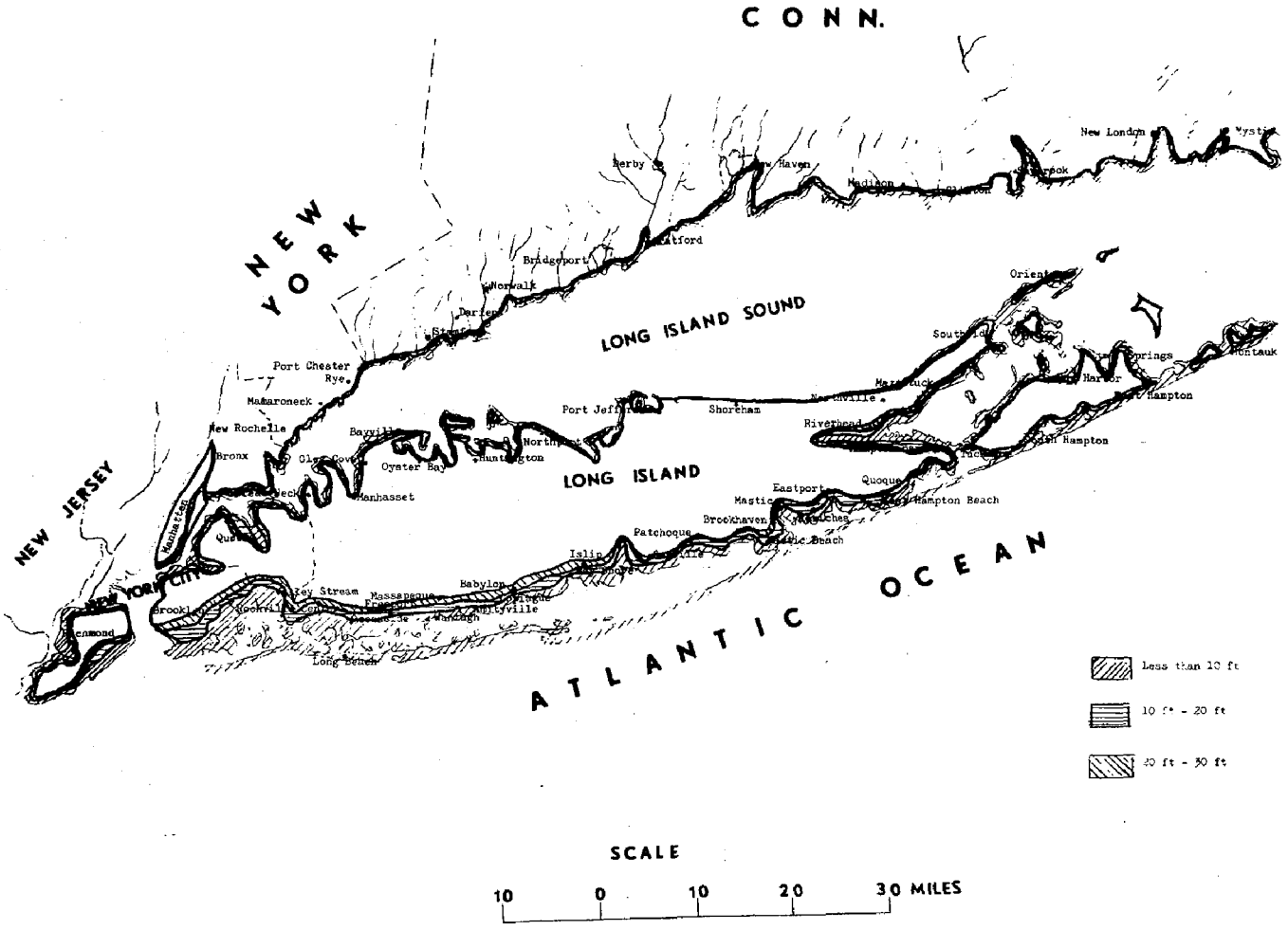
CONN.
NEW YORK
NEW JERSEY
LONG ISLAND SOUND
LONG ISLAND
ATLANTIC OCEAN
Derby
New Haven
Madison
New London
Bridgeport
Norwalk
Darien
Port Chester
Rye
Mamaroneck
New Rochelle
Bronx
Oyster Bay
Huntington
Port Jefferson
Shoreham
Northport
Manhasset
Patchogue
Islip
Babylon
Massapequa
Key Stream
Long Beach
Orient
Riverhead
Eastport
Quogue
Hampton Beach
Brookhaven
Montauk
Harbor
Springs
Hampton
Less than 10 ft
10 ft - 20 ft
20 ft - 30 ft
SCALE
10 0 10 20 30 MILES

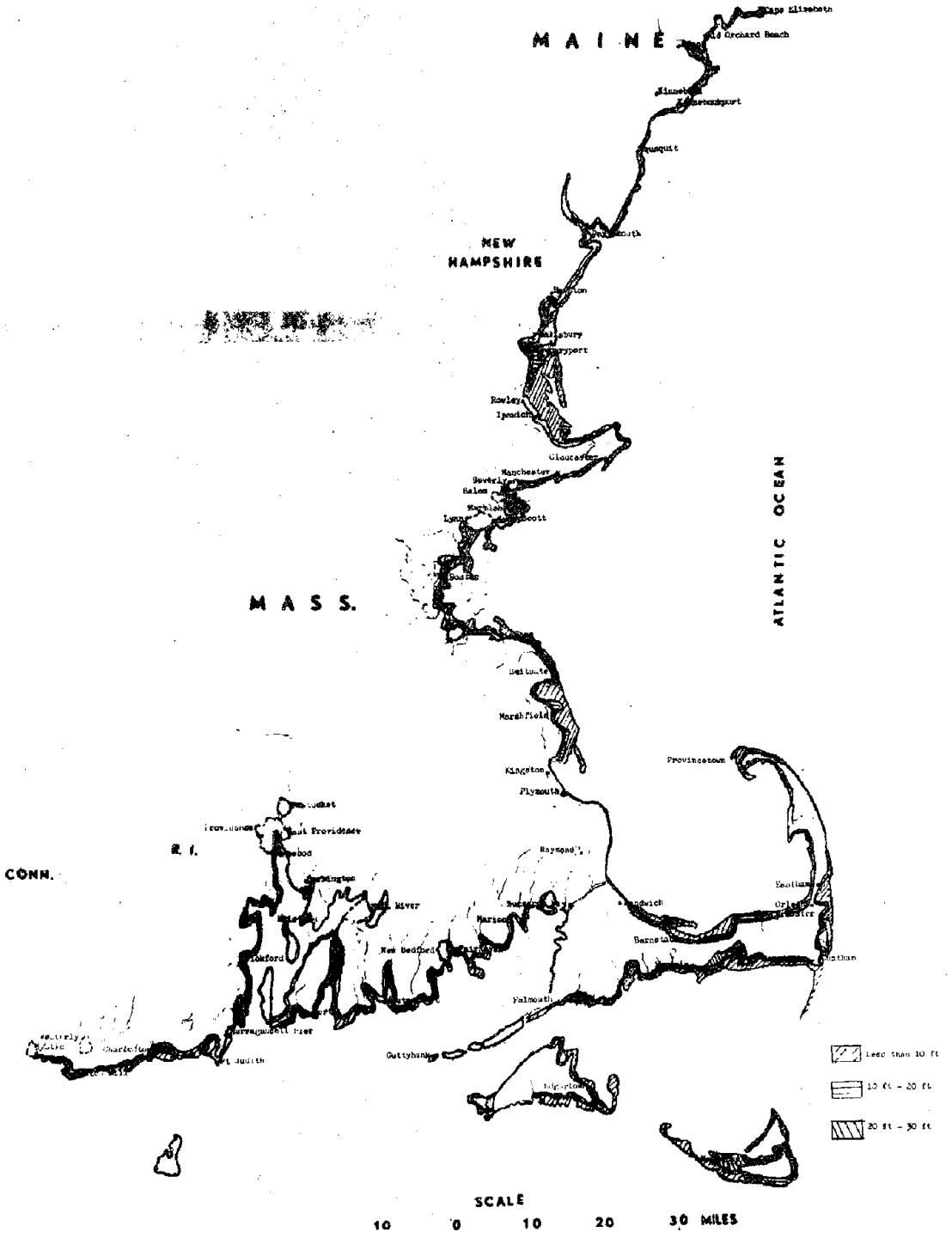
MAINE
NEW HAMPSHIRE
MASS.
R. I.
CONN.
ATLANTIC OCEAN
Cape Elizabeth
Old Orchard Beach
Provincetown
Less than 10 ft
10 ft - 20 ft
20 ft - 30 ft
SCALE
10 0 10 20 30 MILES

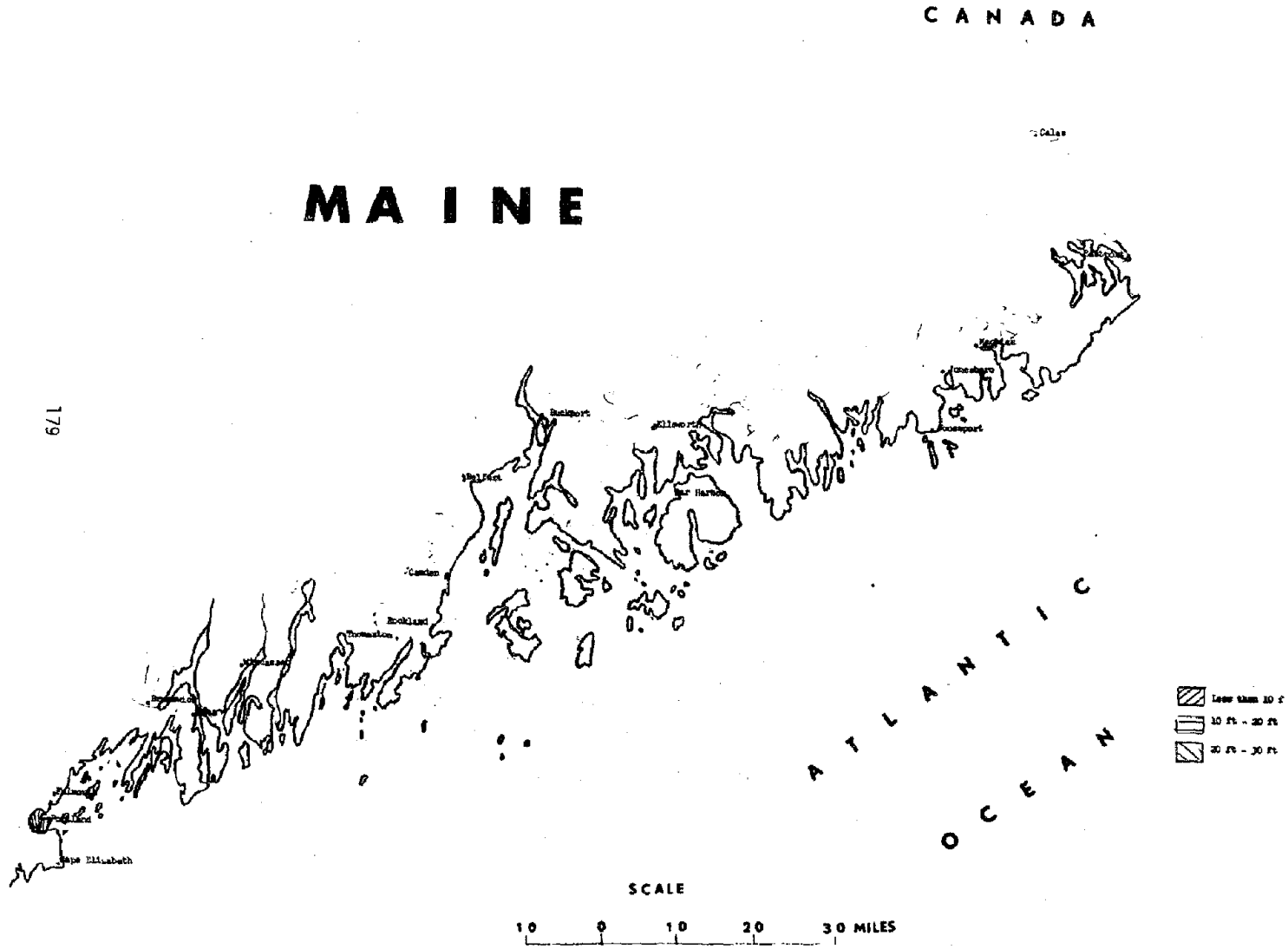
CANADA
MAINE
ATLANTIC
OCEAN
SCALE
10 0 10 20 30 MILES

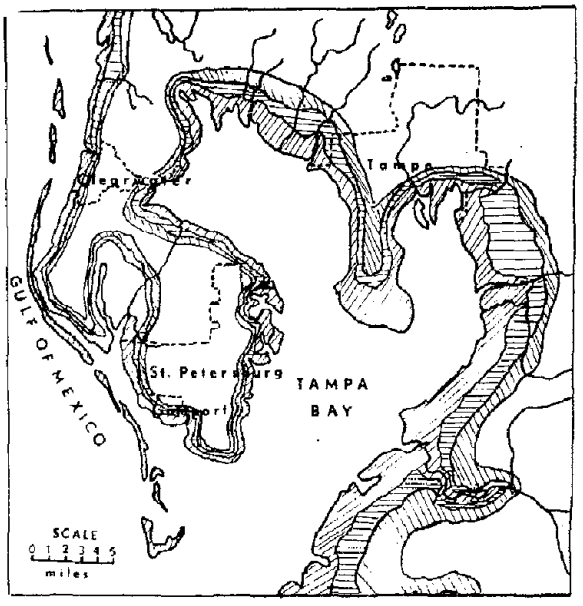

TAMPA AREA

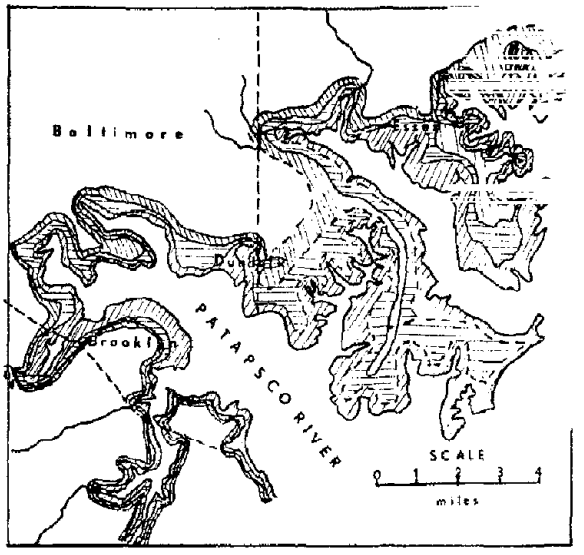

BALTIMORE AREA

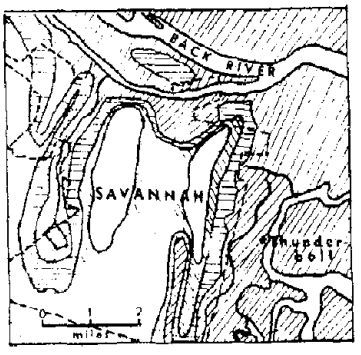

SAVANNAH AREA

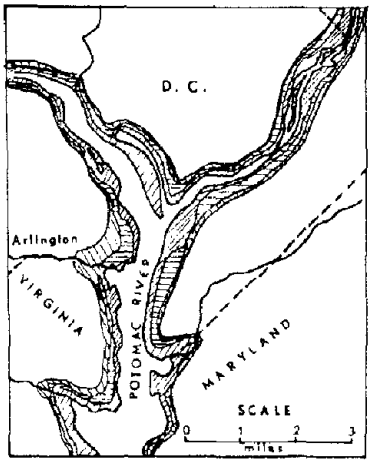

WASHINGTON AREA

- Less than 10 feet
- 10 feet - 20 feet
- 20 feet - 30 feet

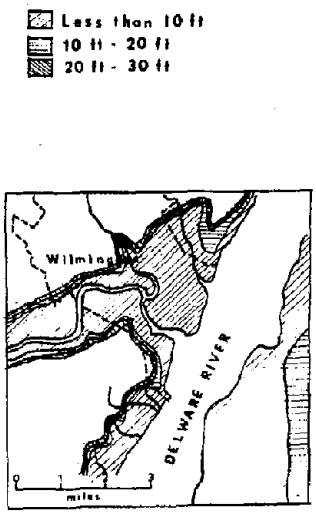

WILMINGTON AREA

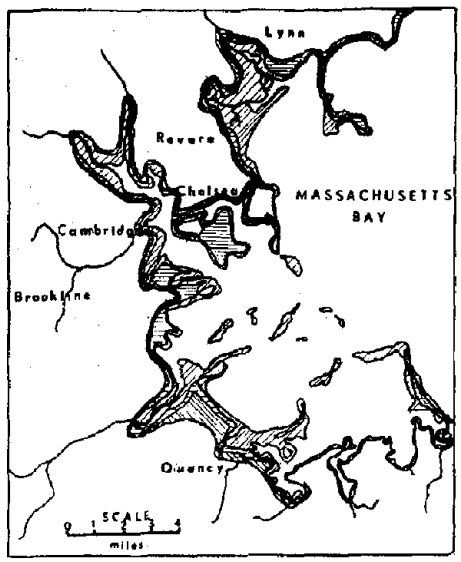

BOSTON AREA

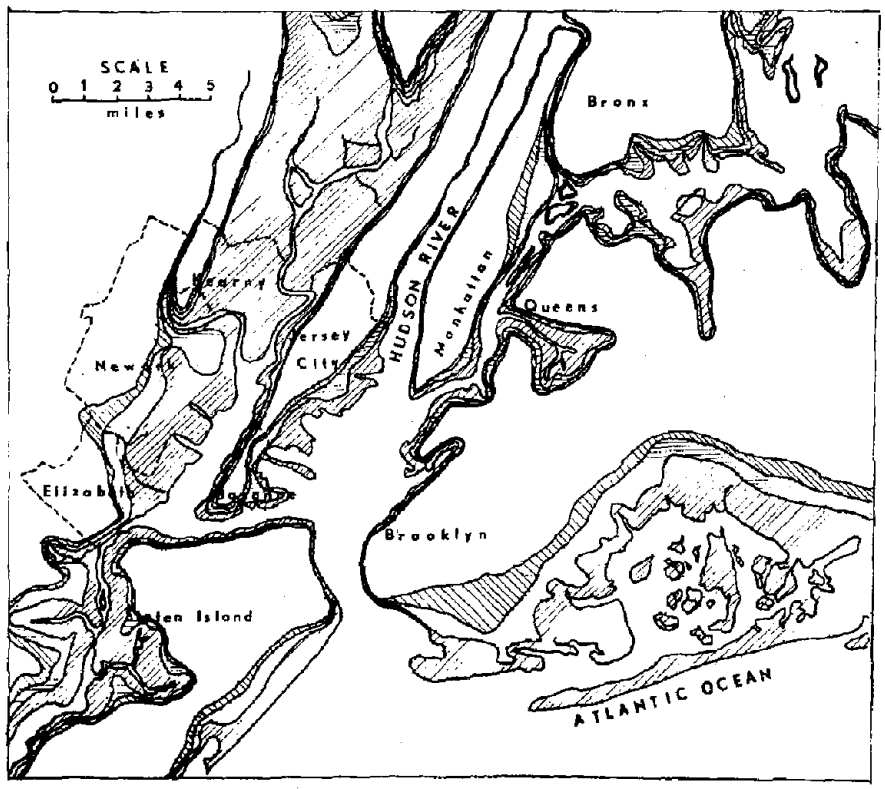

NEW YORK CITY AREA

REFERENCES

Algermissen, S. T.
1969 "Seismic Risk Studies in the United States." Proceedings of the Fourth World Conference on Earthquake Engineering. Santiago, Chile: Chilean Association on Seismology and Earthquake Engineering.

1973 "The Problem of Seismic Zoning." Pages 112-125 in National Bureau of Standards Building Practices for Disaster Mitigation. NBS Building Science Series #46. U. S. Department of Commerce. Washington: U. S. Government Printing Office.

Allen, C. R., *et al.*
1965 "Relationship Between Seismicity and Geologic Structure in the Southern California Region." Bulletin of the Seismological Society of America 65, pp. 743-797.

Blume, J. A.
1969 "Response of Highrise Buildings to Ground Motion from Underground Nuclear Detonations." Bulletin of the Seismological Society of America 59, pp. 2343-2370.

1970 "The Motion and Damping of Buildings Relative to Seismic Response Spectra." Bulletin of the Seismological Society of America 60, pp. 231-259.

1972 "Highrise Building Characteristics and Response Determined from Nuclear Seismology." Bulletin of the Seismological Society of America 62, pp. 519-540.

Blume, J. A. and R. L. Monroe
1971 The Spectral Matrix Method of Predicting Damage from Ground Motion. San Francisco, California: John A. Blume and Associates, Research Division.

Bodine, B. R.
1969 Hurricane Surge Frequency Estimated for the Gulf Coast of Texas. Technical Memo #26. Coastal Engineering Research Center. Washington: U. S. Army Corps of Engineers.

1971 Storm Surge on the Open Coast: Fundamentals and Simplified Prediction. Technical Memo #35. Coastal Engineering Research Center. Washington: U. S. Army Corps of Engineers.

Brune, J. N.
1970 "Tectonic Stress and the Spectra of Seismic Shear Waves from Earthquakes." Journal of Geophysical Research 75 (#26), pp. 4997-5009.

California Divison of Mines and Geology
1966 "Geologic Map of California." In Geology of Northern California. Bulletin #190. Sacramento, California.

Corps of Engineers
1965 Grand Isle and Vicinity, Louisiana Interim Hurricane Survey. 88th Congress, 1st Session. House Document No. 184. Washington: U. S. Government Printing Office.

Cry, G. W.
1965 Tropical Cyclones of the North Atlantic Ocean--Tracks and Frequencies of Hurricanes and Tropical Storms 1871-1963. Technical Paper #55. U. S. Weather Bureau. Washington: U. S. Government Printing Office.

Davis, L. L. and L. R. West
1973 "Observed Effects of Topography on Ground Motion." Bulletin of the Seismological Society of America 63, pp. 283-298.

Donovan, N. C.
1973 "Earthquake Hazards for Buildings." Pages 82-111 in National Bureau of Standards Building Practices for Disaster Mitigation. NBS Building Sciences Series #46. U. S. Department of Commerce. Washington: U. S. Government Printing Office.

Douglas, B. M., *et al.*
1970 "Spectral Characteristics of Central Nevada Microearthquakes." Bulletin of the Seismological Society of America 60, pp. 1547-1559.

Duke, C. M. and S. E. Jacobsen
1973 Optimization of Water Resource Systems Incorporating Earthquake Risk: 1973 Contributions. Water Resources Center Contribution #141. Los Angeles: University of California.

Duke, C. M., *et al.*
1972 Effects of Site Classification and Distance on Instrumental Indices in the San Fernando Earthquake Laboratory. School of Engineering and Applied Science. Los Angeles: University of California.

Dunn, G. E. and B. T. Miller
1964 Atlantic Hurricanes. Baton Rouge: Louisiana State University Press.

Environmental Science Services Administration
1967 Hurricane. U. S. Department of Commerce. Washington: U. S. Government Printing Office.

Ergin, K.
1969 "Observed Intensity-Epicentral Distance Relations in Earthquakes." Bulletin of the Seismological Society of America 59, pp. 1227-1238.

Evernden, J. F., R. R. Hibbard and J. F. Schneider
1972 "Interpretation of Seismic Intensity Data." Pages 363-378 in Proceedings of the International Conference on Microzonation for Safer Construction, Research and Application, Volume I. Washington: National Science Foundation.

Frank, N.
1974 "The Hard Facts About Hurricanes." NOAA 4 (#3). Washington: U. S. Department of Commerce.

Friedman, D. G.
1961 The Use of Climatological Probabilities as an Aid in Making Extended Coverage Rate Level Adjustments. Unpublished Report. Hartford, Connecticut: The Travelers Insurance Company.

1964 Frequency of Hurricane Winds in Various Sections of the Gulf States Compared with Frequencies in the South Atlantic States. Unpublished Report. Hartford, Connecticut: The Travelers Insurance Company.

1966 The Hurricane Hazard in Louisiana. Unpublished Report. Hartford, Connecticut: The Travelers Insurance Company.

1969 "Computer Simulation of the Earthquake Hazards." Pages 153-181 in Office of Emergency Preparedness, Geologic Hazards and Public Problems, Conference Proceedings. Executive Office of the President. Washington: U. S. Government Printing Office.

1971 The Storm Surge Hazard Along the Gulf and South Atlantic Coastlines. Unpublished Report. Hartford, Connecticut: The Travelers Insurance Company.

1972 "Insurance and the Natural Hazards." International Journal of Actuarial Studies in Non-Life Insurance and Risk Theory 7 (Part I), pp. 4-58. Amsterdam, the Netherlands.

1973 "Analysis for Earthquake Insurance." Earthquakes and Insurance. Pasadena: California Institute of Technology.

1973a "Prospective View of Natural Disasters in the United States." Paper presented at the First International Symposium of the System Safety Society on Safety and the Consumer. Denver, Colorado.

1974 "Computer Simulation in Natural Hazard Assessment." Paper presented to the 70th Annual Meeting of the Association of American Geographers. Seattle, Washington.

Friedman, D. G. and M. Bocaccino
1972 Computer Simulation of the Effects of Adjustments to the Inland Flood Hazard. Unpublished Report. Hartford, Connecticut: The Travelers Insurance Company.

Friedman, D. G. and T. S. Roy
1966 Simulation of Total Flood Loss Experience on Dwellings on Inland and Coastal Flood Plains. Report Prepared for the U. S. Department of Housing and Urban Development. Hartford, Connecticut: The Travelers Insurance Company.

1969 Computer Simulation of Earthquake Hazard. Unpublished Report. Hartford, Connecticut: The Travelers Insurance Company.

Friedman, D. G. and P. A. Shortell
1967 Prospective Weather Hazard Rating in the Midwest with Special Reference to Kansas and Missouri. Unpublished Report. Hartford, Connecticut: The Travelers Insurance Company.

Fujita, T. T.
1970 Estimate of Maximum Wind Speeds of Tornadoes in Three Northwestern States. Satellite and Mesometeorology Research Project. Department of Geophysical Science Research Paper #92. Chicago: University of Chicago.

Furumoto, A. S.
1966 "Seismicity of Hawaii, Part 1: Frequency-Energy Distribution of Earthquakes." Bulletin of the Seismological Society of America 56, pp. 1-12.

Goodyear, H. V.
1968 Frequency and Areal Distribution of Tropical Storm Rainfall in the United States Coastal Region of the Gulf of Mexico. ESSA Technical Report #WB-7. Silver Spring, Maryland: U. S. Department of Commerce.

Gutenberg, B. and C. F. Richter
1942 "Earthquake Magnitude, Intensity, Energy and Acceleration." Bulletin of the Seismological Society of America 32, pp. 163-191.

1956 "Earthquake Magnitude, Intensity, Energy and Acceleration." (Second paper.) Bulletin of the Seismological Society of America 46, pp. 105-146.

Harris, D. L.
1963 Characteristics of the Hurricane Storm Surge. Technical Paper #48. U. S. Weather Bureau. Washington: U. S. Department of Commerce.

Hays, W. W., *et al.*
1972 Effects of Site Conditions on Ground Motion (Part II). National Conference on Earthquake Engineering, February 7-10. School of Engineering and Applied Sciences. Los Angeles: University of California.

Housner, G. W.
1973 "The Role of Earthquake Ground Motion in Earthquake Engineering." Pages 73-82 in Research Papers Submitted to Fifth World Conference on Earthquake Engineering. Earthquake Engineering Research Laboratory Report #EERL 73-02. Pasadena: California Institute of Technology.

Housner, G. W. and P. C. Jennings
1973 "Problems in Seismic Zoning." Pages 1-10 in Research Papers Submitted to Fifth World Conference on Earthquake Engineering. Earthquake Engineering Research Laboratory Report #EERL 73-02. Pasadena: California Institute of Technology.

Hudson, D. E.
1972 "Local Distribution of Strong Earthquake Ground Motions." Bulletin of the Seismological Society of America 62, pp. 1765-1786.

Hudson, D. E., *et al.*
1971-73 Analysis of Strong-Motion Earthquake Accelerograms. Earthquake Engineering Research Laboratory. Pasadena: California Institute of Technology.

Hudson, D. E. and F. E. Udwadia
1973 "Local Distribution of Strong Earthquake Ground Motion." Pages 11-20 in Research Papers Submitted to Fifth World Conference on Earthquake Engineering. Earthquake Engineering Research Laboratory Report #EERL 73-02. Pasadena: California Institute of Technology.

Insurance Information Institute
1949-1974 Insurance Facts: Selected Data of General Interest Relating to Property and Liability Insurance. New York.

Isacks, B. and J. Oliver
1964 "Seismic Waves with Frequencies from 1 to 100 Cycles per Second Recorded in a Deep Mine in Northern New Jersey." Bulletin of the Seismological Society of America 54, pp. 1941-1979.

Jelesnianski, C. P.
1967 "Numerical Computations of Storm Surges with Bottom Stress." Monthly Weather Review 95 (#11), pp. 740-756.

1972 SPLASH (Special Program to List Amplitudes of Surges from Hurricanes), 1: Landfall Storms. Publication #NOAA TM-NWS TDL-46. System Development Office. Silver Spring, Maryland: U. S. Department of Commerce.

Jelesnianski, C. P. and A. D. Taylor
1973 A Preliminary View of Storm Surges Before and After Storm Modifications. Publication #ERL WMPO-3, NHRL-102. National Oceanic and Atmospheric Administration. Washington: U. S. Department of Commerce.

Jenkins, O. P.
1965 Geologic Guidebook of the San Francisco Bay Counties. Sacramento: California Division of Mines and Geology.

Jennings, P. C.
1971 Engineering Features of the San Fernando Earthquake, Feb. 9, 1971. Earthquake Engineering Research Laboratory Publication #EERL 71-02. Pasadena: California Institute of Technology.

Johnson, R. A.
1973 "An Earthquake Spectrum Prediction Technique." Bulletin of the Seismological Society of America 63, pp. 1255-1274.

Jones, D. E., Jr.
1971 "Flood Damage and Flood Protection." In Urban Water Resources Management. Report of the Third Conference on Urban Water Resources Research, Deerfield Academy, 1970. New York: American Society of Civil Engineers.

Kaplan, M.
1972 "Actuarial Aspects of Flood and Earthquake Insurance." Proceedings of the Conference of Actuaries in Public Practice 21, pp. 474-511.

Lastrico, R. M., C. M. Duke and Y. Ohta
1972 "Effects of Site and Propagation Path on Recorded Strong Earthquake Motions." Bulletin of the Seismological Society of America 62, pp. 933-954.

Lomnitz, C.
1966 "Statistical Prediction of Earthquakes." Review of Geophysics 4, pp. 377-393.

1974 Global Tectonics and Earthquake Risk. Amsterdam, the Netherlands: Elsevier Scientific Publishing Company.

Lynch, R. D.
1969 "Response Spectra for Pahute Mesa Nuclear Events." Bulletin of the Seismological Society of America 59, pp. 2295-2309.

Lysmer, J., *et al.*
1970 Influence of Baserock Characteristics on Ground Response. Earthquake Engineering Research Center Report #EERC 70-7. Berkeley: University of California.

Medvedev, S. V.
1962 Engineering Seismology. Translated from Russian. Jerusalem: Israel Program for Scientific Translations.

Munich Reinsurance
1973 Earthquakes. Munich, West Germany.

Murphy, J. R. and J. A. Lahoud
1969 "Analysis of Seismic Peak Amplitudes from Underground Nuclear Explosions." Bulletin of the Seismological Society of America 59, pp. 2325-2341.

Murphy, J. R., *et al.*
1972 Calculated San Fernando Earthquake Response Spectra. National Conference on Earthquake Engineering, Feb. 7-10. School of Engineering and Applied Sciences. Los Angeles: University of California.

Nadolski, M. E.
1969 "Architectural Damage to Residential Structures from Seismic Disturbances." Bulletin of the Seismological Society of America 59, pp. 487-502.

National Oceanic and Atmospheric Administration
1972 A Study of the Earthquake Losses in the San Francisco Bay Area: Data and Analysis. Report prepared for the Office of Emergency Preparedness. U. S. Department of Commerce. Washington: U. S. Government Printing Office.

1973 A Study of the Earthquake Losses in the Los Angeles Area. Report prepared for the Office of Emergency Preparedness. Department of Commerce. Washington: U. S. Government Printing Office.

Newmark, N. M. and W. J. Hall
1973 "Procedures and Criteria for Earthquake-Resistant Design (Part II)." Pages 209-236 in National Bureau of Standards Building Practices for Disaster Mitigation. NBS Building Science Series #46. U. S. Department of Commerce. Washington: U. S. Government Printing Office.

Nickerson, J. W.
1971 Storm-Surge Forecasting. Navy Weather Research Facility Technical Paper #10-71. Norfolk, Virginia.

Nuttli, O. W.
1973 "The Mississippi Valley Earthquakes of 1811 and 1812: Intensities, Ground Motion and Magnitudes." Bulletin of the Seismological Society of America 63, pp. 227-248.

1973a State-of-the Art for Assessing Earthquake Hazards in the United States: Design Earthquakes for the Central United States. Army Engineers Waterways Experiment Station Publication #AD 756-447. Washington: U. S. Government Printing Office.

Office of the Assessor, Los Angeles County
1973 Personal Communication to E. J. Baker. Los Angeles, California.

Perez, V.
1973 "Velocity Response Envelope Spectrum as a Function of Time, for the Pacoima Dam, San Fernando Earthquake, February 9, 1971." Bulletin of the Seismological Society of America 63, pp. 299-313.

Richter, C. F.
1958 Elementary Seismology. San Francisco: W. H. Freeman and Company.

1959 "Seismic Regionalization." Bulletin of the Seismological Society of America 49, pp. 123-162.

Schnabel, P. B. and H. B. Seed
1973 "Accelerations in Rock for Earthquakes in the Western United States." Bulletin of the Seismological Society of America 63, pp. 501-516.

Schnabel, P., H. B. Seed and J. Lysmer
1972 "Modification of Seismograph Records for Effects of Local Soil Conditions." Bulletin of the Seismological Society of America 62, pp. 1649-1664.

Scholl, R. E.
1974 "Statistical Analysis of Low-Rise Building Damage Caused by the San Fernando Earthquake." Bulletin of the Seismological Society of America 64, pp. 1-24.

Scholl, R. E. and I. Farhoomand
1973 "Statistical Correlation of Observed Ground Motion with Low-Rise Building Damage." Bulletin of the Seismological Society of America 63, pp. 1515-1537.

Seed, H. B. and I. M. Idriss
1969 "Influence of Soil Conditions on Ground Motions During Earthquakes." Journal of the Soil Mechanics and Foundations Division (SMI), Proceedings of the American Society of Civil Engineers 95, pp. 99-137.

1969a Rock Motion Accelerograms for High Magnitude Earthquakes. Earthquake Engineering Research Center Report #EERC 69-7. Berkeley: University of California.

1970 "Analyses of Ground Motions at Union Bay, Seattle During Earthquakes and Distant Nuclear Blasts." Bulletin of the Seismological Society of America 60, pp. 125-136.

Shteinburg, V. V.
1969 "Studies of the Spectra of Ground Vibration Caused by Nearby Earthquakes." Proceedings of the Fourth World Conference on Earthquake Engineering. Santiago, Chile: Chilean Association on Seismology and Earthquake Engineering.

Slemmons, D. B., A. E. Jones and J. I. Gimlette
1965 "Catalog of Nevada Earthquakes, 1852-1960." Bulletin of the Seismological Society of America 55, pp. 561-565.

Steinbrugge, K. V.
1973 "Earthquake Insurance Losses for Single-Family Wood Frame Dwellings." Paper presented to the National Committee on Property Insurance. San Francisco: Earthquake Department of Insurance Services Office.

Steinbrugge, K. V., *et al.*
1971 San Fernando Earthquake: February 9, 1971. San Francisco: Pacific Fire and Rating Bureau.

Sugg. A. L., *et al.*
1971 Memorable Hurricanes of the United States Since 1873. NOAA Technical Memo NWS SR-56. National Weather Service. Washington: U. S. Government Printing Office.

Thatcher, W. and T. C. Hanks
1973 "Source Parameters of Southern California Earthquakes." Journal of Geophysical Research 78 (#35), pp. 8547-8576.

Thom, H. C. S.
1968 "New Distributions of Extreme Winds in the United States." Journal of the Structural Division, Proceedings of the American Society of Civil Engineers 94, pp. 1787-1800.

Townley, S. D. and M. W. Allen
1939 "Descriptive Catalog of Earthquakes of the Pacific Coast of the United States 1769-1928." Bulletin of the Seismological Society of America 29, pp. 1-297.

Trifunac, M. D.
1971 "Response Envelope Spectrum and Interpretation of Strong Earthquake Ground Motion." Bulletin of the Seismological Society of America 61, pp. 343-356.

1973 "Analysis of Strong Earthquake Ground Motion for Prediction of Response Spectra." Earthquake Engineering and Structural Dynamics 2 (#1), pp. 59-69.

Trifunac, M. D. and J. N. Brune
1970 "Complexity of Energy During the Imperial Valley, California Earthquake of 1940." Bulletin of the Seismological Society of America 60, pp. 137-160.

Trifunac, M. D., F. E. Udwadia, and A. G. Brady
1973 "Recent Developments in Data Processing and Accuracy Evalutions of Strong Motion Acceleration Measurements." Research Papers Submitted to the Fifth World Conference on Earthquake Engineering. Earthquake Engineering Research Laboratory Report #EERL 73-02. Pasadena: California Institute of Technology.

Udwadia, F. E. and M. D. Trifunac
1973 "Comparison of Earthquake and Microtremor Ground Motion in El Centro, California." Bulletin of the Seismological Society of America 63, pp. 1227-1253.

1973a "Damped Fourier Spectrum and Response Spectra." Bulletin of the Seismological Society of America 63, pp. 1775-1783.

U. S. Coast and Geodetic Survey
1966 Earthquake History of the United States. Part II: Stronger Earthquakes of California and Western Nevada. Washington: U. S. Government Printing Office.

U. S. Department of Commerce
1937-1970 United States Earthquakes: Annual Earthquakes. Washington: U. S. Government Printing Office.

1950-1973 Climatological Data, National Summaries. National Oceanic and Atmospheric Administration, Environmental Data Service. Asheville, North Carolina: National Climatic Center.

1961 Climatological Data, National Summary, Annual 1961. Volume 12 (#13). National Oceanic and Atmospheric Administration Environmental Data Service. Asheville, North Carolina: National Climatic Center.

1967 Studies in Seismicity and Earthquake Damage Statistics, Parts 1 and 2. Reports prepared for Department of Housing and Urban Development by ESSA of the Department of Commerce. Washington.

1969 Studies in Seismicity and Earthquake Damage Statistics, 1969: Summary of Recommendations. A report prepared for Department of Housing and Urban Development by ESSA of Department of Commerce. Washington.

1972 County Business Patterns. U. S. Bureau of the Census. Washington: U. S. Government Printing Office.

1973 Preliminary Determination of Epicenters. National Oceanic and Atmospheric Administration. Boulder, Colorado.

Wesson, R. L. and W. L. Ellsworth
1973 "Seismicity Preceding Moderate Earthquakes in California." Journal of Geophysical Research 78 (#35), pp. 8527-8546.

Whitcomb, J. H., *et al.*
1973 "San Fernando Earthquake Series, 1971: Focal Mechanisms and Tectonics." Reviews of Geophysics and Space Physics II (#3), pp. 693-697.

White, Gilbert F. and J. Eugene Haas
1975 Assessment of Research on Natural Hazards. Cambridge, Massachusetts: MIT Press.

Whitman, R. V., *et al.*
1973 Damage Statistics for High-Rise Buildings in the Vicinity of the San Fernando Earthquake. Structures Publication #363. Cambridge, Massachusetts: Massachusetts Institute of Technology.

University of Colorado
Institute of Behavioral Science

Program on Technology, Environment and Man
Monograph Series

Friedman, Don G. *Computer Simulation in Natural Hazard Assessment.* NSF-RA-E-75-002.

Cochrane, Harold C. *Natural Hazards and Their Distributive Effects.* NSF-RA-E-75-003.

Warrick, Richard A., *et al.* *Drought Hazard in the United States: A Research Assessment.* NSF-RA-E-75-004.

Ayre, Robert S., *et al.* *Earthquake and Tsunami Hazards in the United States: A Research Assessment.* NSF-RA-E-75-005.

White, Gilbert F., *et al.* *Flood Hazard in the United States: A Research Assessment.* NSF-RA-E-75-006.

Brinkmann, Waltraud A. R., *et al.* *Hurricane Hazard in the United States: A Research Assessment.* NSF-RA-E-75-007.

Baker, Earl J. and Joe Gordon-Feldman McPhee. *Land Use Management and Regulation in Hazardous Areas: A Research Assessment.* NSF-RA-E-75-008.

Ericksen, Neil J. *Scenario Methodology in Natural Hazards Research.* NSF-RA-E-75-010.

Brinkmann, Waltraud A. R., *et al.* *Severe Local Storm Hazard in the United States: A Research Assessment.* NSF-RA-E-75-011.

Warrick, Richard A. *Volcano Hazard in the United States: A Research Assessment.* NSF-RA-E-75-012.

Mileti, Dennis S. *Natural Hazard Warning Systems in the United States: A Research Assessment.* NSF-RA-E-75-013.

(The above publications are available from the Institute of Behavioral Science #1, University of Colorado, Boulder, CO 80302.)

Mileti, Dennis S. *Disaster Relief and Rehabilitation in the United States: A Research Assessment.* NSF-RA-E-75-009.

Sorensen, John H. with J. Kenneth Mitchell. *Coastal Erosion Hazard in the United States: A Research Assessment.* NSF-RA-E-75-014.

Huszar, Paul C. *Frost and Freezing Hazard in the United States: A Research Assessment.* NSF-RA-E-75-015.

Sorensen, John H., Neil J. Ericksen and Dennis S. Mileti. *Landslide Hazard in the United States: A Research Assessment.* NSF-RA-E-75-016.

Assessment of Research on Natural Hazards Staff. *Snow-Avalanche Hazard in the United States: A Research Assessment.* NSF-RA-E-75-017.

Cochrane, Harold C. and Brian A. Knowles. *Urban Snow Hazard in the United States: A Research Assessment.* NSF-RA-E-75-018.

Brinkmann, Waltraud A. R. *Local Windstorm Hazard in the United States: A Research Assessment.* NSF-RA-E-75-019.

Ayre, Robert S. *Technological Adjustments to Natural Hazards.* NSF-RA-E-75-020.

(The above publications are available from the National Technical Information Service, Springfield, VA 22151.)

White, Gilbert F. and J. Eugene Haas. *Assessment of Research on Natural Hazards.* Cambridge, Massachusetts: MIT Press. NSF-RA-E-75-001.